Table of contents

Chapter 1

Formulas of sediment transport capacity

1.1 INTRODUCTION

The object of this research is to evaluate the Longshore Sediment Transport Capacity (LST) along the Catalan coast. The LST of a stretch of coast depends on its morphology, the characteristics of the sediment that forms the stretch and the characteristics of the waves that break over it. Taking this in account, many models have been developed in order to estimate LST, giving as a result several formulas. In this first chapter are revised and described the most widely used of them. The objective is to give an idea about the process of obtaining these formulas and to explain the influence of which parameters is considered in each formula. In the following chapters, some of the formulas will be applied to the stretches of beach of the Catalan coast. In that sense it is necessary to know which parameters are the most important to apply the formulas and to obtain them among the available data that has been collected along the Catalan coast up to day.

1.1 CERC FORMULA

The so-called "CERC formula" was adopted by the U.S Army Corps of Engineers in its coastal design manual published in 1966. This formula had been developed by Savage (1962) after summarizing the available data from field and laboratory studies. Imman and Bagnold (1963) suggested the use of an immersed weight transport rate, rather than a volumetric rate. An immersed weight sediment transport equation was calibrated by Komar and Inman (1970). Based on this relationship and other available field data, the CERC formula was updated from its 1966 version and presented in several editions of the *Shore Protection Manual* (1977, 1984).

A representation of the longshore sediment transport rate is an immersed weight transport rate I_l related to the volume transport rate by

$$I_l = (\rho_s - \rho)g\,(1 - n)Q_l \tag{1}$$

or

$$Q_l = \frac{I_l}{(\rho_s - \rho)g(1-n)} \tag{2}$$

The potential longshore sediment transport rate, dependent on an available quantity of littoral material, is most commonly correlated with the so-called longshore component of wave energy flux or power:

$$P_l = (EC_g)_b \sin\alpha_b \cos\alpha_b \tag{3}$$

where E_b is the wave energy evaluated at the breaker line:

$$E_b = \frac{1}{8}\rho\, g\, H_b^2 \tag{4}$$

and C_{gb} is the wave group speed at the breaker line:

$$C_{gb} = \sqrt{gd_b} = \left(g\frac{H_b}{\kappa}\right)^{1/2} \tag{5}$$

where κ is the breaker index H_b/d_b. The term $(EC_g)_b$ is the "wave energy flux" evaluated at the breaker zone, and α_b is the wave breaker angle relative to the shoreline. The immersed weight transport rate is I_l has the same units as P_l, so that the relationship

$$I_l = KP_l \tag{6}$$

is homogeneous, as the empirical coefficient K is dimensionless. Equation 6 is commonly referred to as the CERC formula.

Equation 4 may be written:

$$I_l = KP_l = K(EC_g)_b \sin\alpha_b \cos\alpha_b \tag{7}$$

which, on assuming shallow water breaking, gives

$$I_l = K\left(\frac{\rho g H_b^2}{8}\right)\left(\frac{gH_b}{\kappa}\right)^{1/2} \sin\alpha_b \cos\alpha_b \tag{8}$$

$$I_l = K\left(\frac{\rho g^{3/2}}{8\kappa^{1/2}}\right) H_b^{5/2} \sin\alpha_b \cos\alpha_b \tag{9}$$

$$I_l = K\left(\frac{\rho g^{3/2}}{16\kappa^{1/2}}\right) H_b^{5/2} \sin(2\alpha_b) \tag{10}$$

By using Equation 2, the relationship for I_l can be converted to a volume transport rate:

$$Q_l = \frac{K}{(\rho_s - \rho)g(1-n)} P_l \tag{11}$$

$$Q_l = K\left(\frac{\rho\sqrt{g}}{16\kappa^{1/2}(\rho_s - \rho)g(1-n)}\right) H_b^{5/2} \sin(2\alpha_b) \tag{12}$$

The K coefficient defined here on utilizing the rms breaking wave height $H_{b,rms}$. The *Shore Protection Manual* presented a dimensionless coefficient $K_{SPM\ sig}$ = 0.39 based on computations utilizing the significant wave height. The value of this SPM coefficient corresponding to the rms wave height $H_{b\ rms}$ is $K_{SPM\ rms}$ = 0.92.

Earlier, in 1970, Kommar and Imman had introduced a design value of the K coefficient for use with rms breaking wave height: $K_{K\&I\ rms}$ = 0.77. This value is commonly seen in many longshore transport rate computations.

Following are presented some methods used to obtain a more exactly value of *K* considering grain characteristics or breaking conditions.

Determination of the *K* coefficient

Variation of K with median grain size

- Bailard

An energy-based model was developed by Bailard (1981, 1982), which presents *K* as a function of the breaker angle and the ratio of the orbital velocity magnitude and the sediment fall speed, also based on the rms height at breaking. Using laboratory data sets, Bailard developed the following equation:

$$K = 0.05 + 2.6\sin^2(2\alpha_b) + 0.007\frac{u_{mb}}{w_f} \qquad (13)$$

where u_{mb} is the maximum oscillatory velocity magnitude, obtained as:

$$u_{mb} = \frac{\kappa}{2}\sqrt{gd_b} \qquad (14)$$

and w_f is the fall speed of the sediment.

Bailard's relationship is based on a limited data set, as the similar relationship presented by Walton (1979) and Walton and Chiu (1979).

Others have proposed empirically based relationships for increasing *K* with decreasing grain size, or equivalently, fall speed (Bruno, Dean and Gable 1980; Dean et al. 1982; Kamphuis et al. 1986; Dean, 1987). Komar (1988) suggested that *K* should depend on sediment grain size, and the absence of such a trend in his analysis must result from the imperfect quality of the data.

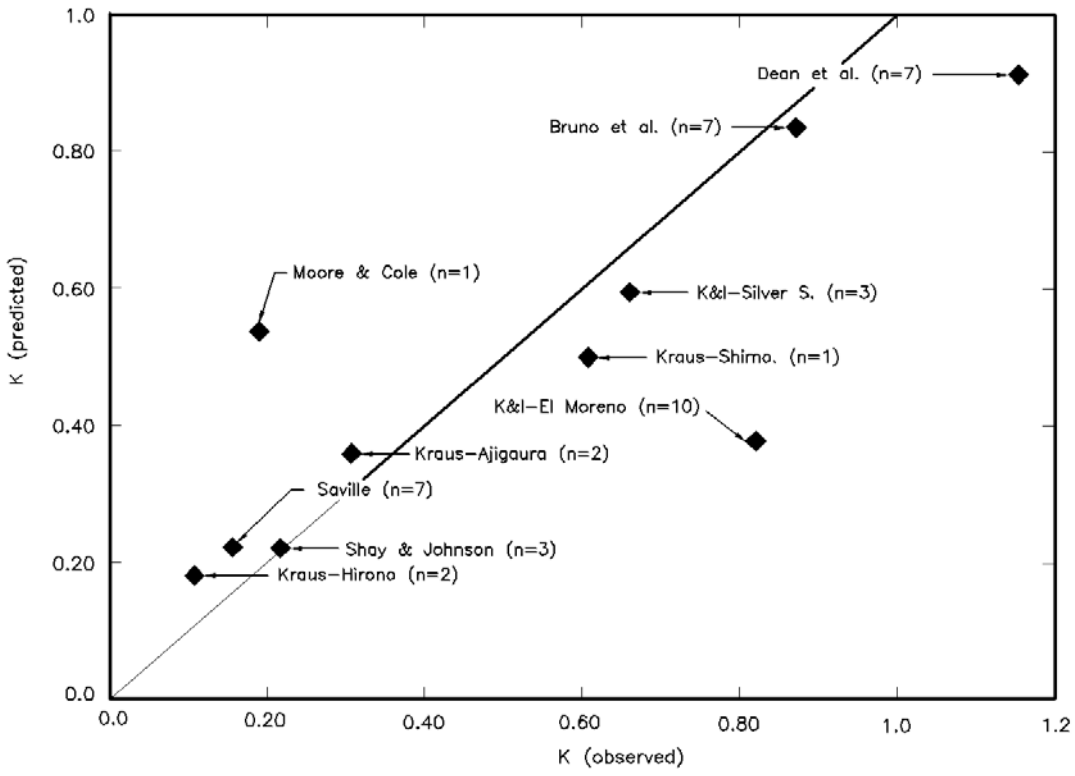

Measured and predicted K coefficients using Bailard's equation. Source: *Coastal Engineering Manual*, Chapter 2.

- Del Valle, Medina and Losada

An empirically based relationship was presented by del Valle, Medina and Losada (1993) for the K parameter, adding sediment transport data representing a range in median sediment grain sizes (0.40 mm to 1.5 mm) from the Adra River Delta, Spain to the available database as modified by Komar (1988). Del Valle, Medina and Losada obtained wave parameters from buoy and visual observations, and sediment transport rates were evaluated from aerial photographs documenting a 30-year period of shoreline evolution. Results of their analysis reinforce a decreasing trend in the empirical coefficient K with sediment grain size. The empirically based relationship is to applied with rms breaking wave height:

$$K = 1.4e^{-2.5D_{50}} \qquad (15)$$

where D_{50} is the median grain size of the beach sediment in millimeters. This relationship is based on limited data and depends strongly on the data from the Adra River Delta.

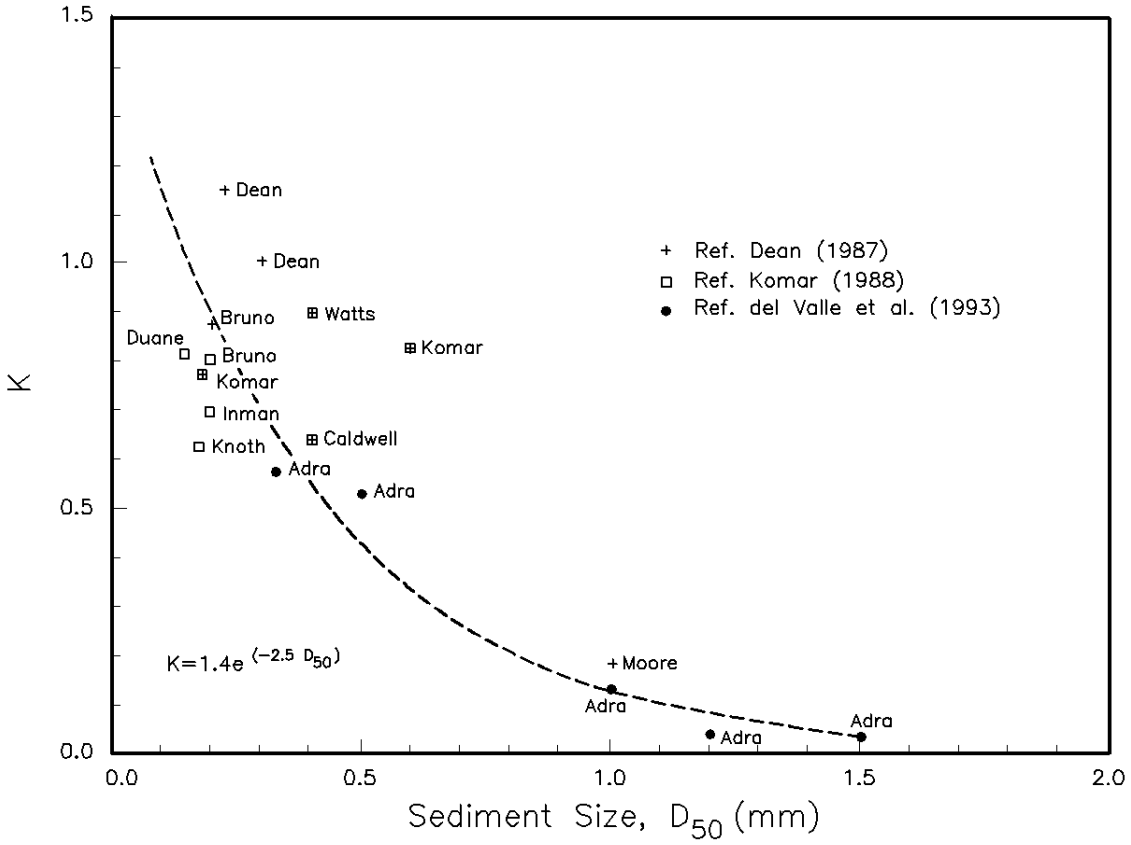

Coefficient K versus median grain size D_{50} (del Valle, Medina and Losada 1993). Source: *Coastal Engineering Manual*, Chapter 2.

Variation of K with surf similarity

- Kamphuis and Readshaw

From laboratory data, a relationship between K and the surf parameter

$$\xi_b = m / (H_b / L_0)^{1/2} \qquad (16)$$

has also been observed (Kamphuis and Readshaw 1978). These data suggest that the value of *K* increases with increasing value of the surf similarity parameter.

Practical considerations in LST calculations

According to the *Coastal Engeenering Technical Note-II-24 (12/90)* published by the Coastal Engeenering Research Center, some limitations must be considered when using the CERC formula to predict LST.

Threshold for significant transport

A threshold for significant transport was determined and expressed in terms of a *longshore discharge parameter*, R, defined as

$$R = V X_b H_{sb} \qquad (17)$$

where

V = average longshore current speed in the surf zone (m/s), and
X_b = average width of the surf zone (m)

The critical value of the longshore discharge parameter, Rc, below which significant sand transport did not occur, was empirically determined to be $R_c = 3.71$ m^3/s (Kraus and Dean 1987; Kraus, Gingerich and Rosati 1988).

The longshore current velocity on an open coast can be expressed (Komar and Inman 1970) as

$$V = 1.35\, u_m \sin(2\theta_b) \qquad (18)$$

where

$u_m = 0.5\, H_{sb}\, (g / d_b)^{1/2}$ is the maximum wave orbital velocity at breaking.

Assuming a plane beach profile ($X_b = d_b$ / tanβ = H_{sb} / (γ tanβ), where tanβ is the bottom slope, and combining EquationS 17 and 18 gives

$$R = \frac{1.35}{2}\sqrt{\frac{g}{\gamma}}\frac{H_{sb}^{5/2}}{\tan\beta}\sin 2\theta_b \qquad (19)$$

For values of $|R| \le R_c = 3.71$ m^3/s, there will not occur appreciable sand transport.

Estimating uncertaintly in Q

Due to uncertainties based on instrumentation accuracy there are breaking wave height and wave angle uncertainty values ΔH_{sb} and $\Delta\theta_b$, respectively. Associated LST ΔQ can be calculated. Considering

$$Q \sim H_{sb}^{5/2} \sin(2\theta_b) \qquad (20)$$

Including uncertainties in breaking wave height and angle:

$$Q \pm \Delta Q \sim (H_{sb} \pm \Delta H_{sb})^{5/2} \sin 2(\theta_b \pm \Delta\theta_b) \qquad (21)$$

Assuming that the wave angle at breaking is small, and using the first two tems of a Taylor series expansion of Equation 21, the uncertainty in the longshore transport rate is estimated as:

$$\Delta Q \sim Q\left(\pm\frac{\Delta\theta_b}{\theta_b} \pm \frac{5}{2}\frac{\Delta H_{sb}}{H_{sb}}\right)$$

The uncertainty in wave height is much large than the uncertainty in wave angle.

Comments

Some of the objections against the CERC formula are that the predicted sediment transport does not depend on the grain size of the sediment or the shape or slope of the coastal

profile. Several formulations for Kc were suggested in order to consider these parameters. Bodge and Kraus (1991) proposed a formulation for Kc as a function of the Iribarren number of the beach. It predicted less transport on more dissipative beaches and more transport on more reflective beaches. Dean et al. (1982) suggested a Kc coeficient wich reflects the influence of the grain size of the beach. They found that the coefficient Kc decreses for increasing the grain size. Kamphuis et al (1986) analysed field and laboratory data and developed an equation in wich the transport rate is proportional to the beach slope and inversely proportional to the grain size of the beach sediment.

1.2 BIJKER FORMULA

Bijker (1971) distinguises between bed load and suspended load, where the bed load transport depends on the total bottom shear stress by waves and currents. The suspended load is obtained by integrating the product of the concentration and velocity profiles along the vertical, where the reference concentration for the suspended sediment is expressed as a function of the bed load transport. The Bijker transport formula is, in principle, applicable for both breaking and non-breaking waves. However, different empirical coefficient values are needed in the formula.

Bijker used the Kalinske-Frijlink formula (1952) for bed load and the Einstein's method for evaluate the suspended load to obtain wich took into account both waves and currents. This formula is popular among European engineers.

The bed load transport rate ($q_{b,B}$; in $m^3/s/m$, including pores) is calculated from:

$$q_{b,B} = A d_{50} \frac{V}{C} \sqrt{g} \exp\left[\frac{-0.27(s-1) d_{50} \rho g}{\mu \tau_{b,wc}} \right] \qquad (1)$$

where A is an empirical coefficient (1.0 for non-breaking waves and 0.5 for breaking waves), d_{50} the median particle diameter, V the mean longshore current velocity, C the Chezy coefficient based on d_{50}, g the acceleration of gravity, s ($=\rho_s/\rho$) the relative sediment density, ρ_s the density of the bed material, ρ the density of water, μ a ripple factor, and $\tau_{b,wc}$ the bottom shear stress due to the waves and current. The first part of the above expression represents a transport parameter, whereas the second part (the exponent) is a stirring parameter. The ripple factor, wich indicates the influence of the form of the bottom roughness on the bed load transport, is expressed as

$$\mu = \left(\frac{C}{C_{90}} \right)^{1.5} \tag{2}$$

where C_{90} is the Chezy coefficient based on D_{90}, exceede 10% by weight. The combined shear stress at the bed (C) inducced by waves and current is (valid for a 90º angle between the waves and current),

$$\tau_{b,wc} = \tau_{b,c} \left[1 + \frac{1}{2} \left(\xi \frac{u_0}{V} \right)^2 \right] \tag{3}$$

in wich $\tau_{b,c}$ is the bed shear stress due to current only and u_0 the maximum wave orbital velocity near the bed. The coefficent ξ is given by

$$\xi = C \sqrt{\frac{f_w}{2g}} \tag{4}$$

in wich f_w is the wave friction factor (Jonsson, 1966).

The bedload is assumed to occur in a bottom layer having a thickness equal to the bottom roughness (r). The concentration of material in the bed load layer (c_b) is

$$c_b = \frac{q_{b,B}}{6.34\sqrt{\frac{\tau_{b,c}}{\rho}}r} \tag{5}$$

Over the thickness, c_b is assumed to be constant.

The concentration distribution is obtained from

$$c(z) = c_b\left[\frac{r}{h-r}\frac{h-z}{z}\right]^{\frac{w\sqrt{\rho}}{k\sqrt{\tau_{b,wc}}}} \tag{6}$$

where z is the elevation, h the water depth, w the sediment fall speed, and κ von Karman's constant. By integrating along the vertical from the reference hight to the water surface, the load suspended sediment load is determined as

$$q_{s,B} = 1.83q_{b,B}\left[I_1 \ln\left(\frac{33h}{r}\right) + I_2\right] \tag{7}$$

where I_1 and I_2 are the Einstein integrals for the suspended load:

$$I_1 = \int_{\delta}^{1}\left(\frac{1-y}{y}\right)^A dy \tag{8-a}$$

$$I_2 = \int_{\delta}^{1}\left(\frac{1-y}{y}\right)^A \ln y dy \tag{8-b}$$

where $A = W_S / \kappa(\tau_{cw}/\rho)^{0.5}$ is a function determining the rate of the suspension, κ=0.41 is the Von Karman constant, and W_S the settling velocity.

The total load is computed as the sum of bed load and suspended load:

$$q_{t,B} = q_{b,B} + q_{s,B} \qquad (9)$$

Comparision with field and experimental data

A study carried out by Camemen and Larroudé shows that the Bijker formula tends underestimate solid transport mainly for wave-current interaction. In this case the errors can be very important, reaching several orders of magnitude. The authors explain this by the fact that the Bijker formula takes into account waves only as an active term for suspension. Although the wave orbital velocity is high, if the steady current is very low, the net sediment transport will be very low. In cases with only waves the results are very scattered. In cases without waves the results are better but less good that the obtained with the other formulae. Furthermore, these results seems to be very sensitive to the metod used to compute the roughness: using skin friction results in serious under-estimation, particulary for the coarsest sediments.

In a study by Bayram, Larson, Miller and Kraus (2001) of comparision between predictive formulas and field mesurements the result of comparing the Bijker formula was that it systematically overestimated the trasnport rates for all conditions considered.

1.3 ENGELUND AND HANSEN FORMULA

The formula developed by Engelund and Hansen compute the bed load due to the current. Later the formula was modified to compute the total load. Also it was modified to compute the load due to wave stirring and not only due to current. However, their theory has limitations when applied to graded sediments containing large amount of fine fractions, causing predicted transport rates to be smaller than the actual trasnport rates. The same coefficient values are used for monochromatic and random waves. The final formula calculates the total load as

$$q_{t,EH} = V \frac{0.05\tau_{b,c}^2 \left[1 + \frac{1}{2}\left(\xi \frac{u_0}{V}\right)^2\right]^2}{(s-1)^2 d_{50} \rho^2 g^{5/2}} + A\left[\frac{(\tau_{b,w} - \tau_{b,cr})V}{\rho g}\right] \qquad (1)$$

The first part of the formula is the current term, wich computes the bed and suspended load due to the current. In this term the same coefficient value (=0.05) is apply for both monochromatic and random waves in the original formula. The second part, the wave term, is the Watanabe formula (1992) to compute the total load due to wave stirring. In this term the coefficient A is about 0.5 for monochromatic waves and 2.0 for random waves. $\tau_{b,cr}$ is the critical bed shear stress for incipient motion and is determined from the Shield curve for oscillatory flow.

Comparision with field data

The comparision of the Engelund and Hansen formula predictions with field data sets realized by Bayram, Larson, Miller and Kraus (2001) pointed out that this formula produces reasonable over the entire range of wave conditions investigated, but displaying significant scatter.

1.4 ACKERS AND WHITE FORMULA

As in the case of Engelund and Hansen, the formula proposed by Ackers and White (1973) initially predicted the total load transport under a current. Later it was amplied by Van De Graaff and Van Overeem (1979) to compute the wave load. The original Ackers-White formula was

$$q_{t,AW} = V \frac{1}{1-p} d_{35} \left(\frac{V}{V^*}\right)^n \frac{C_{d,gr}}{A^m} (F_C - A)^m \qquad (1)$$

where p is the porosity of the sediment, d_{35} the particle diameter exceeded by 65% of the weight, V^* the shear velocity due to the current, n, m, $C_{d,gr}$, and A dimensionless parameters and F_C a sediment mobility number. The dimensionless parameters are written as

$$n = 1 - 0.2342 \ln(d_{gr}) \tag{2}$$

$$m = \frac{9.66}{d_{gr}} + 1.34 \tag{3}$$

$$C_{d,gr} = \exp\left[2.86 \ln(d_{gr}) - 0.4343 (\ln d_{gr})^2 - 8.128\right] \tag{4}$$

$$A = \frac{0.23}{\sqrt{d_{gr}}} + 0.14 \tag{5}$$

where

$$d_{gr} = d_{35} \left(\frac{g(s-1)}{\upsilon^2} \right)^{1/3} \tag{6}$$

and υ is the kinematic viscosity. The sediment mobility number is defined as

$$F_C = \frac{V \left(\frac{V^*}{V} \right)^n C_d^n}{C_d g^{n/2} \sqrt{(s-1) d_{35}}} \tag{7}$$

where

$$C_d = 18 \log\left(\frac{10h}{d_{35}} \right) \tag{8}$$

The modified equation by Van De Graaff and Van Overeem (1979), which accounts the wave stirring, is written as

$$q_{t,AWM} = V \frac{1}{1-p} d_{35} \left(\frac{V'_{wc}}{V^*_{wc}} \right)^n \frac{C_{d,gr}}{A^m} \left[\frac{V'_{wc} \left(\frac{V^*_{wc}}{V'_{wc}} \right)^n C_d^n}{C_d g^{n/2} \sqrt{(s-1)d_{35}}} - A \right]^m \qquad (9)$$

where

$$V^*_{wc} = V^* \left[1 + \frac{1}{2} \left(\xi \frac{u_0}{V} \right)^2 \right]^{1/2} \qquad (10\text{-a})$$

and

$$V'_{wc} = V^* \left[1 + \frac{1}{2} \left(\xi' \frac{u_0}{V} \right)^2 \right]^{1/2} \qquad (10\text{-b})$$

In this formulation, ξ' is based on D_{35} and ξ on the bed roughness r.

Comparison with field data

In the comparison with field data sets by Bayram, Larson, Miller and Kraus (2001) the Ackers and White formula gave satisfactory results for all conditions considered, but scatter was marked both for swell and storm.

1.5 BAILARD AND INMAN FORMULA

Bailard and Inman (1981) extended the formula introduced by Bagnold to oscillatory flow in combination with a steady current over a plane sloping bottom. The instantaneous bed load ($q'_{b,BI}$) and suspended load ($q'_{s,BI}$) transport rate vectors are expressed as

$$q'_{b,BI} = \frac{0.5 f_w \rho e_b}{(\rho_s - \rho) g \tan\gamma} \left[\left| U'_t \right|^2 U'_t - \frac{\tan\beta}{\tan\gamma} \left| U'_t \right|^3 i\beta \right] \qquad (1)$$

$$q'_{s,BI} = \frac{0.5 f_w \rho e_s}{(\rho_s - \rho) g w} \left[\left| U'_t \right|^3 U'_t - \frac{e_s}{w} \tan\beta \left| U'_t \right|^5 i\beta \right] \qquad (2)$$

in which tanβ is the local bottom slope, tanγ a dynamic friction factor, U'_t the instantaneous velocity vector near the bed due to waves and current and $i\beta$ is a unit vector in the direction of the bed slope.

Assuming that a weak longshore current prevails, neglecting effects of the slope term on the total transport rate for near-normal incident waves, the local time-averaged LST rate is

$$q_{t,BI} = 0.5\rho f_w u_0^3 \frac{e_b}{(\rho_s - \rho) g \tan\gamma} \left(\frac{\delta_v}{2} + \delta_v^3 \right) + 0.5\rho f_w u_0^4 \frac{e_s}{(\rho_s - \rho) g w_s} \left(\delta_v u_3^* \right) \qquad (3)$$

where e_b and e_s are efficiency factors, and:

$$\delta_v = \frac{V}{u_0} \qquad (4)$$

$$u_3^* = \frac{\left\langle \left| U'_t \right|^3 \right\rangle}{u_0} \qquad (5)$$

The following coefficient values are typically used in calculations: e_b=0.1, e_b=0.02, tanγ=0.63. The efficiency factors are assumed to be constant, although work has indicated that e_b and e_s are related to the bed shear stress and the particle diameter.

Estimation of the friction coefficient f_{cw} and comparison with field and experimental data

Madsen and Grant defined a method to extract the frcition coefficient f_{cw} from the total shear stress τ_{cw}. Using these method good results are obtained in some cases, but a clear

overestimation has been observed in the case of wave-current interaction. In Fig. 1 is observed a good agreement with experimental data using the Madsen and Grant's method with the skin friction due to waves. As it has been explained, a slight scatter can be observed for wave-current interaction cases, as the *Jansen* data, in which there is an overestimation, and for the *Dibajnia* data, when the formula present an underestimation.

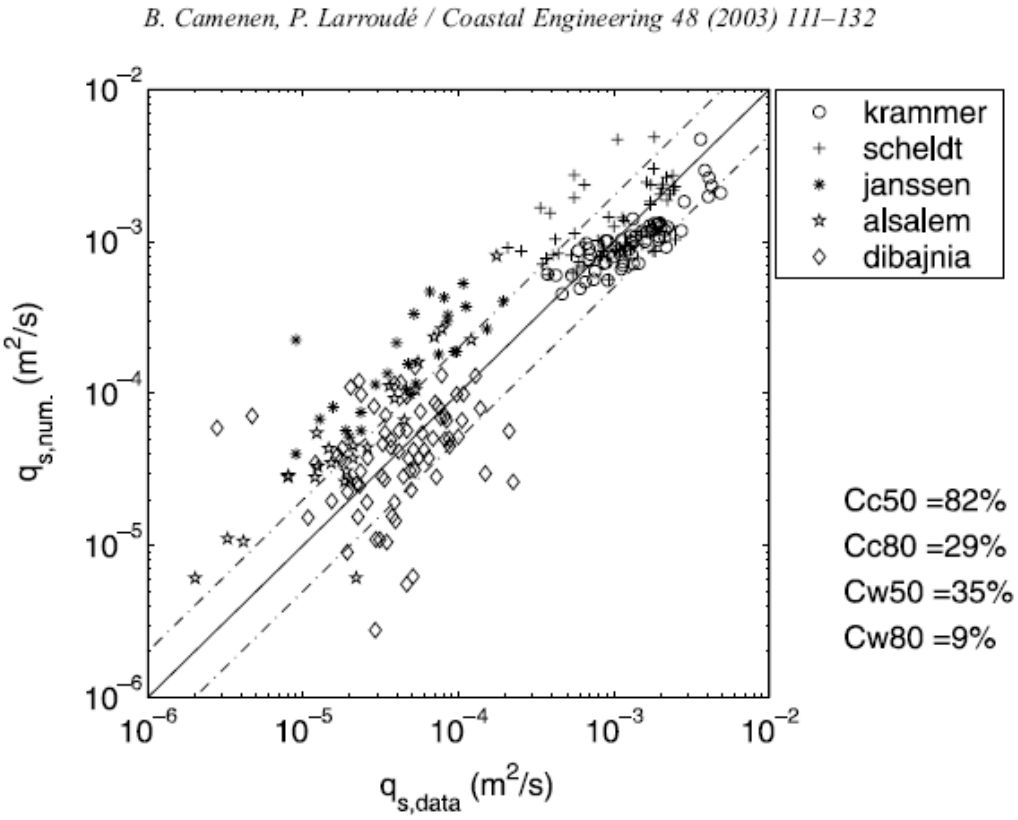

Fig. 1.1 Comparison between the Bailard formula and experimental data.

In the comparison by Bayram, Larson, Miller and Kraus the Bailard and Imman formula it overestimated the transport systematically during swell and underestimated during storm.

1.6 DIBAJNIA AND WATANABE FORMULA

Dibajnia and Watanabe (1992) developed a model similar to Bailard and Ribberink. This model breaks down the sediment transport into two half cycles due to the presence of

waves. During the first half-cycle, sediment moves in the direction of the wave, just as it moves in the opposite direction during the second half-cycle. The formula takes into account a possible quantity of sand still in suspension after each half-cycle, and hence moving in the other direction.

The solid volume flux is given by the following equation:

$$\vec{q}_S = A_{dw} W_S d \frac{\vec{\Gamma}}{\Gamma} \Gamma^{B_{dw}} \tag{1}$$

where A_{dw}=0.001 and B_{dw}=0.55: coefficients of calibration, and

$$\vec{\Gamma} = \frac{T_{wc}\vec{u}_{wc}\left(\Omega_c^3 + \Omega_c'^3\right) + T_{wt}\vec{u}_{wt}\left(\Omega_t^3 + \Omega_t'^3\right)}{\left(u_{wc} + u_{wt}\right)T_w} \tag{2}$$

where T_w, T_{wc}, T_{wt} are the period and half-periods of wave taking into account the effect of a current. Ω_c and Ω_t are the amount of sand entrained and settled during the half-period T_{wc} and T_{wt}, respectively. Ω_c' and Ω_t' are amount of suspended sand remaining from the positive and the negative half-cycle, respectively. u_{wc} and u_{wt} are quadratic velocity (wave + current) over each half-period expressed as

$$u_{wj}^2 = \frac{2}{T_{wj}} \int_t^{t+T_{wj}} u^2(t)dt + 2U_c^2 \sin^2\theta \tag{3}$$

where j can be c or t, $u(t) = U_c\cos\theta + u_w(t)$. $u_w(t)$ is the instantaneous wave orbital velocity. θ is the angle between wave direction and current direction.

If $\omega_j \leq \omega_{cr}$ then $\Omega_j = \omega_j \frac{2W_s T_{wj}}{d}$

and $\Omega'_j = 0$ (4-a)

If $\omega_j \geq \omega_{cr}$ then $\Omega_j = \frac{2W_s T_{wj}}{d}$

and $\Omega'_j = (\omega_j - 1)\frac{2W_s T_{wj}}{d}$ (4-b)

with:

$$\omega_j = \frac{u_{wj}^2}{2(s-1)gW_S T_{wj}} \quad (5)$$

where *j* can be *c* or *t*

ω_{cr} is a ripple parameter

$$\omega_{cr} = 0.03 \quad \text{if } \Psi_{cw(max)} \leq 0.2$$

$$= 1 - 0.97\left(1 - \left(\frac{\Psi_{cw(max)} - 0.2}{0.4}\right)^2\right)^{0.5} \quad \text{if } 0.2 < \Psi_{cw(max)} < 0.6$$

$$= 1 \quad \text{if } 0.6 < \Psi_{cw(max)} \quad (6)$$

where $\Psi_{cw(max)}$ is the maximum Shields parameter due to wave-current interaction, computed following method of Soulsby.

Comparison with field and experimental data

Studied by Camemen and Larroudé, Dibajnia and Watanabe formula gives good results for most of the cases studied. However, a slight underestimation can be observed in Fig. 2 for the *Scheldt* and *Krammer* data, and a slight overestimation for the *Janssen* and *Alsalem* data. Nevertheless, the results remain less scattered than with some of the other formulae.

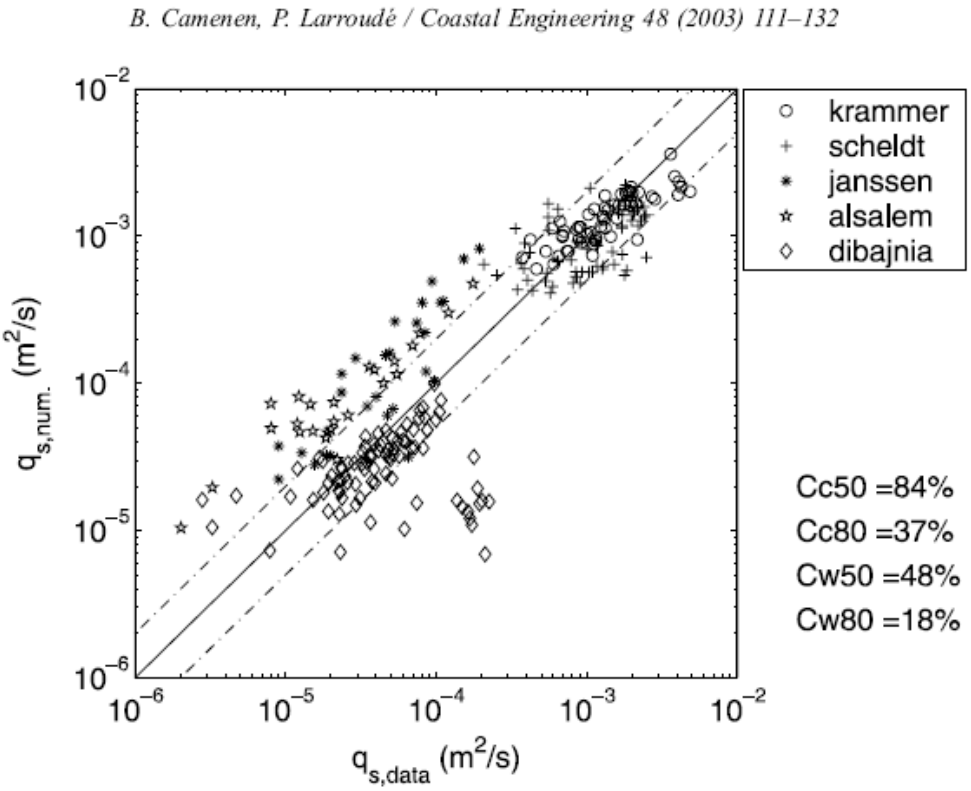

Fig. 1.2. Comparison between the Dibajnia and Watanabe formula and experimental data.

Dibajnia and Watanabe formula yielded the best predictions for storm conditions in the comparison by Bayram, Larson, Miller and Kraus but markedly overestimated the transport rates for swell waves.

1.7 RIBBERINK FORMULA

The model proposed by Ribberink is a quasy-steady model of bed load transport where the instantaneous flux is assumed to be proportional to a function of the difference between the actual time-dependent bed shear stress. This formulation has been calibrated towards several flume data sets including wave-current interaction in a plane regime, considering the suspended load negligible. It accounts field data obtained from unidirectional flows in rivers.

The expression for the sand transport is the following:

$$\overrightarrow{q_{sb}} = m_{Rib}\sqrt{(s-1)gd^3}\left\langle\left(\left|\overrightarrow{\Psi(t)}\right| - \Psi_{cr}\right)^{n_{Rib}}\frac{\overrightarrow{\Psi(t)}}{\left|\Psi(t)\right|}\right\rangle \qquad (1)$$

where $\overrightarrow{\Psi(t)} = 0.5 f_{cw}|u(t)|\overrightarrow{u(t)}/[(s-1)gd]$ is the time dependent Shields parameter with the instantaneous velocity $\overrightarrow{u(t)} = \overrightarrow{U_c} + \overrightarrow{u_w(t)}$ and the wave-current friction factor f_{cw} computed according to the Madsen and Grant's method. Ψ_{cr} is the critical Shields parameter. $\langle\ \rangle$ means time-averaged over several periods and m_{Rib} and n_{Rib} are adjusted coefficients.

As in the Bailard formula, an equivalent wave-current friction coefficient has to be computed. Ribberink proposed to use the Madsen and Grant's method. He also proposed to compute the total roughness as

$$k_{st} = \max\left(k_s; d\left[1 + 6\left(\left\langle\left|\Psi(t)\right|\right\rangle/\Psi_{cr} - 1\right)\right]\right) \qquad (2)$$

where k_s is skin roughness high.

Comparison with field and experimental data

The Riberink formula has given good results in case of wave-current interaction, but significantly underestimates the sediment transport in the cases with strong currents, and thus with high suspended load (Camemen and Larroudé, 2001). This can be due to the fact that this formula was adjusted only for cases with bed and sheet flow, and without significant suspension load.

The wave-current friction coefficient is difficult to estimate, as occurs in the Bailard formula.

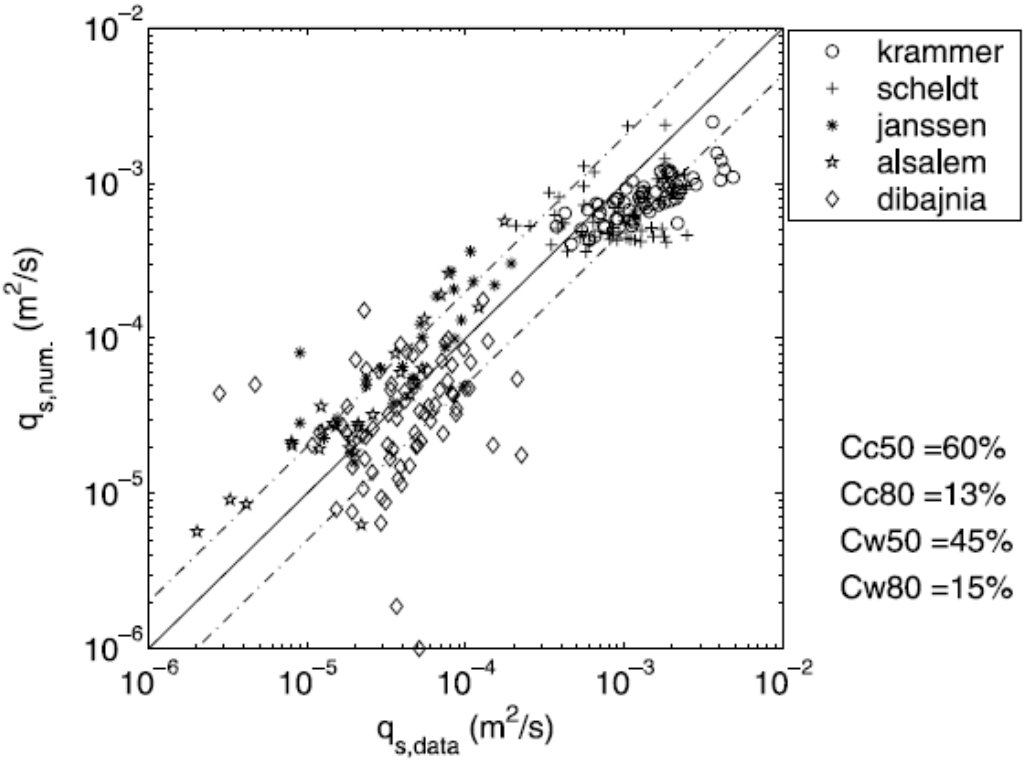

Fig.1.3. Comparison between the Ribberink formula and experimental data.

1.8 KAMPHUIS FORMULA

J. William Kamphuis developed a longshore sediment transport formula (1991) based on physical model texts. Here are shown the steps for obtaining the expression and the results of comparing it with the field data.

Sediment transport rate may be expressed as

$$Q_S = f(H, T, d, \mu, g, x, y, t, \rho_s, D) \quad (1)$$

where Q_S is sediment transport rate, H and T are wave height and period; d, ρ and μ are the depth, density and dynamic viscosity of the water, g is the acceleration due to gravity; x, y and z are directions, t is the time; ρ_s and D are the sediment density and diameter. If Q_S is defined in kg/sec Eq. 1 may be reduced to a dimensionless version:

$$\frac{Q_S}{\rho_S H^3/T} = \Phi\left(\frac{d}{H}, \frac{\rho}{\rho_S}, \frac{\mu/\rho_S}{H^2/T}, \frac{gT^2}{H}, \frac{x}{H}, \frac{y}{H}, \frac{z}{H}, \frac{t}{T}, \frac{D}{H}\right) \quad (2)$$

For doing the dimensionless parameters to be more useful, the terms of Eq. 2 are combined as

$$\frac{Q_S}{\rho_S H^3/T} = \Phi\left(\frac{d}{H}, \frac{\rho}{\rho_S}, \left\{\frac{H^2/T}{\mu/\rho_S}\sqrt{\frac{gT^2}{H}\frac{\rho}{\rho_S}}\right\}, \frac{2\pi H}{gT^2}, \left\{\frac{H}{x}, \frac{z}{H}\right\}, \left\{\frac{y}{H}\frac{H}{x}\right\}, \frac{z}{H}, \frac{t}{T_P}, \frac{H}{D}\right) \quad (3)$$

Because alongshore sediment transport takes place in the breaking zone and is related to wave breaking, the significant breaking wave height $H_{s,b}$ is used as determining parameter. T_P is used to define the wave period and Eq. reduces to

$$\frac{Q_S}{\rho_S H^3/T} = \Phi\left(\frac{H_{s,b}}{d_b}, \frac{\rho_S}{\rho}, \frac{H_{S,b}\sqrt{gH_{S,b}}}{\mu/\rho}, \frac{H_{S,b}}{L_{O,p}}, m_b, \alpha_b \frac{z}{H_{S,b}}, \frac{t}{T_P}, \frac{H_{S,b}}{D_{50}}\right) \quad (4)$$

Equation 4 states that the dimensionless sediment transport rate is a function of breaker index; relative density of the sediment, a breaking wave Reynolds Number, wave steepness, beach slope, wave angle, vertical distance in terms of wave height, time as number of waves, and ratio of (wave height)/(grain diameter). Some ratios can be removed from the analysis, without loss of generality. The breaker index ($H_{s,b}/d_b$) is determined by the breaking process itself and is therefore not a free parameter. Only transport of sand, gravel, cobble, etc is considered and hence the density ratio will be relatively constant. The breaking process is turbulent, which makes the dependence on breaking Reynolds Number small. Since Q_s is an integrated value over the vertical, the $z/H_{s,b}$ term becomes irrelevant. Similarly, since Q_s is an averaged value over many wave periods, t/T_p is irrelevant. Finally, existing wave and transport theory indicates that the dependence on wave angle can be related to ($\sin 2\langle_b$). This results in

$$\frac{Q_S}{\rho_S H^3/T} = K \cdot \left(\frac{H_{S,b}}{L_{o,p}}\right)^p \cdot m_b^q \cdot \left(\frac{H_{S,b}}{D_{50}}\right)^r \cdot \sin^s(2\alpha_b) \quad (5)$$

Known field data were represented (Kamphuis et al., 1986) and the exponent and constant were then derived from the model tests, resulting in K=7.9x10^4, p=-1.25, q=0.75, r=0.25 and s=0.6

$$\frac{Q_S}{(\rho_S-\rho)H^3/T} = 7.9\text{x}10^{-4}\cdot\left(\frac{H_{S,b}}{L_{o,p}}\right)^{-1.25}\cdot m_b^{0.75}\cdot\left(\frac{H_{S,b}}{D_{50}}\right)^{0.25}\cdot\sin^{0.6}(2\alpha_b) \qquad (7)$$

Analysis of the model results:

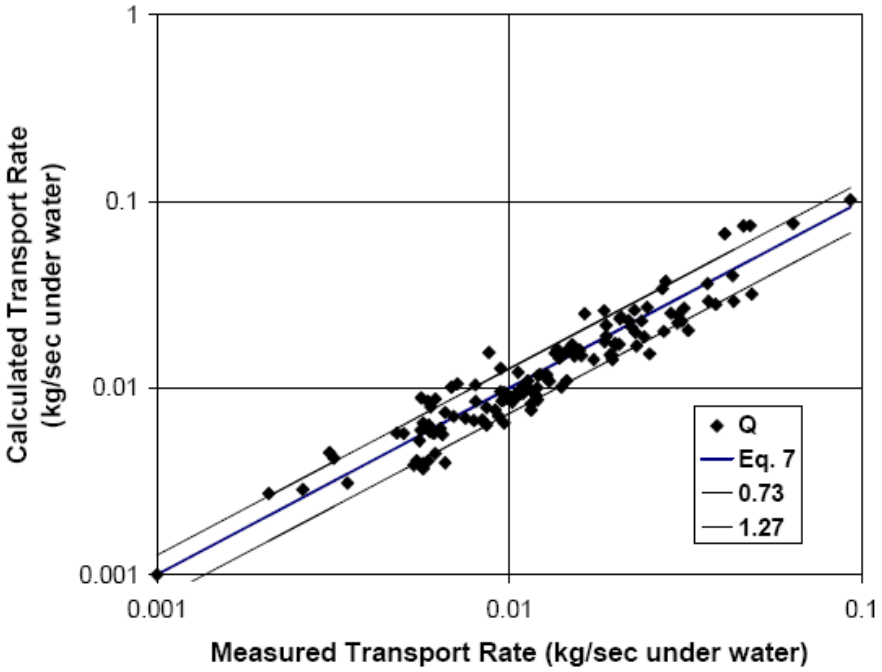

Fig. 1.4. Predicted transport rate versus measured transport rate. Alongshore Transport of Sand (Kamphuis, 2002).

Eq. 7 may be simplified to

$$Q_u = 7.9x10^{-4}(\rho_s-\rho)\left(\frac{g}{2\pi}\right)^{1.25} H_{S,b}^2 T_p^{1.5} m_b^{0.75} D_{50}^{-0.25}\sin^{0.6}(2\alpha_b) \qquad (8)$$

or

$$Q_u = 2.27\, H_{S,b}^2 T_p^{1.5} m_b^{0.75} D_{50}^{-0.25}\sin^{0.6}(2\alpha_b) \qquad \textit{kg/s (underwater mass)} \qquad (9)$$

The "breaking slope", m_b in these expressions is the slope that *causes* the breaking, hence the slope over one or two wave lengths offshore of the breaker. The coefficient and exponents of Eq. 7 were obtained by minimizing $S_{y/x}$, where

$$S_{y/x} = \sqrt{\frac{\Sigma(\log Q_{u,calc} - \log Q_{u,meas})^2}{n-2}} \qquad (10)$$

and n is the number of experimental points. It is found that 68% of the data lie within one standard deviation, between $1 \pm \sigma$.

Among the data from field analysis and from the model was observed there was a scale difference. That indicates there was a little scale effect in the model tests.

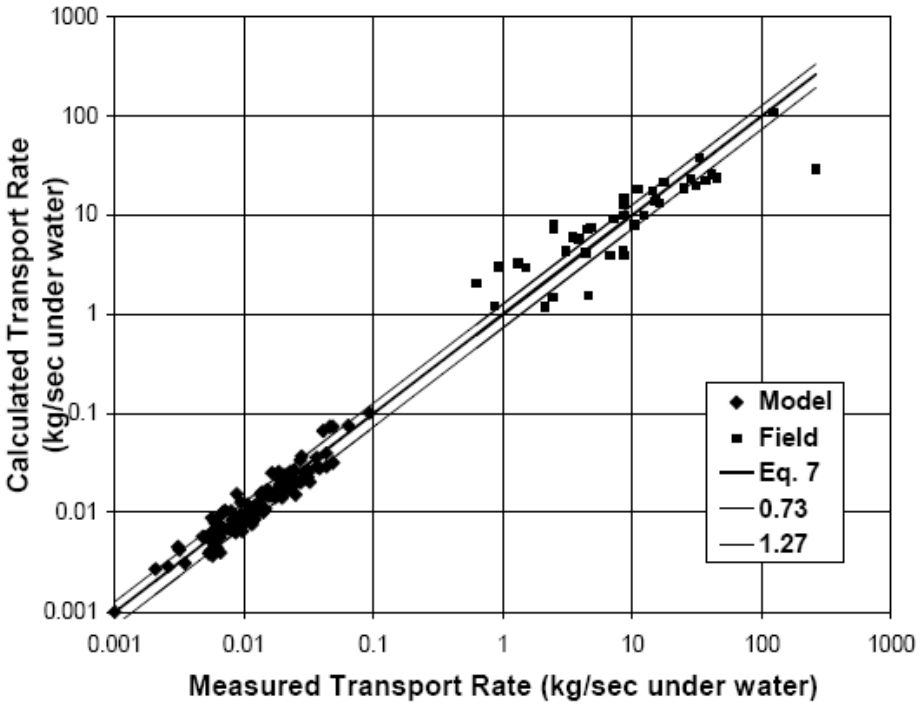

Fig. 1.5. Predicted transport rate versus measured transport rate. Alongshore Transport of Sand (Kamphuis, 2002).

However, field and model data should both be used, as although field data can seem more real they alone are less certain.

Other equations

It is more practical to work using the unit of transport volume than using underwater sediment transport rate . So the equations 7 to 9 can be translate to be used with the new unit. For kg/s (dry mass), the relevant equations are:

$$\frac{Q_S}{\rho_S H^3/T} = 7.9\text{x}10^{-4} \cdot \left(\frac{H_{S,b}}{L_{o,p}}\right)^{-1.25} \cdot m_b^{0.75} \cdot \left(\frac{H_{S,b}}{D_{50}}\right)^{0.25} \cdot \sin^{0.6}(2\alpha_b) \qquad (11)$$

$$Q_u = 3.65\, H_{S,b}^2 T_p^{1.5} m_b^{0.75} D_{50}^{-0.25} \sin^{0.6}(2\alpha_b) \qquad \textit{kg/s (dry mass)} \qquad (12)$$

For sediment transport volume, the equations are:

$$\frac{Q_v}{H_{s,b}^3/T_p} = 7.9\text{x}10^{-4} \cdot \left(\frac{H_{S,b}}{L_{o,p}}\right)^{-1.25} \cdot m_b^{0.75} \cdot \left(\frac{H_{S,b}}{D_{50}}\right)^{0.25} \cdot \sin^{0.6}(2\alpha_b) \qquad (13)$$

For sand porosity of 0.32 and for units in m_3/hr

$$Q_v = 7.9\text{x}10^{-4} \cdot \left(\frac{3600}{(1-0.32)}\right)\left(\frac{g}{2\pi}\right)^{-1.25} \cdot H_{s,b}^2 T_p^{1.5} m_b^{0.75} \cdot D_{50}^{-0.25} \cdot \sin^{0.6}(2\alpha_b) \qquad (14)$$

$$Q_v = 7.3\, H_{S,b}^2 T_p^{1.5} m_b^{0.75} D_{50}^{-0.25} \sin^{0.6}(2\alpha_b) \qquad m^3/hr \qquad (15)$$

Comparison with field data

Field results with single wave condition

The data for this comparison were taken from original sources and as quoted and reduced by Van Rijn (2001). These are a set from Lake Michigan (Lee, 1975), Indian Rocks beach in Florida (Wang and Kraus, 1999), the field facility of the US Army Corps of Engineers at Duck, North Carolina (Miller, 1999) and the experiments of Balouin et al (2002) at the

Barra Nova inlet on the Algarve Coast of Portugal. The new data cover a whole range from very approximate to very detailed measurement.

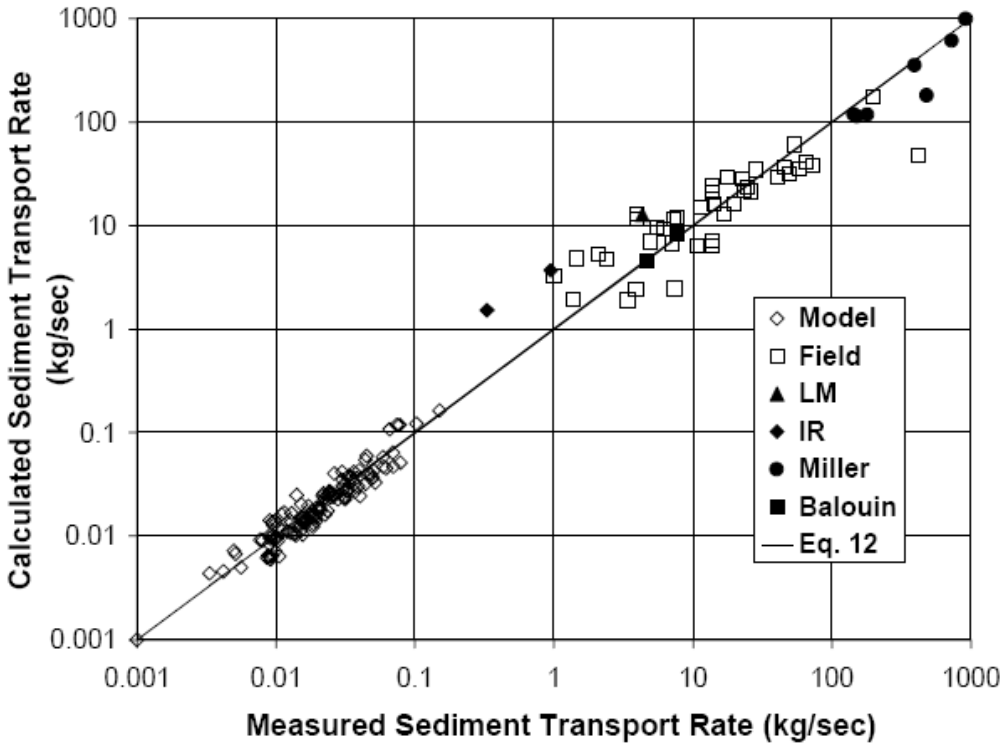

Fig. 1.6. Kamphuis. Field results for single wave conditions. Source: Alongshore Transport of Sand (Kamphuis, 2002).

Figure 6 indicates that the equation predicts the sediment transport well. The data which presents most difference with predicted results are Lake Michigan and Indian Rocks. These are the earliest data and according to Kamphuis the overestimation by a factor 3 to 5 can be possibly as a result of few exactly measurement of the transport or the wave conditions. Nevertheless, two of the Miller (new data) points are overestimated by a factor of 2 to 2.5.

Field results with a wave climate

The comparisons made with wave climate show that field measurements with detailed wave climate are difficult to use for improving basic sediment transport equations. In the case of predominantly bi-directional transport, the morphological changes are related to the net transport, a small value obtained by subtraction of many large values. The many parameters, such as sediment transport rate obtained from air photo interpretation, and

representative beach slope and grain size contain much subjectivity and the time dependency of the parameters present additional difficulty.

1.9 VAN RIJN FORMULA

A detailed process based model (CROSMOR2000) was developed by Leo C. van Rijn (2000) to be used in computing the longshore sand transport distribution along the crossshore bed profile. After testing this model using the available field data sets it was applied to study the effects on the longshore transport process of particle size, wave period and profile shape. Hence, the main overall result the study was a general expression for longshore transport of sand and gravel/shingle, including the effects of profile slope and tidal velocity. To obtain it are used combining the results of the model and the field data.

Schoonees and Theron (1993) have made an extensive inventory of the available data sets of longshore sand transport rates, but most of these data sets refer to mild wave conditions and not for storm conditions.

CROSMOR2000model

It computes a cross-shore distribution of wave height, longshore velocity and longshore sand transport (Van Rijn, 2000). The CROSMOR 2000 model comprises three submodules: hydrodynamics (waves, currents), sand transport, and bed level evolution (morphology).

Analysis of field data

The data sets has been selected for testing and come from several beaches in United States. Among them there are the data from Duck, obtained by the USACE in minor to major storm conditions (Miller, 1999).

The measured total longshore sand transport rates can be plotted as function of the parameter $W= (H_{s,b})^3 \sin(2\theta_b)$ and the trend line can be represented by

$$Q_t = 40\ (H_{s,b})^3 \sin(2\theta_b) \qquad (1)$$

with: Q_t = longshore sand transport (in kg/s; dry mass); $H_{s,b}$ = significant wave height at breaker line (in m); θ_b = wave incidence angle (to shore normal) at breaker line (degrees). Equation (7) is valid for sand in the range of 0.15 to 0.5 mm and beach slopes in the range of 0.02 to 0.1.

Development of new equation for longshore sand transport

The simplified formula for the longshore sand transport (incl. all effects) reads as:

$$Q_t = K_0\ K_{swell}\ K_{grain}\ K_{slope}\ (H_{s,b})^{2.5}\ V_{eff,L} \qquad (2)$$

with:

Q_t = longshore sand transport (in kg/s, dry mass);

$H_{s,b}$ = significant wave height at breaker line (m);

$V_{eff,L} = [(V_{wave,L})^2 + (V_{tide,L})^2]^{0.5}$ = effective longshore velocity at mid surf zone (m/s) for tidal velocity and wave-induced velocity in same direction (minus sign for opposing conditions);

$V_{wave,\,L} = 0.3(gH_{s,b})^{0.5}\sin(2\theta_b)$ = wave induced longshore velocity in mid surf zone (incl. wind effect);

$V_{tide,L}$ = longshore velocity in mid surf zone due to tidal forcing (=0 m/s for non tidal cases; 0.1 m/s for microtidal, 0.3 m/s for mesotidal and 0.5 m/s for macrotidal cases);

θ_b = wave incidence angle at the breaker line (to shore normal; in degrees);

Ko = 42;

K_{swell} =T_{swell}/T_{ref} = swell correction factor for swell waves (<2 m);
with T_{ref} = reference wave period = 6 s ; K_{swell} =1 for wind waves;

K_{grain} = ($d_{50,ref}/d_{50}$) = particle size correction factor ($d_{50,ref}$ = 0.2 mm), with $K_{grain,min}$ = 0.1 for d_{50} >2 mm;

K_{slope} = $(\tan\beta/\tan\beta_{ref})^{0.5}$ = bed slope correction factor ($K_{slope,max}$ =1.25, $K_{slope,min}$ = 0.75);
tanβ =actual bed slope, $\tan\beta_{ref}$ = 0.01 (reference slope of Egmond profile).

Determination of K coefficients and validity ranges

To determine the correction factors (K) accounting for the effect of basic parameters, the following parameters have been considered:

- wave period of swell waves;
- particle size: the sediment particle size has been varied in the range of 0.15 mm to 10 mm for one wave condition (offshore wave incidence angle of 30 degrees and offshore wave height of 3 m);
- additional wind-induced and tide-induced longshore velocity at seaward boundary for various offshore wave conditions;
- profile shape, using profiles from three barred sites (Duck, USA; Egmond and Noordwijk, Netherlands) for various offshore wave conditions.

Effect of grain size

An analysis of the model for several particle sizes was carried out to determine K_{grain}.
The particle size correction factor K_{grain} has been set to a constant value of 0.1 for particle sizes larger than 2 mm. For smaller particles sizes is found that for a change from 0.2 to 0.4 mm the longshore sediment transport decreases by a factor of 2 to 3. The
decrease in LST is largest (factor 3) for the larger waves (Hs,o>3m). The LST decreases strongly for particle sizes in the range between 0.15 and 10 mm. For coarse materials the bed-load transport is dominant and not much dependent on particle diameter, which can be seen from existing bed-load transport formulae. For gravels may be realistic a constant K_{grain} for the gravel and shingle range (2 to 50mm), but is not realistic for larger sizes.

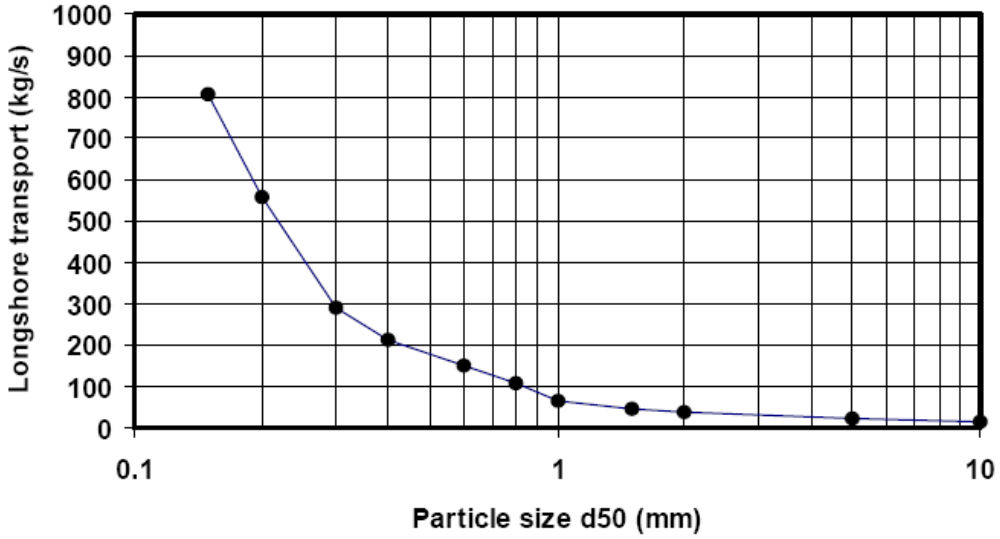

Fig. 1. 7 Effect of particle size on longshore sediment transport (based on CROSSMORE2000 results).

Equation (10) is valid for sand beaches and gravel/shingle beaches.

Conclusions of the analysis by Van Rijn

Analysis of the field data

The knowledge of the characteristics of the field data sets used to compare with the results obtained with the Van Rijn formula will be useful to know in which cases can be assured good results using this formula.

- Range of the available field data sets: from about 0.1 to 1000 kg/s or 5.4 to 54000 m^3/day. The bulk density is about 1600 kg/m^3.

- Relationship between transport (kg/s), wave height and wave incidence angle suggested by the field data: $Q_{t,mass} = 40(H_{s,br})^3 \sin(2\theta_{br})$.

- Between transport, particle size and beach slope the field data sets do not show any systematic relationship.

- Longshore velocities range: 0.5 to 1 m/s (minor storms) and 1 to 1.5 m/s (storms).

Parameterization results

Following is shown the influence of each parameter observed in the LST. Using this information it will possible to define the determination of which parameters has most importance.

- Range of variation of the LST of 0.2 mm along a barred profile: 5 to 5000 kg/s or 300 to 300 000 m^3/day for wave heights between 1 and 5 m and wave incidence angles between 10º and 70º at depth of 15 m.

- Variation of the LST with the wave period: An increase or decrease of the wave period of about 10% to 20% at the same wave height does not produce a variation of the current velocity, but the longshore sand transport sand transport becomes almost twice as large for long period swell waves. A correction factor can be used to represent this effect.

- Variation of the LST with the particle size: For particle sizes smaller than about 0.3 mm the LST increases significantly. That occurs due to dominance of the suspended load. The LST for shingle and gravel roughly is a factor 10 smaller than that for the sand for the same wave conditions.

- Effect of additional longshore velocity: It is largest for a small wave incidence angle. The effect of the additional longshore velocity is less important for offshore wave angles larger than 20º, particularly for storm conditions when wave-induced forcing is dominant.

- Influence of the profile shape: A relatively steep profile leads to somewhat larger wave heights at the breaker line and somewhat larger longshore current velocities and transport rates in the surf zone. A relatively flat profile leads to smaller wave heights at the breaker line and smaller current velocities and transport rates in the surf zone.

Comparison with field data by Bayram, Larson, Miller and Kraus

The Van Rijn formula gave the most reliable predictions over the entire range of wave conditions (swell and storm) studied, based on criteria involving the scatter, trend and clustering of the predictions around the measurements.

1.10 EXPLANATION OF THE GRAPHS 1, 2 AND 3

The type of the data comprised by Camemen and Larroudé are the following:

- Strong currents without waves: *Scheldt* and *Krammer*
- Laboratory data in an oscillating flume according to:
    - Al Salem (1993), Ribberink and Al Salem (1994): *Al Salem*
    - Dohmen-Janssen (1999): *Janssen*
    - Dibajnia and Watanabe (1992): *Dibajnia*

It is often considered that the estimation of sediment flux is acceptable when it is between 0.5 and 2 times the experimental data. Therefore, in the graphs, the curves $q_{s(num)} = q_{s(data)}$ (solid line) and $q_{s(num)} =$ 0.5 or 2 $q_{s(data)}$ (dashed lines) are given. For each comparison with the data, the percentage of points with less than 50% error and less than 20% error is also computed for "current only" data and "wave-current" data (i.e., Cc50, Cc80, Cw50, Cw80, respectively). In case of negative data (current direction opposite to wave direction), the absolute value is presented on the graph only if the formula predict the correctly induced direction of the sediment transport. If the direction of transport is predicted incorrectly, an error up to 100% is considered.

Chapter 2

Characterization of the coastal parameters for sediment transport in the Catalan coast

2.1 WAVES

The quantity of sediment moved in a period of time depends on the height, period and direction (angle of incidence) of the waves that have been crashing against the beach during this period. The available data referred to wave characteristics come from historical series collected by six buoys situated along the Catalan coast. A zonification of the wave climate in the Catalan coast was made and is shown in figure 2.1. According to this zonification, each stretch of the coast can be considered to be exposed to the wave climate defined from the data collected by a specific buoy. That buoy can be in general the closest, but not necessarily, so an studied definition of something like an "area of influence" for each buoy was required. Therefore in each point where LST has been calculated, it has been assigned the wave climate provided by the buoy in its zone the point comes. On the list of points and its characteristics appears the historical series of waves (numbered these series from 1 to 6) used to calculate the LST in the point.

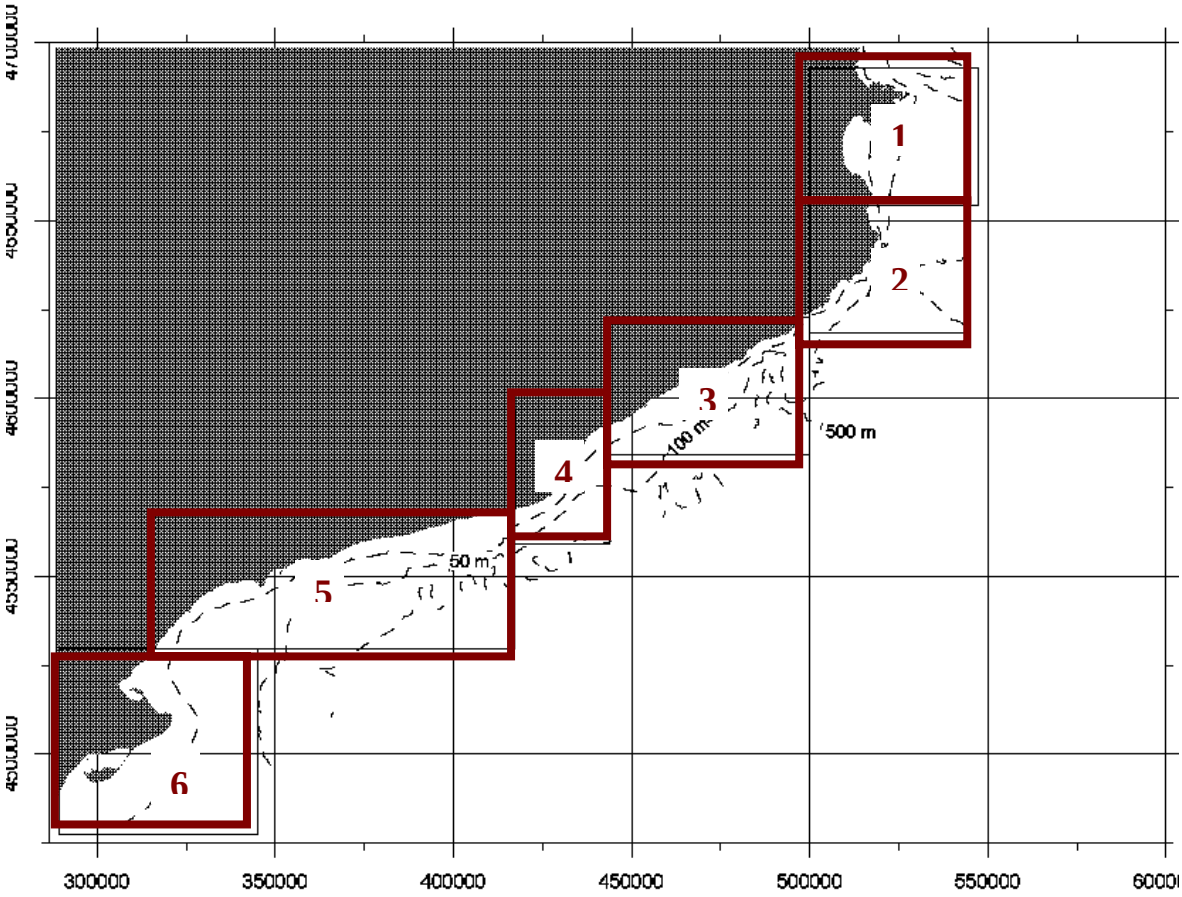

Figure 2.1: Assignation of coastal zones to a wave climate provided by a buoy.

Each series of wave data contains the following variables ordered in consecutive columns:

- Definition of the moment in which data was recorded: year/month/day/hour
- Wave significant height – Hs (cm).
- Period (sec).
- Direction – angle to the north (deg).

These series are a required input for the program used to calculate the LST by using CERC and Khampuis formulas. Each measurement of the series that has been taken during a period of time has an Hs, a significant period and a direction. These values, adding to sediment parameters, can be introduced in the formula used to calculate LST, either CERC

or Khampuis. The result is a quantity of sediment moved per unit of time (seconds). Therefore, it must be multiplied by the average time (seconds) that this conditions appear in a year. Then, all the quantities moved by each combination of wave conditions during its total time of appearing per year can be added up. Now the result is the total movement of sediment per year.

Issues related to the treatment of wave data:
- Measured in deep water. The program is able to propagate the characteristics of the waves to shallow water.
- Gamma Index for wave breaking considered: 0.65.

2.2 SEDIMENT CHARACTERISTICS

The fundamental characteristic of the sediment in terms of evaluating the LST is the grain size, which determines the weight of each grain and hence its resistance to be moved by the water in movement and its faster or slower fall to the bottom once it is raised from there. The most usual is to consider the medium grain diameter of the sediment, D_{50}. Data of that variable has been obtained from many points along the beaches of the Catalan coast, and it has been used to assign a grain diameter to each stretch in which the coast line has been divided. On the maps of the coast are shown the points where measurements of D_{50} has been carried out and are available to be used in this research.

In some cases these measurements has been taken in several points distributed in a defined zone of a beach. The sediment of these zones has been studied for some purpose in the past, and its area of study doesn't use to be very extensive. Indeed, is always much smaller than the length of the stretch it belongs to (in the next section is carefully explained the process to determine the stretches with constant characteristics assigned). Therefore, is sufficiently precise to obtain an average value of the measures of D_{50} for each stretch.

2.2 MORPHOLOGY

2.2.1 Coast orientation

The line of the coast is in general irregular and its orientation to the north is impossible to define exactly, as it is very variable and only very short stretches of the coast have a constant orientation. The angle between the waves and the shoreline is a fundamental variable to estimate the LST, as it depends hardly on the angle of incidence of the wave.

In order to determinate the orientation of each stretch of coast an approximation of the Catalan coast by long straight sections has been made. This sections are considered entirely beach or non beach. In the sections which are considered to be beach it will be supposed that exists sediment transport capacity and not in which are considered to not be beach. Each straight section has an orientation that is considered to be the orientation of this stretch of beach in all their points. Following are shown several maps on which appears the entire Catalan coast with the stretches defined as beach and non beach. From these pictures is obtained the orientation of each stretch by measuring its angle to the north. The straight sections have been drawn seeking an approximation to the real line of the coast sufficiently similar.

The Catalan coast follows approximately the direction North East – South West, being exposed to the winds coming from East and South. In fact, the predominant winds are those with East direction. Along the line of the coast there are not important bays or gulfs, apart from the Gulf of Roses, despite it is not very closed and the shoreline inside the gulf is almost an straight line with South-North direction closed by two capes in its ends. The rest of the coast is formed by zones with small and large coves (mainly in the north part, known as Costa Brava) alternating with zones of long and straight beaches. We can find these mainly along the central part of the coast of Catalonia and the south part, known as Costa Daurada.

Although in general the orientations of the shoreline are variable, we can find its major part between the North-South direction (0º) and the West-East direction (90º).

2.2.2 Beach profile – slope

As it has been difficult to obtain data on beach slopes along the Catalan coast, it has been considered estimated medium beach slopes profiles according to the models which relate grain size with the beach profile. A theoretical beach profile has been assigned to each point of the coast that corresponds with the grain size in the point.

Equilibrium profile

A simple approximation to the equilibrium beach profile has been considered. It consist in estimate a medium slope according to the characteristics of the sediment and the degree of exposition of the beach. This approximation is done, in general, from empirical diagrams, as Wiegel's (1964), where is given the expected slope for the beach as function of the medium diameter of exposed, moderately protected, and protected beaches to wave action. The diagram by Wiegel has been used to determinate the beach slope in the points of the Catalan coast where the grain size is known for this study. Each beach has been considered to be exposed, moderately protected or protected.

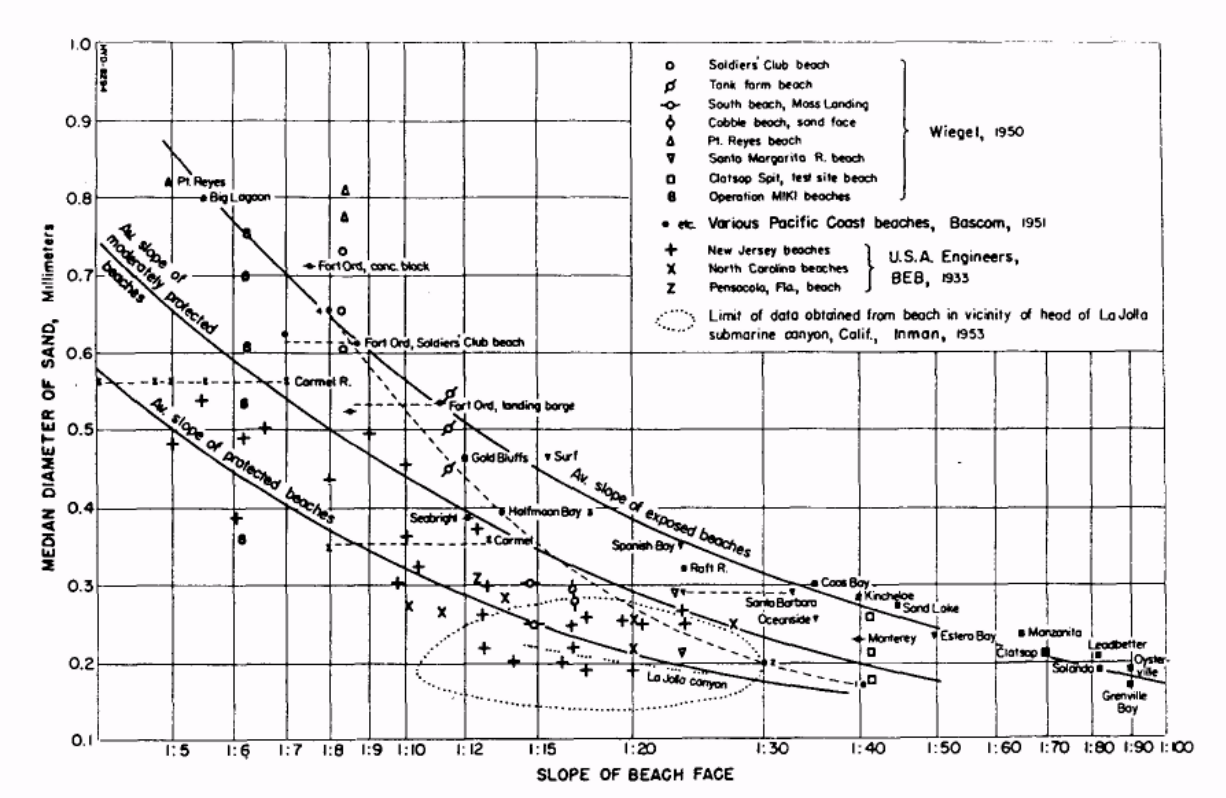

Figure 2.2Wiegel Diagram. Equilibrium slopes for various grain sizes and degree of exposition.

Similar research for the beach slope in function of the sediment and wave characteristics has been carried out by Dalrymple and Thompson (1976), Sunamura (1984), Kriebel et al (1991) and Jiménez and Sánchez-Arcilla (1992), among others.

The points in which slope was unknown are the following. Estimation using Wiegel's diagram is shown:

	Diameter (mm)	**Degree of exposition** P = Protected MP = Moderately protected E = Exposed	**Slope (Wiegel)**	
Girona				
La Rovina (Nord):	0,26	MP	1:25	0,04
La Rovina (Centre):	0,25	MP	1:25	0,04
Ca'n Comes:	0,34	MP	1:15	0,07
Sant Pere Pescador:	0,33	E	1:25	0,04
Sant Martí d'Empúries:	0,33	MP	1:16	0,06
L'Estartit (Nord):	0,29	MP	1:20	0,05
L'Estartit (Centre):	0,29	MP	1:20	0,05
Pals:	0,51	MP	1:08	0,13
Cala La Fosca	0,29	P	1:12	0,08
Palamós:	1,05	P	1:06	0,17
Sant Antoni de Calonge:	0,88	MP		
Platja d'Aro (Centre):	1,76	E		
Platja d'Aro (Sud):	0,80	E		
S'Agaró	0,27	MP	1:24	0,04
Sant Pol (Nord):	0,38	P	1:08	0,13
Sant Pol (Sud):	0,36	P	1:08	0,13
Lloret:	1,46	P		
Lloret (Sud):	1,99	P		
Santa Cristina	0,81			
S'Abanell (Nord):	1,19	P		
S'Abanell (Centre):	1,67	P		
Tordera:	0,55	E	1:11	0,09
Barcelona				
Mataró	0,50	E	1:12	0,08
El Masnou	1,12			
Castelldefels	0,18	E	1:90	0,01

Tarragona				
Creixell	0,15	E	1:100	0,01
Cambrils	0,15	MP	1:60	0,02
Barra del Trabucador	0,20	E	1:75	0,01

Table 2.1 Slope of beaches obtain using Wiegel Diagram

The values of slopes that are not on this table are known from bathymetry.

2.2.3 Mapping of the coast line of Catalunya

The following series of maps comprise the entire coast of Catalunya. In each map are identified the points where measures of the sediment characteristics are available and the name of the beach which the point belongs to. The lines drawn on the maps represent the simplification of the coast line for estimation of the LST purpose. The stretches in white are which are considered to be beach and therefore to have transport capacity. The stretches in dark green are considered to don't be beach.

Figure 2.3 Representation of the Catalan coast. Map numbers.

1. Portbou - Begur

Figure 2.4 Map of stretch Portbou - Begur.

2. Begur – Palamós

Figure 2.5 Map of stretch Begur - Palamós.

3. Palamós – Pola-Giverola

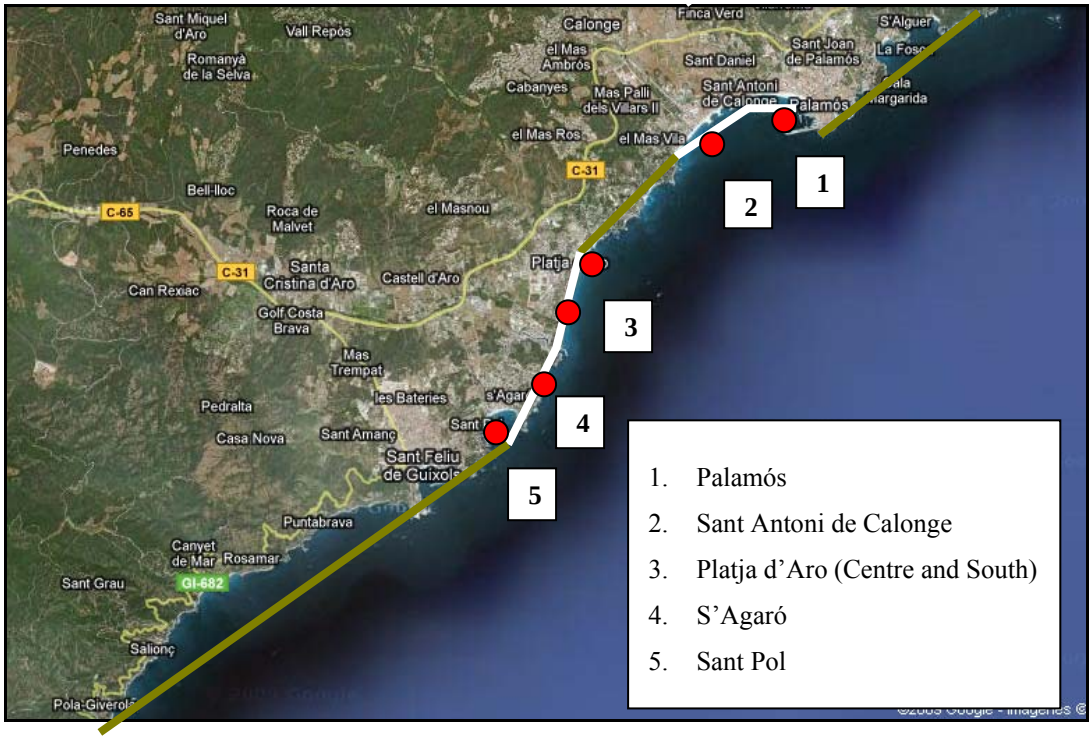

Figure 2.6 Map of stretch Palamós – Pola-Giverola.

4. Pola-Giverola - Tordera

Figure 2.7 Map of stretch Pola-Giverola – La Tordera.

5. Tordera – Mataró

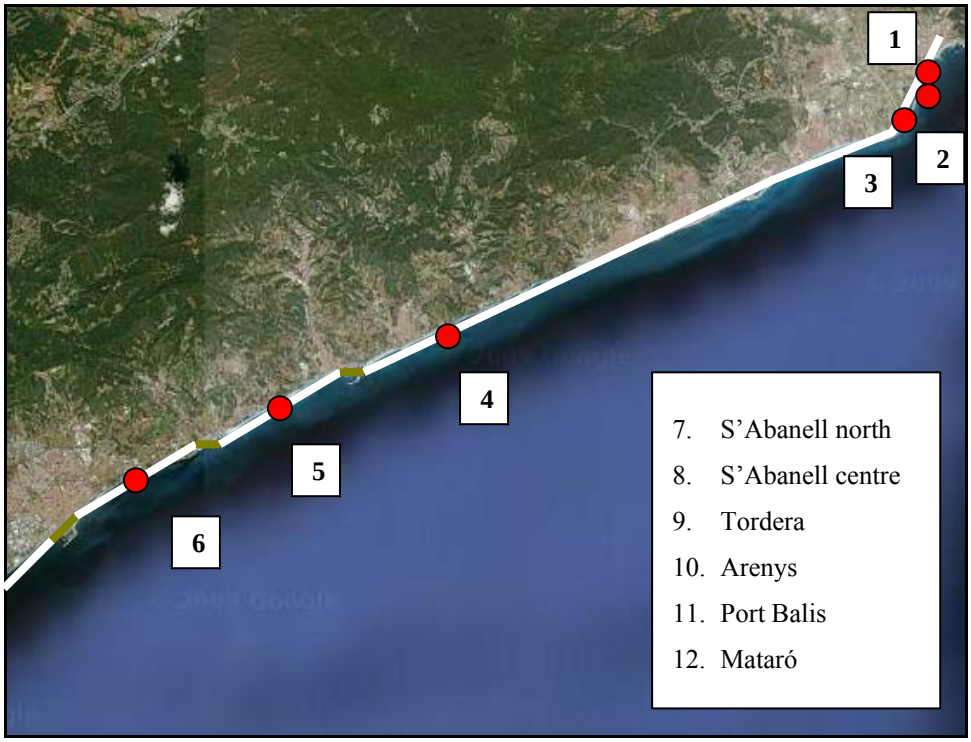

Figure 2.8 Map of stretch La Tordera - Mataró.

6. Mataró - Barcelona

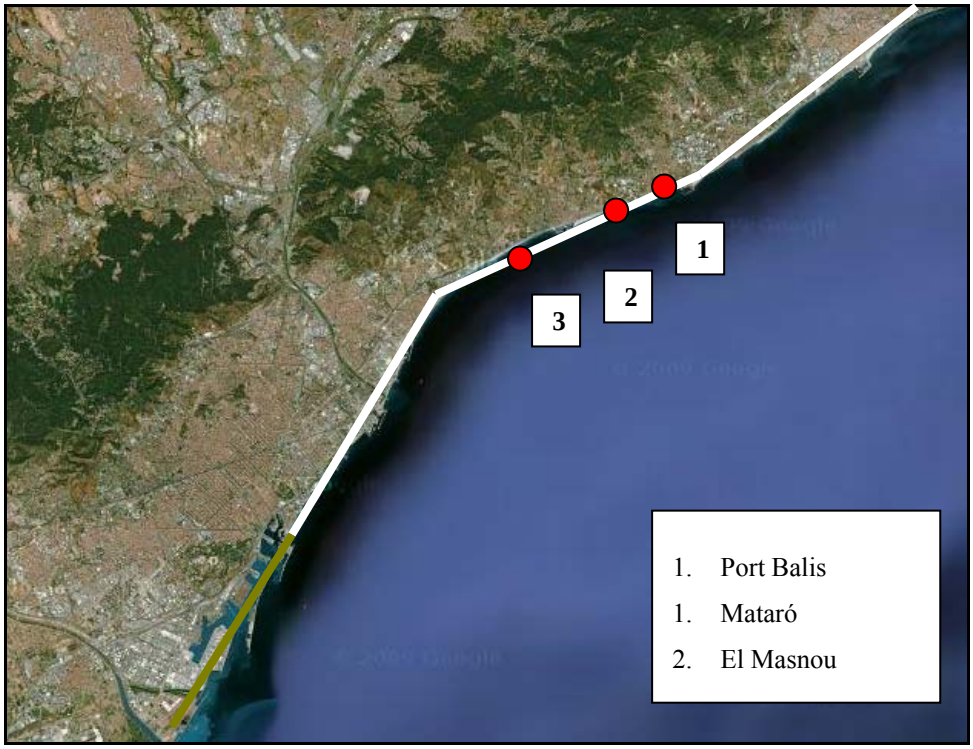

Figure 2.9 Map of stretch Mataró – Barcelona.

7. Barcelona - Sitges

Figure 2.10 Map of stretch Barcelona – Sitges.

8. Sitges – Segur de Calafell

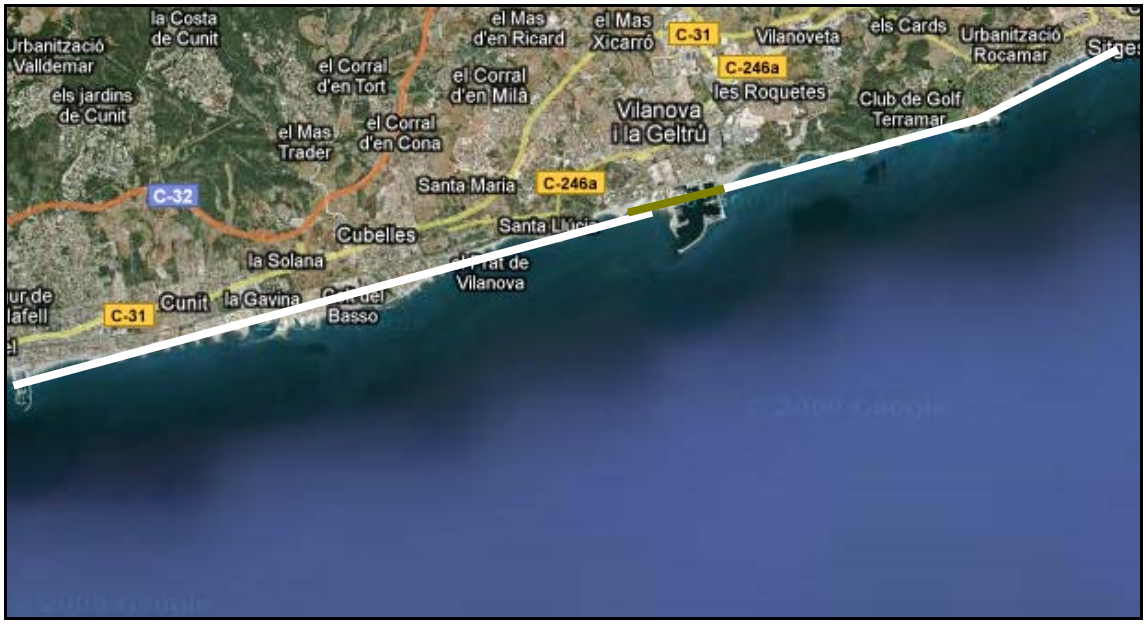

Figure 2.11 Map of stretch Sitges – Segur de Calafell.

9. Segur de Calafell - Torredembarra

Figure 2.12 Map of stretch Segur de Calafell – Torredembarra.

10. Torredembarra – Cala Romana

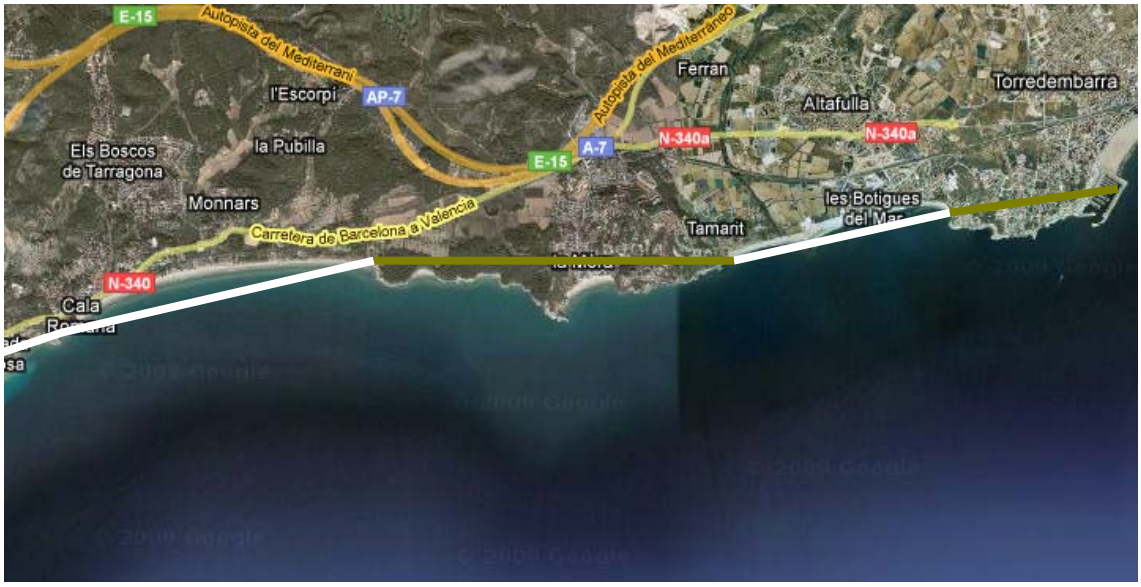

Figure 2.13 Map of stretch Segur de Torredembarra – Cala Romana.

11. Cala Romana - Cambrils

Figure 2.14 Map of stretch Segur de Cala Romana - Cambrils.

12. Cambrils – Miami Platja

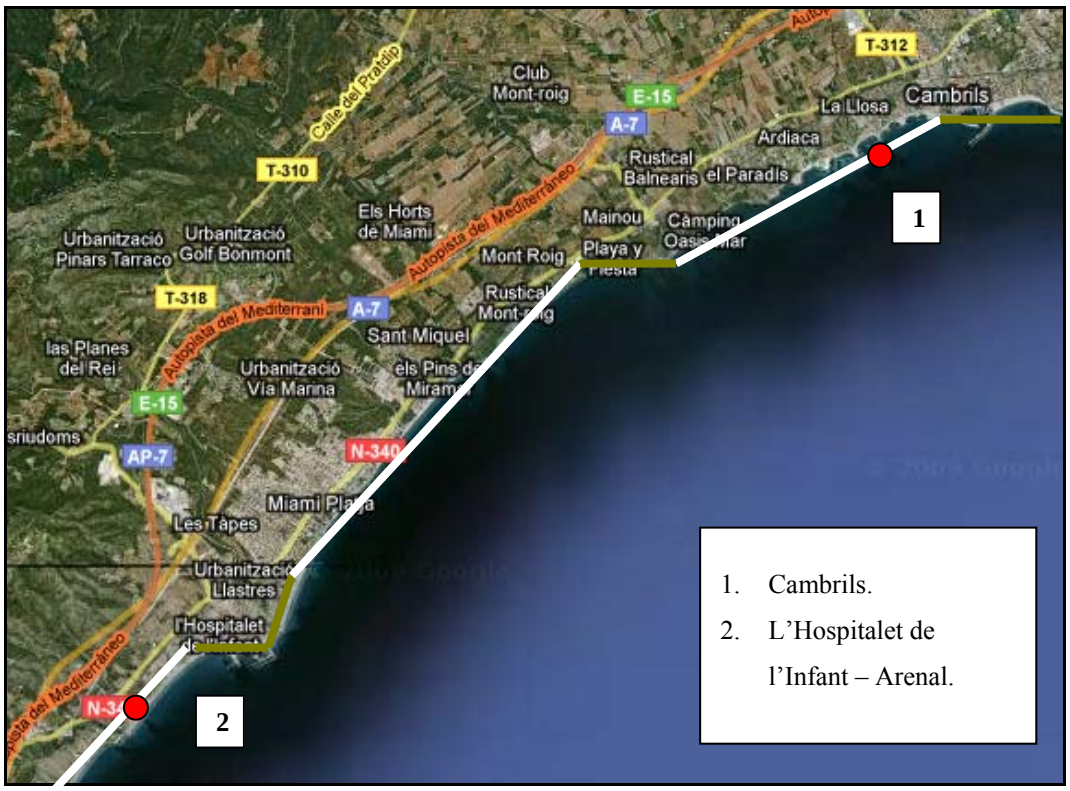

Figure 2.15 Map of stretch Segur de Cala Romana - Cambrils.

13. Ebre Delta

Figure 2.16 Map of stretch Segur de Ebre Delta.

Chapter 3

Sediment Transport evaluation in the specified zones

3.1 INTRODUCTION

In the last chapter there were represented the points where we have available data on the parameters needed to aply the CERC formula. In this third chapter are presented the results given by the application of the formula at the characterized sites and the analysis carried out over the LST values like distribution throughout the year, sediment budget along the beach or Littoral Drift Roses.

This chapter of results is divided in to parts. The first one is the study of each physiographic unit identified. For each one of these unit is presented a set of results: LST time series, monthly distribution of LST, LST values (total, contribution by wave direction and contribution of storm periods), sediment budget using LST capacity, resume of storm contribution and Littoral Drift Rose. The second part (General Conclusions) is constituted by global results extracted from the study of all the units. It includes a resume of LST values along the Catalan coast, monthly distribution of LST, proportion of LST caused by storms and the evolution of LST total values per year in the course of the years.

3.2 LST CALCULATION

It must be defined a set of parameters where some of them can be measured or estimated and others must be supposed. Formula used for LST calculation has been CERC Formula, which needs the following parameters to be applied. There are included the values considered for the ones that must be supposed.

- Orientation of the shoreline.
- Gamma index for wave breaking: 0.65

- Initial depth wave conditions: 100m
- Characteristic parameter for wave height: Hs
- Median grain size diameter.
- Beach profile - bed slope (see chapter 2.2.2)
- Obtaining Krms for CERC calculation: calculation of Krms by del Valle, Medina and Losada (1993). Needs sediment size.
- Data set of wave conditions (see chapter 2.1). Includes:
    - Date of each measure, as it is registered the time in which wave measurement start and time in it ends.
    - Hs
    - Tp (Period)
    - Direction.

Description of the analysis done for each physiographic unit

Results are presented following always the same structure. Here is explained which are the results given and how have them been obtained.

LST time series

The software used to apply CERC formula gives an LST value for each measurement from wave data time series. For every measurement we know the date when it was recorded. Then, as a first step to give an idea of the magnitude and main direction of LST, is presented a graphic of time-ordered LST values. These graphics are useful not to know exactly the sediment drift that has taken place in a certain year but to see and identify the years with anomaly high values of transport. Adding to this, we can see easily on these graphics the difference in magnitude of the transport in both directions along a beach, as they graphics for each direction are presented separately.

To better comparison among the different zones of a unique unit the same scale has been used for all the graphics representing the same physiographic unit.

Monthly distribution of LST

Before showing the distribution over the years the study regards the distribution throughout an average year of the LST. The objective is to see the variation of the magnitude of LST over the months and specially to calculate with certain exactitude the proportion of sediment moved during winter time and summer time. Obviously the first one is expected to be quite higher but it will be interesting to know exactly how higher is. Identification of months with specially high or low values of LST will be done as well. For a better analysis of these results it might be useful to look at the tables of monthly distribution of wave height, included on Appendix 2.

LST estimation in average year: total, by wave direction and proportion caused by Hs>2m.

These values are presented on a table. It appears total drift towards each direction, drift caused by waves coming from each wave direction (ex. transport produced by waves coming from East) and proportion of transport caused by storms (that means to add up the transport produced by waves with Hs > 2m). We can see next to these values the percentage they represent. Characterization parameters of each one of the beaches that make up the unit appear on the table: orientation angle, sediment grain size and bottom slope.

Sediment budget using LST capacity

We can see here a diagram with the different magnitudes and directions of littoral drift along the unit and the quantification of sediment gained or lost yearly in each sector.

Storm contribution

The storm contribution in global terms for each sector. Gives a better idea about its magnitude than the list of values by direction given on the table of results.

Littoral Drift Rose

This polar graphic shows, for a certain stretch of coast, the variation of LST with the shoreline orientation. Many beaches tend to change its orientation at different times of the year. The drift rose makes it possible to foresee the range of values reached by the LST at a beach with variable orientation by knowing the range of orientations taken by the beach throughout a year. A drift rose can be representative of a stretch of coast with sufficiently

similar parameters of grain size, bottom slope and to be exposed to the same waves. That's due to the fact that only for the variable shoreline orientation are given different values (more information about Littoral drift rose in Walton and Dean: *Longshore sediment transport via litoral drift rose*). Characteristic values of a site are not always constant along a wide zone but maybe quite similar. That use to happen in beach sectors composing the same physiographic unit. It wouldn't be very useful to create a large number of drift roses applicable only at a small part of the unit, so all the units studied on this research are described by one or two drift roses. These are made using average parameters of the zone corresponding to the rose. In the case that characteristic parameters were extremely different the area has been divided and another rose developed. On the description of the unit there are specified the values of the parameters used to design the roses.

General conclusions

Some aspects of the LST characterization have been analyzed as a global resume. The aim is to achieve some results or conclusions applicable to the entire Catalan coast or to more or less wide zones of this coast. The points presented on this part are the following:

- LST by Net/Gross and by direction of transport (South/North)
- Monthly Distribution
- Proportion of LST caused by storms
- Annual deviation over the mean

3.2.1 Gulf of Roses

Situation of the Gulf of Roses.

Beach definition and main parameters

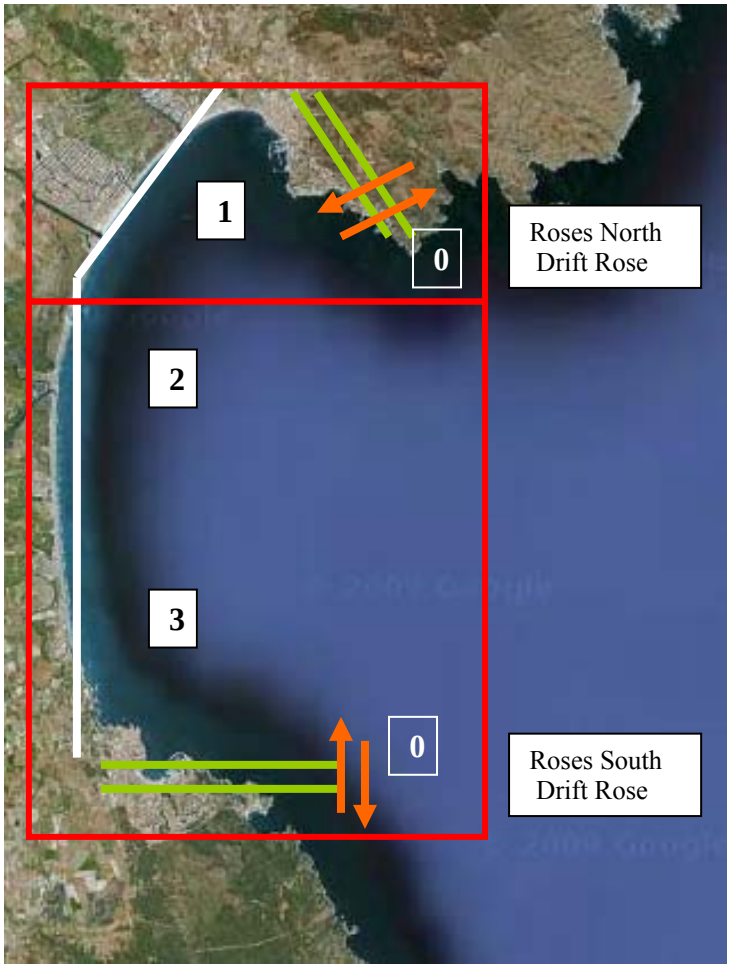

Figure 3.1 Definition of the beach of Gulf of Roses.

	Diameter (D_{50})	Orientation (deg)	Slope	Wave effective Dir.
1. La Rovina	0.26	37	0.04	102-170
2. Sant Pere Pescador	0.33	0	0.04	61-153
3. Sant Martí d'Empúries	0.33	0	0.06	45-140
Data for Drift Roses:				
- Roses North				
Drift Rose	0.33	0-110º	0.05	102-170
- Roses South				
Drift Roses	0.33	325-0º	0.05	45-153

LA ROVINA

Longshore Sediment Transport Time Series

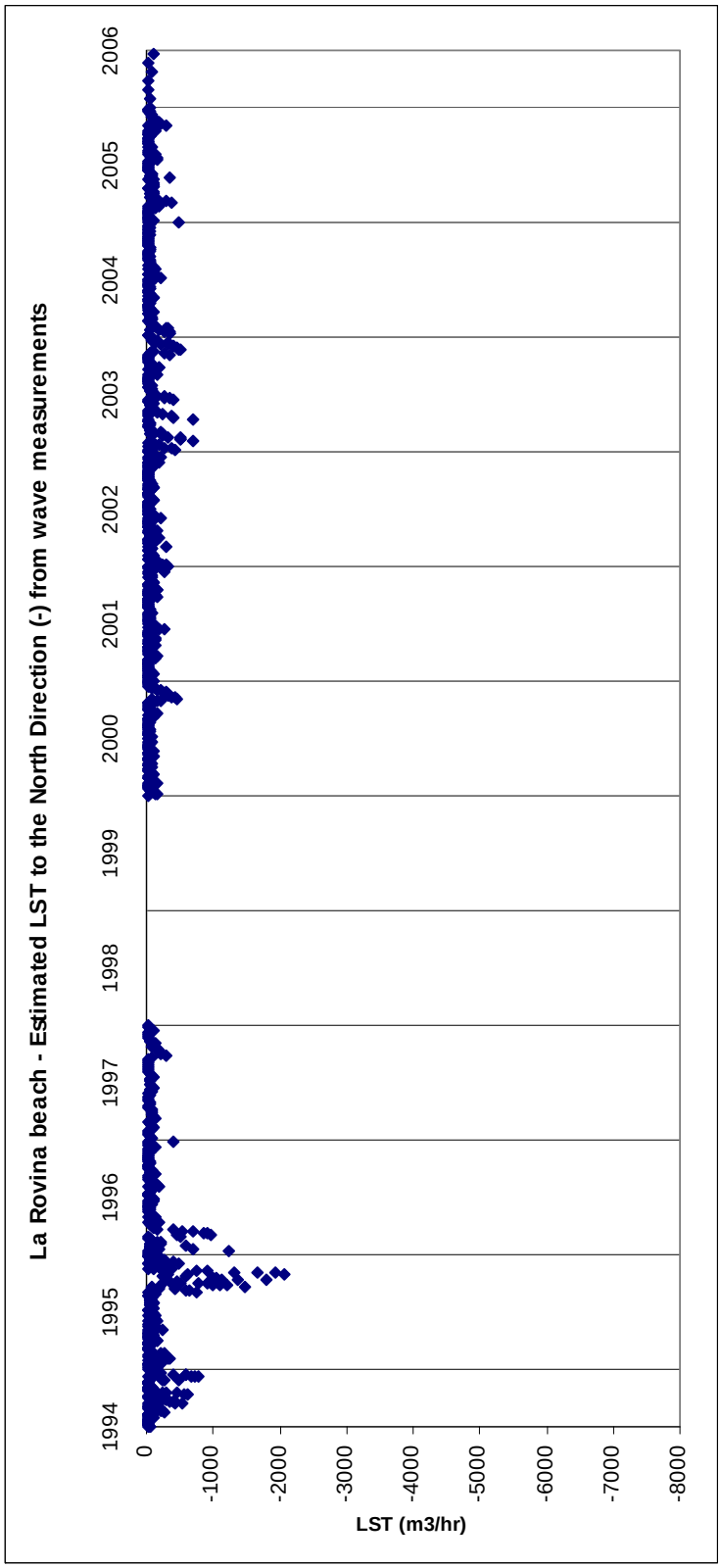

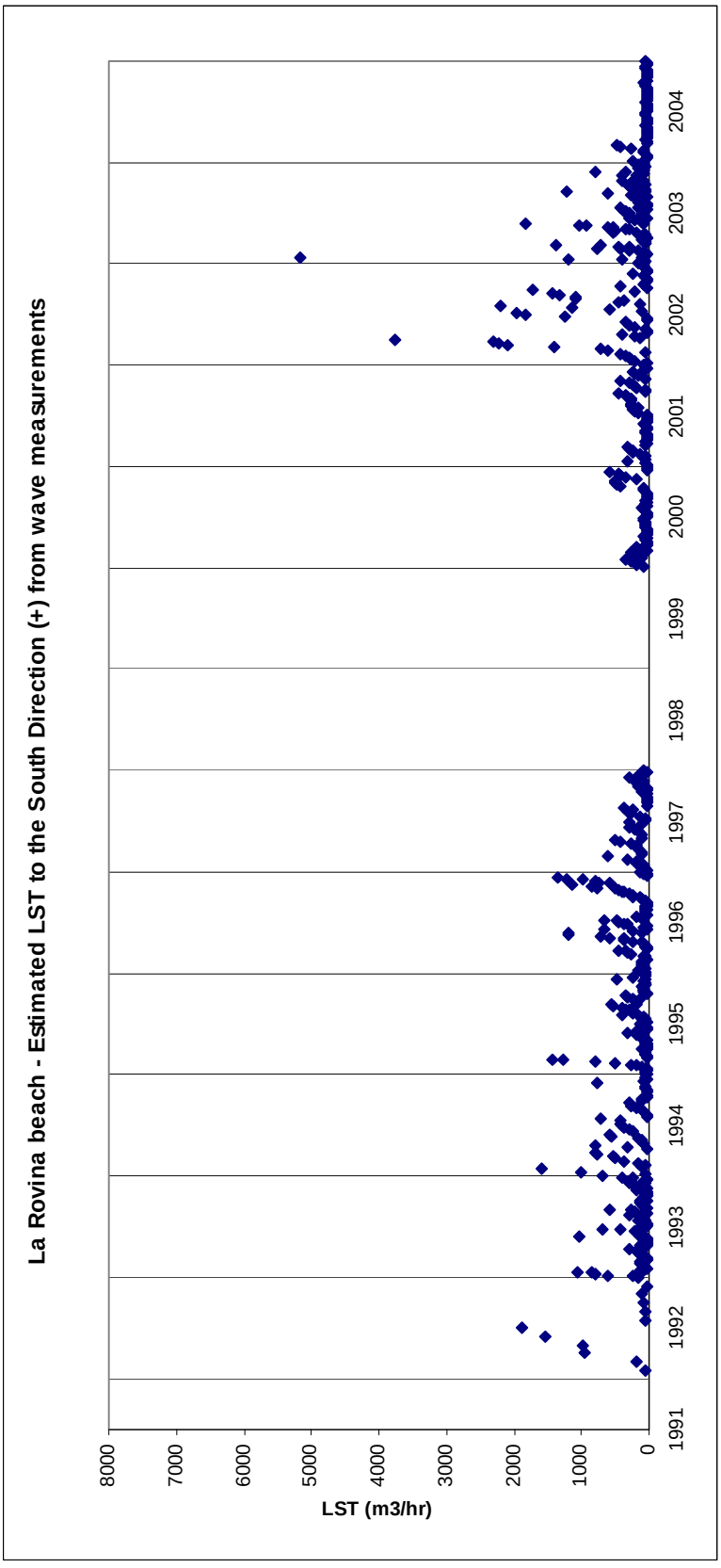
La Rovina beach - Estimated LST to the South Direction (+) from wave measurements
LST (m3/hr)
8000
7000
6000
5000
4000
3000
2000
1000
0
1991
1992
1993
1994
1995
1996
1997
1998
1999
2000
2001
2002
2003
2004

Comments on LST time series

Looking at the time series of La Rovina is easy to notice that the graphic for the North Direction shows a larger number of measurements but with smaller values of transport than the graphic for the South Direction. On this one we can see fewer measurements but however more measurements with a great value of transport (storm measurements). Such storm values don't exist among the larger number of points on the North Direction time table (except a group of points standing out in the end of 1995 and beginning of 1996). That fact is easily understandable when looking at the Wave Height Rose corresponding to the zone of Roses (see "Buoy Zone 1" on *Appendix 1. Wave Height Roses*). As La Rovina is closed in its North end by a long cape only waves coming from a direction greater than 100º can reach the beach, so we have to consider the bottom part of the Wave Rose. Doing so, we see that most of the waves come from the south, producing a small but very frequent sediment transport to the North (as an average, total Net Transport results to be to the North). Nevertheless, the highest wave heights use to come from the East direction, producing an occasional but much more important transport to the South.

Monthly Distribution

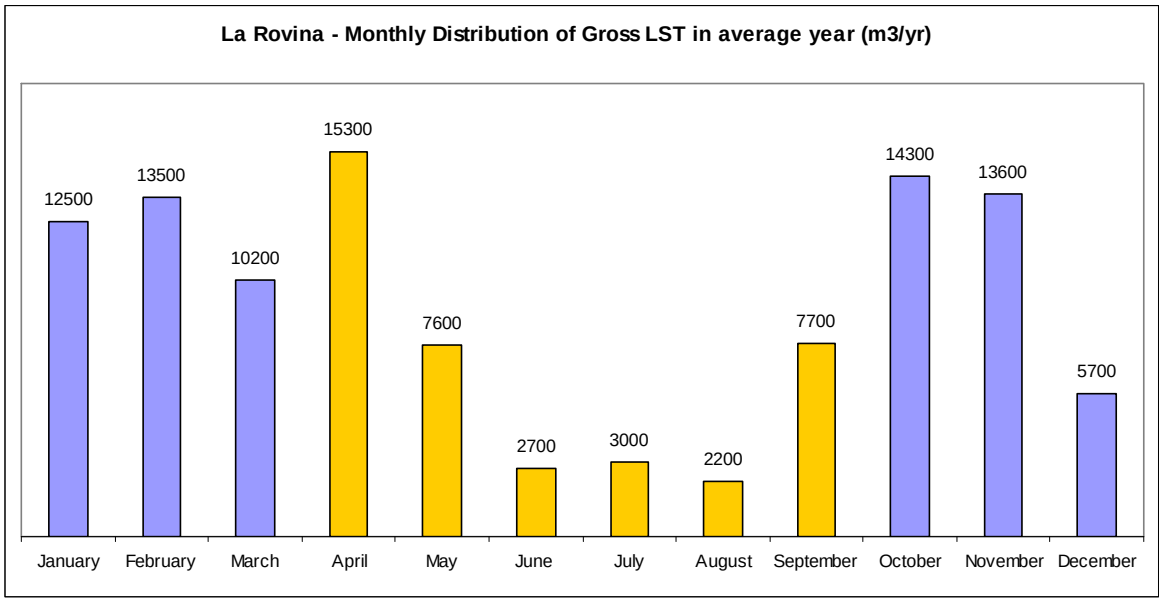

Summer and winter time distribution of Gross LST:

- Oct-Mar: 69 800 (64%)
- Apr-Sep: 38 500 (36%)

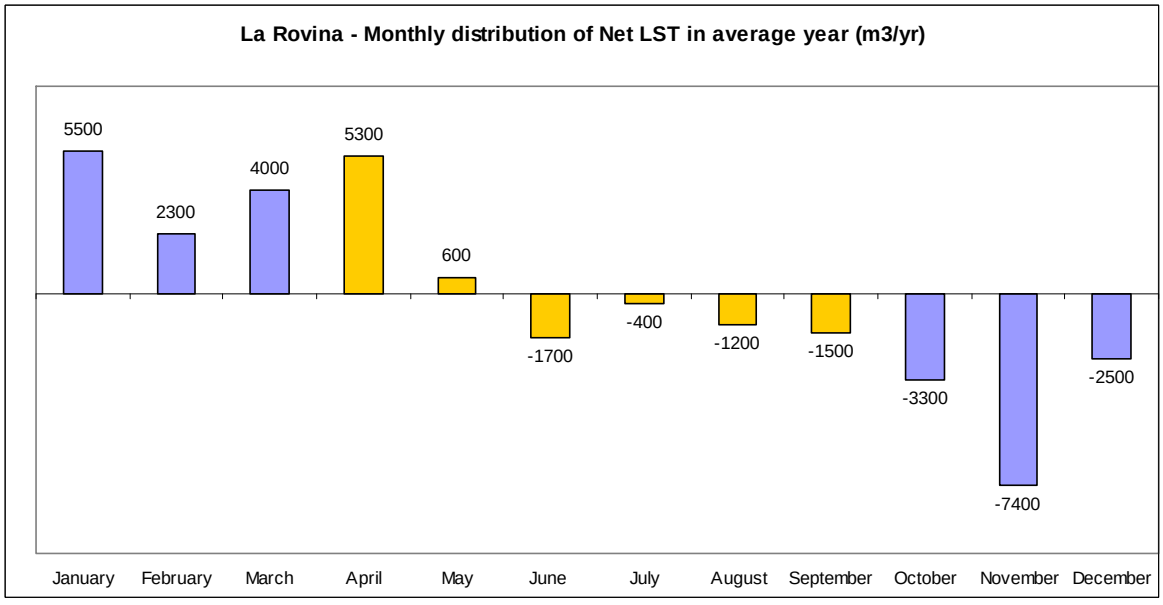

Summer and winter time distribution of Net LST:

- Oct-Mar: 25 000 (70%)
- Apr-Sep: 10 700 (30%)

SANT PERE PESCADOR

Longshore Sediment Transport Time Series

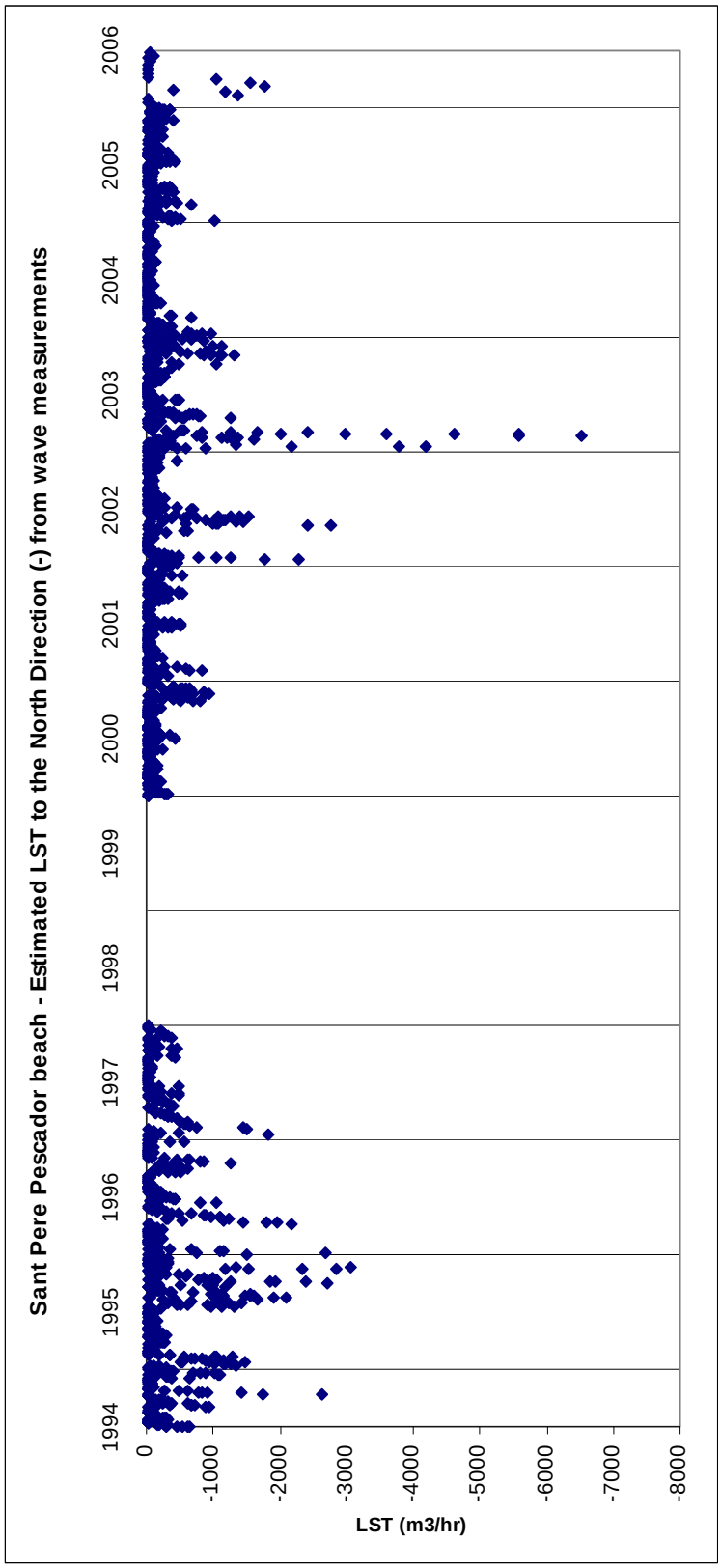

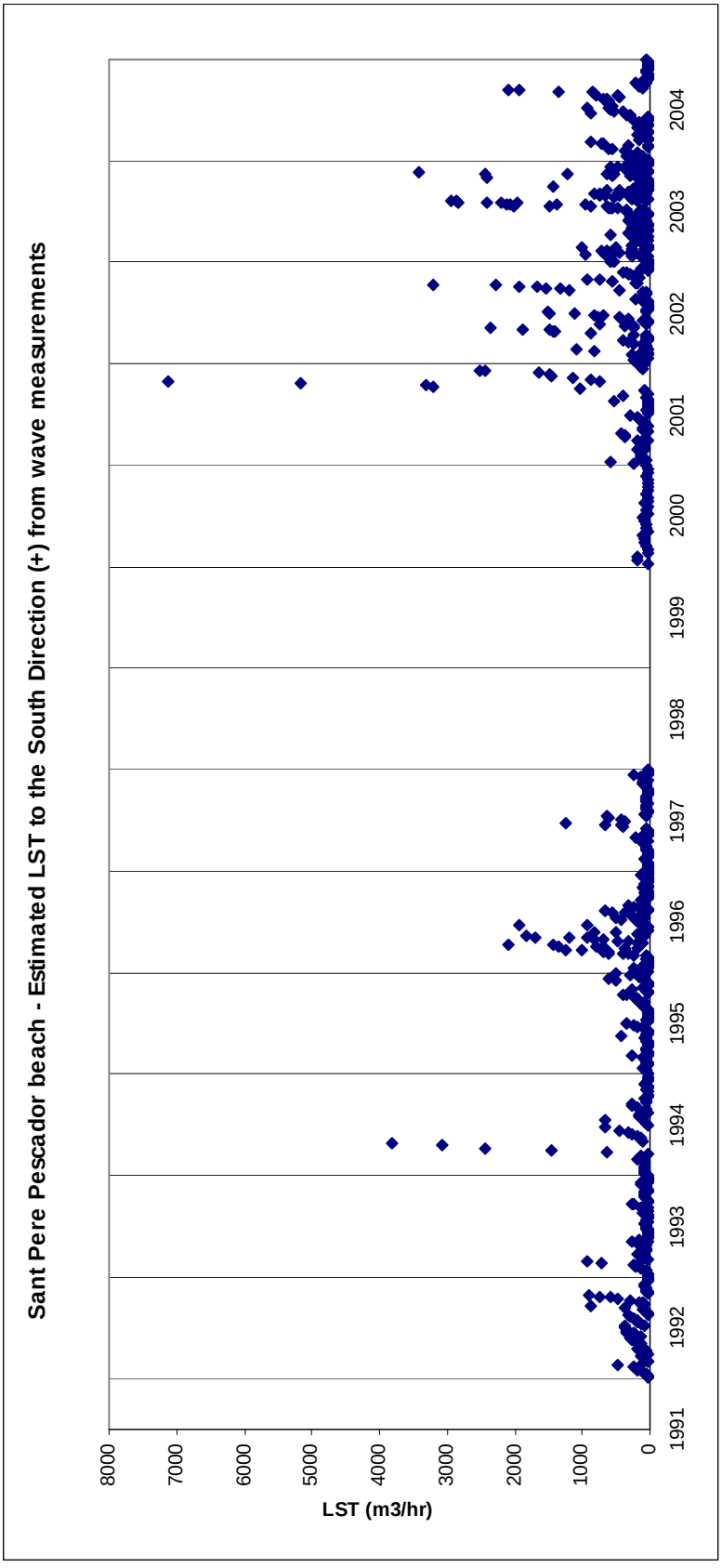
Sant Pere Pescador beach - Estimated LST to the South Direction (+) from wave measurements
LST (m3/hr)
8000
7000
6000
5000
4000
3000
2000
1000
0
1991
1992
1993
1994
1995
1996
1997
1998
1999
2000
2001
2002
2003
2004

Monthly Distribution

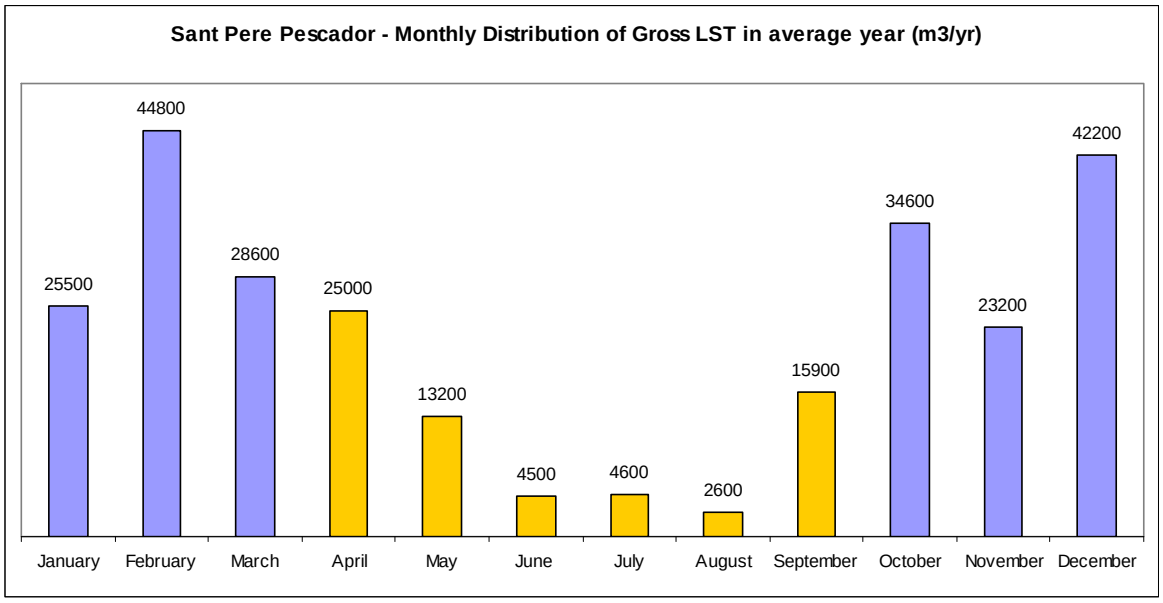

Summer and winter time distribution of Gross LST:

- Oct-Mar: 198 900 (75%)
- Apr-Sep: 65 800 (25%)

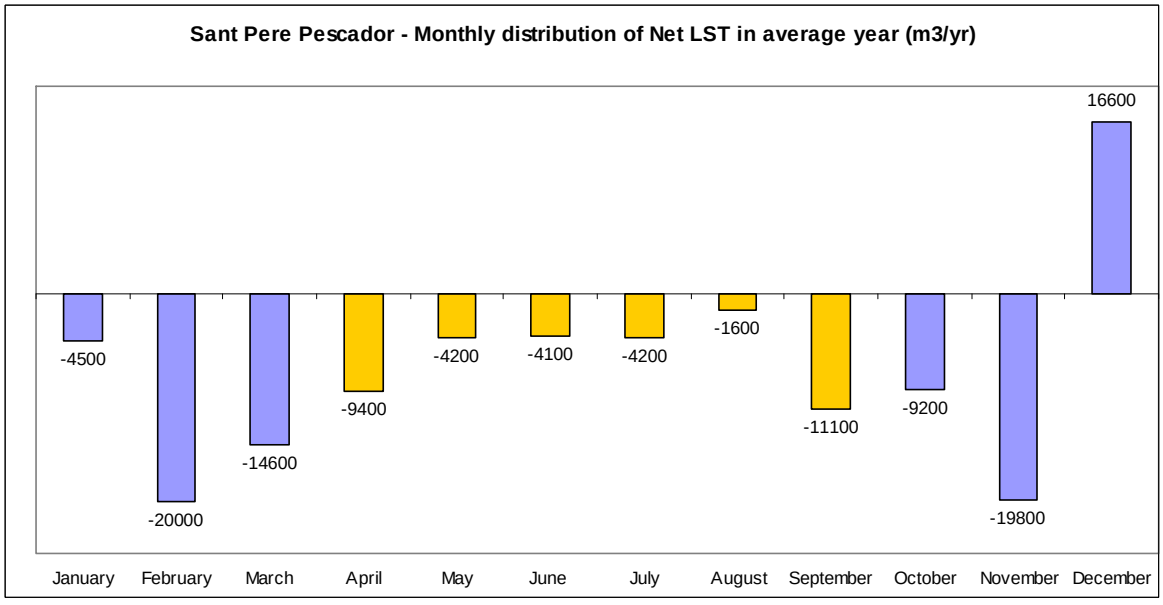

Summer and winter time distribution of Net LST:

- Oct-Mar: 84 700 (71%)
- Apr-Sep: 34 600 (29%)

SANT MARTÍ D'EMPÚRIES

Longshore Sediment Transport Time Series

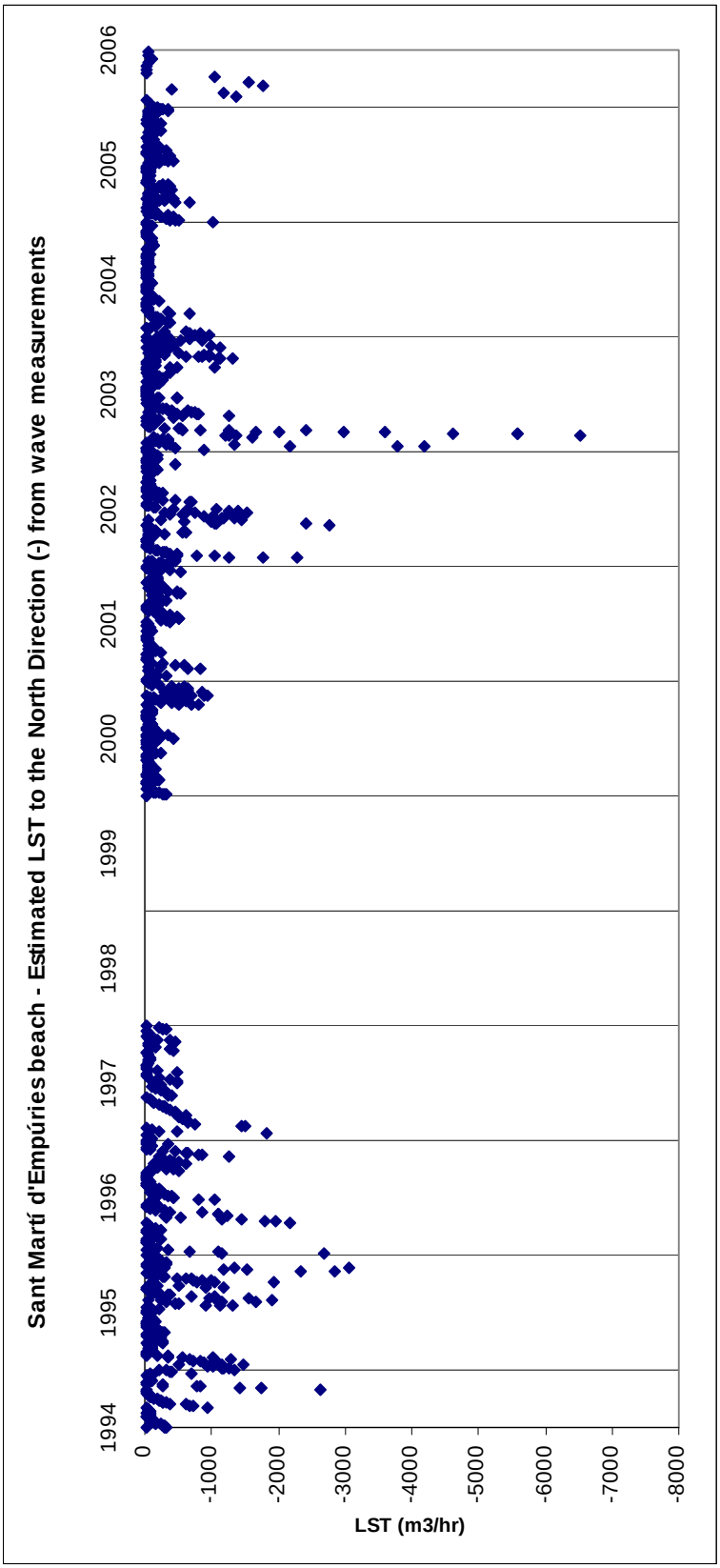

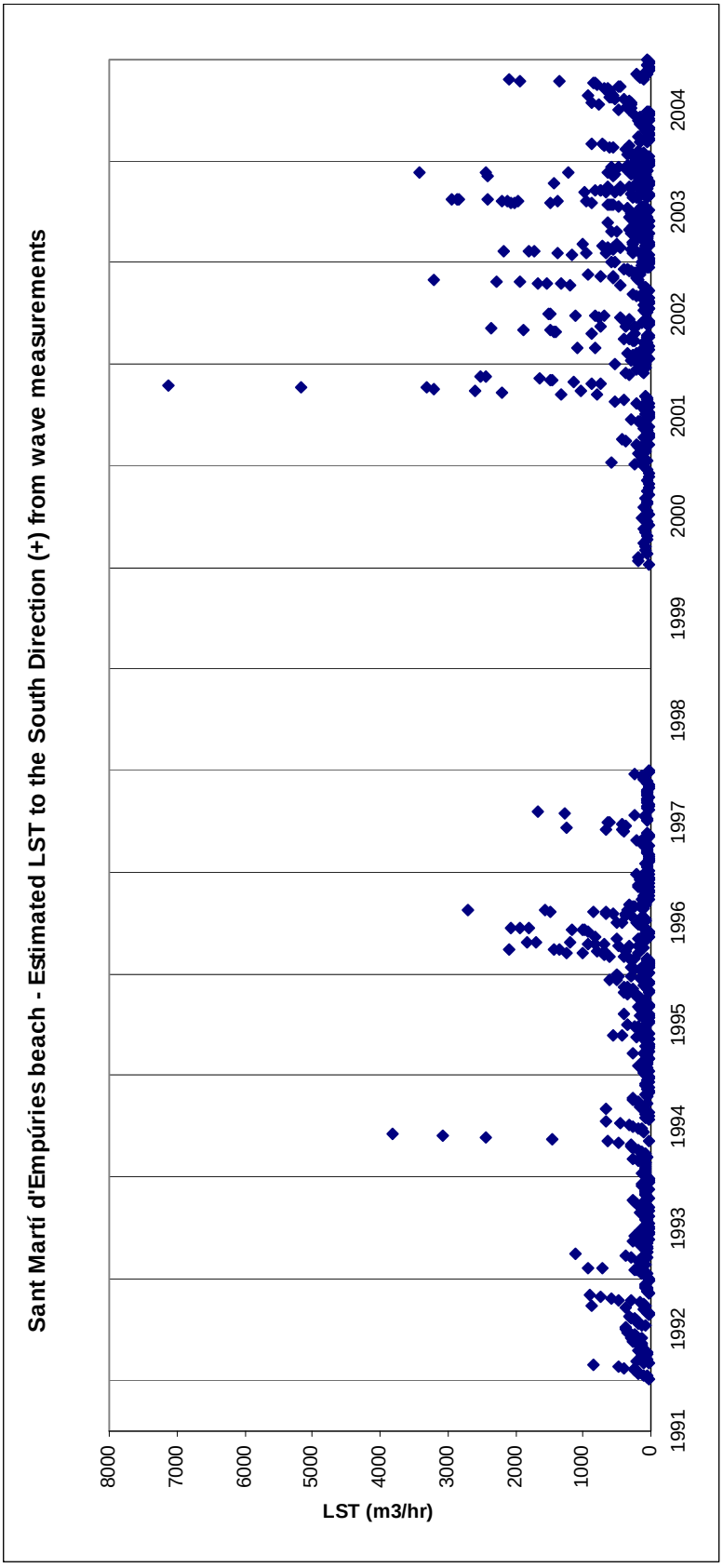
Sant Martí d'Empúries beach - Estimated LST to the South Direction (+) from wave measurements
LST (m3/hr)
8000
7000
6000
5000
4000
3000
2000
1000
0
1991
1992
1993
1994
1995
1996
1997
1998
1999
2000
2001
2002
2003
2004

Comments on LST time series

In the cases of Sant Pere Pescador and Sant Martí d'Empúries there's no so much difference between time series for North and South directions. Theses beaches are more exposed to waves from the East and in consequence, transport is not defined by waves from the South.

Monthly Distribution

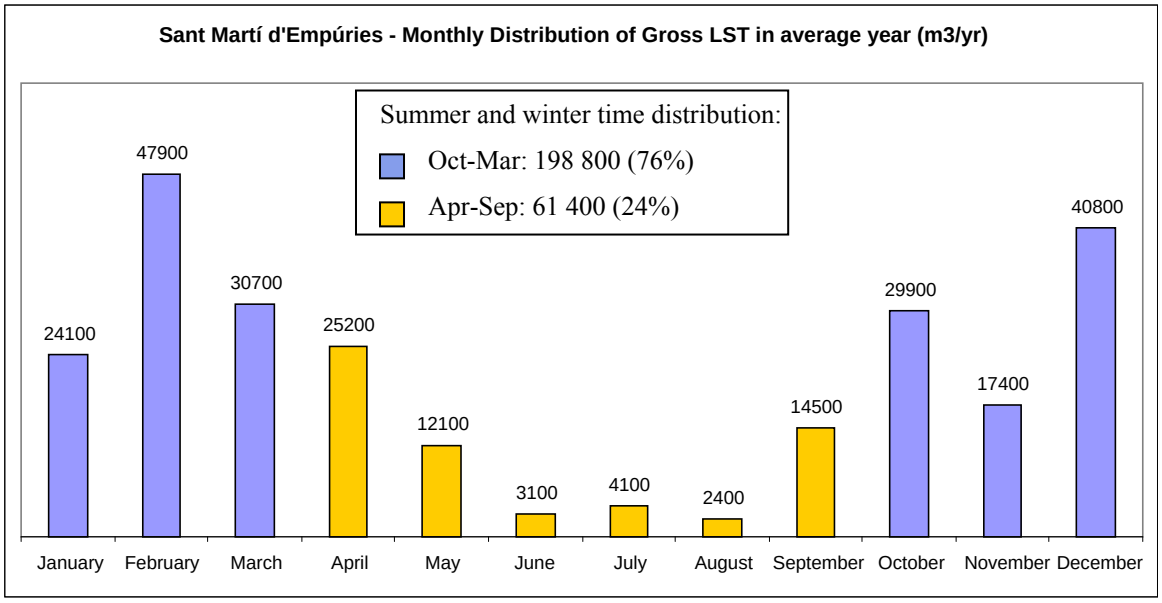

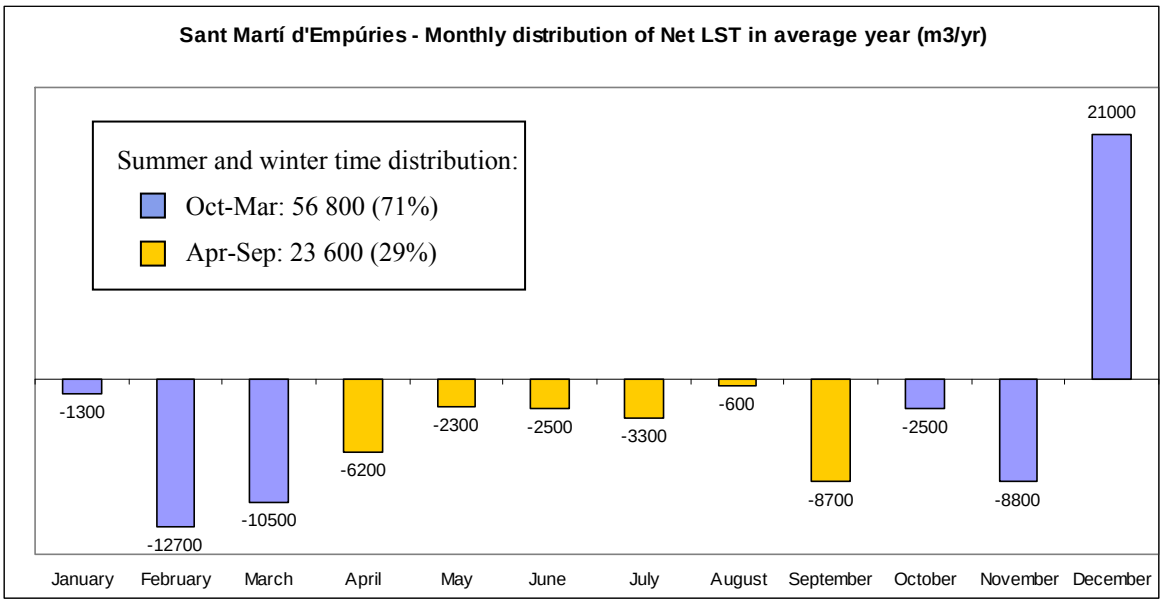

LST estimation in average year: total, by wave direction and proportion caused by Hs>2m.

Beach	Direction of Littoral Drift	Total LST (m3/year)	Wave direction			Hs		Grain size (mm)	Orientation (º)	Slope
			Wave direction	LST (m3/year)	%	LST (Hs>2m)	%			
La Rovina	South	50325	ESE	49175	97.7	24822	50.5	0.26	37	0.04
			SE	1150	2.3	835	72.6			
	North	54379	SE	27721	51.0	12861	46.4			
			SSE	24844	45.7	4035	16.2			
			S	1814	3.3	0	0.0			
Sant Pere Pescador	South	88861	ENE	46799	52.7	30699	65.6	0.33	0	0.04
			E	42062	47.3	34996	83.2			
	North	175441	E	11521	6.6	7163	62.2			
			ESE	58544	33.4	27538	47.0			
			SE	96043	54.7	49216	51.2			
			SSE	9333	5.3	3614	38.7			
Sant Marti d'Empuries	South	106931	NE	14549	13.6	7775	53.4	0.33	0	0.06
			ENE	50762	47.5	32669	64.4			
			E	41620	38.9	34996	84.1			
	North	145215	E	11361	7.8	7163	63.0			
			ESE	57944	39.9	27538	47.5			
			SE	75910	52.3	39767	52.4			

	La Rovina	**Sant Pere Pescador**	**Sant Martí d'Empúries**
Gross LST(m^3/yr)	105 700	264 300	252 100
Net LST (m^3/yr)	-4 000 (to North)	-86 600 (to North)	-38 300 (to South)

Sediment Budget using LST Capacity

Figure 3.2 Evaluation of LST along the Gulf of Roses. Values in m^3/year.

Storm contribution: proportion of transport caused by storm conditions (Hs>2m)

	La Rovina	Sant Pere Pescador	Sant Martí d'Empúries
South Direction	51%	74%	71%
North Direction	31%	50%	52%

North Roses Littoral Drift Rose

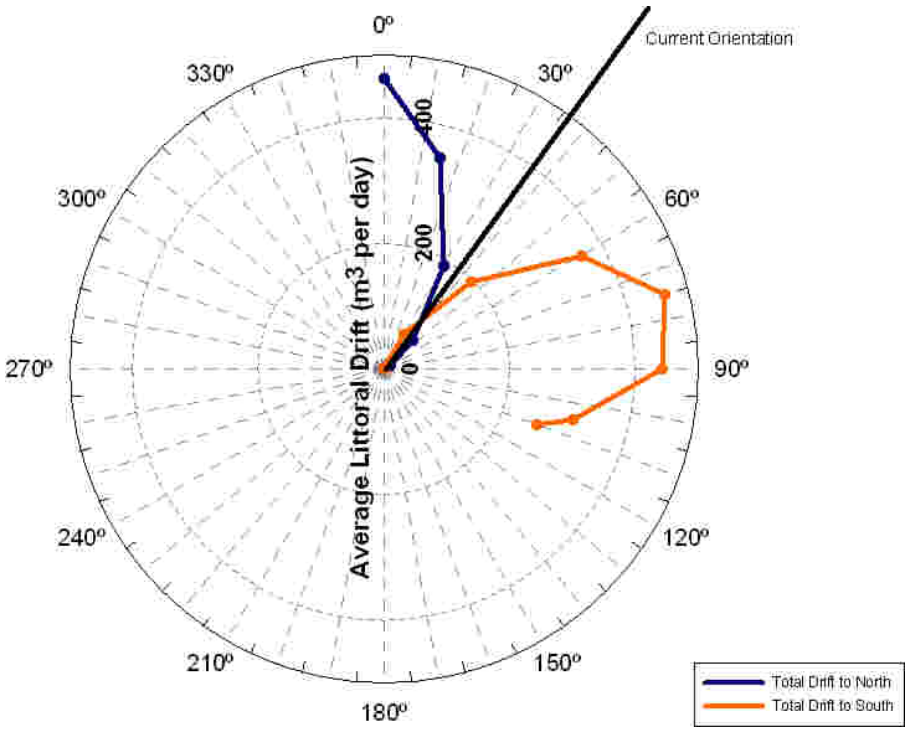

South Roses Littoral Drift Rose

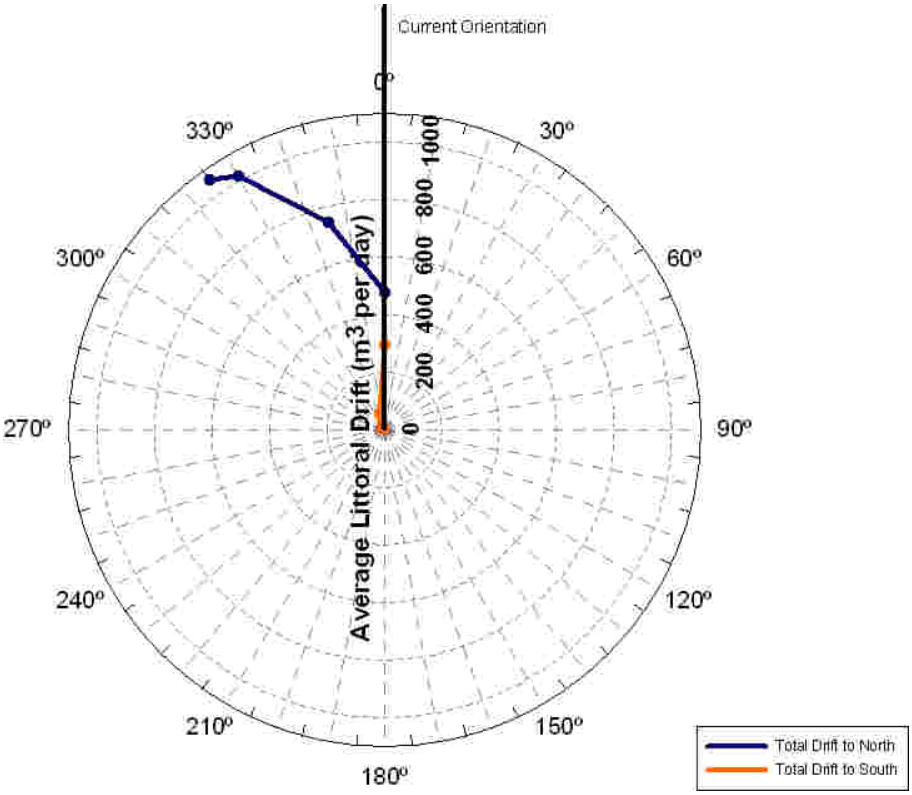

Comments on Drift Roses

The whole Gulf of Roses is an example of equilibrium beach. As we can see on the Drift Roses the current orientation is a minimum transport orientation in both North and South zones. These beaches have changed its shape and orientation freely in the course of the years until the present situation.

3.2.2 L'Estartit – Pals

Situation of L'Estartit – Pals beach.

Beach definition and main parameters

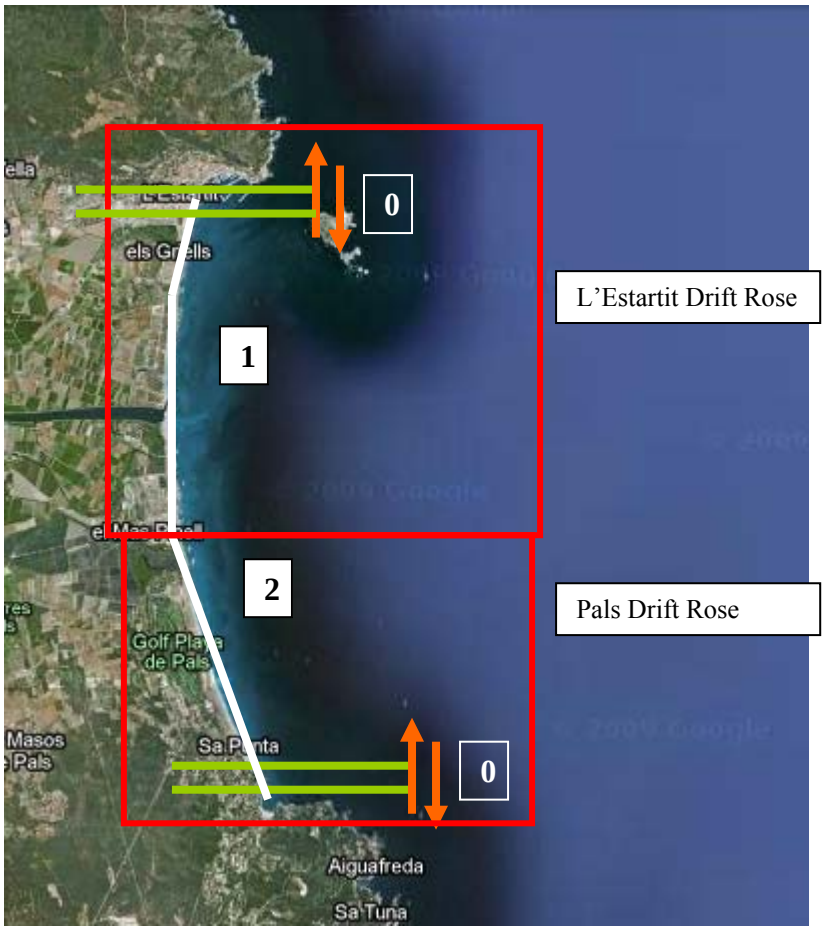

Figure 3.3 Definition of the beach of L'Estartit – Pals. Values in m^3/yr.

	Diameter (D_{50})	**Orientation (deg)**	**Slope**	**Wave effective Dir.**
1. L'Estartit	0.29	0	0.05	15-165
2. Pals	0.51	340	0.13	0-145
Data for Drift Roses:				
- L'Estartit Drift Rose	0.29	350-20º	0.05	0-165
- Pals Drift Rose	0.51	325-0º	0.13	0-145

L'ESTARTIT

Longshore Sediment Transport Time Series

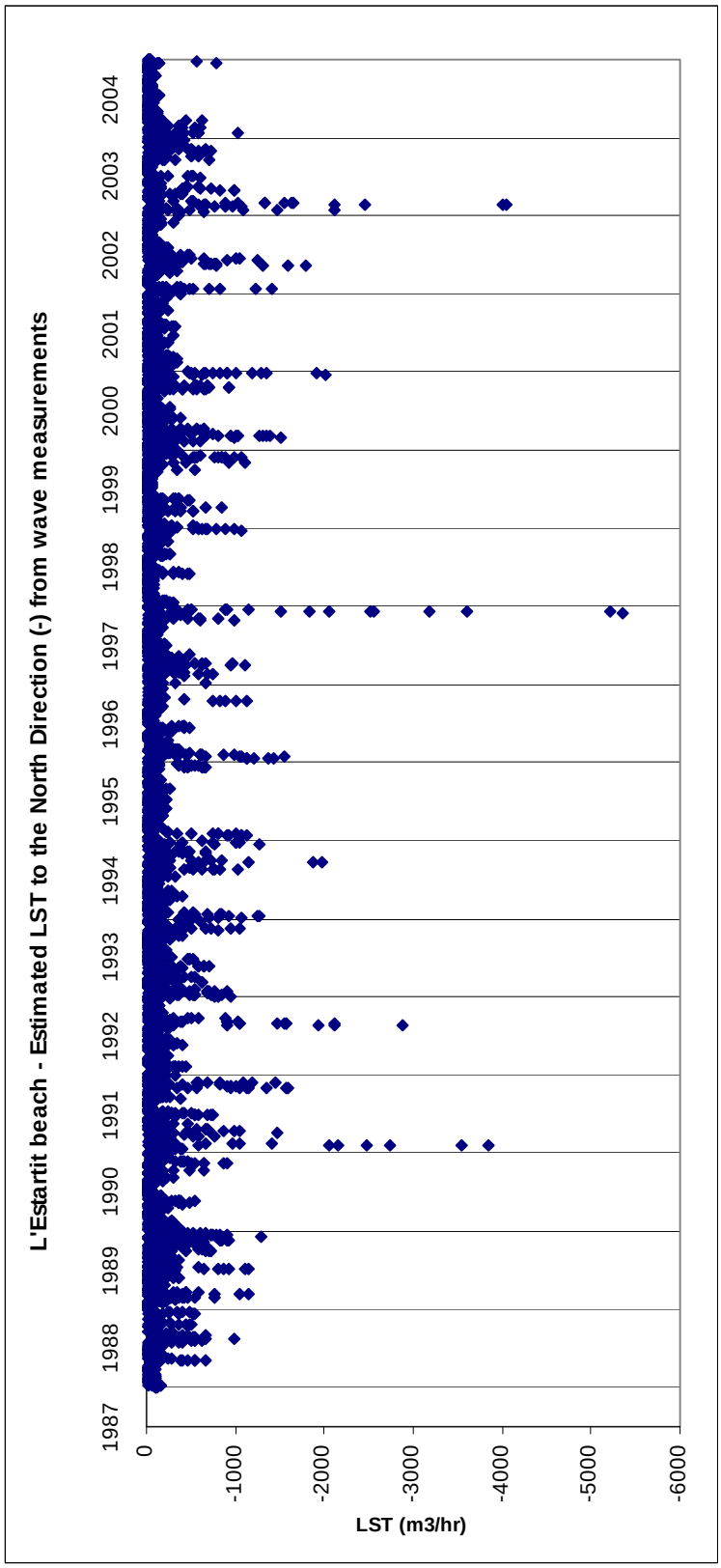

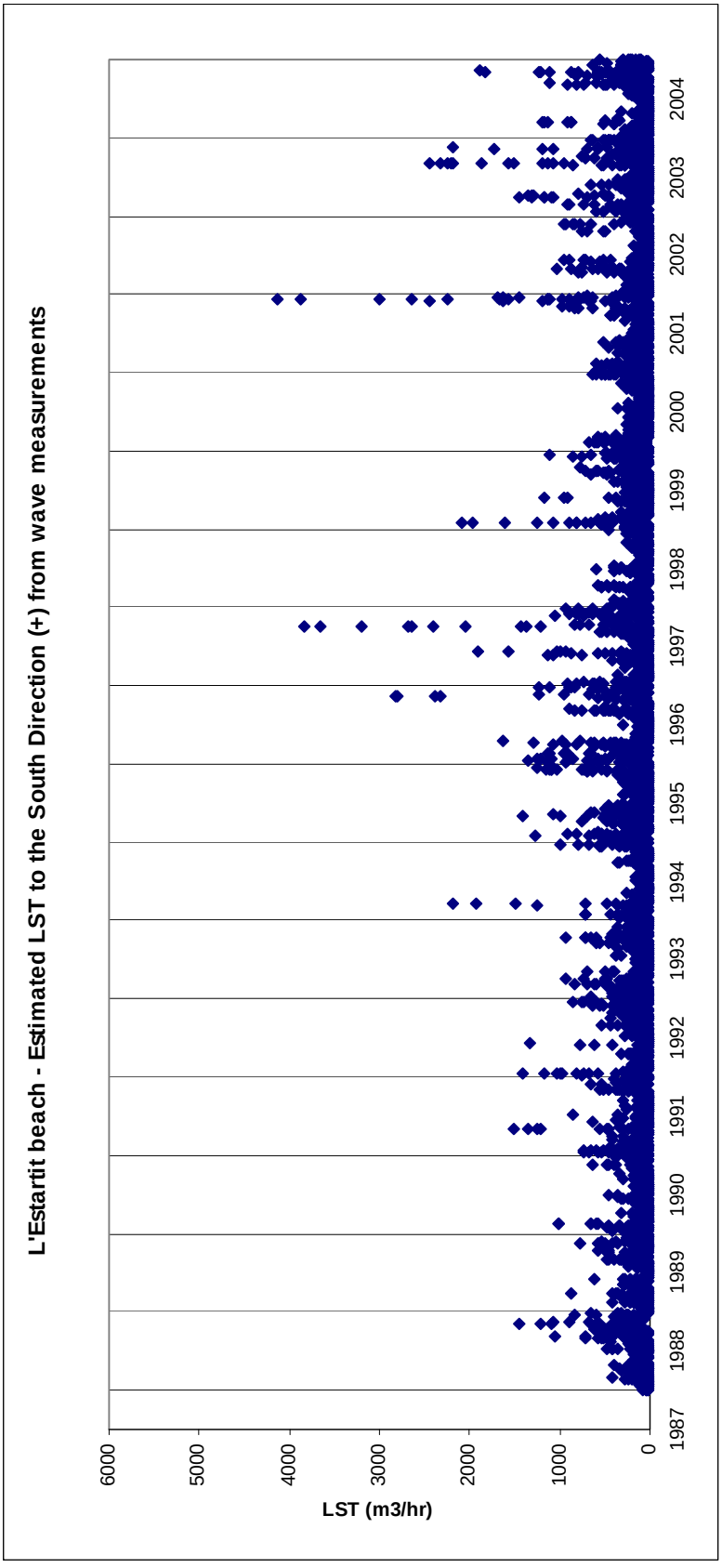
L'Estartit beach - Estimated LST to the South Direction (+) from wave measurements
LST (m3/hr)
6000
5000
4000
3000
2000
1000
0
1987
1988
1989
1990
1991
1992
1993
1994
1995
1996
1997
1998
1999
2000
2001
2002
2003
2004

Monthly Distribution

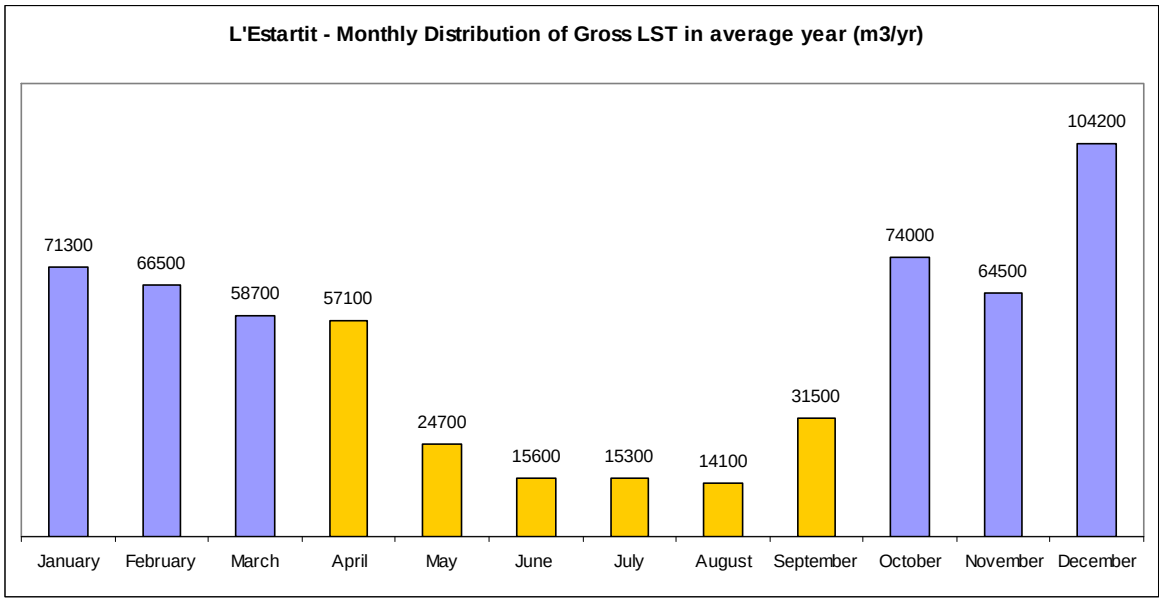

Summer and winter time distribution of Gross LST:

- Oct-Mar: 439 200 (74%)
- Apr-Sep: 158 300 (26%)

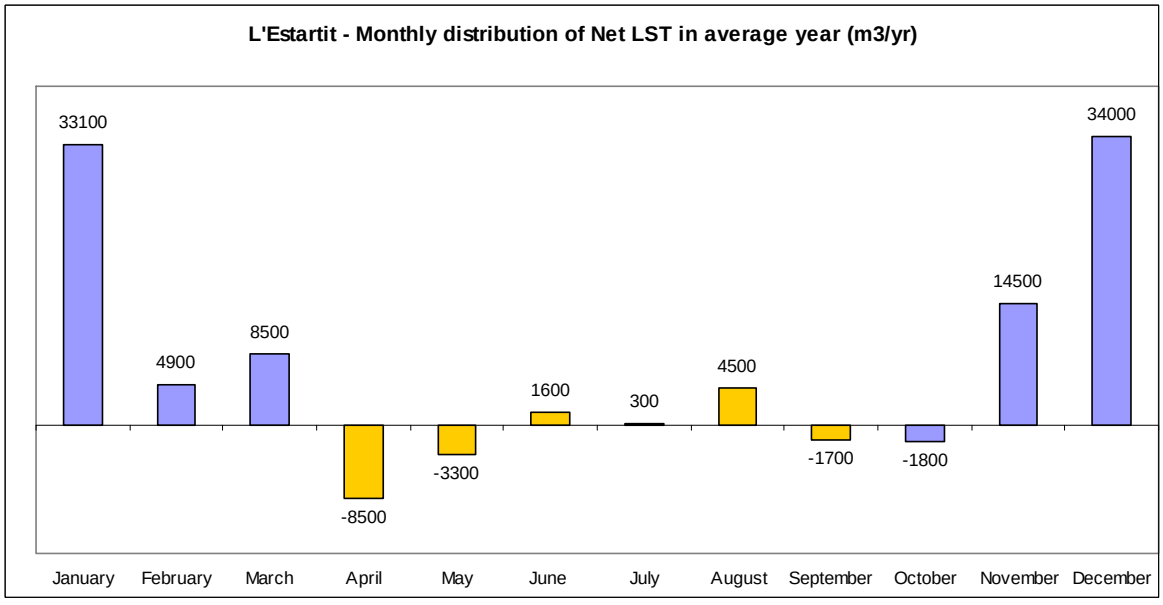

Summer and winter time distribution of Net LST:

- Oct-Mar: 96 800 (83%)
- Apr-Sep: 19 900 (17%)

PALS

Longshore Sediment Transport Time Series

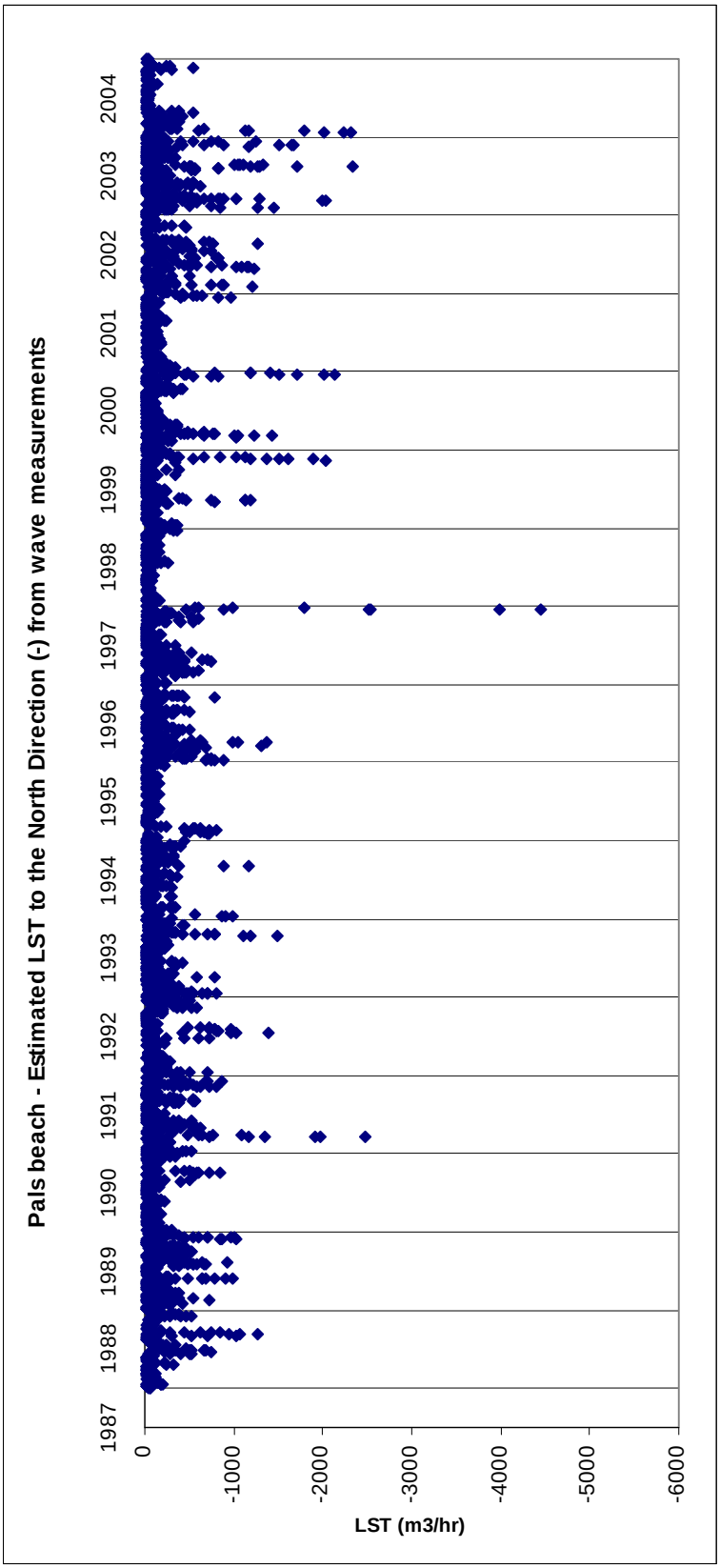

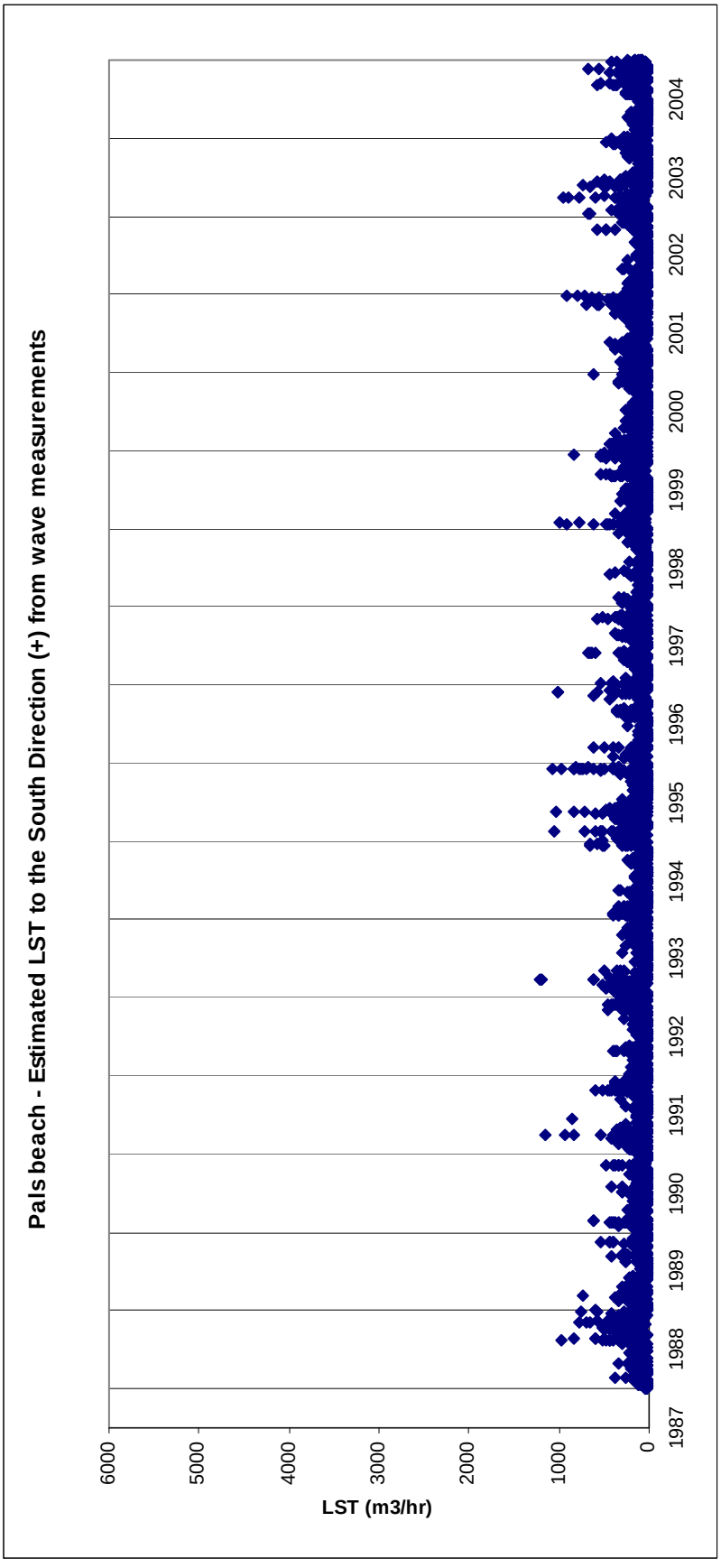
Pals beach - Estimated LST to the South Direction (+) from wave measurements
LST (m3/hr)
6000
5000
4000
3000
2000
1000
0
1987
1988
1989
1990
1991
1992
1993
1994
1995
1996
1997
1998
1999
2000
2001
2002
2003
2004

Monthly Distribution

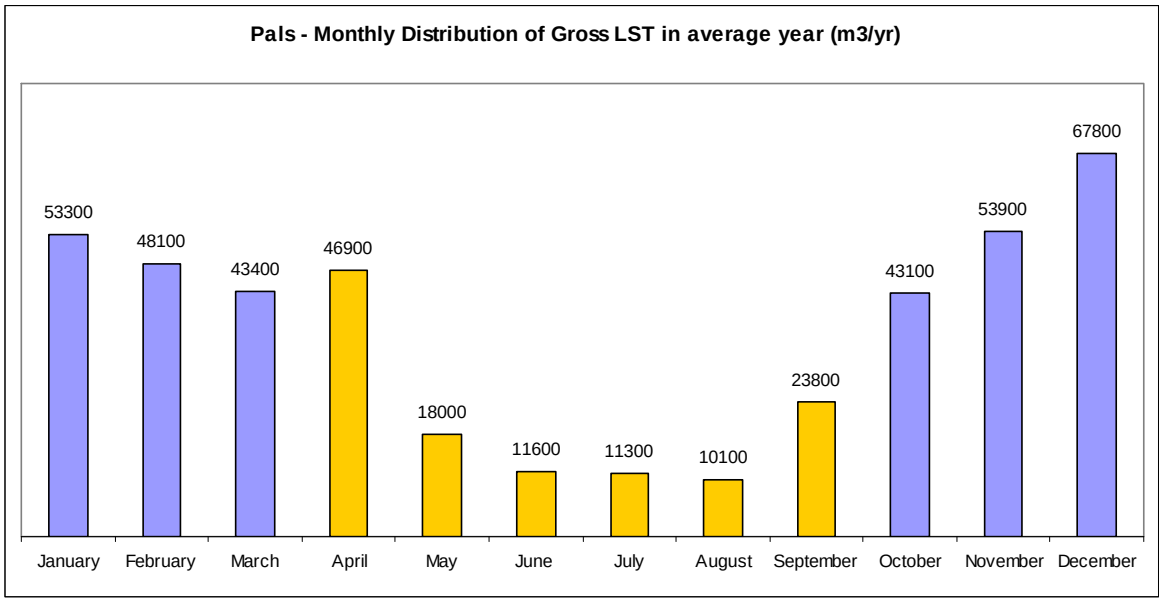

Summer and winter time distribution of Gross LST:

- Oct-Mar: 309 600 (72%)
- Apr-Sep: 121 700 (28%)

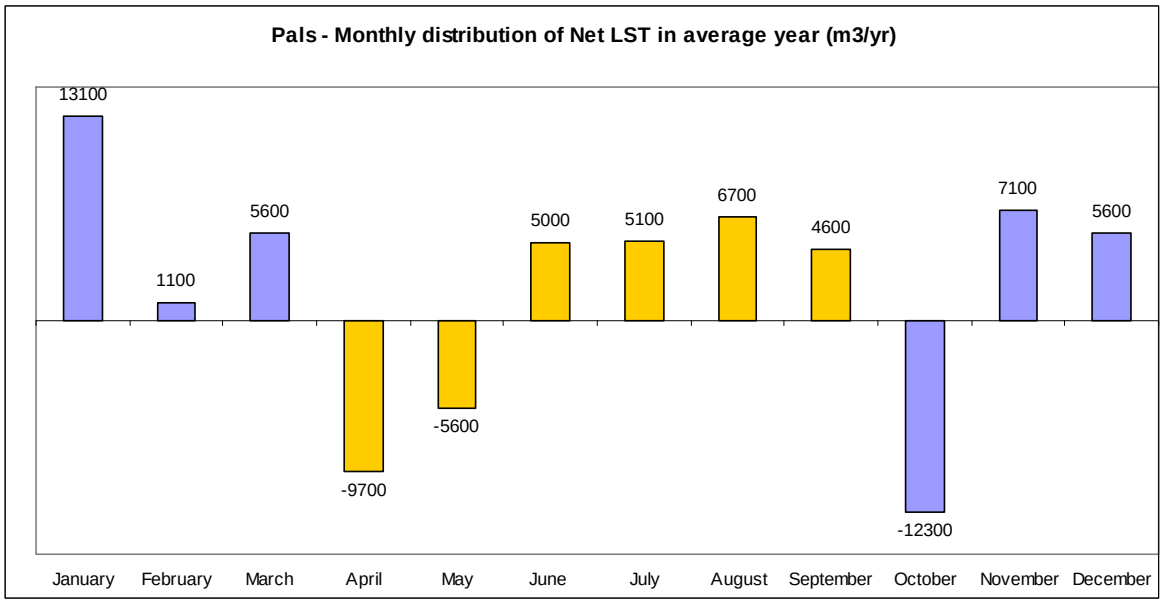

Summer and winter time distribution of Net LST:

- Oct-Mar: 44 800 (55%)
- Apr-Sep: 36 700 (45%)

LST estimation in average year: total, by wave direction and proportion caused by Hs>2m.

Beach	Direction of Littoral Drift	Total LST (m3/year)	Wave direction			Hs		Grain size (mm)	Orientation (º)	Slope
			Wave direction	LST (m3/year)	%	LST (Hs>2m)	%			
L'Estartit	South	341599	NNE	141840	41.5	33227	23.4	0.29	0	0.05
			NE	72582	21.2	26445	36.4			
			ENE	91297	26.7	54386	59.6			
			E	35880	10.5	26552	74.0			
	North	255635	E	17130	6.7	11608	67.8			
			ESE	93335	36.5	50365	54.0			
			SE	115867	45.3	47923	41.4			
			SSE	29303	11.5	8677	29.6			
Pals	South	228917	N	42475	18.6	6613	15.6	0.51	340	0.13
			NNE	148238	64.8	33227	22.4			
			NE	32827	14.3	12639	38.5			
			ENE	5377	2.3	3367	62.6			
	North	202563	ENE	6927	3.4	5217	75.3			
			E	77351	38.2	53031	68.6			
			ESE	73161	36.1	41046	56.1			
			SE	45124	22.3	21095	46.7			

	L'Estartit	**Pals**
Gross LST(m^3/yr)	597 200	431 500
Net LST (m^3/yr)	86 000 (to South)	26 400 (to South)

Sediment Budget using LST Capacity

Figure 3.4 Evaluation of LST along the beach of L'Estartit – Pals. Values in m^3/yr.

Storm contribution: proportion of transport caused by storm conditions (Hs>2m)

	L'Estartit	Pals
South Direction:	45%	29%
North Direction:	50%	62%

Littoral Drift Rose of L'Estartit

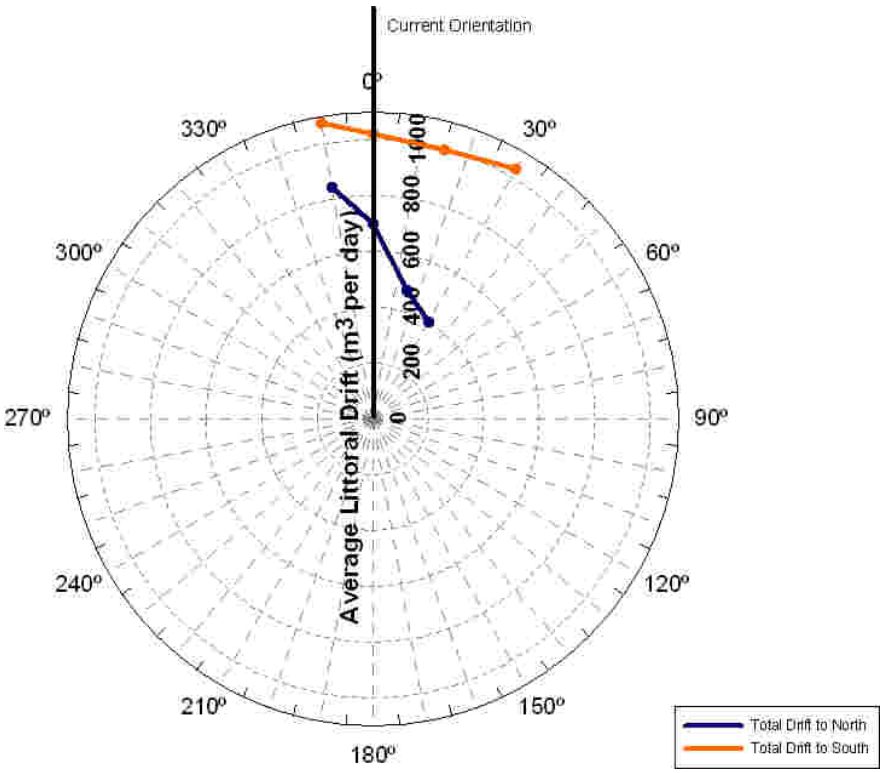

Litoral Drift Rose of Pals

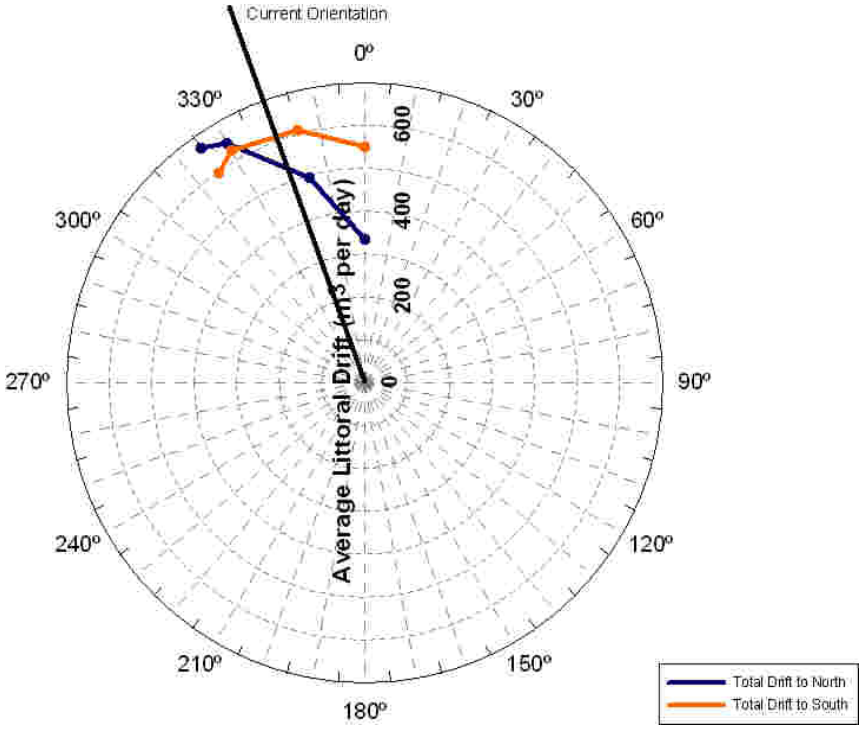

3.2.3 Palamós

Situation of Palamós.

Beach definition and main parameters

Figure 3.5 Definition of the beach of Palamós. Is composed by two stretches: Palamós and Sant Antoni de Calonge.

	Diameter (D_{50})	**Orientation (deg)**	**Slope**	**Wave effective Dir.**
1. Palamós	1.05	108	0.20	169-220
2. Sant Antoni de Calonge	0.88	50	0.20	80-210
Data for Drift Rose:				
- Palamos Drift Rose	0.90	25-130º	0.20	110-220

The beach near the Port of Palamos has a variable orientation that has been approximated in to stretches for a deep analysis. The one named as "Palamos" is closer to the port and the other one ("Sant Antoni de Calonge") is the continuation to the South. The deck of the port avoids a quite wide range of waves to come to the protected part near the port. The part of Sant Antoni de Calonge remains more exposed to those waves. This fact will make the transport to be negative (to the North) at zone close to the port and positive (to the South) as we go away from the protected zone.

PALAMÓS

Longshore Sediment Transport Time Series

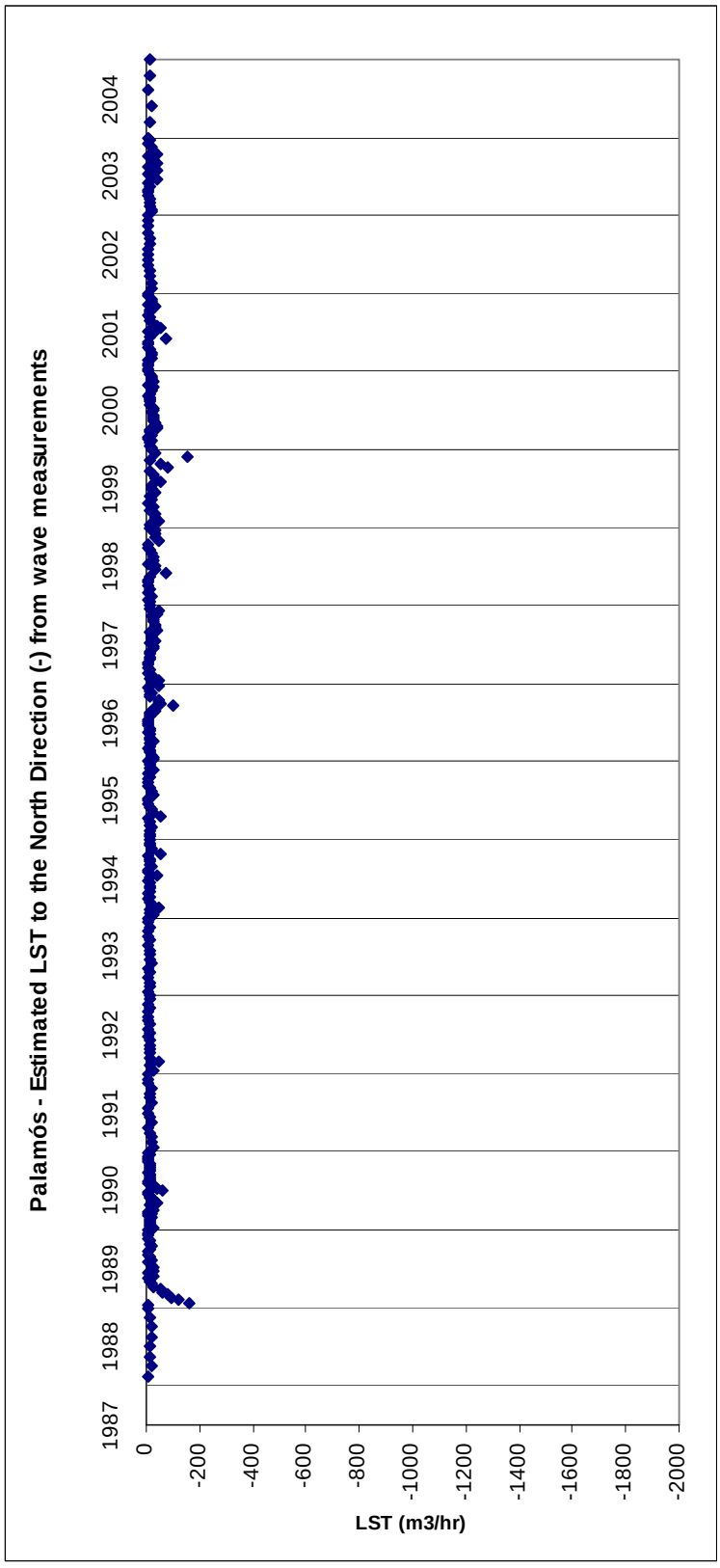

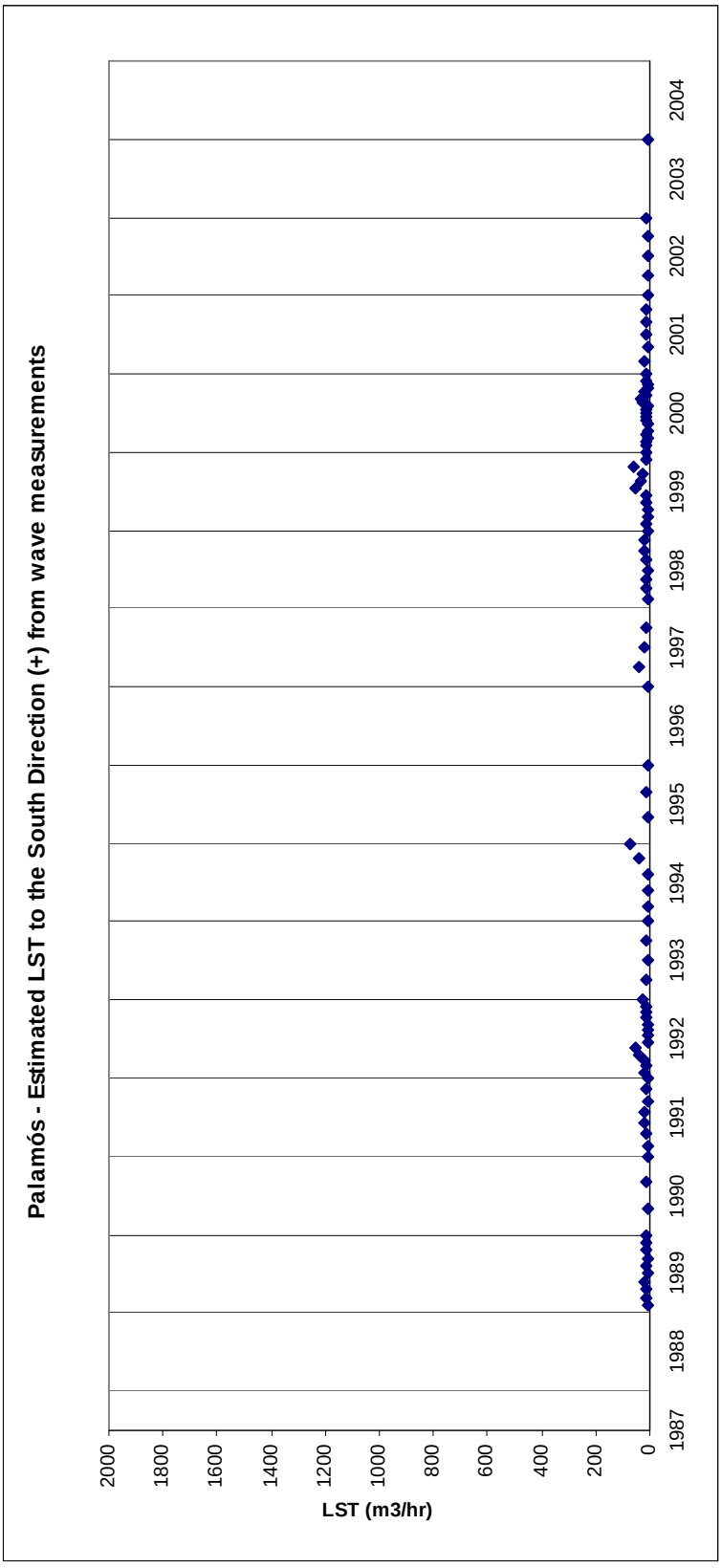
Palamós - Estimated LST to the South Direction (+) from wave measurements
LST (m3/hr)
2000
1800
1600
1400
1200
1000
800
600
400
200
0
1987
1988
1989
1990
1991
1992
1993
1994
1995
1996
1997
1998
1999
2000
2001
2002
2003
2004

Monthly Distribution

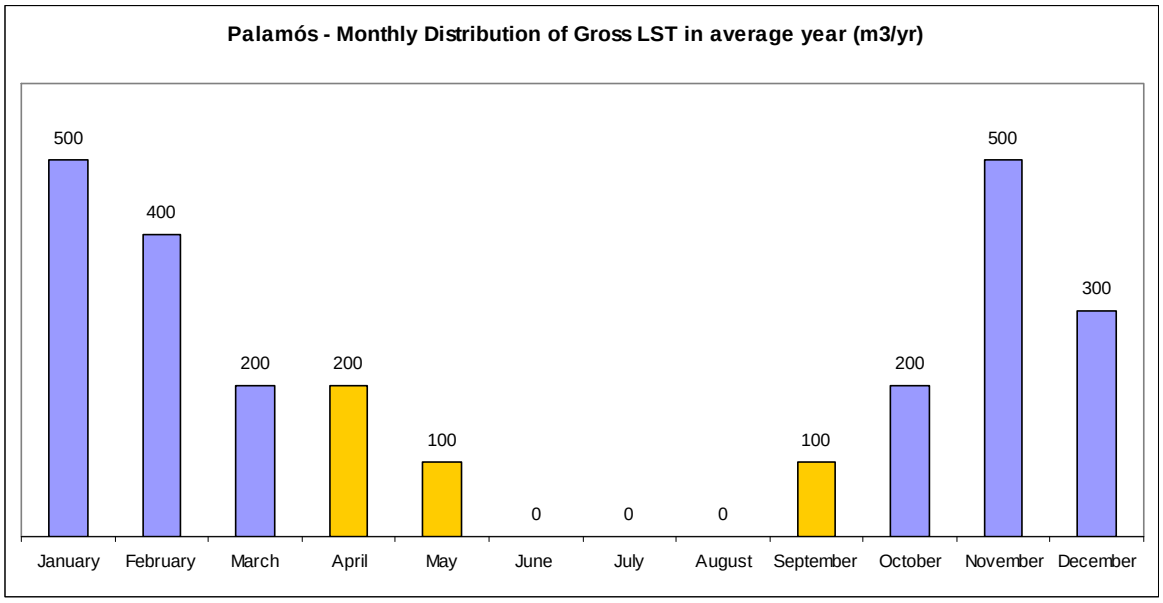

Summer and winter time distribution of Gross LST:

- Oct-Mar: 2100 (84%)
- Apr-Sep: 400 (16%)

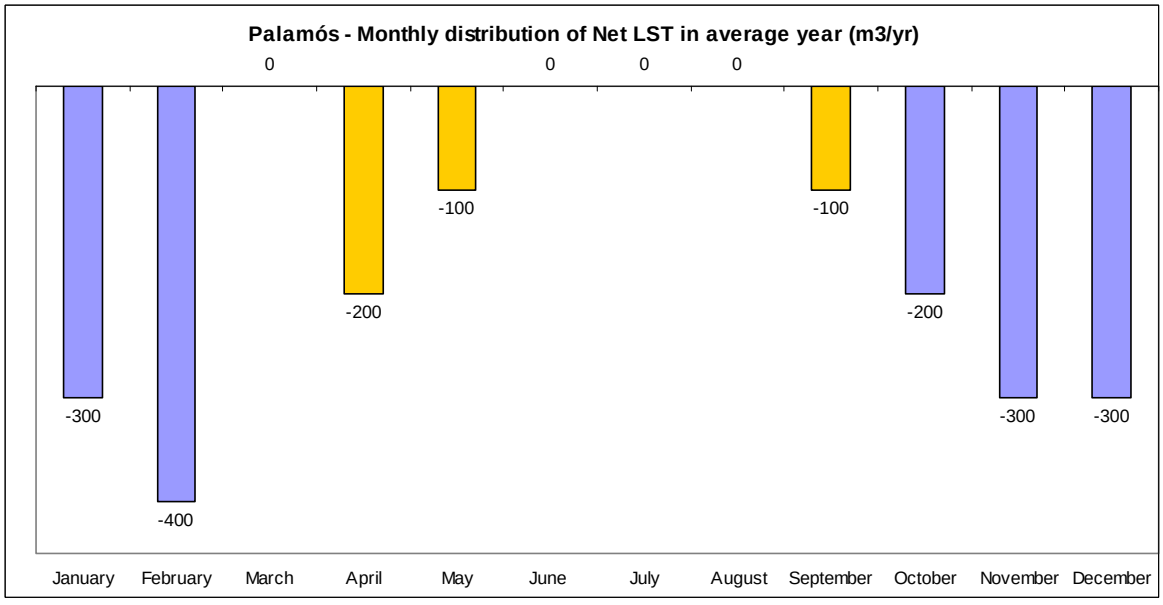

Summer and winter time distribution of Net LST:

- Oct-Mar: 1500 (79%)
- Apr-Sep: 400 (21%)

SANT ANTONI DE CALONGE

Longshore Sediment Transport Time Series

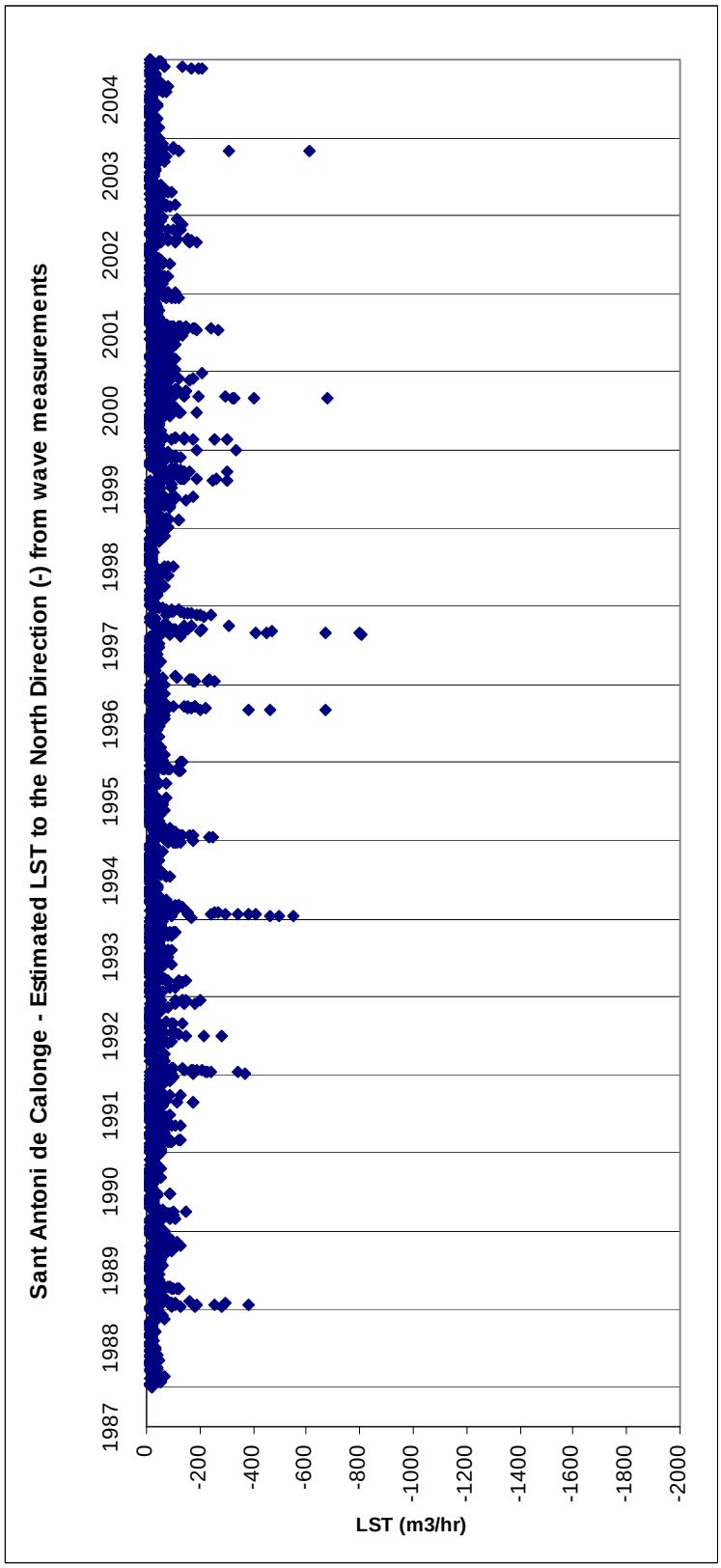

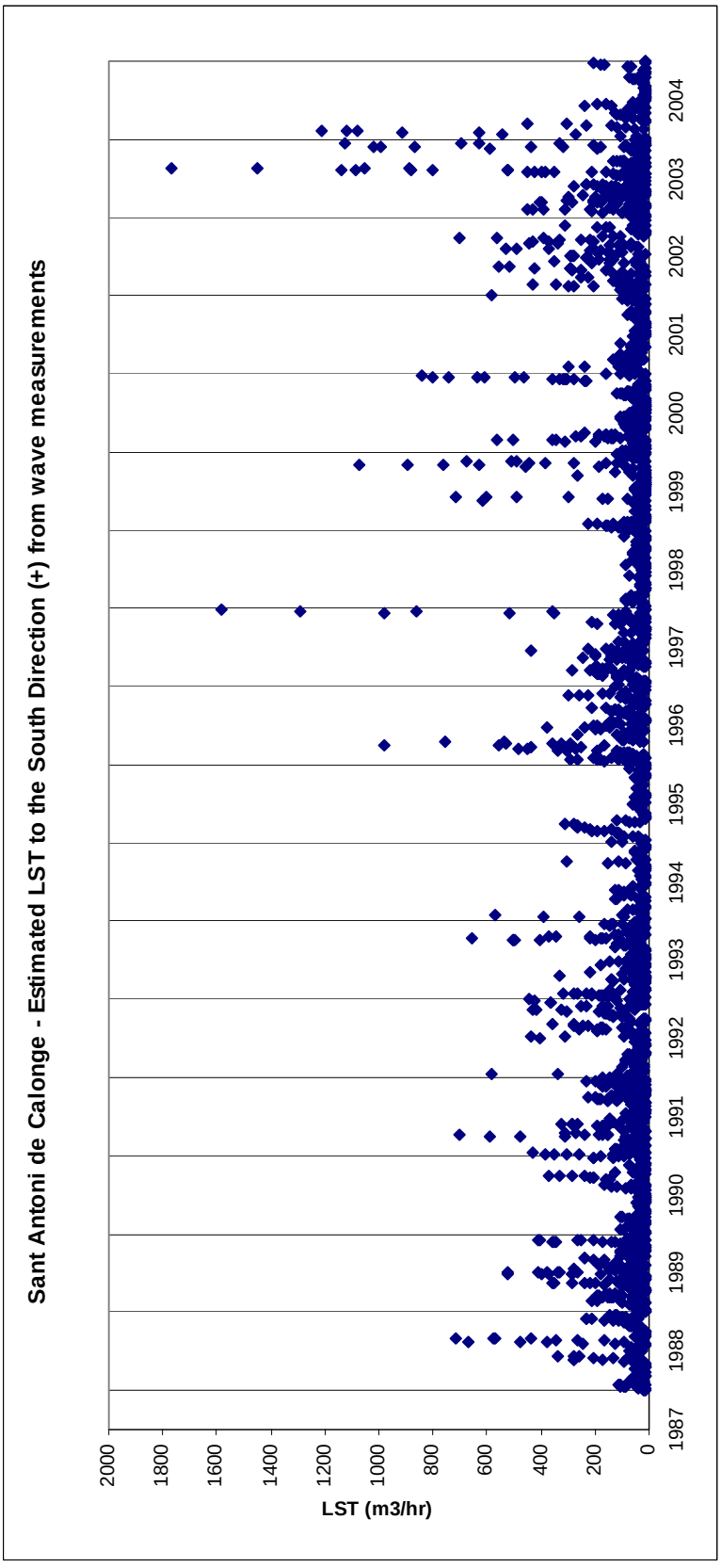
Sant Antoni de Calonge - Estimated LST to the South Direction (+) from wave measurements
LST (m3/hr)
2000
1800
1600
1400
1200
1000
800
600
400
200
0
1987
1988
1989
1990
1991
1992
1993
1994
1995
1996
1997
1998
1999
2000
2001
2002
2003
2004

Monthly Distribution

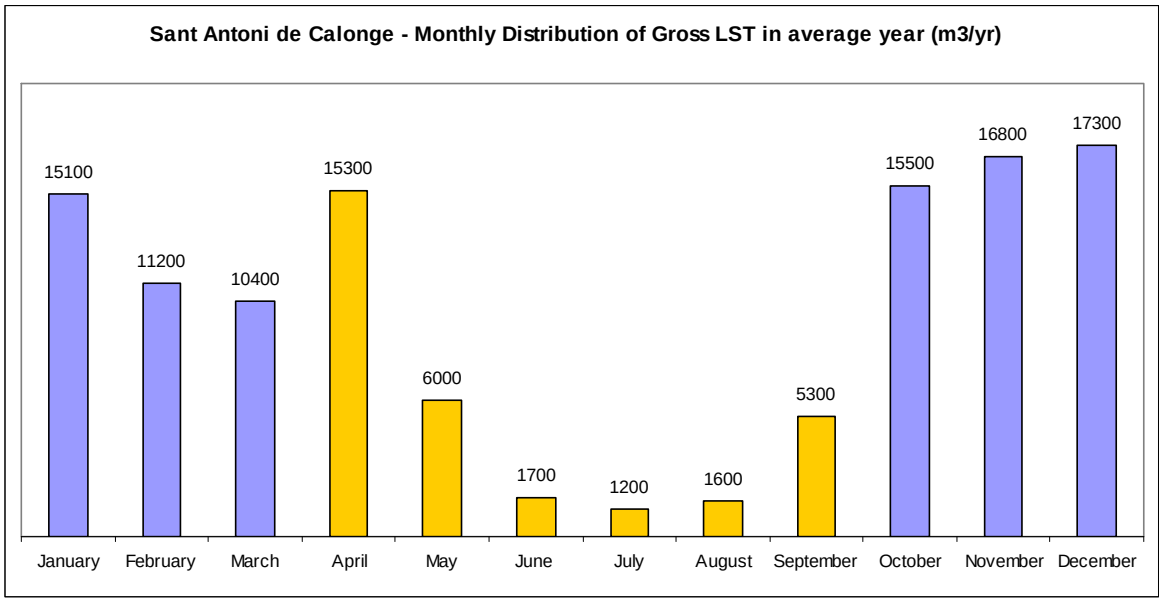

Summer and winter time distribution of Gross LST:

- Oct-Mar: 86 300 (74%)
- Apr-Sep: 31 100 (26%)

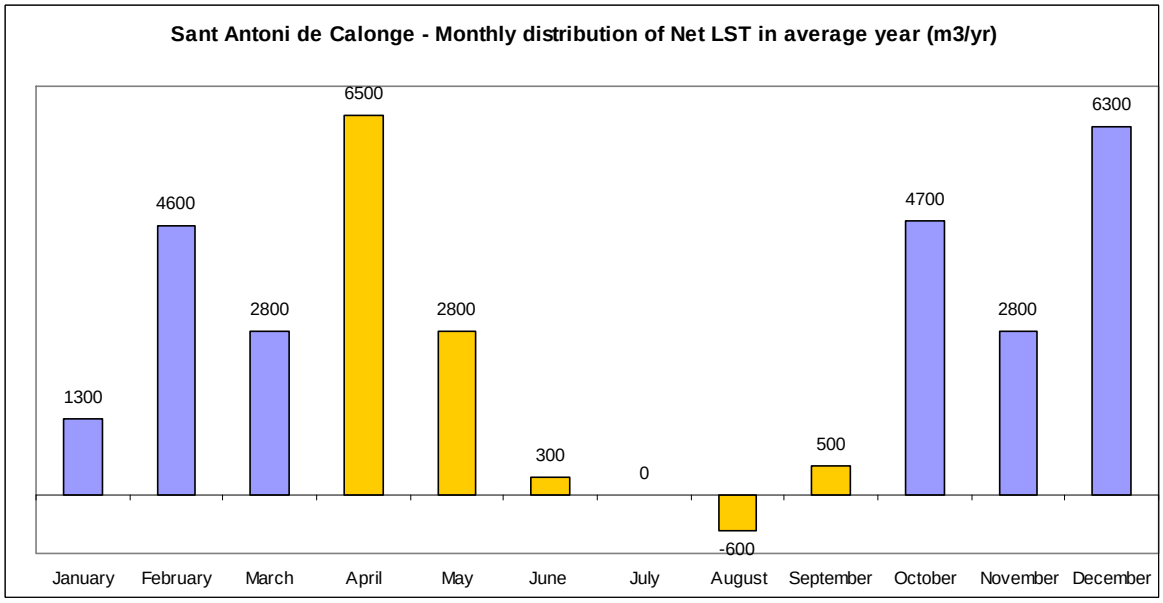

Summer and winter time distribution of Gross LST:

- Oct-Mar: 22 500 (68%)
- Apr-Sep: 10 700 (32%)

LST estimation in average year: total, by wave direction and proportion caused by Hs>2m.

Beach	Direction of Littoral Drift	Total LST (m3/year)	Wave direction			Hs		Grain size (mm)	Orientation (º)	Slope
			Wave direction	LST (m3/year)	%	LST (Hs>2m)	%			
Palamós	West	437	SSW	437	100.0	246	56.3	1.05	108	0.2
	East	2215	SSW	1297	58.6	343	26.4			
			SW	918	41.4	195	21.2			
Sant Antoni de Calonge	South	74642	E	44906	60.2	30978	69.0	0.88	50	0.2
			ESE	24050	32.2	14162	58.9			
			SE	5686	7.6	3341	58.8			
	North	42798	SE	275	0.6	184	66.9			
			SSE	4930	11.5	1845	37.4			
			S	18630	43.5	5731	30.8			
			SSW	18963	44.3	4103	21.6			

	Palamós	Sant Antoni de Calonge
Gross LST(m^3/yr)	2 700	117 400
Net LST (m^3/yr)	-1 800 (to East)	31 800 (to South)

Sediment Budget using LST Capacity

Figure 3.6 Evaluation of LST along Palamós (right) and Sant Antoni de Calonge (left). Values in m^3/yr.

Storm contribution: proportion of transport caused by storm conditions (Hs>2m)

	Palamós	Sant Antoni de Calonge
South Direction:	40%	68%
North Direction:	31%	32%

Palamós Drift Rose

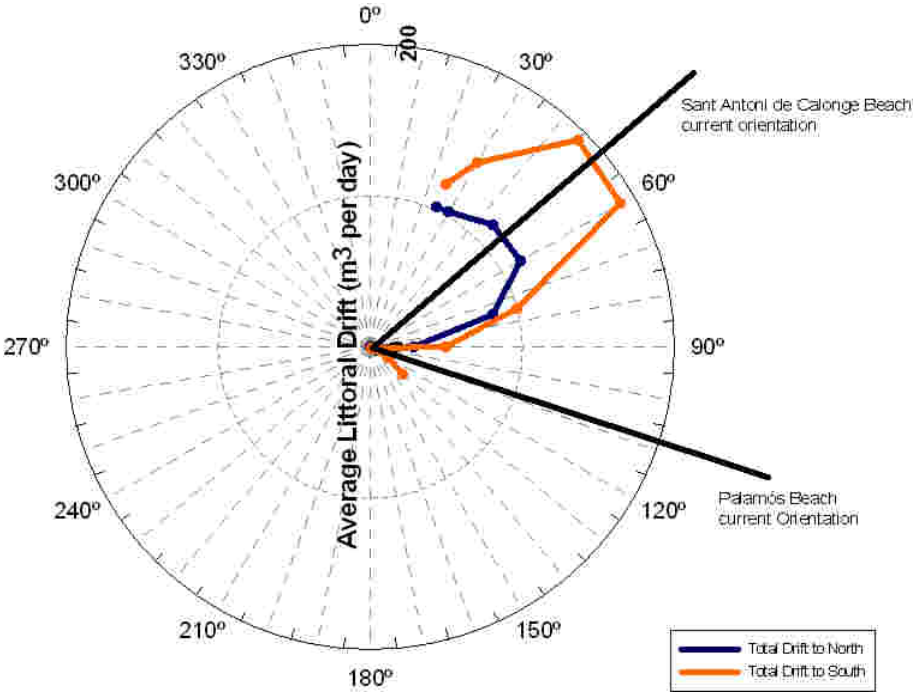

Note that when the orientation producing least transport is impossible to be taken by the beach the real orientation will be a one as far as possible from the orientations in which transport values change rapidly when orientation do. The stretch of Beach of Palamos has clearly adopted an orientation of minimum sediment transport. The other stretch, Sant Antoni de Calonge, takes an orientation of high transport values but little variable with the orientation of the coastline.

3.2.4 Platja d'Aro – Sant Pol

Situation of Platja d'Aro – Sant Pol

Beach definition and main parameters

Figure 3.7 Definition of the beach of Platja d'Aro – Sant Pol.

	Diameter (D_{50})	Orientation (deg))	Slope	Wave effective Dir.
1. Platja d'Aro	0.80	11	0.17	50-190
2. Sant Pol	0.38	37	0.13	101-210
- Platja d'Aro Drift Rose	0.80	0-70º	0.17	50-190

PLATJA D'ARO

Longshore Sediment Transport Time Series

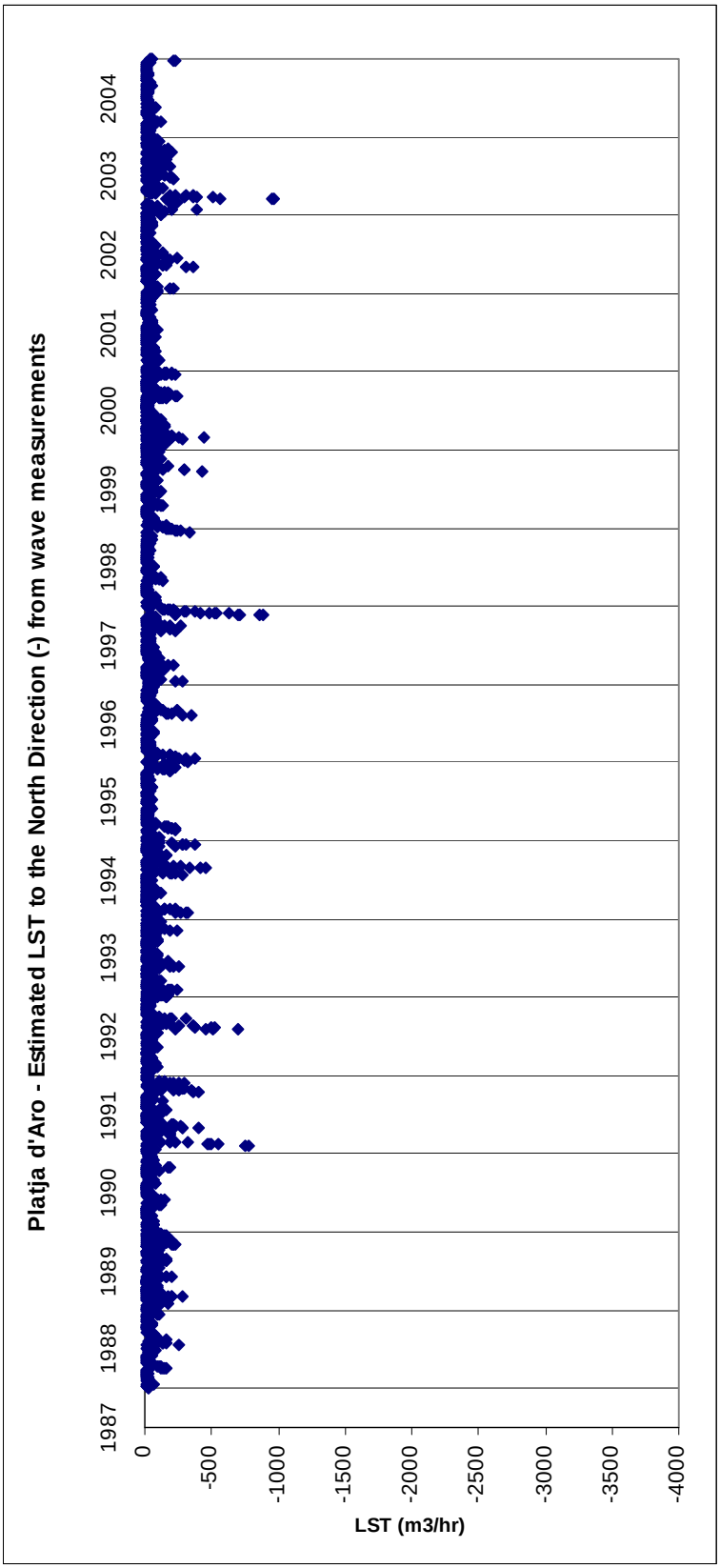

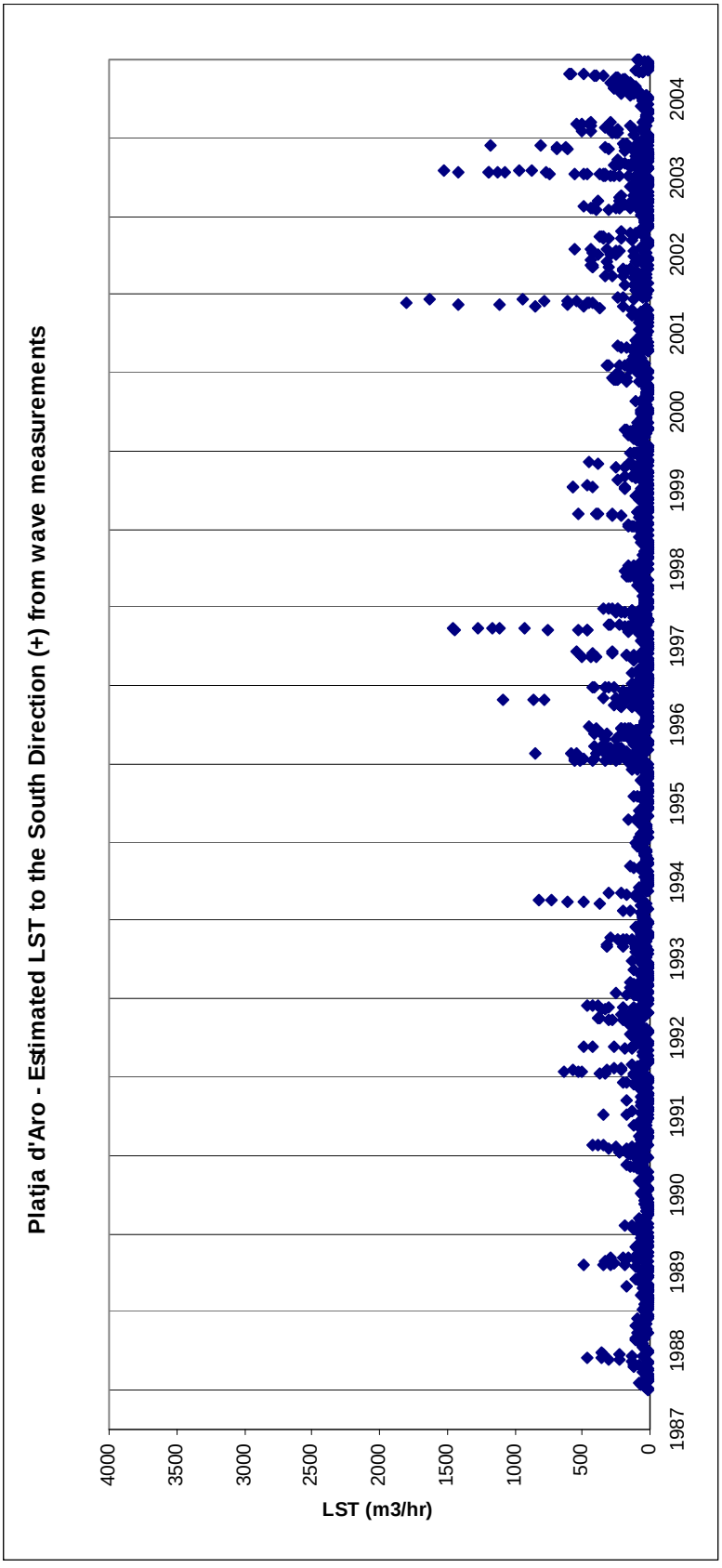
Platja d'Aro - Estimated LST to the South Direction (+) from wave measurements
LST (m3/hr)
4000
3500
3000
2500
2000
1500
1000
500
0
1987
1988
1989
1990
1991
1992
1993
1994
1995
1996
1997
1998
1999
2000
2001
2002
2003
2004

Monthly Distribution

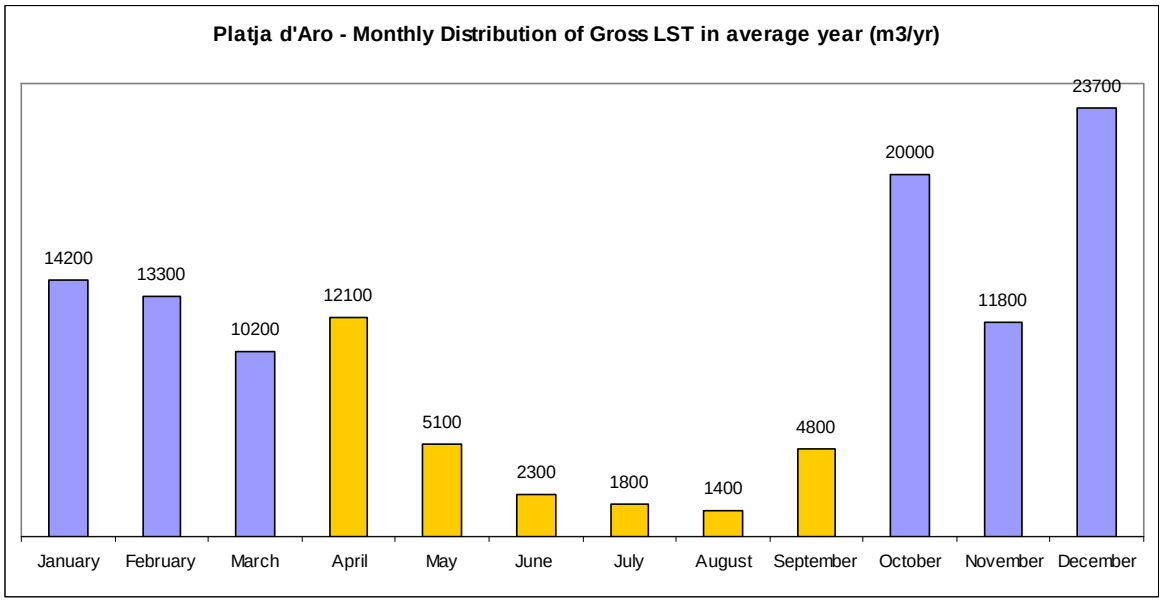

Summer and winter time distribution of Gross LST:

- Oct-Mar: 24 600 (69%)
- Apr-Sep: 11 300 (31%)

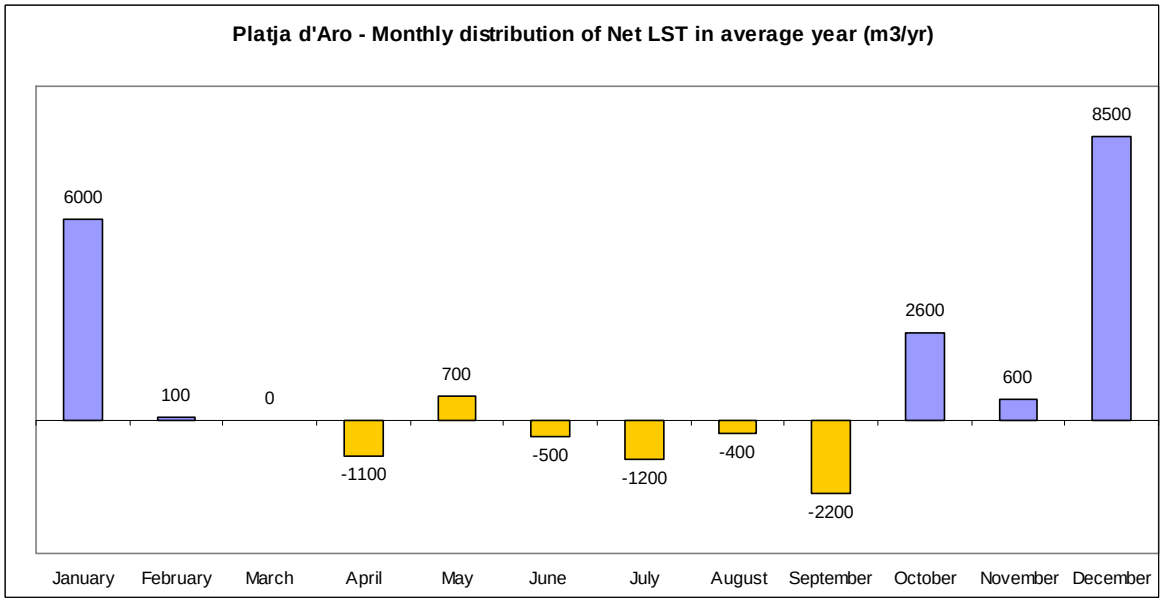

Summer and winter time distribution of Gross LST:

- Oct-Mar: 17 800 (74%)
- Apr-Sep: 6 100 (26%)

SANT POL

Longshore Sediment Transport Time Series

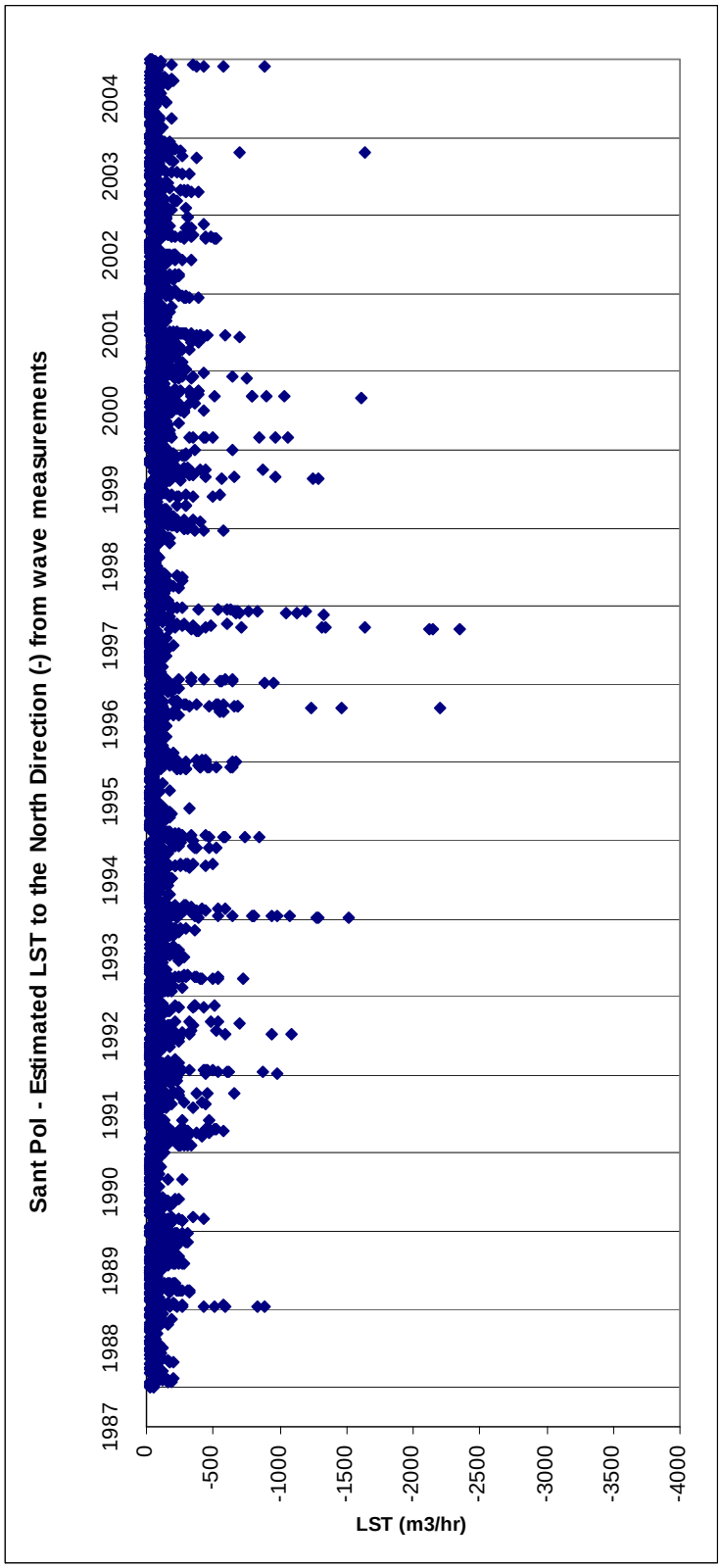

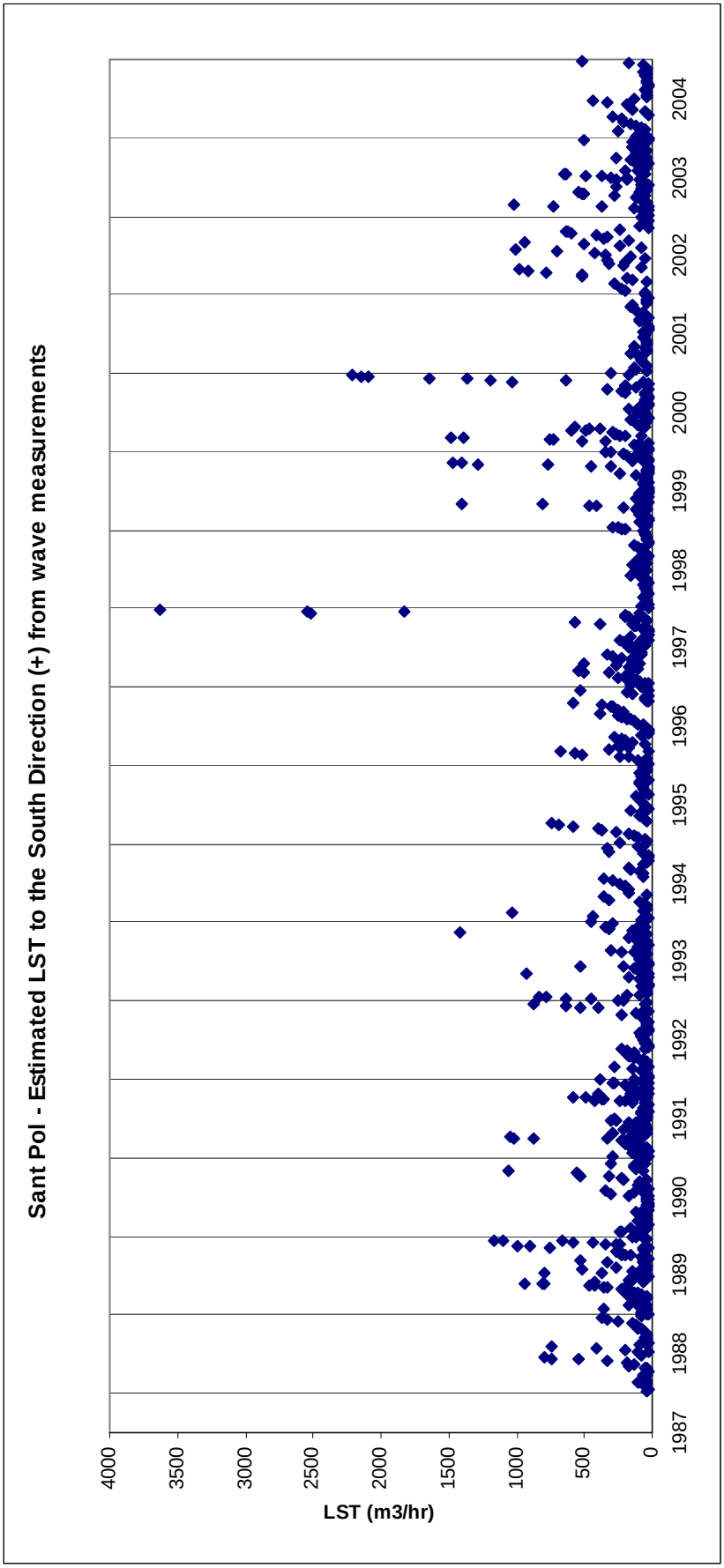
Sant Pol - Estimated LST to the South Direction (+) from wave measurements
LST (m3/hr)
4000
3500
3000
2500
2000
1500
1000
500
0
1987
1988
1989
1990
1991
1992
1993
1994
1995
1996
1997
1998
1999
2000
2001
2002
2003
2004

Monthly Distribution

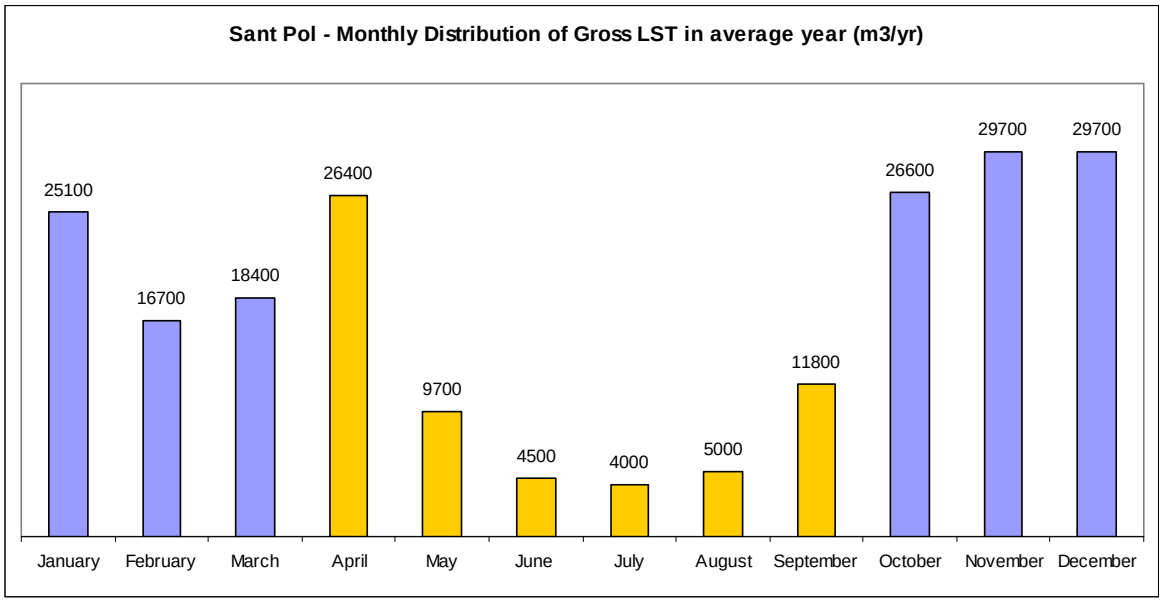

Summer and winter time distribution of Gross LST:

- Oct-Mar: 146 200 (70%)
- Apr-Sep: 61 400 (30%)

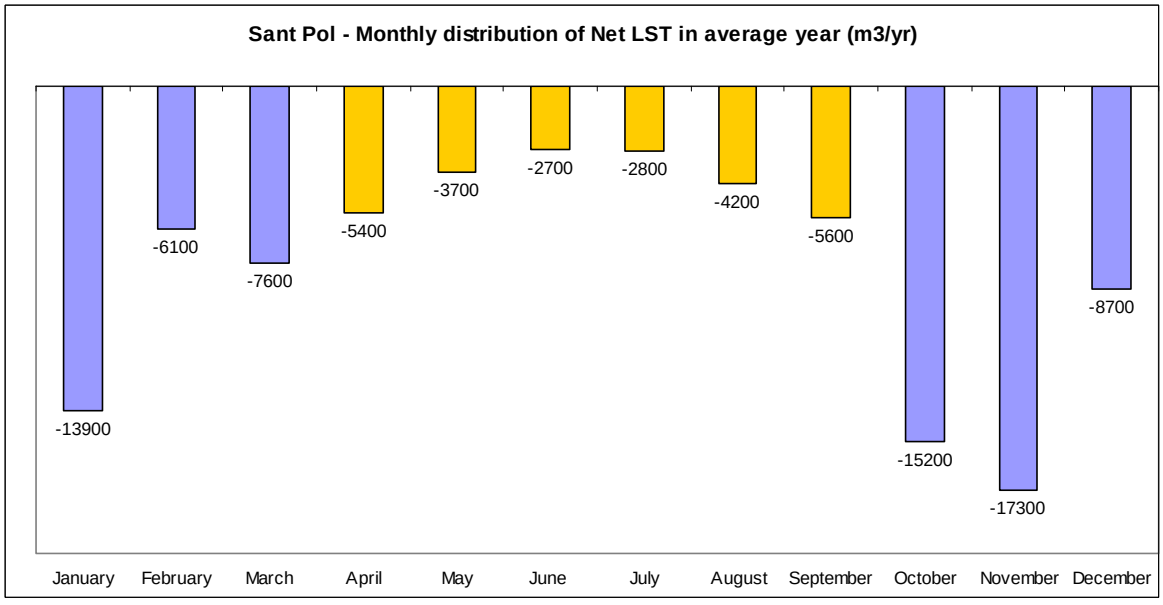

Summer and winter time distribution of Net LST:

- Oct-Mar: 68 800 (74%)
- Apr-Sep: 24 400 (26%)

LST estimation in average year: total, by wave direction and proportion caused by Hs>2m.

Beach	Direction of Littoral Drift	Total LST (m3/year)	Wave direction			Hs		Grain size (mm)	Orientation (º)	Slope
			Wave direction	LST (m3/year)	%	LST (Hs>2m)	%			
Platja d'Aro	South	66933	NE	4849	7.2	1896	39.1	0.8	11	0.17
			ENE	33851	50.6	21100	62.3			
			E	28233	42.2	20703	73.3			
	North	54036	ESE	12455	23.0	7383	59.3			
			SE	27862	51.6	12170	43.7			
			SSE	10631	19.7	3583	33.7			
			S	3088	5.7	1207	39.1			
Sant Pol	South	52285	ESE	51570	98.6	30947	60.0	0.38	37	0.13
			SE	715	1.4	595	83.2			
	North	150318	SE	18552	12.3	7570	40.8			
			SSE	32283	21.5	10040	31.1			
			S	59853	39.8	17294	28.9			
			SSW	39630	26.4	9148	23.1			

	Platja d'Aro	**Sant Pol**
Gross LST(m^3/yr)	121 000	202 600
Net LST (m^3/yr)	12 900 (to South)	-98 000 (to North)

Sediment Budget using LST Capacity

The evaluation in the beach of Sant Pol has not been carried out. The reason is that this beach is placed in a narrow cove that goes deep into the land. That probably will make the waves to enter straight in the cove and to impact always in a perpendicular way over the beach. Therefore, the theoretical LST calculated according to the formulas won't exist in practice. We can expect this beach to remain in the same position with little alternative displacement to one side and to the other through the year.

Figure 3.8 Evaluation of LST along Platja d'Aro.Values m^3/yr.

Storm contribution: proportion of transport caused by storm conditions (Hs>2m)

	Platja d'Aro	Sant Pol
South Direction:	68%	65%
North Direction:	49%	33%

Platja d'Aro Drift Rose

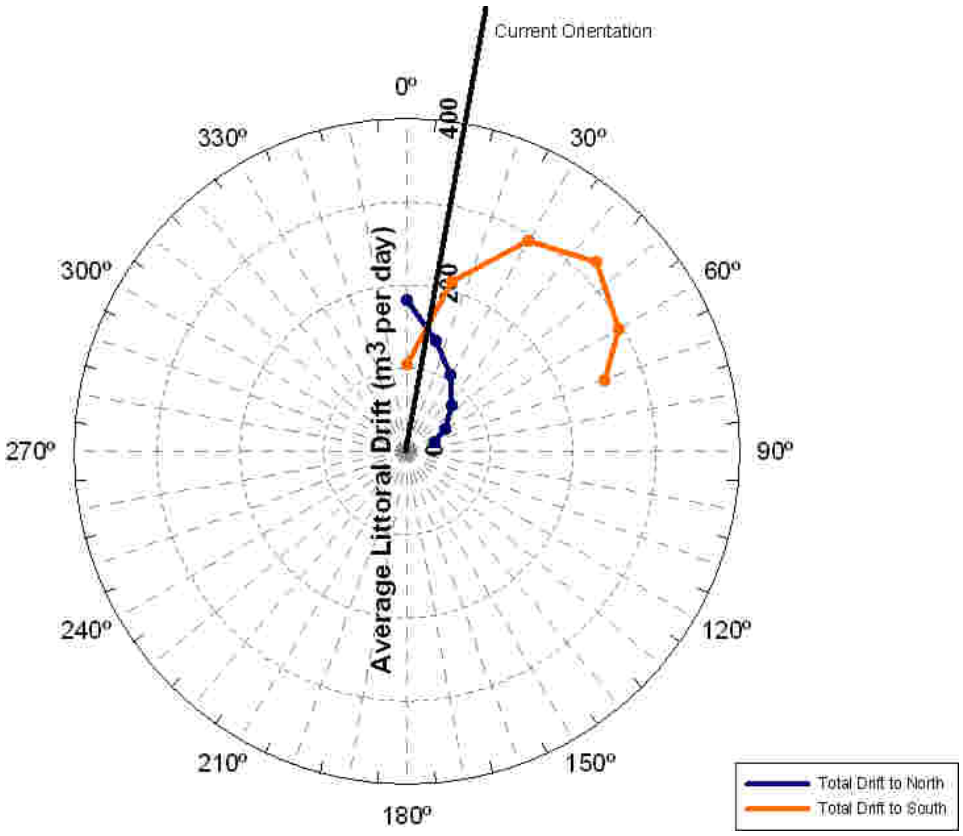

Platja d'Aro is a straight beach exposed to almost all wind directions coming from the sea. There are no big obstacles in its ends nor anything susceptible to produce unpredictable changes on waves characteristics. In such conditions the beach takes the most natural and simple shape and orientation, resulting this the one producing least net total transport.

3.2.5 Lloret de Mar – Santa Cristina

Situation of El Lloret de Mar.

Beach definition and main parameters

Figure 3.9 Definition of the beach of Lloret de Mar – Santa Cristina.

	Diameter (D_{50})	**Orientation (deg)**	**Slope**	**Wave effective Dir.**
1. Lloret north	1.46	63	0.2	80-230
2. Lloret south	1.50	63	0.2	85-225
3. Santa Cristina	0.81	53	0.17	70-225
Data for Drift Rose:				
- Lloret Drift Rose	1.48	30-100º	0.2	80-230

LLORET NORTH

Longshore Sediment Transport Time Series

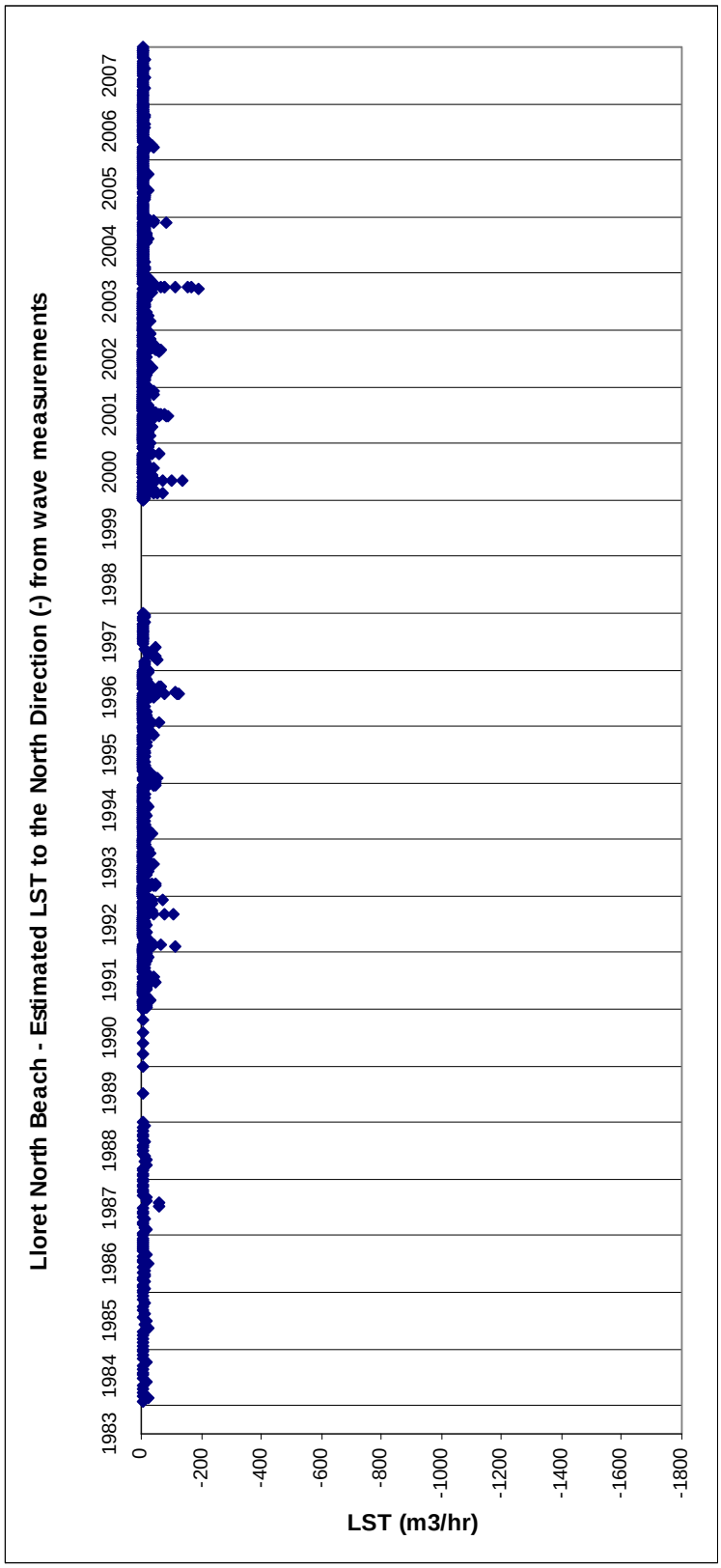

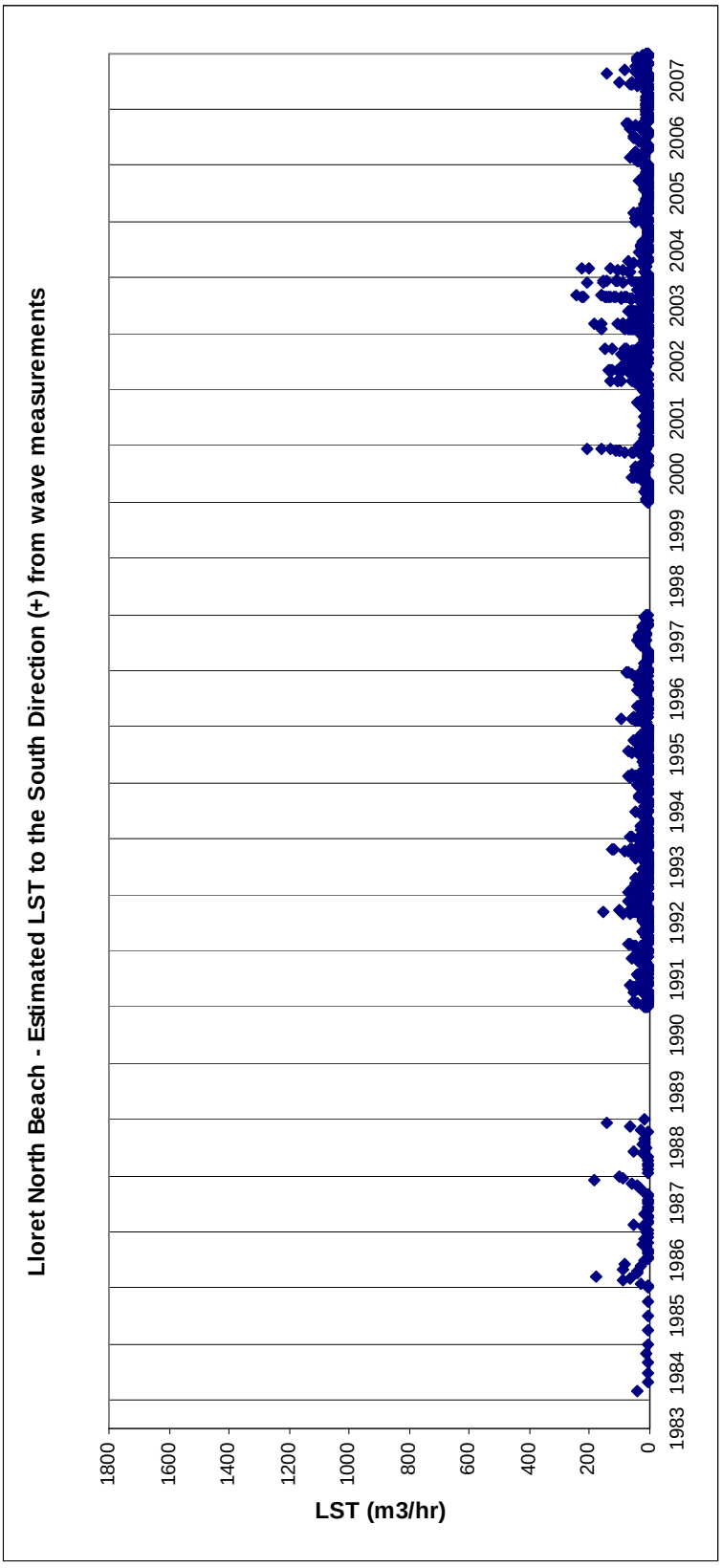
Lloret North Beach - Estimated LST to the South Direction (+) from wave measurements
LST (m3/hr)
1800
1600
1400
1200
1000
800
600
400
200
0
1983
1984
1985
1986
1987
1988
1989
1990
1991
1992
1993
1994
1995
1996
1997
1998
1999
2000
2001
2002
2003
2004
2005
2006
2007

Monthly Distribution

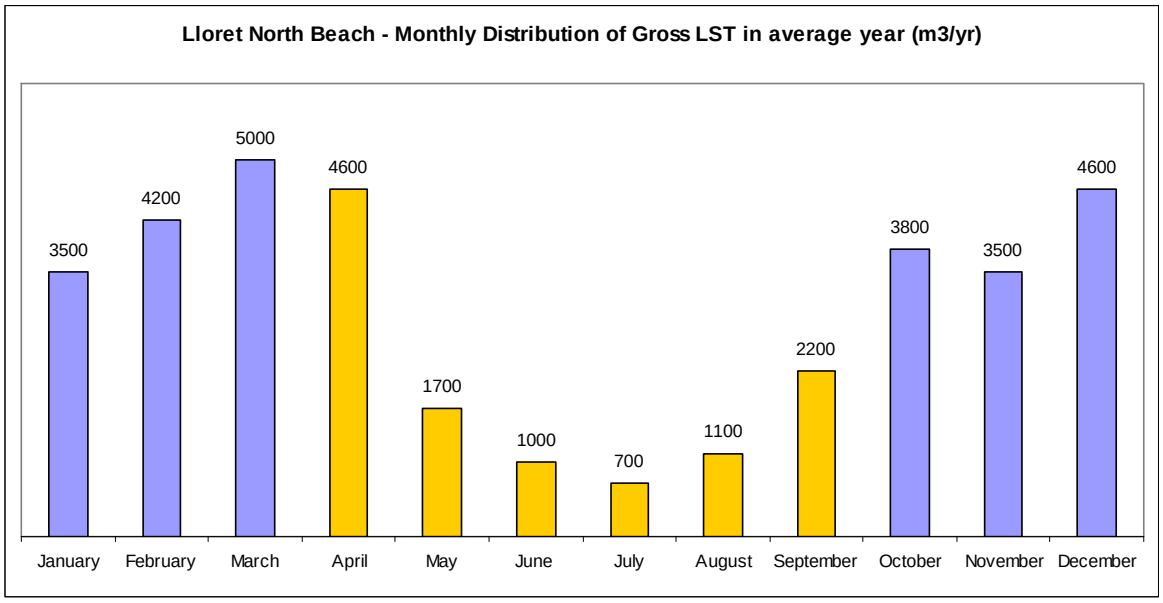

Summer and winter time distribution of Gross LST:

- Oct-Mar: 24 600 (69%)
- Apr-Sep: 11 300 (31%)

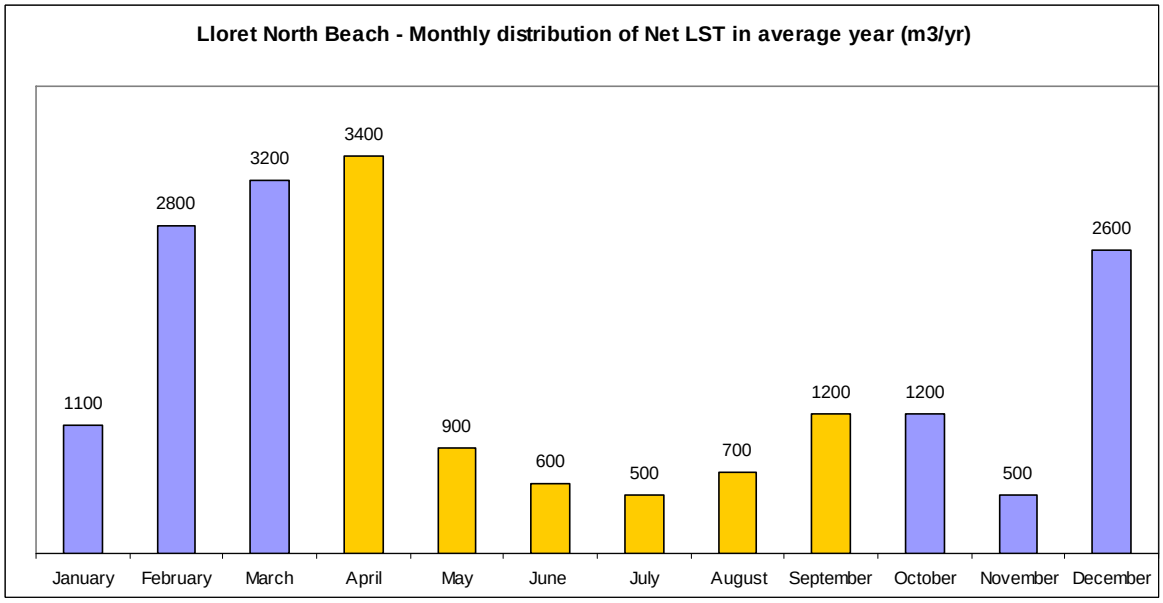

Summer and winter time distribution of Net LST:

- Oct-Mar: 11 400 (61%)
- Apr-Sep: 7 300 (39%)

LLORET SOUTH

Longshore Sediment Transport Time Series

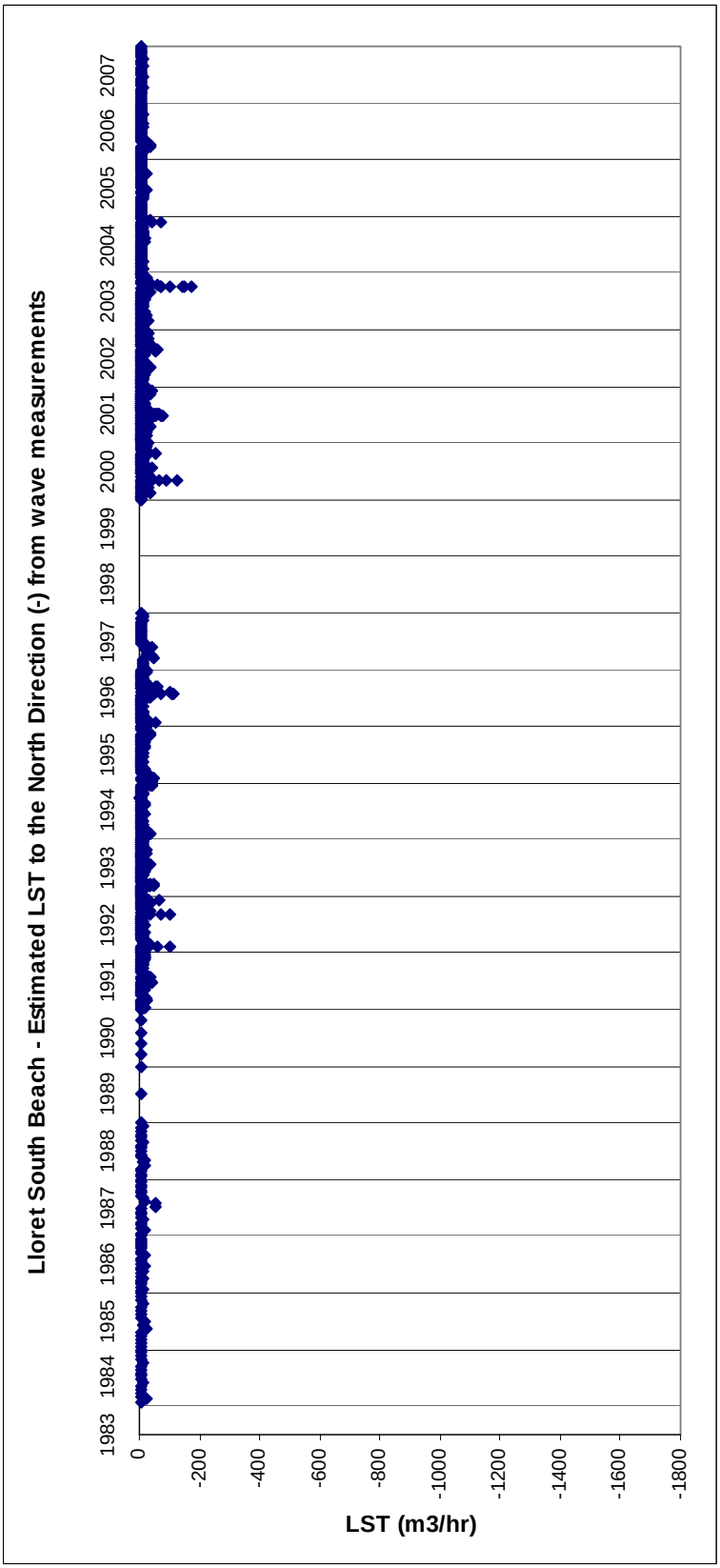

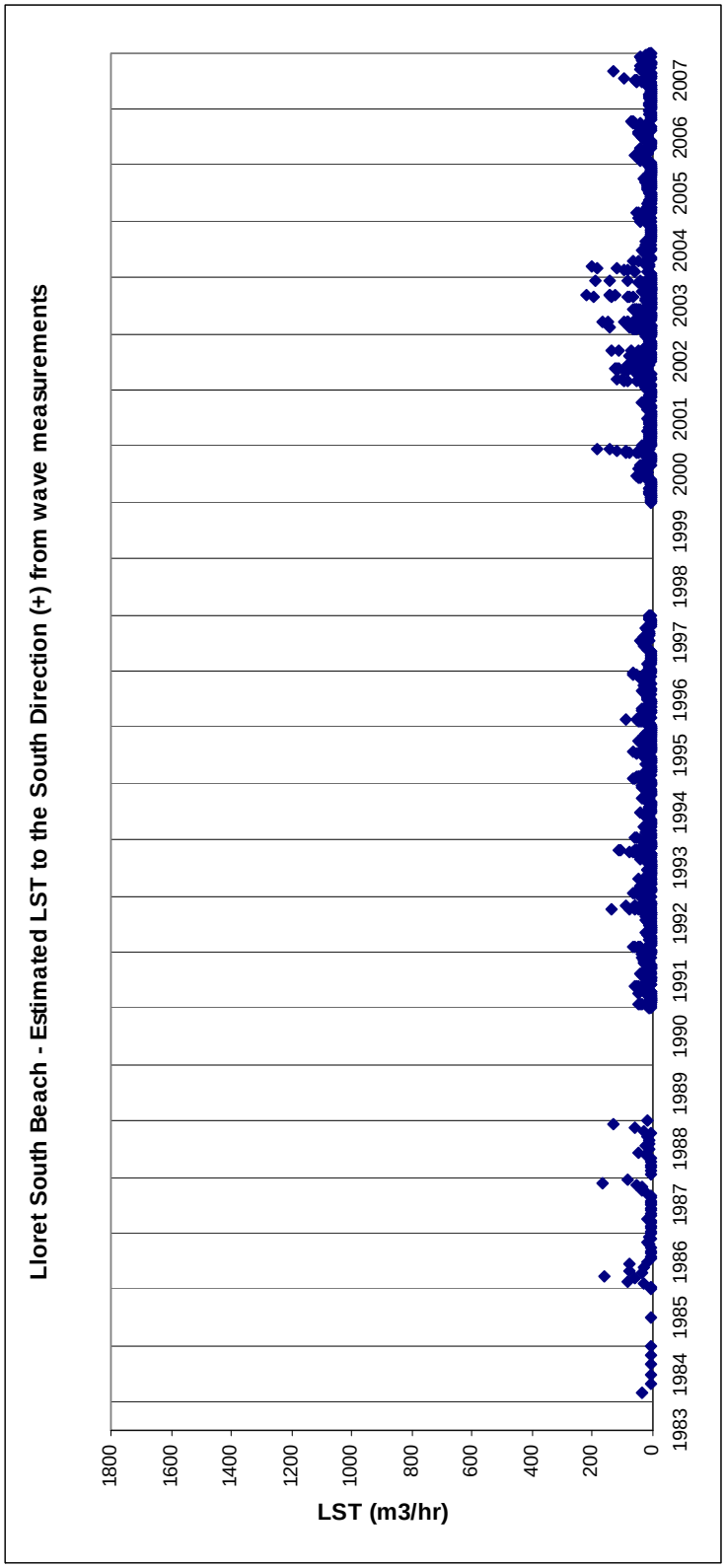
Lloret South Beach - Estimated LST to the South Direction (+) from wave measurements
1800
1600
1400
1200
1000
800
600
400
200
0
LST (m3/hr)
1983
1984
1985
1986
1987
1988
1989
1990
1991
1992
1993
1994
1995
1996
1997
1998
1999
2000
2001
2002
2003
2004
2005
2006
2007

Monthly Distribution

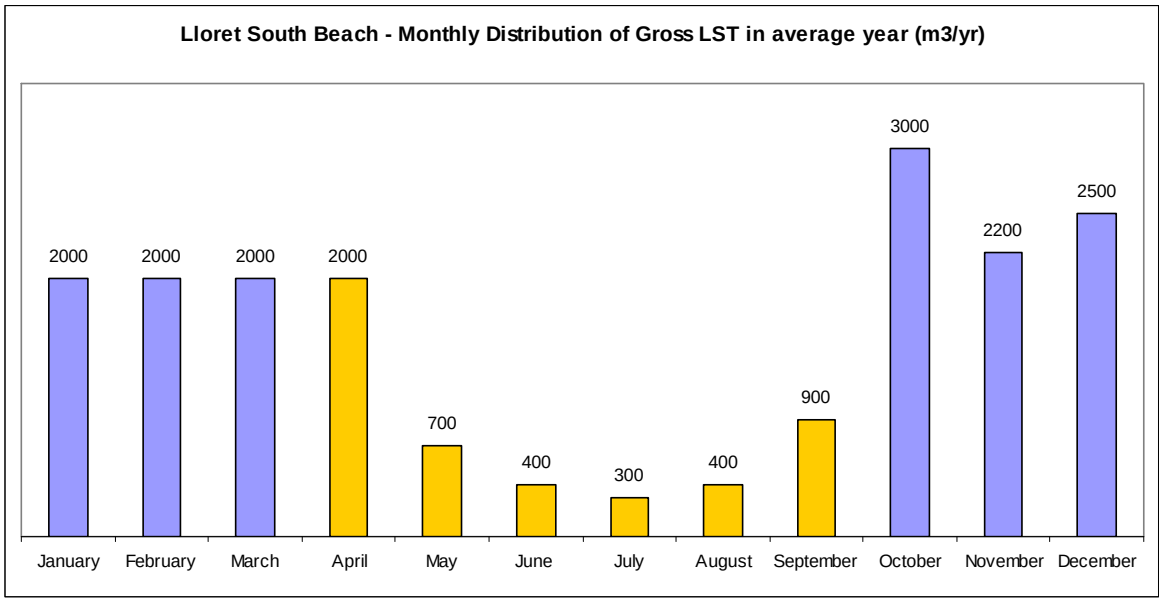

Summer and winter time distribution of Gross LST:

- Oct-Mar: 13 700 (69%)
- Apr-Sep: 4 700 (31%)

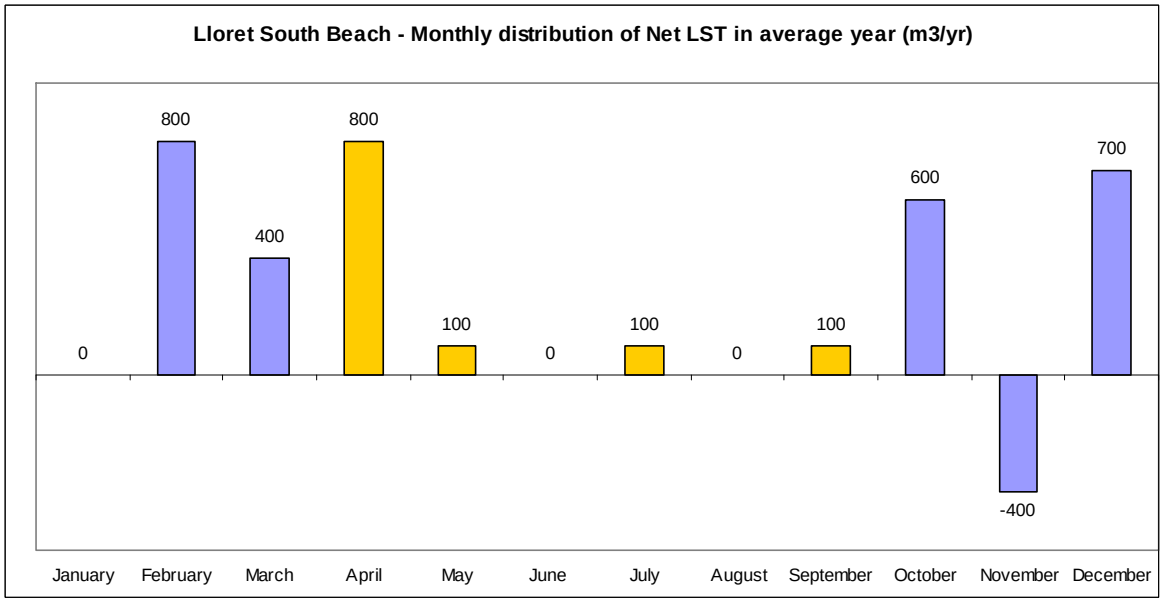

Summer and winter time distribution of Gross LST:

- Oct-Mar: 2 900 (73%)
- Apr-Sep: 1 100 (28%)

SANTA CRISTINA

Longshore Sediment Transport Time Series

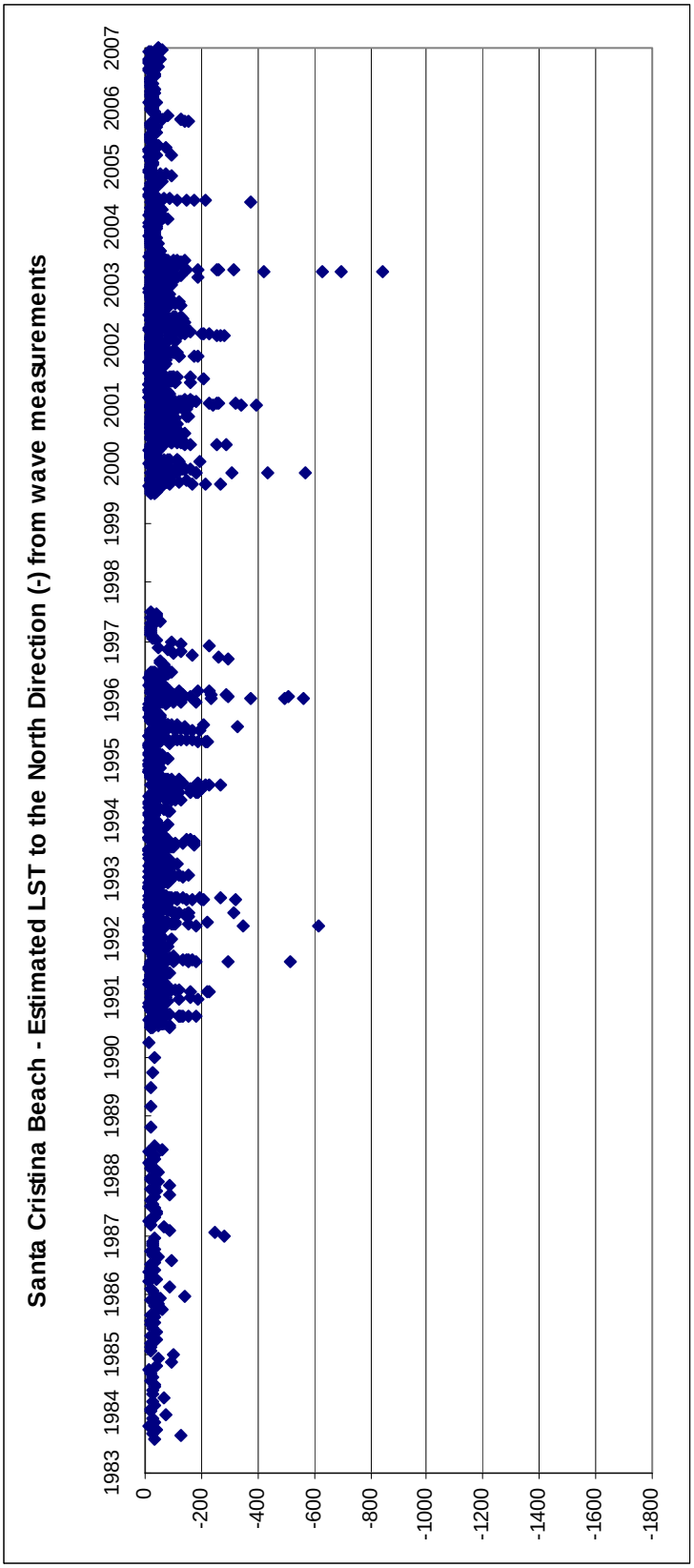

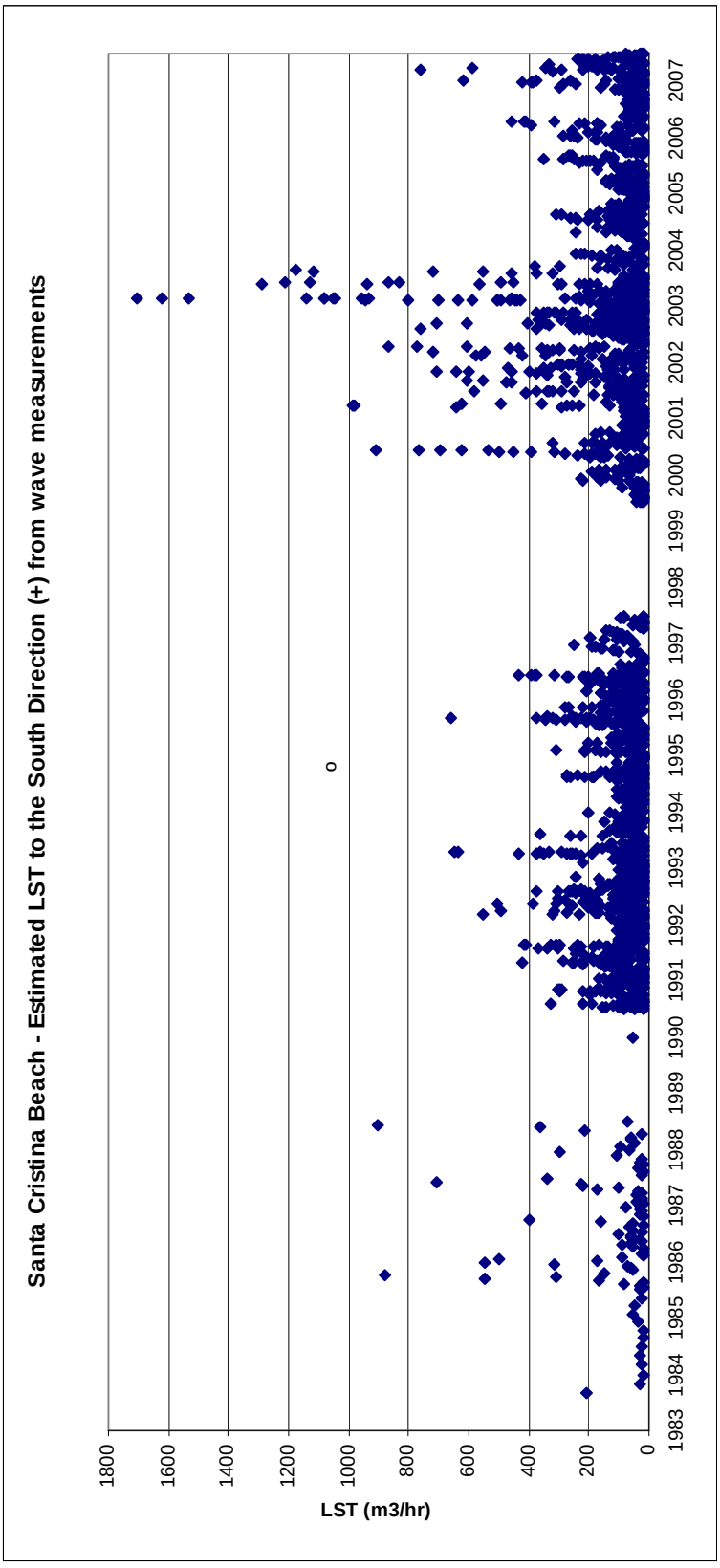
Santa Cristina Beach - Estimated LST to the South Direction (+) from wave measurements
LST (m3/hr)
1800
1600
1400
1200
1000
800
600
400
200
0
1983
1984
1985
1986
1987
1988
1989
1990
1991
1992
1993
1994
1995
1996
1997
1998
1999
2000
2001
2002
2003
2004
2005
2006
2007

Monthly Distribution

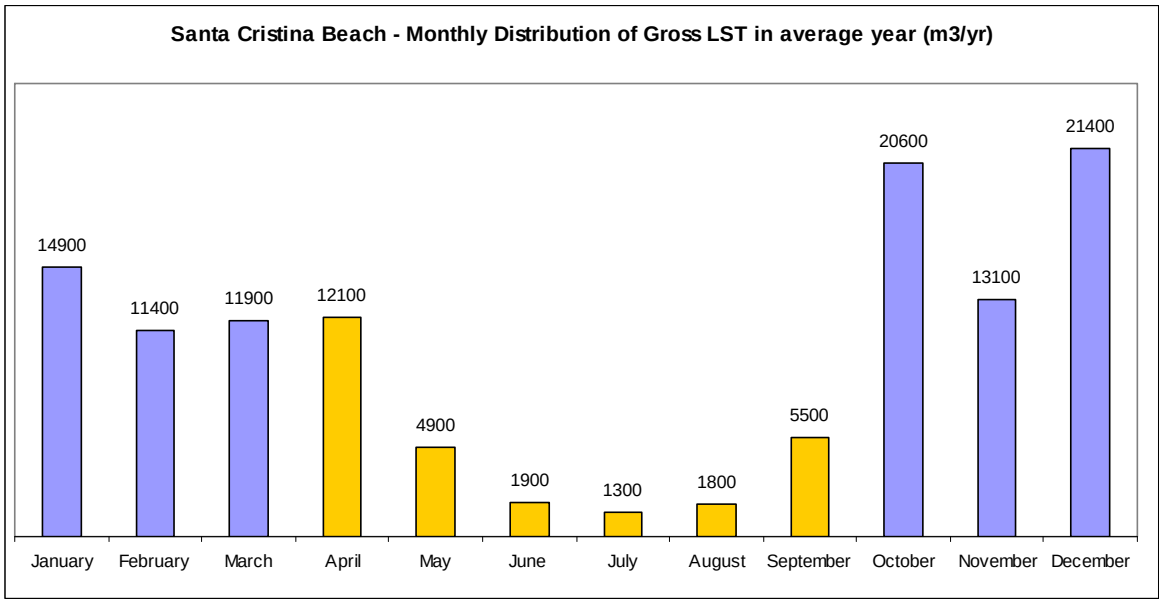

Summer and winter time distribution of Gross LST:

- Oct-Mar: 93 300 (69%)
- Apr-Sep: 27 500 (31%)

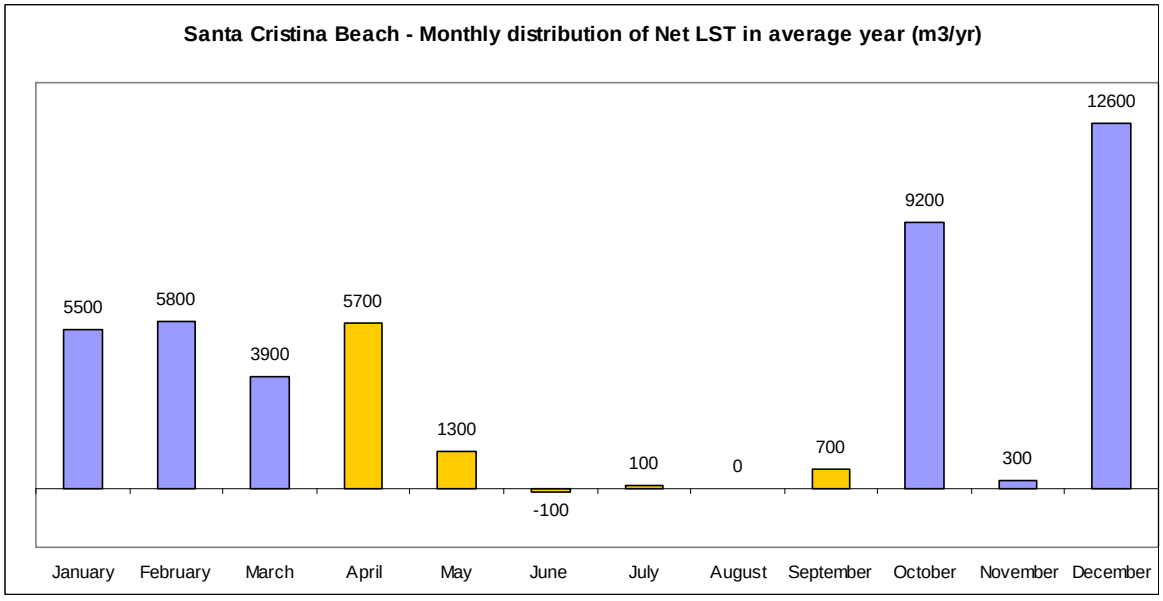

Summer and winter time distribution of Net LST:

- Oct-Mar: 37 300 (83%)
- Apr-Sep: 7 900 (17%)

LST estimation in average year: total, by wave direction and proportion caused by Hs>2m.

Beach	Direction of Littoral Drift	Total LST (m3/year)	Wave direction			Hs		Grain size (mm)	Orientation (º)	Slope
			Wave direction	LST (m3/year)	%	LST (Hs>2m)	%			
Lloret North	South	13450	E	5923	44.0	3561	60.1	1.46	63	0.2
			ESE	5230	38.9	2447	46.8			
			SE	2280	17.0	1103	48.4			
			SSE	17	0.1	5	29.4			
	North	8511	SSE	123	1.4	27	22.0			
			S	1138	13.4	252	22.1			
			SSW	6000	70.5	1460	24.3			
			SW	1250	14.7	169	13.5			
Lloret South	South	10769	E	3959	36.8	2290	57.8	1.5	63	0.2
			ESE	4732	43.9	2214	46.8			
			SE	2063	19.2	998	48.4			
			SSE	15	0.1	5	33.3			
	North	7620	SSE	115	1.5	24	20.9			
			S	1026	13.5	228	22.2			
			SSW	5429	71.2	1321	24.3			
			SW	1050	13.8	149	14.2			
Santa Cristina	South	82255	ENE	10493	12.8	5924	56.5	0.81	53	0.17
			E	41638	50.6	24518	58.9			
			ESE	23605	28.7	2265	9.6			
			SE	6519	7.9	3559	54.6			
	North	37766	SSE	2403	6.4	443	18.4			
			S	7378	19.5	1432	19.4			
			SSW	25028	66.3	6201	24.8			
			SW	2957	7.8	498	16.8			

	Lloret North	**Lloret South**	**Santa cristina .**
Gross LST(m^3/yr)	22 000	18 400	120 000
Net LST (m^3/yr)	4 900 (to South)	3 100 (to South)	44 500 (to South)

Sediment Budget using LST Capacity

Figure 3.10 Evaluation of LST along the zone of Lloret – Santa Cristina. Values in m^3/yr.

Storm contribution: proportion of transport caused by storm conditions (Hs>2m)

	Lloret North	Lloret South	Santa Cristina .
South Direction	53%	51%	55%
North Direction	23%	23%	23%

Lloret Drift Rose

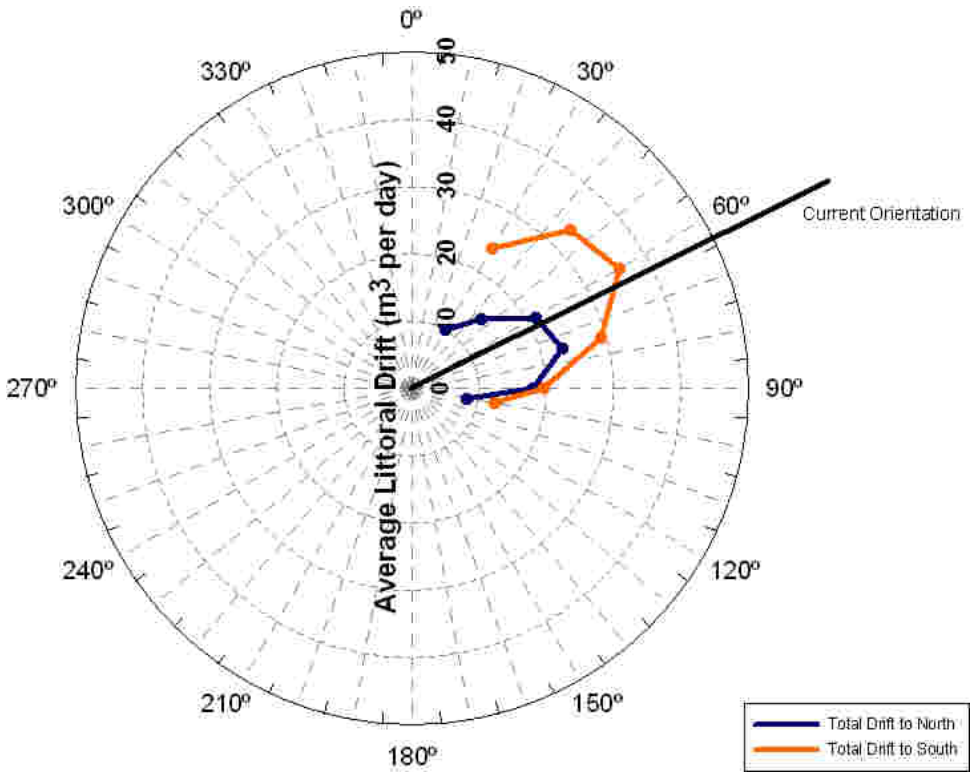

Lloret is not an equilibrium beach. To be more or less stable this beach should be oriented 30º to the North (according to the rose it'll be also possible with an orientation of about 110º but that won't occur in practice, as sediment transport is largely to the south and hence the orientation trends to approach to the North). From the picture (Figure 3.10) it can be noticed that the beach width is increasing in the south part and decreasing in the north. The natural way for this beach (if there weren't limitations) would be to continue this process until the orientation became about 30º. That would mean an important decreasing of the width in the central zone and the complete

3.2.6 Blanes – Arenys de Mar

Situation of the strecht Blanes – Arenys de Mar.

As this unit is quite large its definition is presented divided into several stretches: Blanes – Tordera, Tordera – Calella and Calella – Arenys. It has been considered that there is a free pass of sediment from one stretch to the other.

Beach definition and main parameters

Figure 3.11 Definition of the beach of Blanes – Arenys.

Stretch Blanes – Tordera

Figure 3.12 Definition of the beach of Blanes – Arenys. Stretch Blanes – Tordera (S'Abanell).

Stretch Tordera – Calella

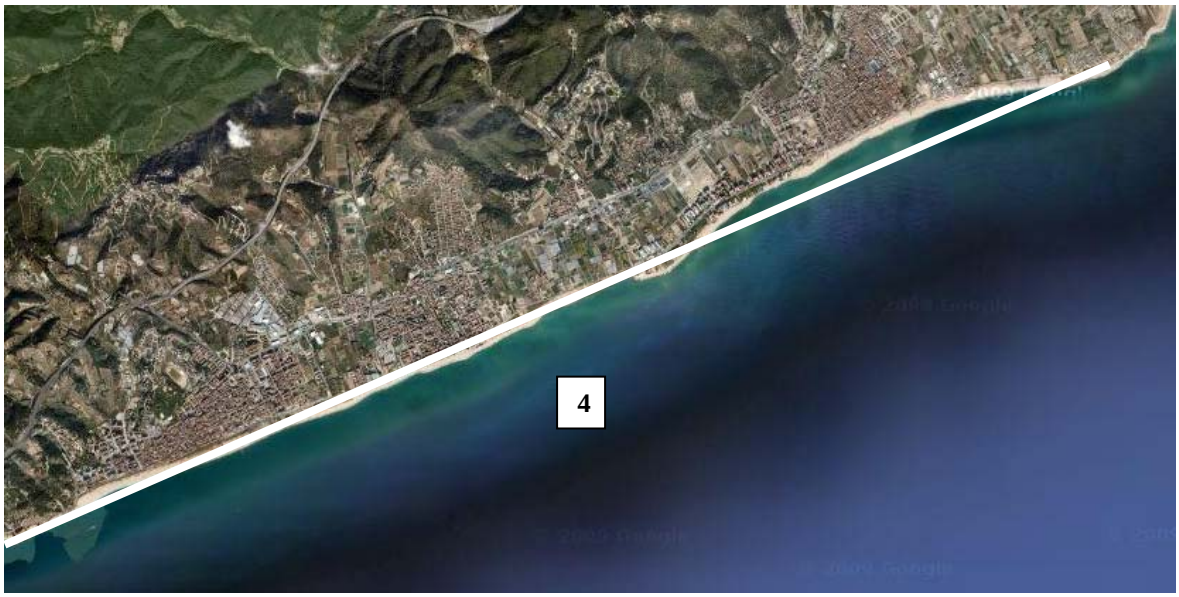

Figure 3.13 Definition of the beach of Blanes – Arenys. Stretch Tordera – Calella.

Stretch Calella – Arenys de Mar

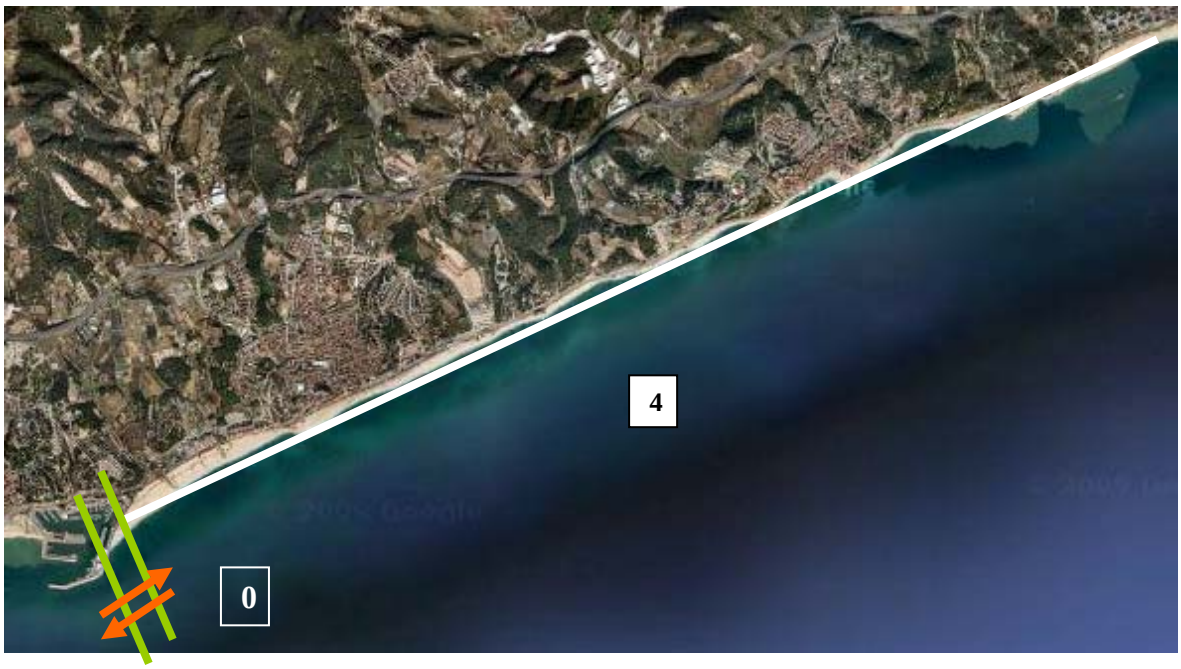

Figure 3.14 Definition of the beach of Blanes – Arenys. Stretch Calella – Arenys de Mar.

	Diameter (D_{50})	**Orientation (deg)**	**Slope**	**Wave effective Dir.**
1. S'Abanell north	1.19	27	0.18	65-205
2. S'Abanell south	1.50	27	0.20	65-205
3. Tordera	0.55	27	0.09	65-205
4. Tordera – Arenys	0.50	65	0.08	65-245
Data for Drift Rose				
- Blanes Drift Rose	1.10	15-60	0.16	65-205

S'ABANELL NORTH

Longshore Sediment Transport Time Series

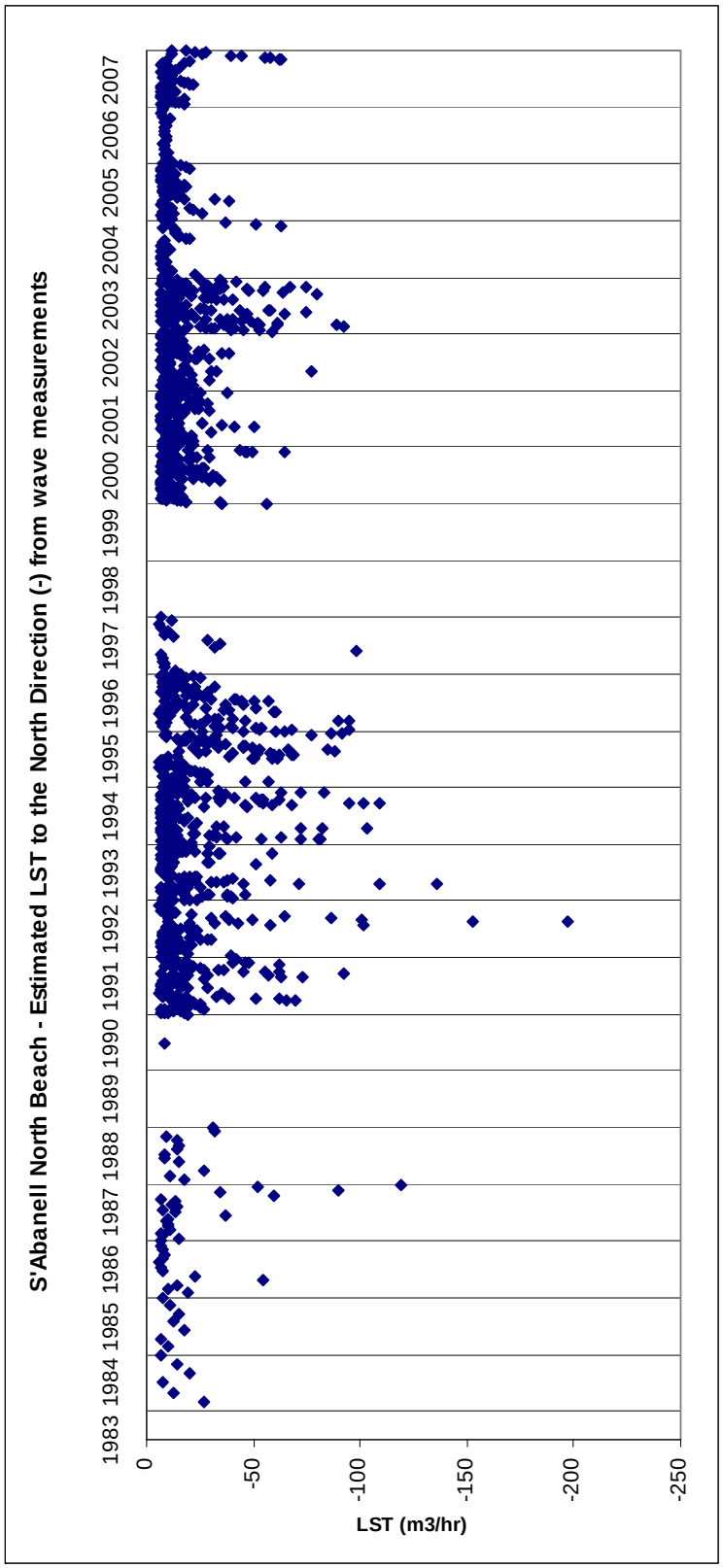

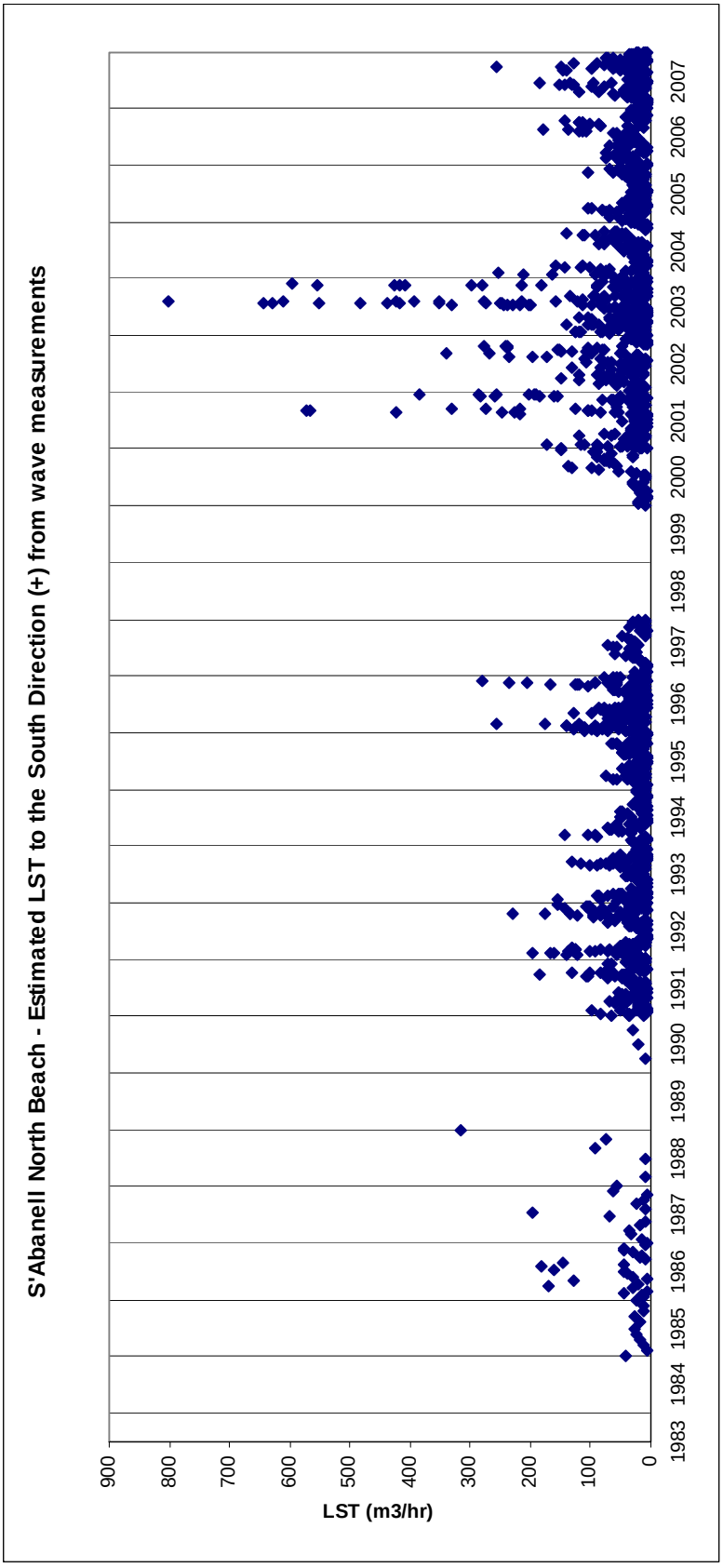
S'Abanell North Beach - Estimated LST to the South Direction (+) from wave measurements
LST (m3/hr)
900
800
700
600
500
400
300
200
100
0
1983
1984
1985
1986
1987
1988
1989
1990
1991
1992
1993
1994
1995
1996
1997
1998
1999
2000
2001
2002
2003
2004
2005
2006
2007

Monthly Distribution

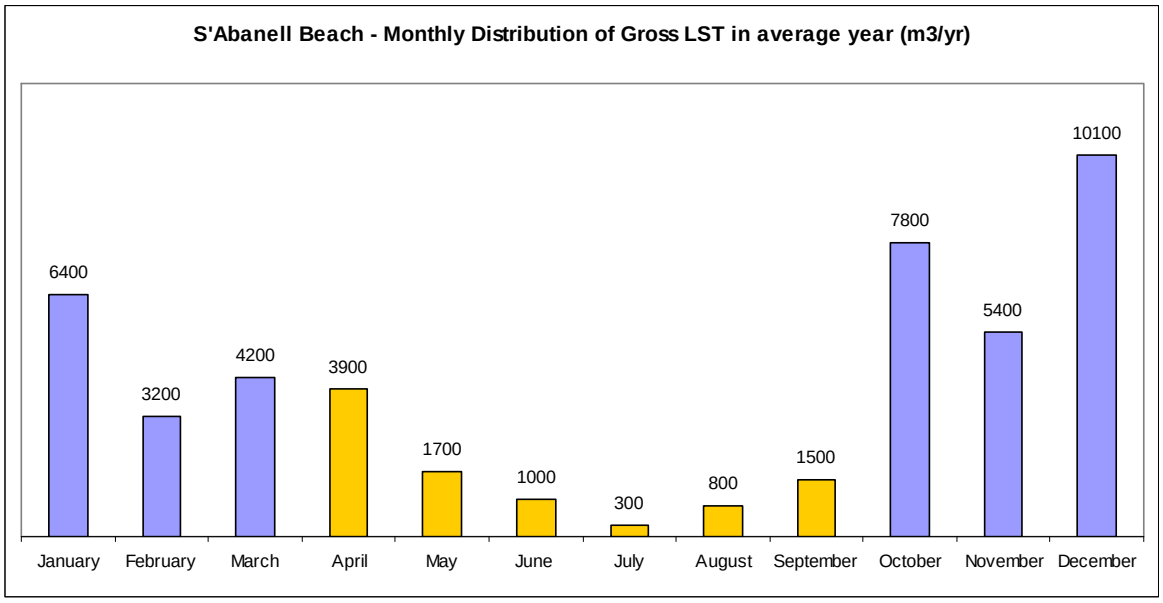

Summer and winter time distribution of Gross LST:

- Oct-Mar: 213 400 (74%)
- Apr-Sep: 73 300 (36%)

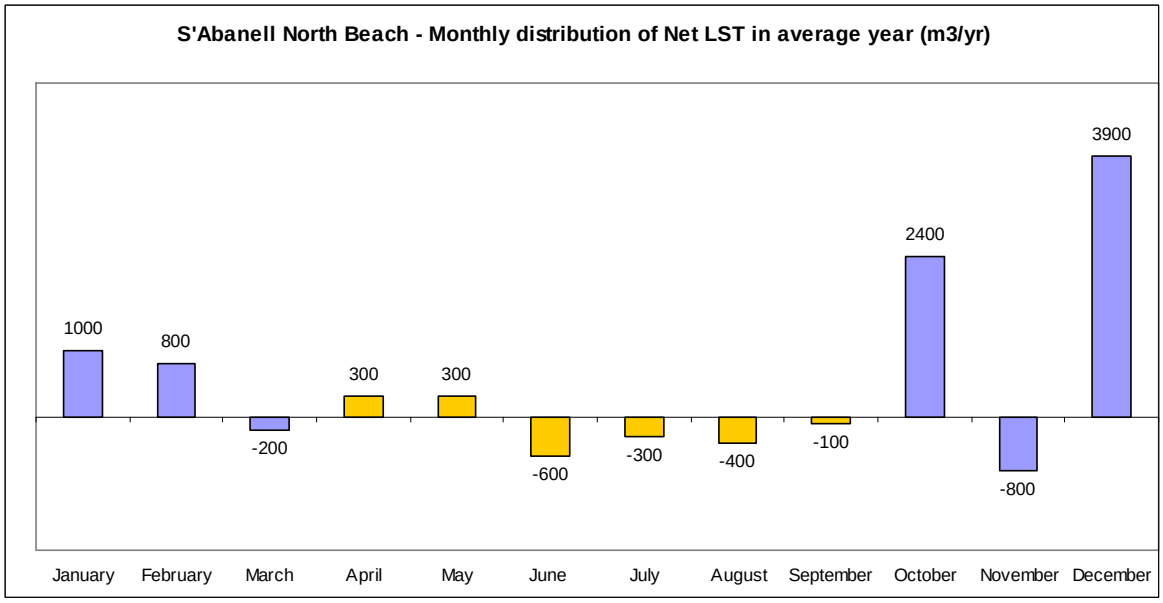

Summer and winter time distribution of Net LST:

- Oct-Mar: 9 100 (82%)
- Apr-Sep: 2 000 (18%)

S'ABANELL SOUTH

Longshore Sediment Transport Time Series

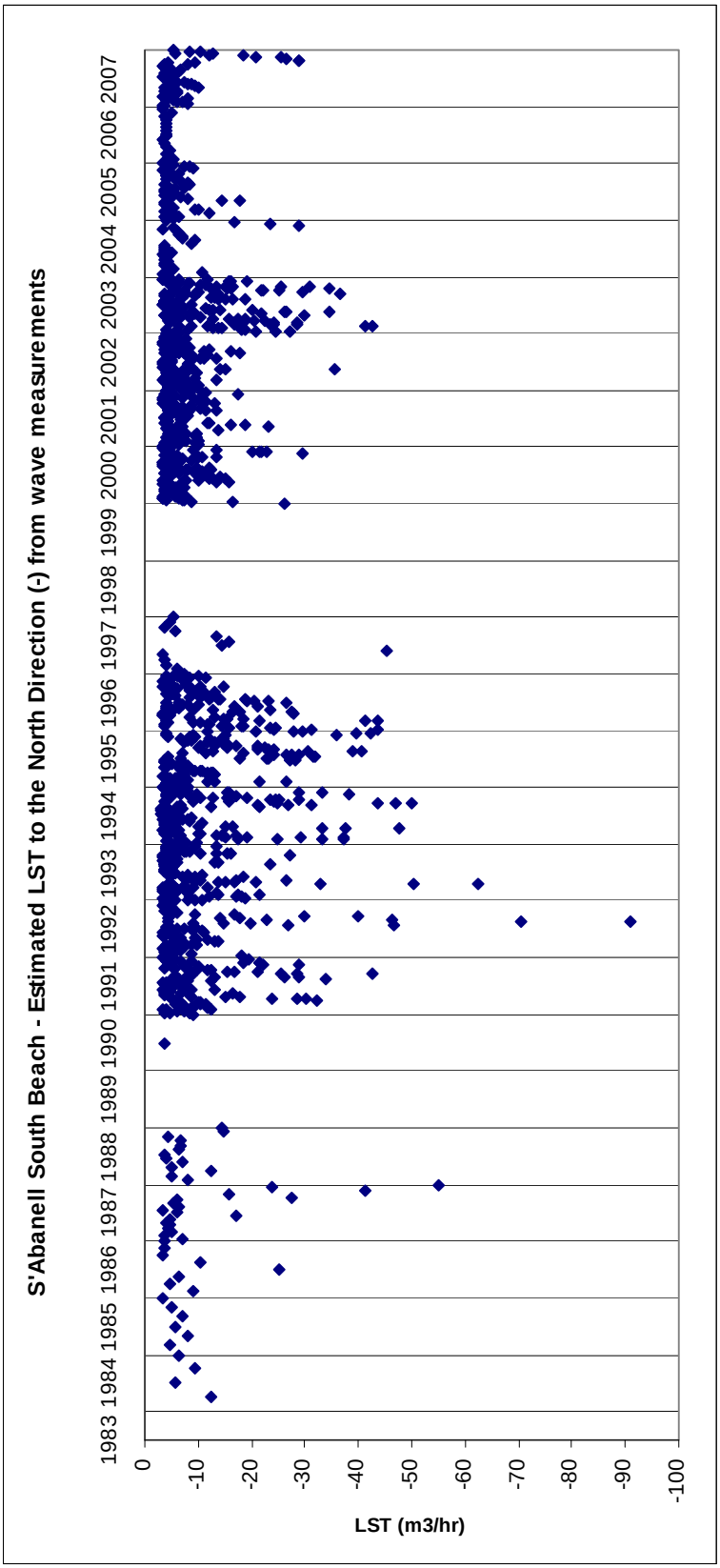

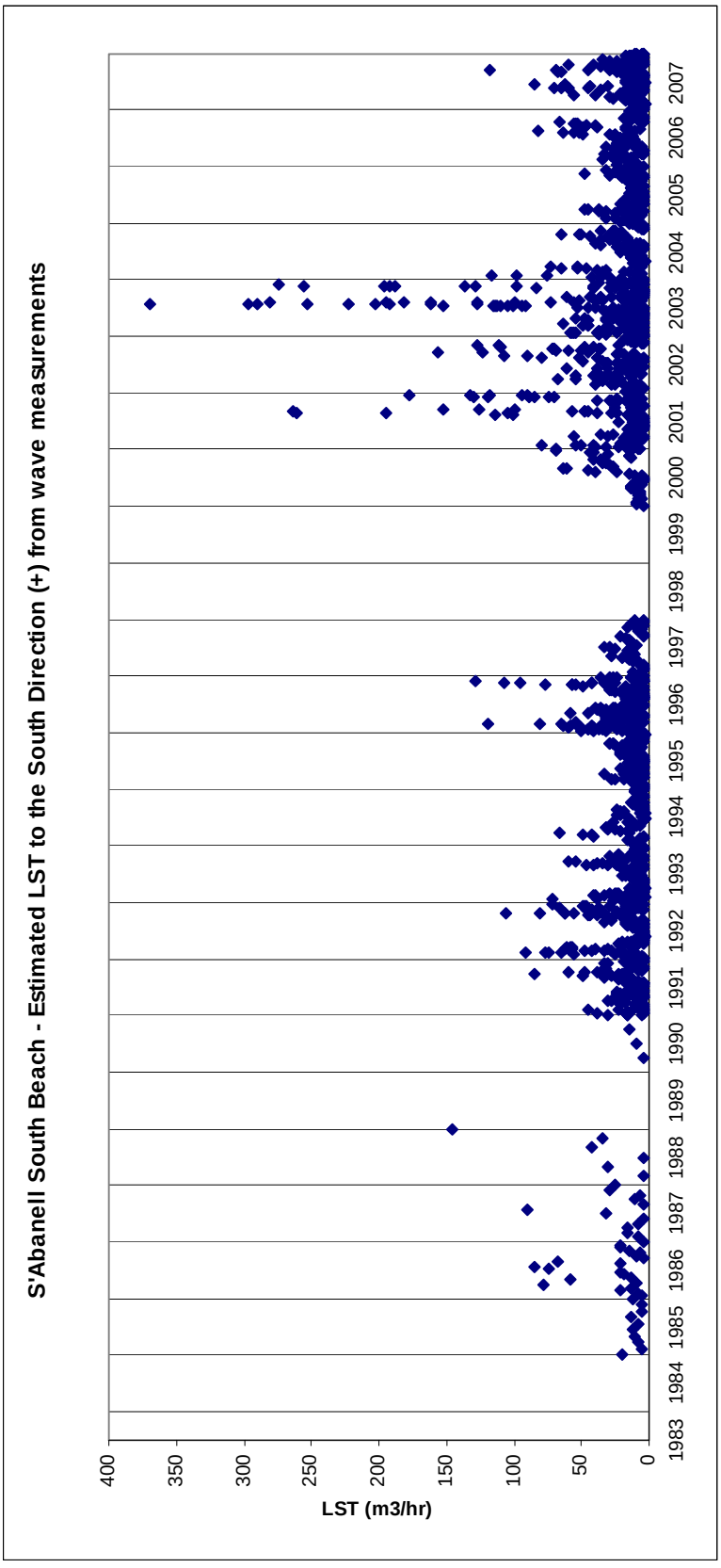
S'Abanell South Beach - Estimated LST to the South Direction (+) from wave measurements
LST (m3/hr)
400
350
300
250
200
150
100
50
0
1983
1984
1985
1986
1987
1988
1989
1990
1991
1992
1993
1994
1995
1996
1997
1998
1999
2000
2001
2002
2003
2004
2005
2006
2007

Monthly Distribution

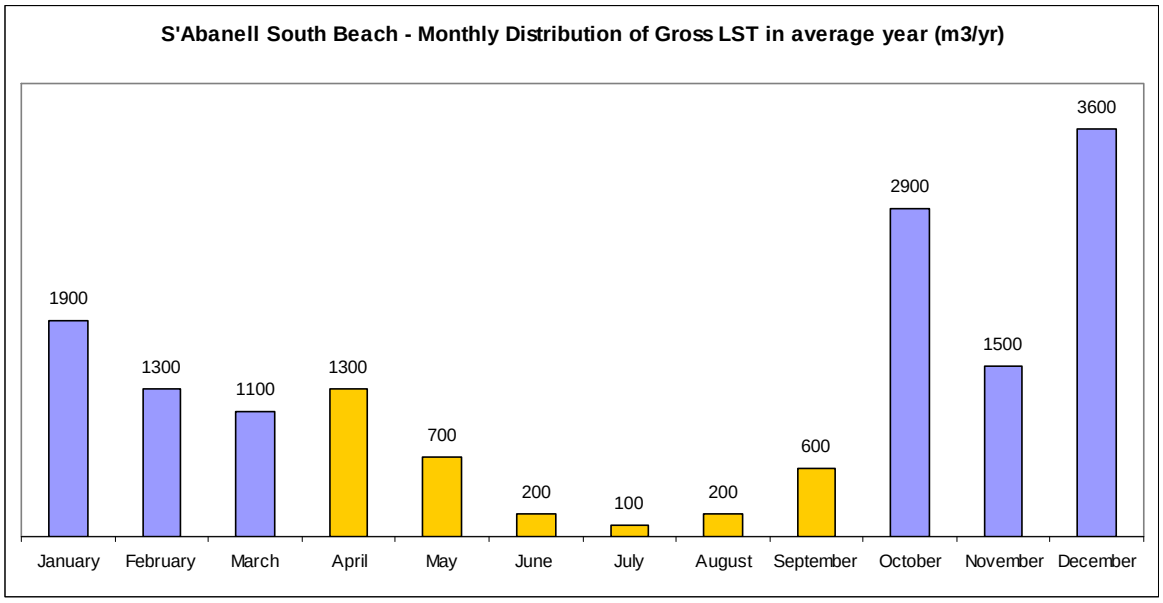

Summer and winter time distribution of Gross LST:

- Oct-Mar: 12 300 (80%)
- Apr-Sep: 3 100 (20%)

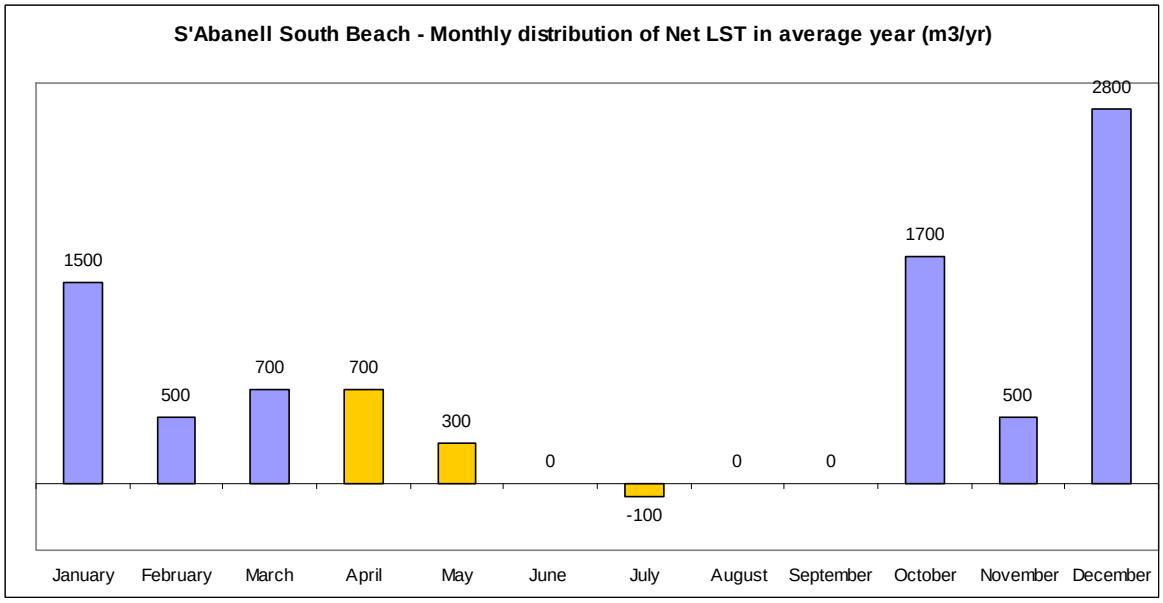

Summer and winter time distribution of Net LST:

- Oct-Mar: 7 700 (88%)
- Apr-Sep: 1 100 (13%)

TORDERA

Longshore Sediment Transport Time Series

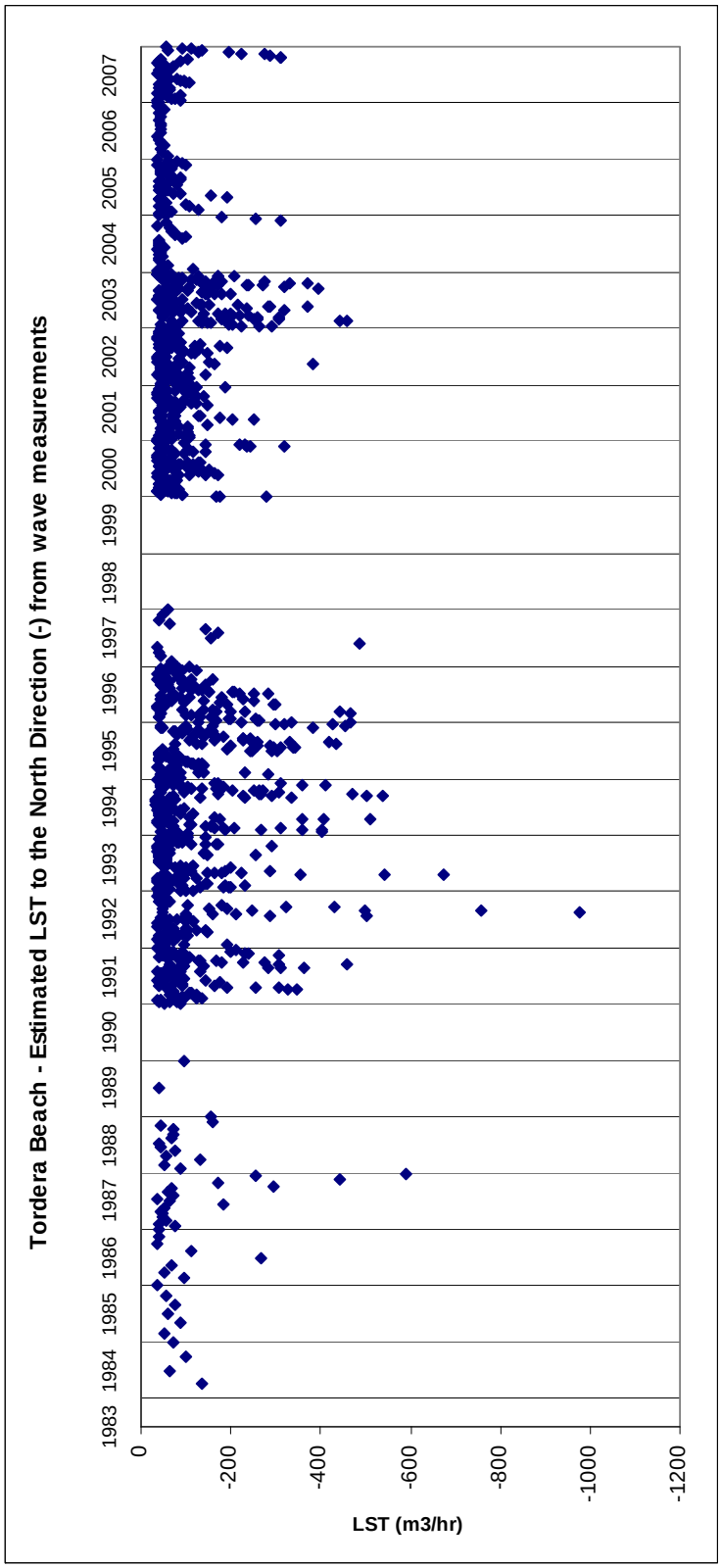

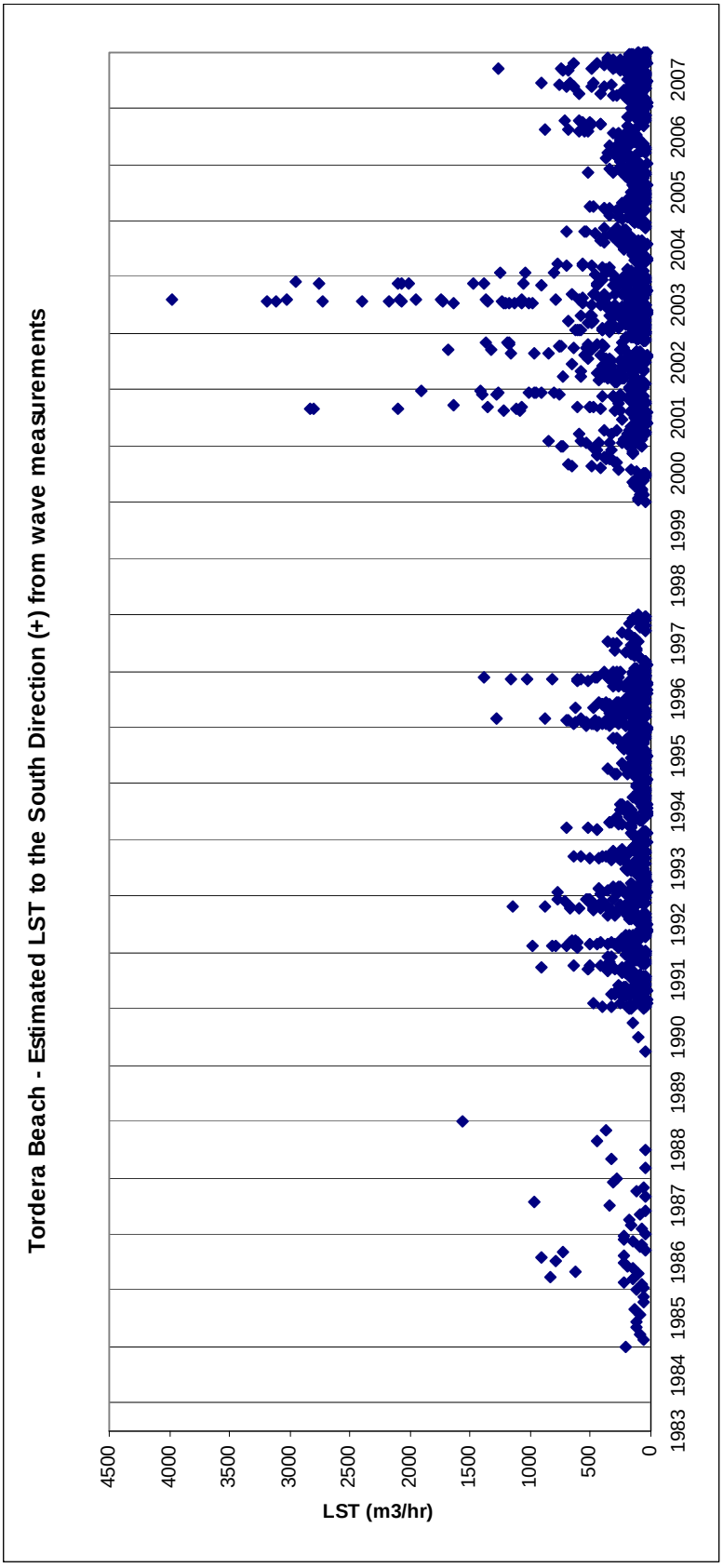
Tordera Beach - Estimated LST to the South Direction (+) from wave measurements
LST (m3/hr)
4500
4000
3500
3000
2500
2000
1500
1000
500
0
1983
1984
1985
1986
1987
1988
1989
1990
1991
1992
1993
1994
1995
1996
1997
1998
1999
2000
2001
2002
2003
2004
2005
2006
2007

Monthly Distribution

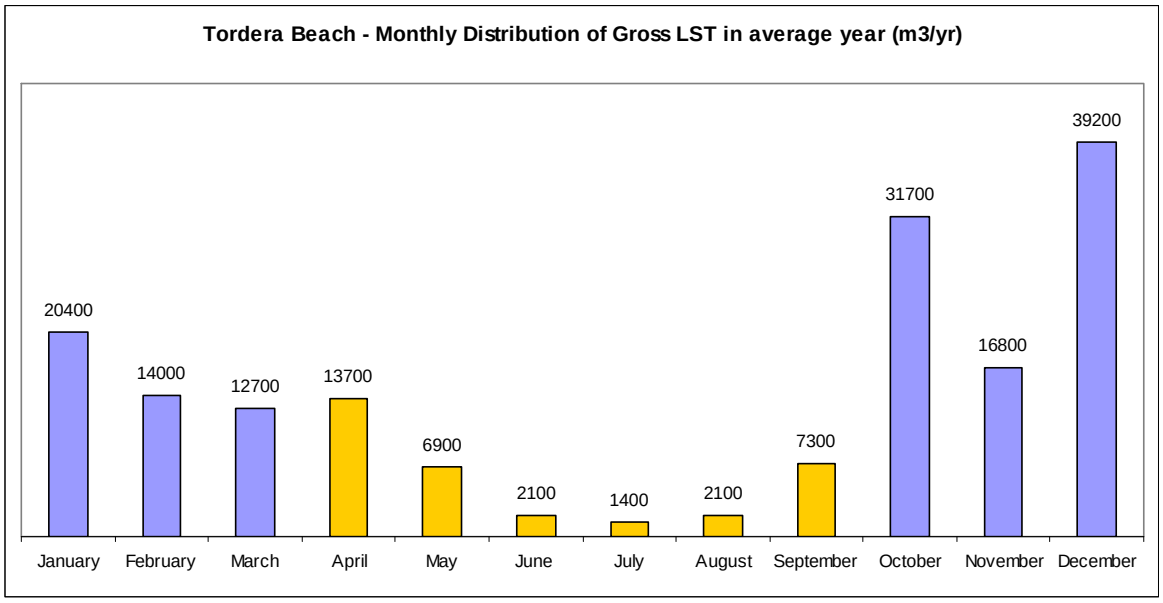

Summer and winter time distribution of Gross LST:

- Oct-Mar: 134 800 (80%)
- Apr-Sep: 33 500 (20%)

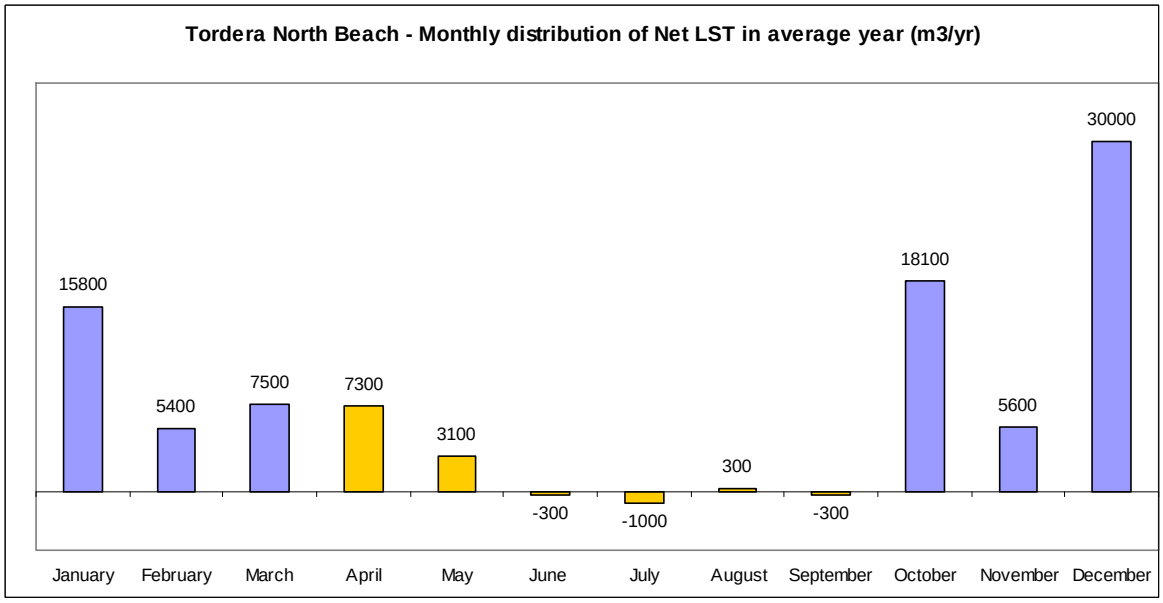

Summer and winter time distribution of Net LST:

- Oct-Mar: 82 400 (87%)
- Apr-Sep: 12 300 (13%)

TORDERA – ARENYS DE MAR

Longshore Sediment Transport Time Series

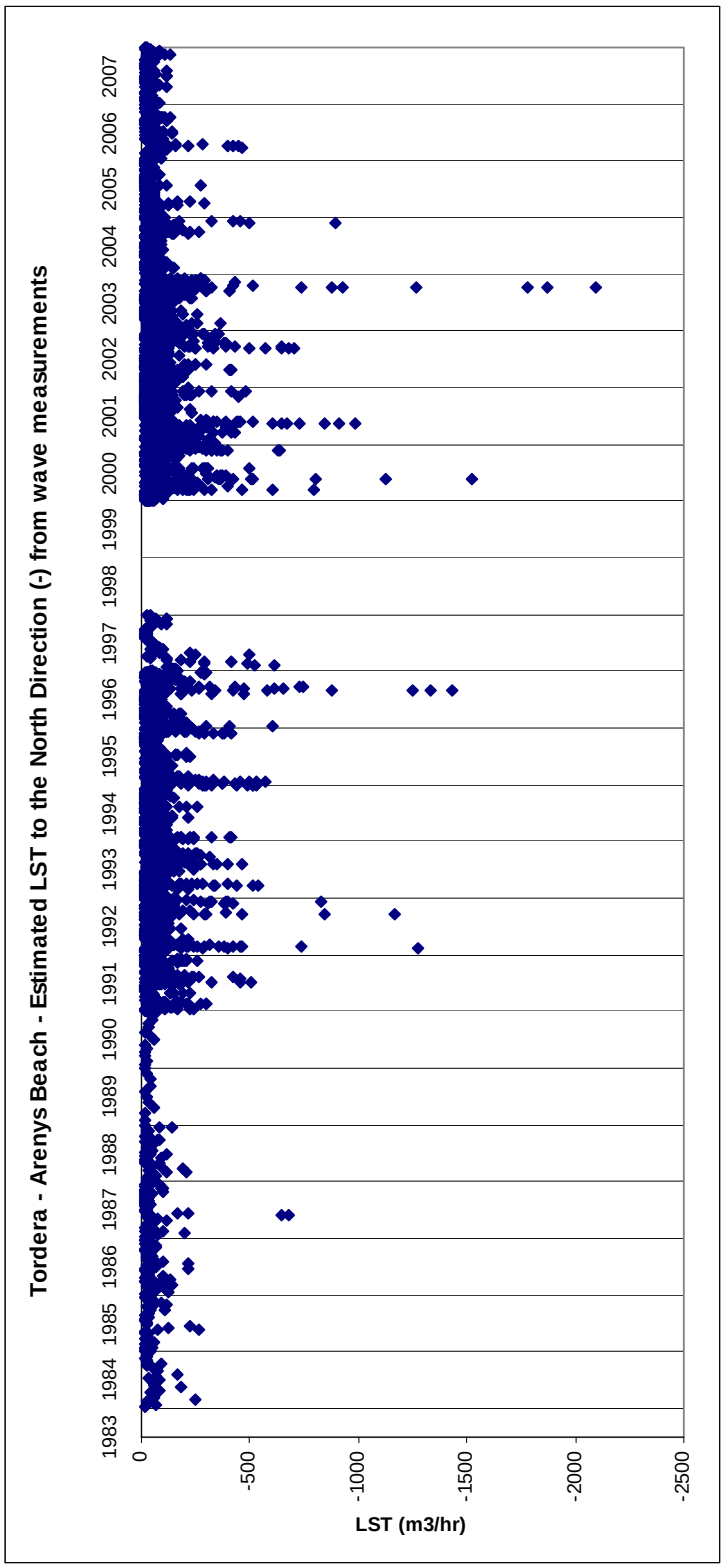

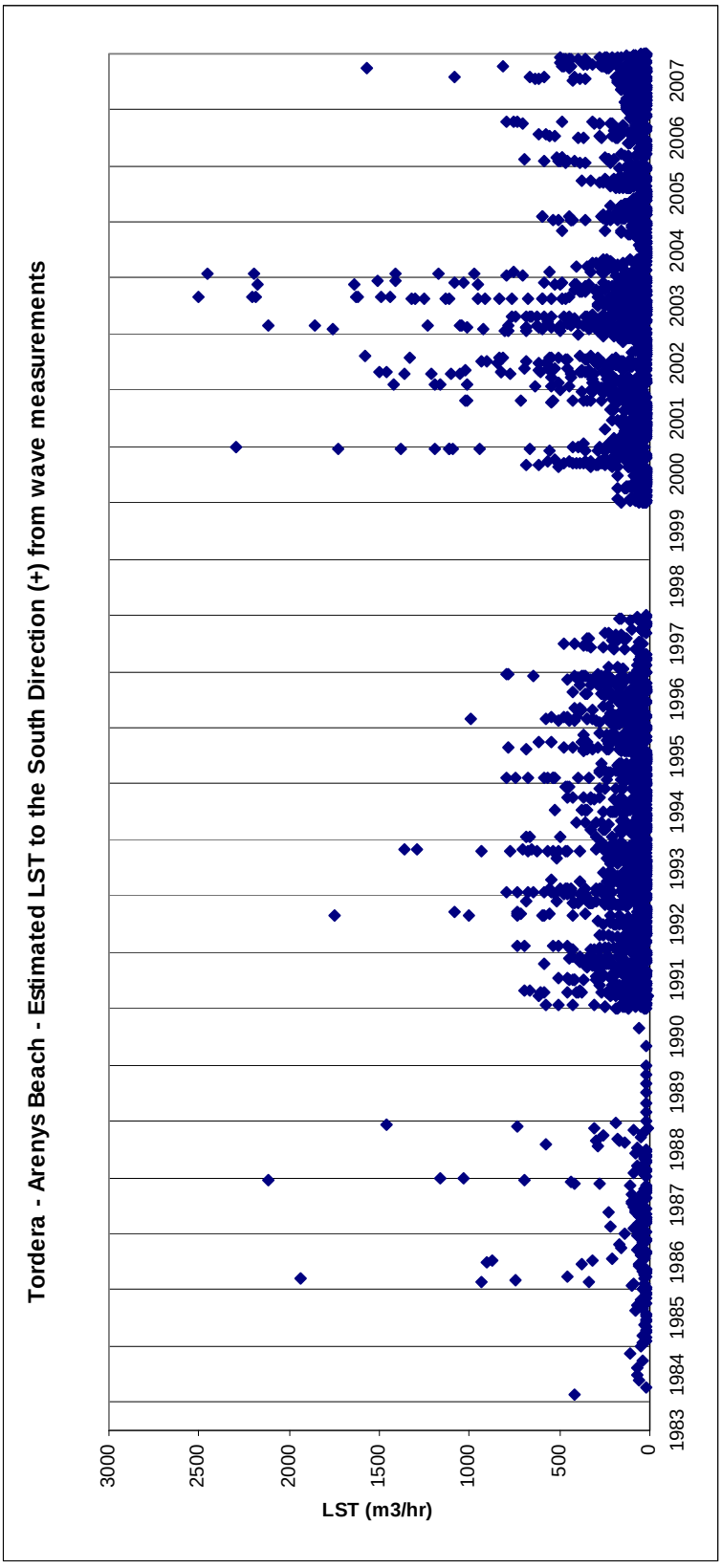
Tordera - Arenys Beach - Estimated LST to the South Direction (+) from wave measurements
LST (m3/hr)
3000
2500
2000
1500
1000
500
0
1983
1984
1985
1986
1987
1988
1989
1990
1991
1992
1993
1994
1995
1996
1997
1998
1999
2000
2001
2002
2003
2004
2005
2006
2007

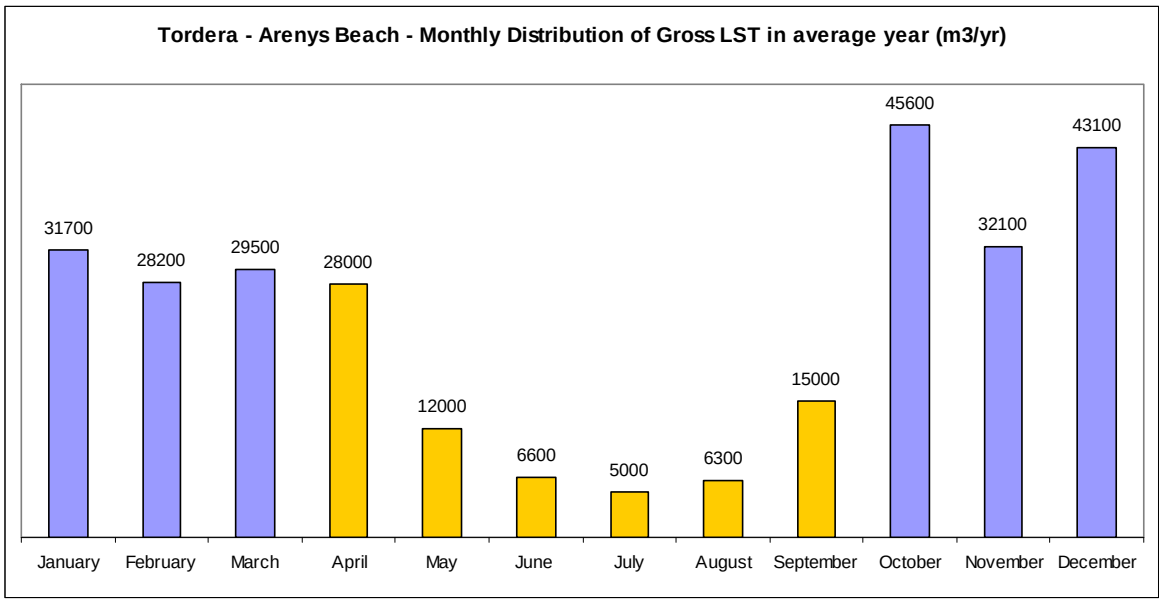

Summer and winter time distribution of Gross LST:

- Oct-Mar: 210 200 (74%)
- Apr-Sep: 72 900 (26%)

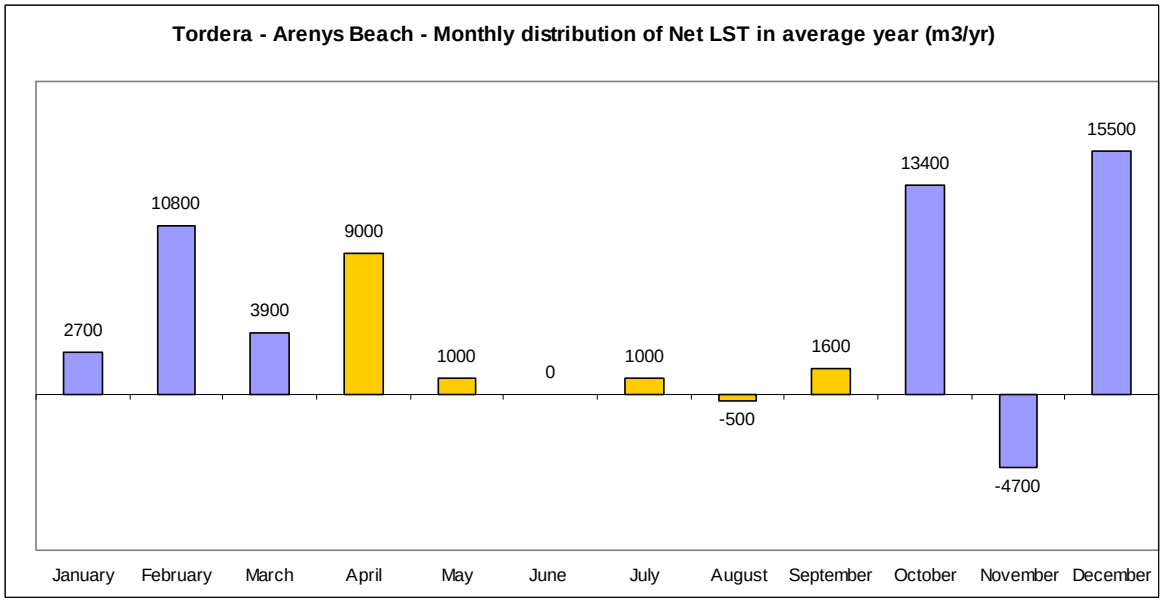

Summer and winter time distribution of Net LST:

- Oct-Mar: 51 000 (80%)
- Apr-Sep: 13 100 (20%)

LST estimation in average year: total, by wave direction and proportion caused by Hs>2m.

Beach	Direction of Littoral Drift	Total LST (m3/year)	Wave direction			Hs		Grain size (mm)	Orientation (º)	Slope
			Wave direction	LST (m3/year)	%	LST (Hs>2m)	%			
S'Abanell North	South	26396	ENE	8666	32.8	4392	50.7	1.19	27	0.2
			E	15651	59.3	9368	59.9			
			ESE	2079	7.9	1268	61.0			
	North	8074	ESE	209	2.6	137	65.6			
			SE	3066	38.0	1206	39.3			
			SSE	2311	28.6	366	15.8			
			S	1813	22.5	379	20.9			
			SSW	675	8.4	292	43.3			
S'Abanell South	South	12544	ENE	4436	35.4	2196	49.5	1.5	27	0.2
			E	7167	57.1	4316	60.2			
			ESE	941	7.5	584	62.1			
	North	3587	ESE	91	2.5	63	69.2			
			SE	1371	38.2	556	40.6			
			SSE	1029	28.7	169	16.4			
			S	805	22.4	175	21.7			
			SSW	291	8.1	133	45.7			
La Tordera	South	148139	ENE	60975	41.2	27715	45.5	0.55	27	0.09
			E	77052	52.0	46398	60.2			
			ESE	10112	6.8	6280	62.1			
	North	38573	ESE	979	2.5	676	69.1			
			SE	14742	38.2	5974	40.5			
			SSE	11068	28.7	1812	16.4			
			S	8654	22.4	1877	21.7			
			SSW	3130	8.1	1428	45.6			
La Tordera - Arenys	South	168268	ENE	9643	5.7	5698	59.1	0.5	65	0.08
			E	65749	39.1	38108	58.0			
			ESE	60999	36.3	26919	44.1			
			SE	31216	18.6	12952	41.5			
			SSE	661	0.4	144	21.8			
	North	114825	SSE	1495	1.3	281	18.8			
			S	15557	13.5	2833	18.2			
			SSW	77843	67.8	16942	21.8			
			SW	19785	17.2	2061	10.4			
			WSW	145	0.1	35	24.1			

	S'Abanell North	**S'Abanell South**	**Tordera .**
Gross LST(m^3/yr)	34 500	16 100	186 700
Net LST (m^3/yr)	18 300 (to South)	9 000 (to South)	109 600 (to South)

	Tordera-Arenys
Gross LST(m^3/yr)	283 100
Net LST (m^3/yr)	53 400 (to South)

Sediment Budget using LST Capacity

Figure 3.15 Evaluation of LST along the zone of Blanes. S'Abanell – La Tordera.

This is the first stretch of the unit with the north end in Blanes and the south end in Arenys the Mar. Until this point there are no obstacles capable to retain an important amount of sand, so the 109 600 m^3 going out from this stretch are transferred to the following stretch (Tordera – Arenys).

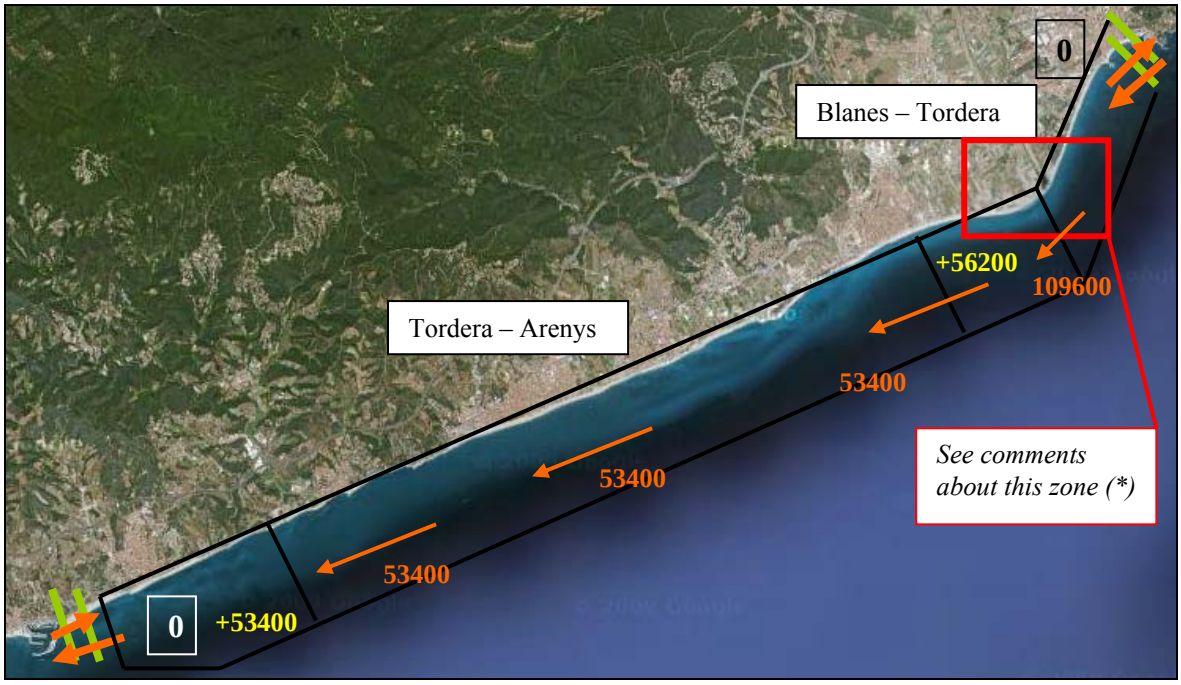

Figure 3.16 Evaluation of LST along the zone of Blanes - Arenys. La Tordera – Arenys.

***Comments on the intermediate zone between stretches**

It is represented an annual drift of 109 600 m^3 along the zone where takes place a change of shoreline orientation. That's the transport produced due to the orientation at the North of this zone, that is currently 27º. With the orientation going past this stretch to the South, that is 65º, the transport produced is 53 400 m^3. Is difficult to say what happens exactly at the intermediate point with the difference between the two drifts. Obviously about a half of the 109 600 m^3 coming from the North are spread and deposited along this zone but without further investigation we cannot say until which point it occurs or to define with certain precision the area where deposit takes place. Adding to this, there's placed at this point the mouth of the Tordera river. The sediment contribution from this river has not been quantified nor the effect of its flow on the littoral drift. In short, in general we can say that along the northern zone close to the river the drift is 109 600 m^3/yr and along the southern stretch the drift is 53 400 m^3/yr. As a simplification, on Figure 3.16 the difference between the two values is supposed to be a deposit along a zone defined at the beginning of the second southern stretch.

Storm contribution: proportion of transport caused by storm conditions (Hs>2m)

	S'Abanell North	S'Abanell South	Tordera .
South Direction	58%	58%	58%
North Direction	31%	31%	31%

	Tordera-Arenys
South Direction	50%
North Direction	19%

Blanes drift Rose

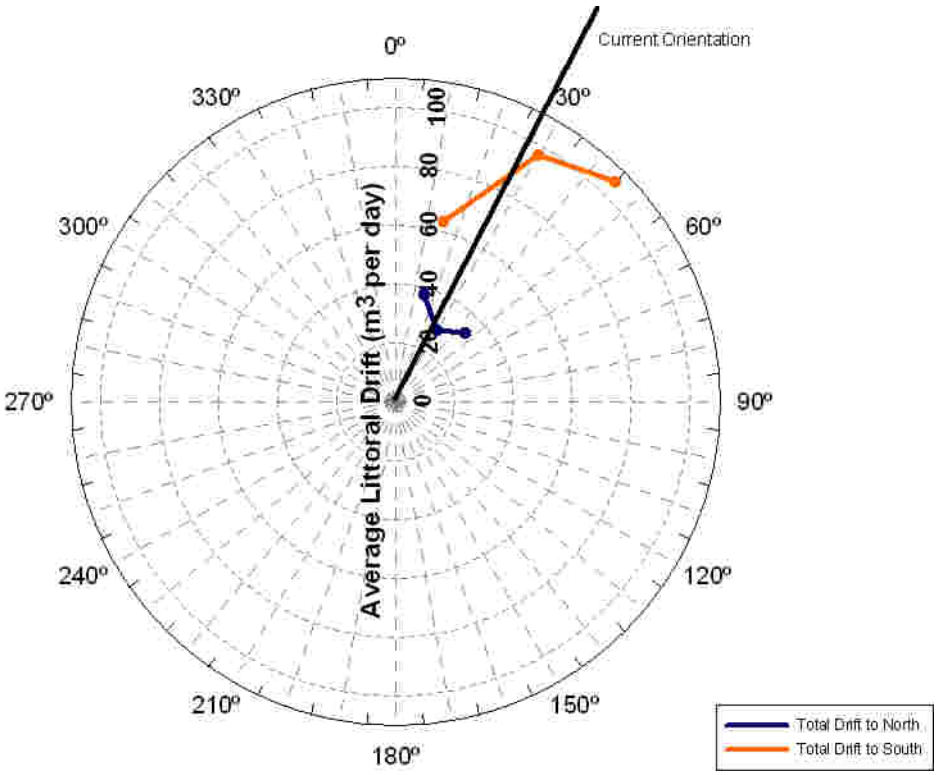

Drift Rose of Tordera – Arenys

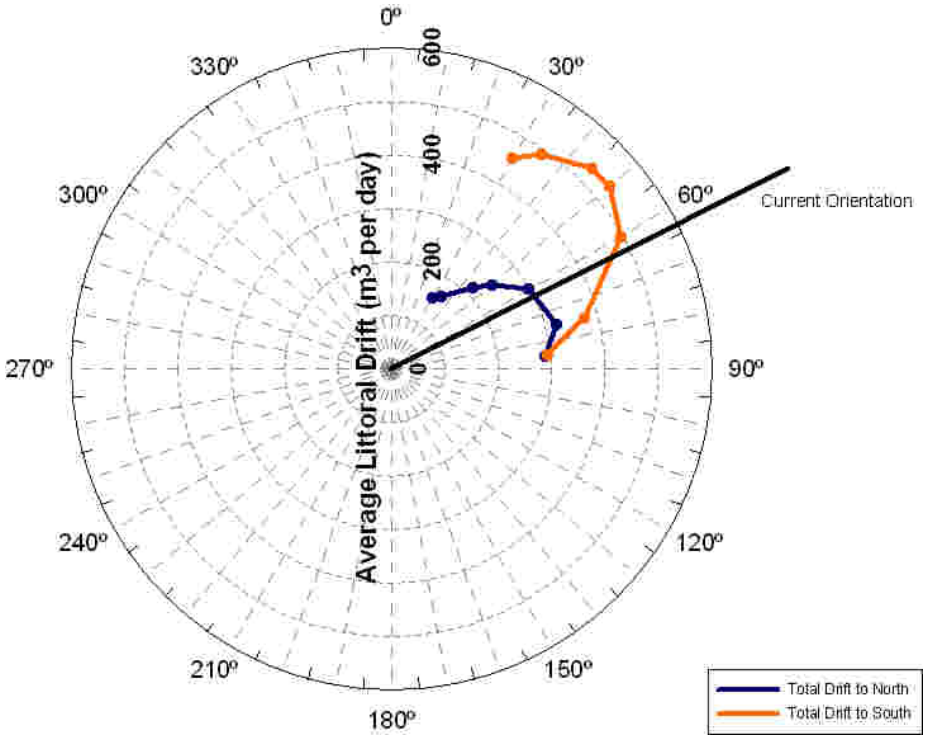

3.2.7 Arenys de Mar – Port Balis

Situation of Arenys – Port Balis beach.

Beach definition and main parameters

Figure 3.17 Definition of the beach of Arenys – Port Balis.

	Diameter (D_{50})	Orientation (deg)	Slope	Wave effective Dir.
1. Arenys – Port Balis	0.50	63	0.08	63-243

Longshore Sediment Transport Time Series

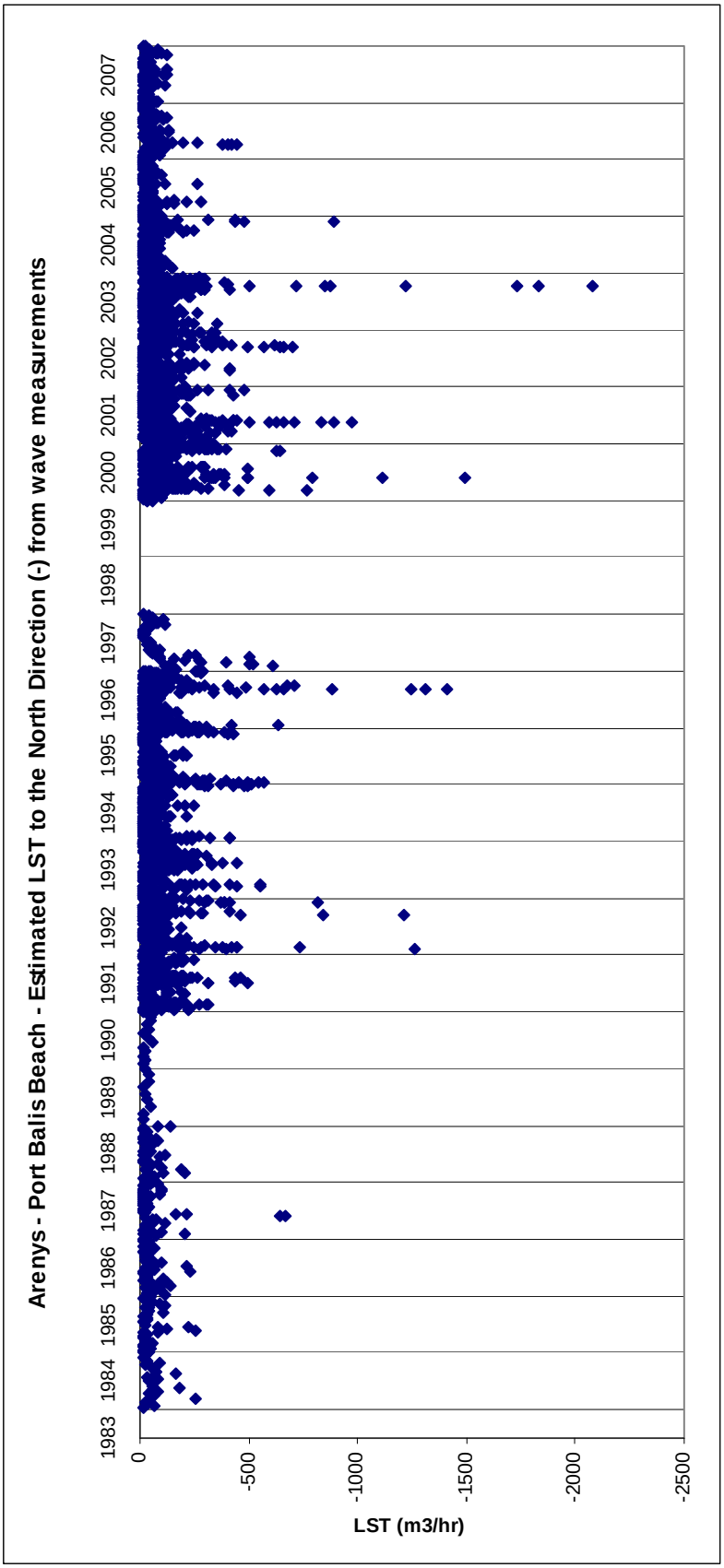

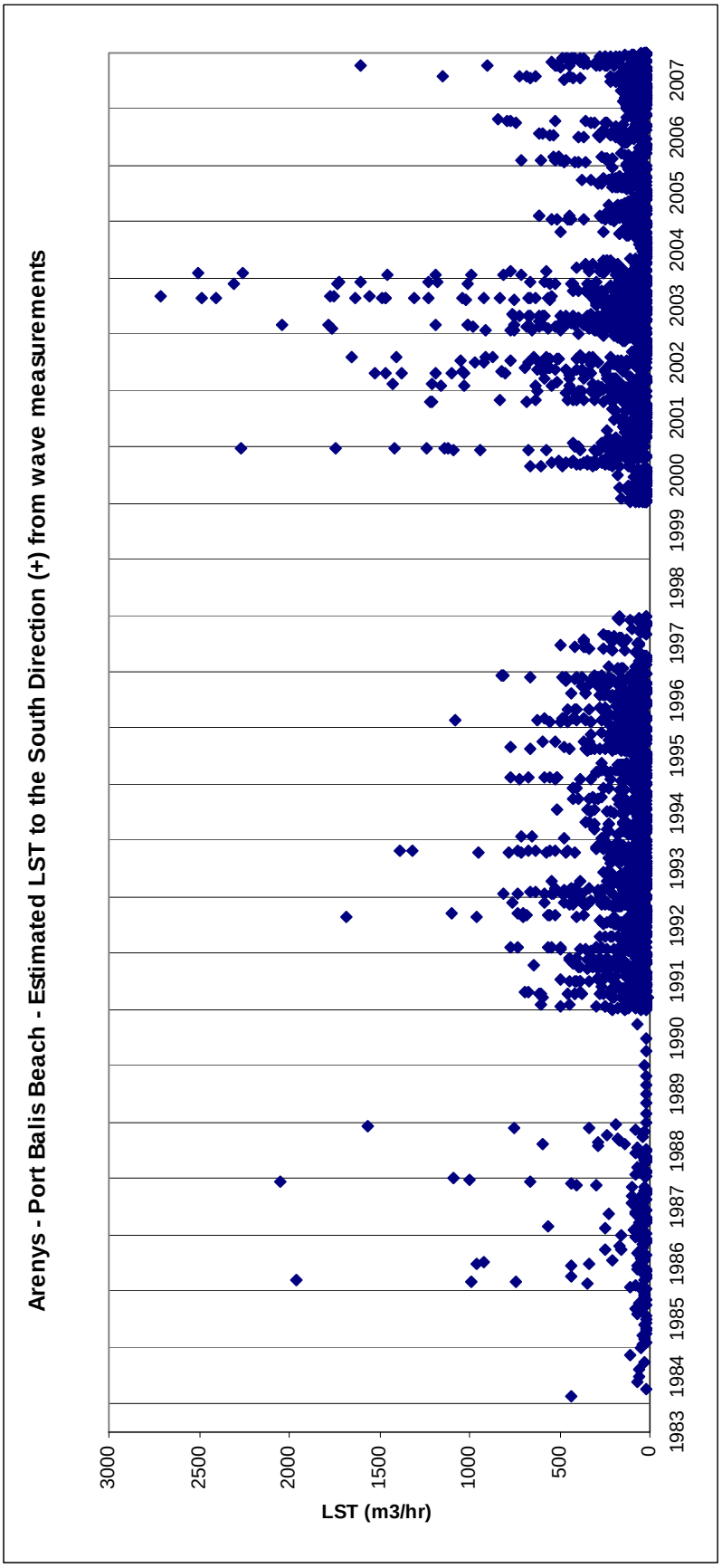
Arenys - Port Balis Beach - Estimated LST to the South Direction (+) from wave measurements
LST (m3/hr)
3000
2500
2000
1500
1000
500
0
1983
1984
1985
1986
1987
1988
1989
1990
1991
1992
1993
1994
1995
1996
1997
1998
1999
2000
2001
2002
2003
2004
2005
2006
2007

Monthly Distribution

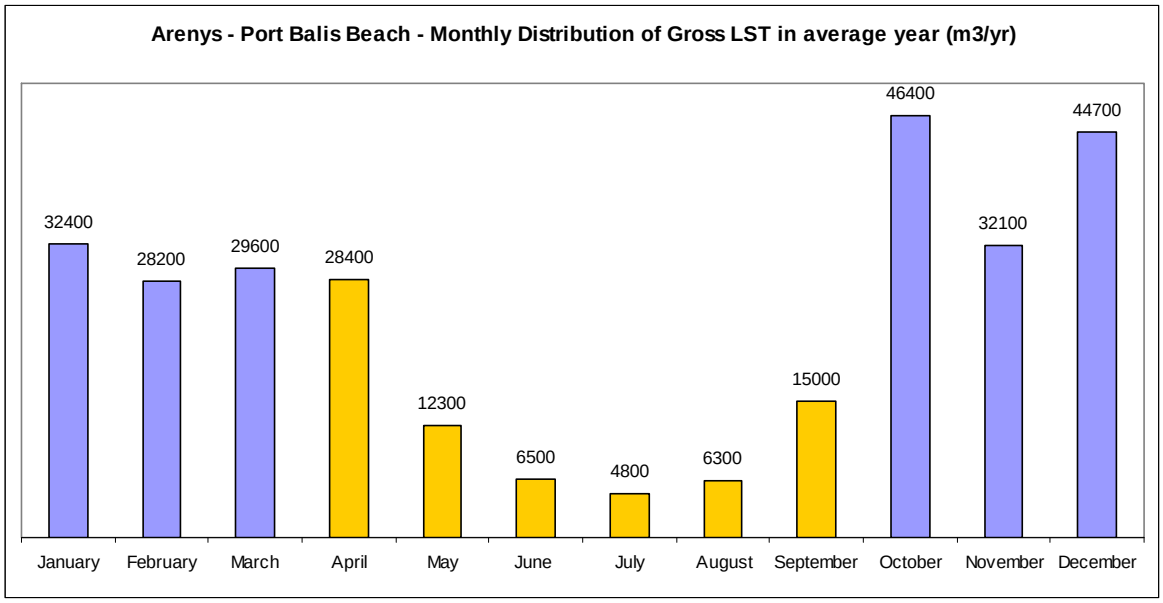

Summer and winter time distribution of Gross LST:

- Oct-Mar: 213 400 (74%)
- Apr-Sep: 73 300 (36%)

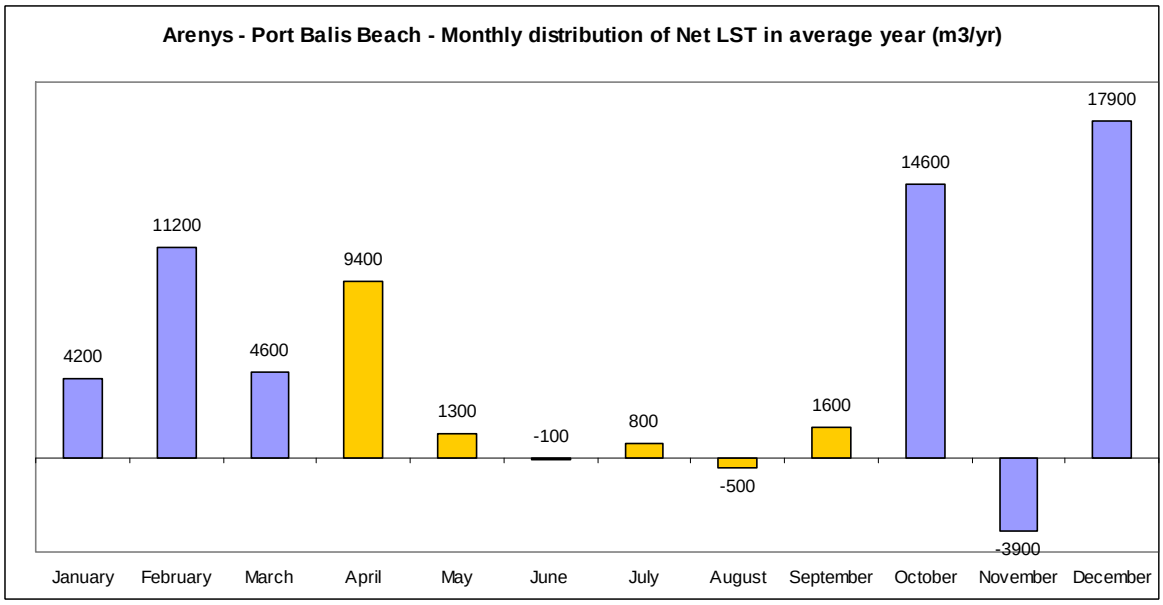

Summer and winter time distribution of Net LST:

- Oct-Mar: 56 400 (80%)
- Apr-Sep: 13 700 (20%)

LST estimation in average year: total, by wave direction and proportion caused by Hs>2m.

Beach	Direction of Littoral Drift	Total LST (m3/year)	Wave direction			Hs		Grain size (mm)	Orientation (º)	Slope
			Wave direction	LST (m3/year)	%	LST (Hs>2m)	%			
Arenys - Port Balis	South	173875	ENE	12509	7.2	7115	56.9	0.5	63	0.08
			E	71209	41.0	40716	57.2			
			ESE	60941	35.0	26974	44.3			
			SE	28879	16.6	12156	42.1			
			SSE	337	0.2	65	19.3			
	North	112779	SSE	2093	1.9	298	14.2			
			S	16424	14.6	2774	16.9			
			SSW	76193	67.6	16088	21.1			
			SW	18022	16.0	1911	10.6			
			WSW	47	0.0	18	38.3			

Arenys – Port Balis .

Gross LST(m^3/yr) 286 700

Net LST (m^3/yr) 61 100 (to South)

Sediment Budget using LST Capacity

Figure 3.18 Evaluation of LST along the beach of Arenys – Port Balis.

Storm contribution: proportion of transport caused by storm conditions (Hs>2m)

South Direction: 50%

North Direction: 19%

Arenys – Port Balis Drift Rose

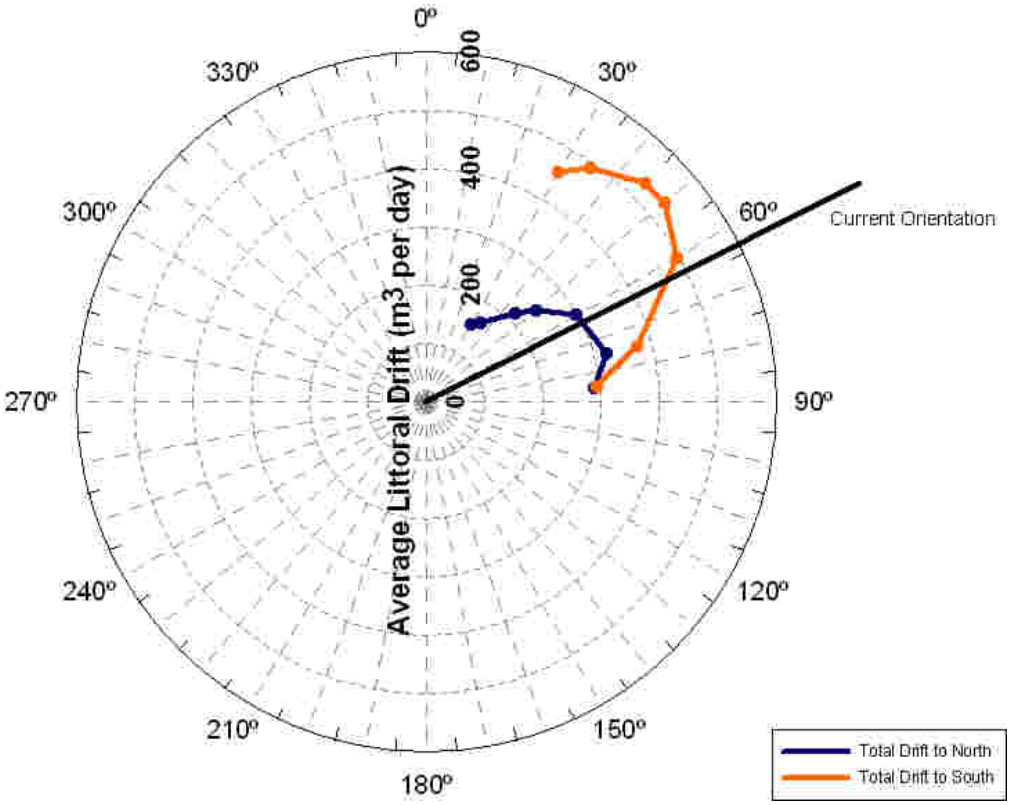

3.2.8 Mataró

Situation of Mataro beach.

Beach definition and main parameters

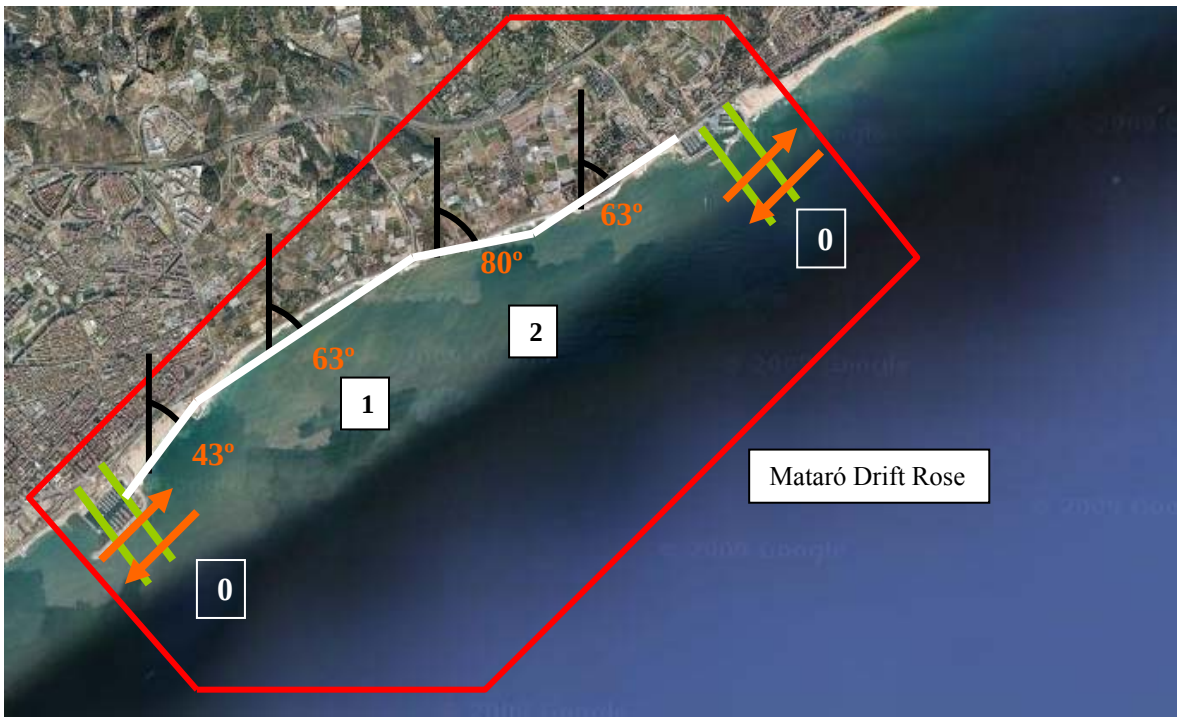

Figure 3.19 Definition of the beach of Mataró.

	Diameter (D_{50})	Orientation (deg)	Slope	Wave effective Dir.
1. Mataró	0.50	63	0.08	63-243
2. Mataró 2	0.50	80	0.08	63-243
- Mataró Drift Rose	0.50	30-85	0.08	63-243

Longshore Sediment Transport Time Series

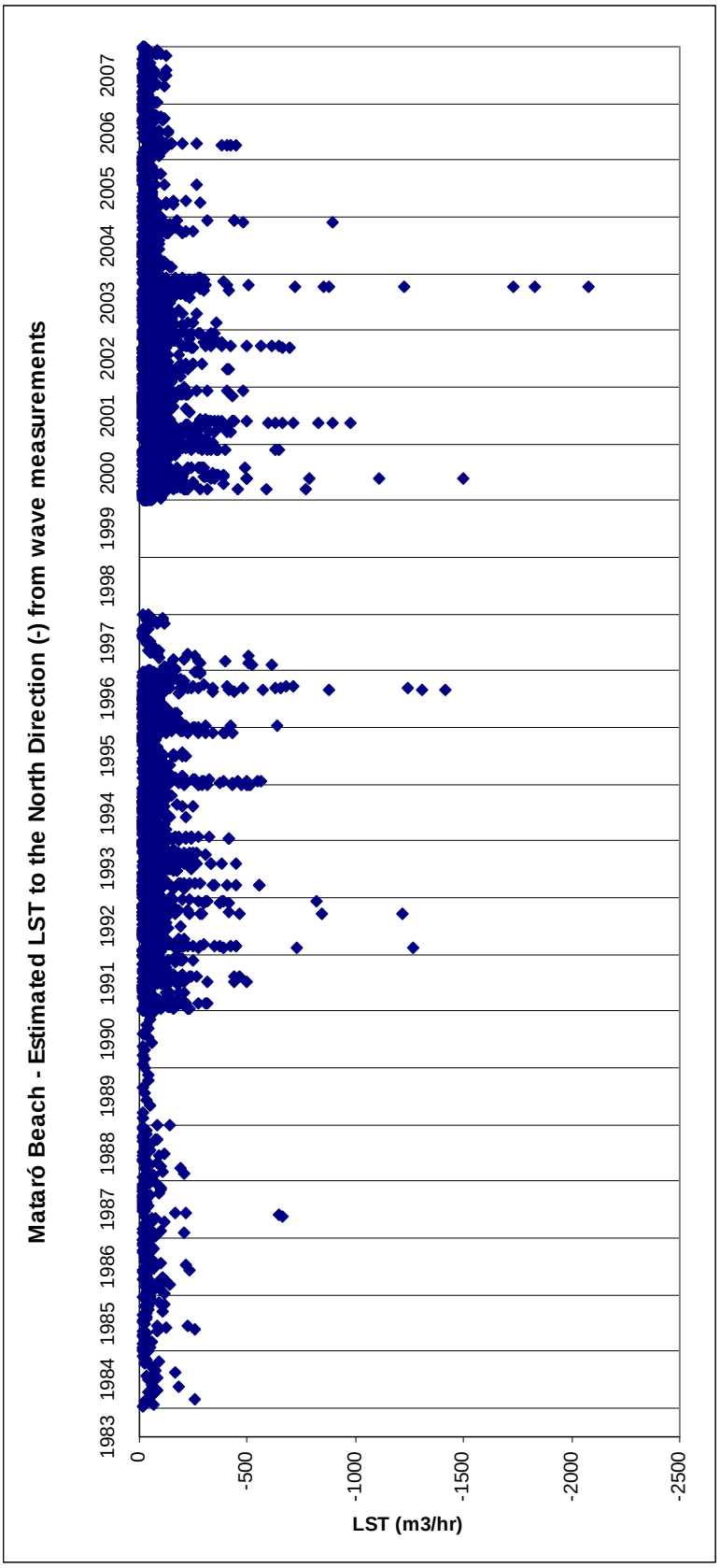

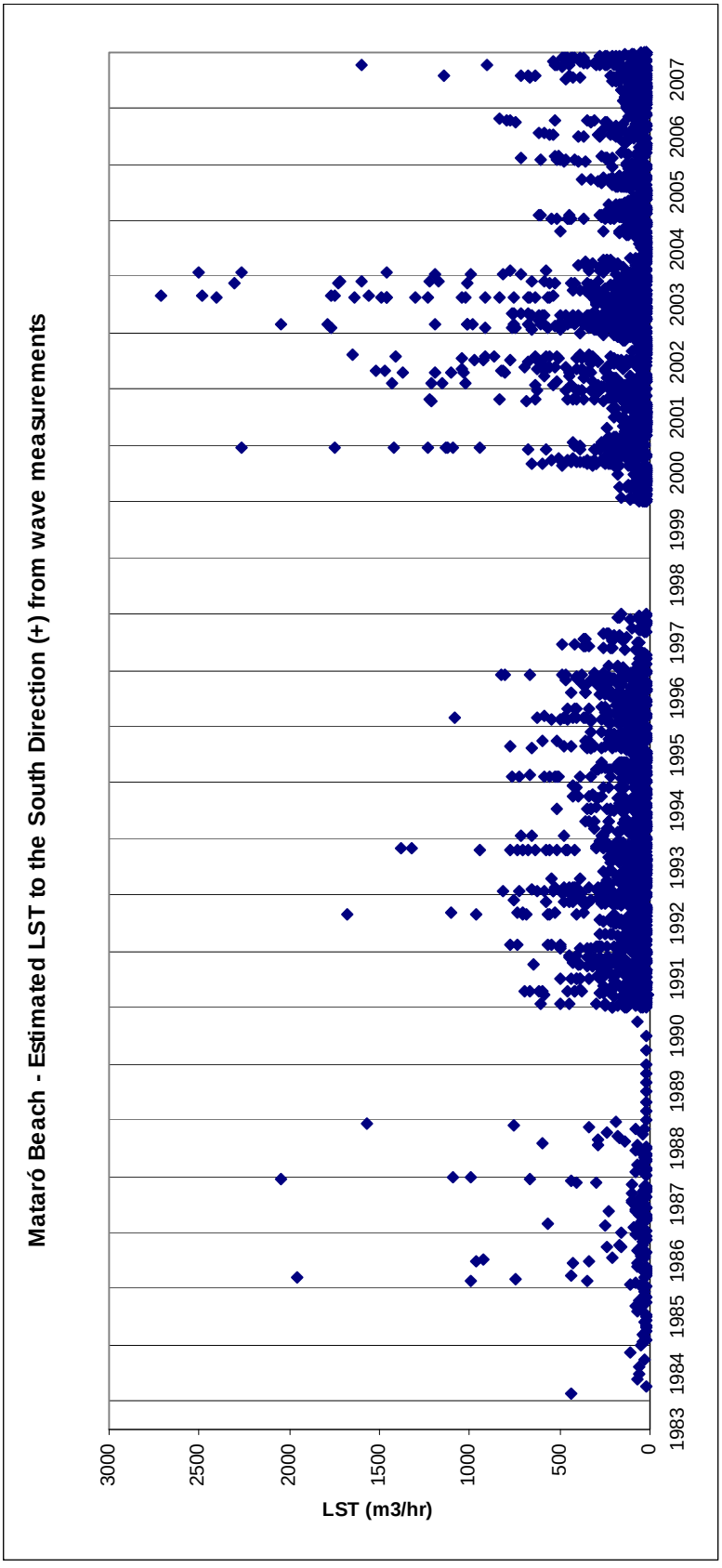
Mataró Beach - Estimated LST to the South Direction (+) from wave measurements
LST (m3/hr)
3000
2500
2000
1500
1000
500
0
1983
1984
1985
1986
1987
1988
1989
1990
1991
1992
1993
1994
1995
1996
1997
1998
1999
2000
2001
2002
2003
2004
2005
2006
2007

Monthly Distribution

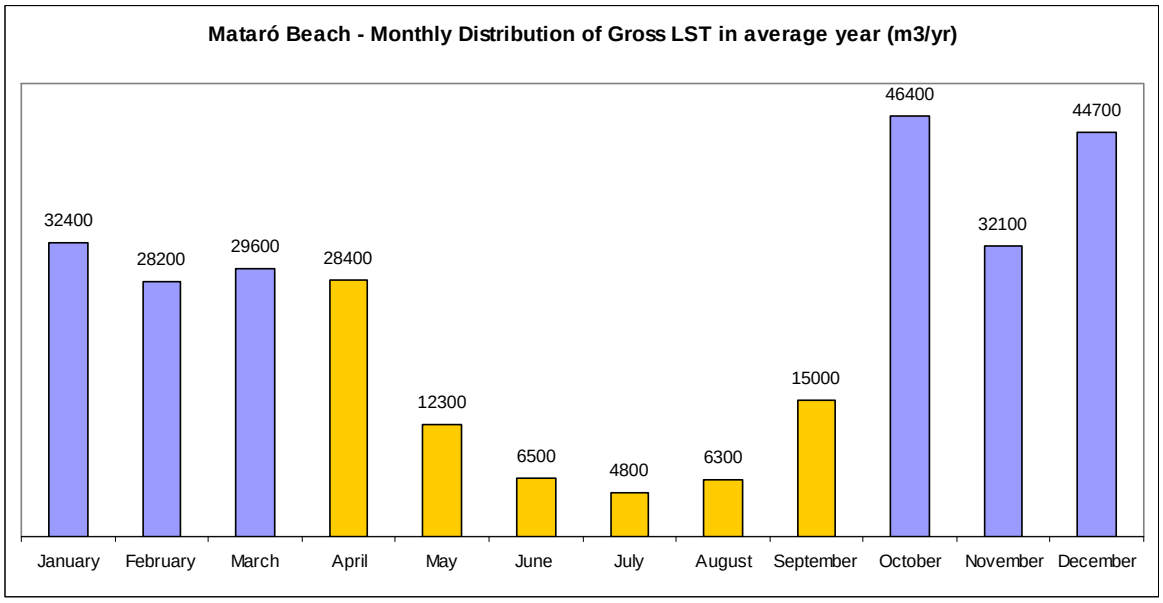

Summer and winter time distribution of Gross LST:

- Oct-Mar: 213 400 (74%)
- Apr-Sep: 73 300 (36%)

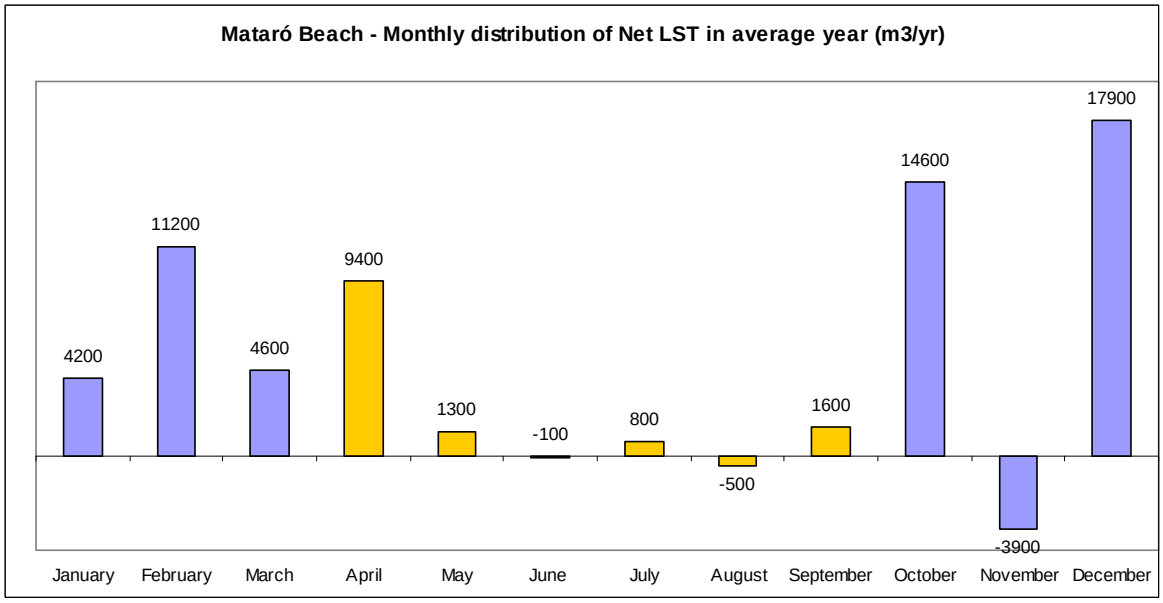

Summer and winter time distribution of Net LST:

- Oct-Mar: 56 400 (80%)
- Apr-Sep: 13 700 (20%)

LST estimation in average year: total, by wave direction and proportion caused by Hs>2m.

Beach	Direction of Littoral Drift	Total LST (m3/year)	By wave direction			By Hs		Grain size (mm)	Orientation (º)	Slope
			Wave direction	LST (m3/year)	%	LST (Hs>2m)	%			
Mataró	South	173875	ENE	12509	7.2	7115	56.9	0.5	63	0.08
			E	71209	41.0	40716	57.2			
			ESE	60941	35.0	26974	44.3			
			SE	28879	16.6	12156	42.1			
			SSE	337	0.2	65	19.3			
	North	112779	SSE	2093	1.9	298	14.2			
			S	16424	14.6	2774	16.9			
			SSW	76193	67.6	16088	21.1			
			SW	18022	16.0	1911	10.6			
			WSW	47	0.0	18	38.3			

	Mataró	**Mataró 2**
Gross LST(m^3/yr)	286 700	234 000
Net LST (m^3/yr)	61 100 (to South)	7 331 (to South)

Sediment Budget using LST Capacity

Figure 3.14 Evaluation of LST along the beach of Mataró.

Storm contribution: proportion of transport caused by storm conditions (Hs>2m)

South Direction: 50%

North Direction: 19%

Mataró Drift Rose

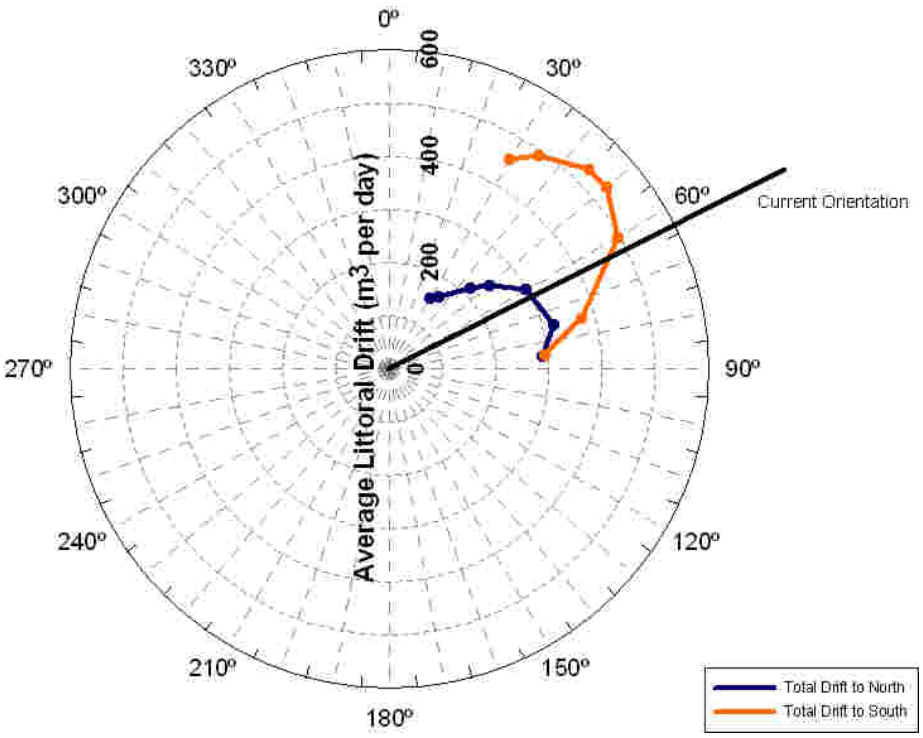

3.2.9 Masnou

Situation of El Masnou

Beach definition and main parameters

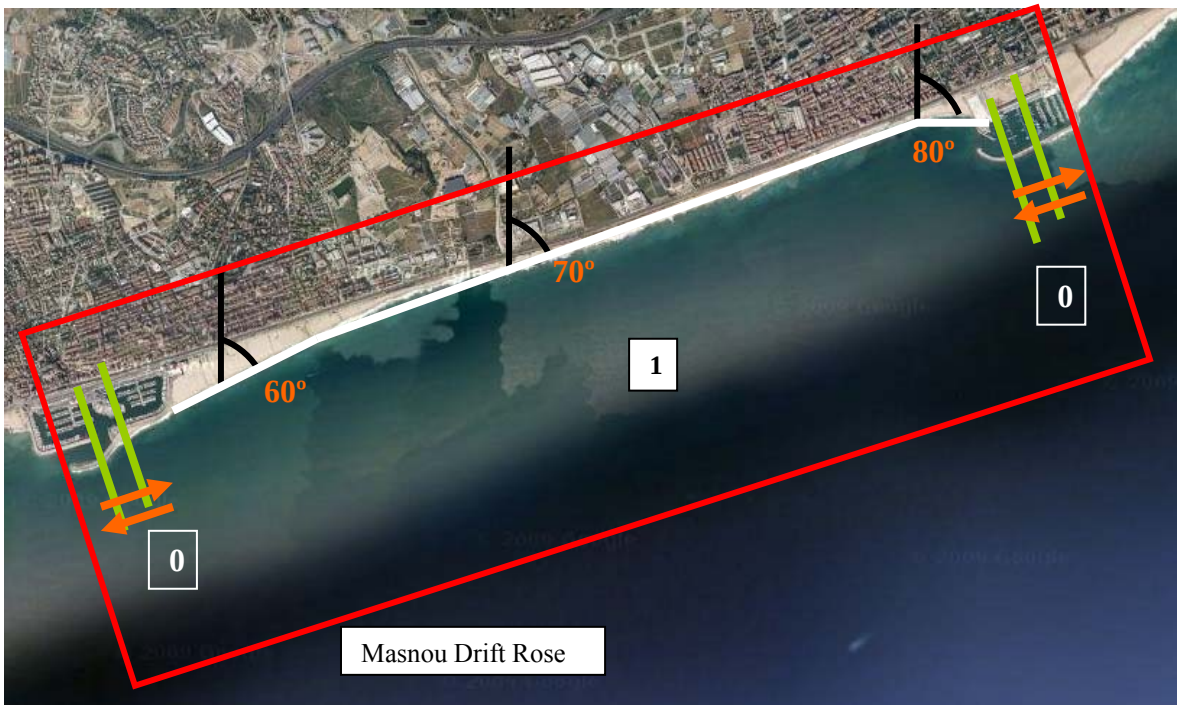

Figure 3.15 Definition of the beach of El Masnou.

	Diameter (D_{50})	Orientation (deg)	Slope	Wave effective Dir.
1. El Masnou	1.12	70	0.19	63-213
Data for Drift Rose				
- Masnou Drift Rose	1.12	60-80	0.19	63-213

Longshore Sediment Transport Time Series

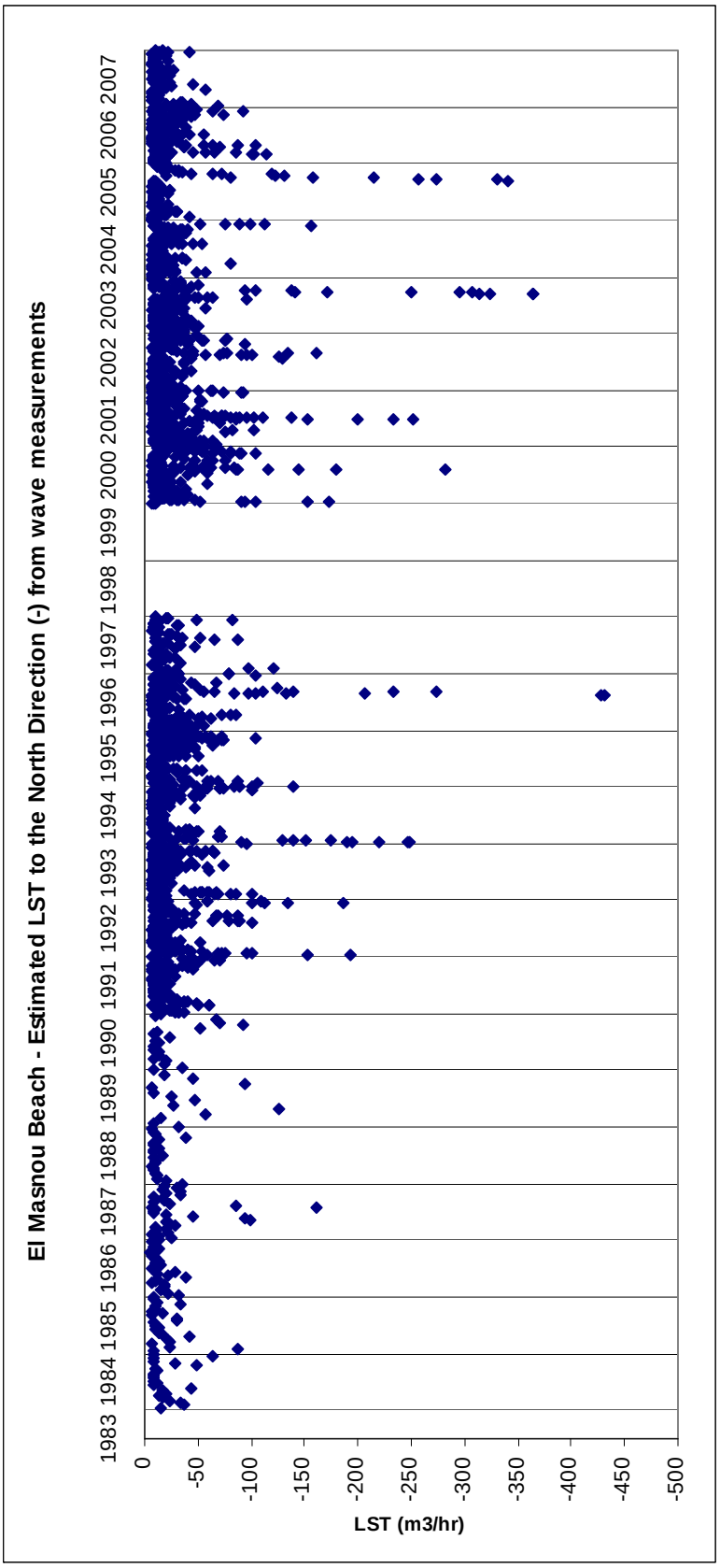

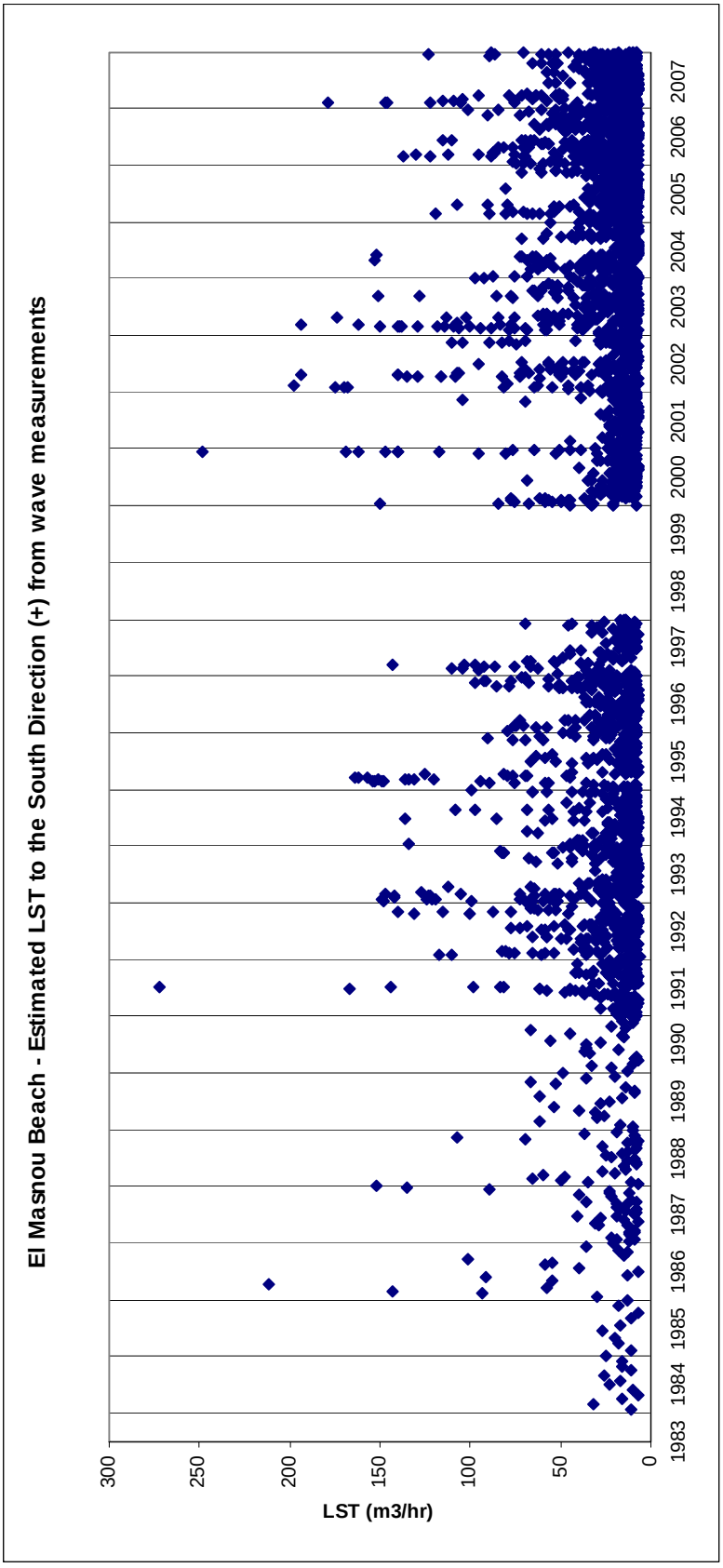
El Masnou Beach - Estimated LST to the South Direction (+) from wave measurements
LST (m3/hr)
300
250
200
150
100
50
0
1983
1984
1985
1986
1987
1988
1989
1990
1991
1992
1993
1994
1995
1996
1997
1998
1999
2000
2001
2002
2003
2004
2005
2006
2007

Monthly Distribution

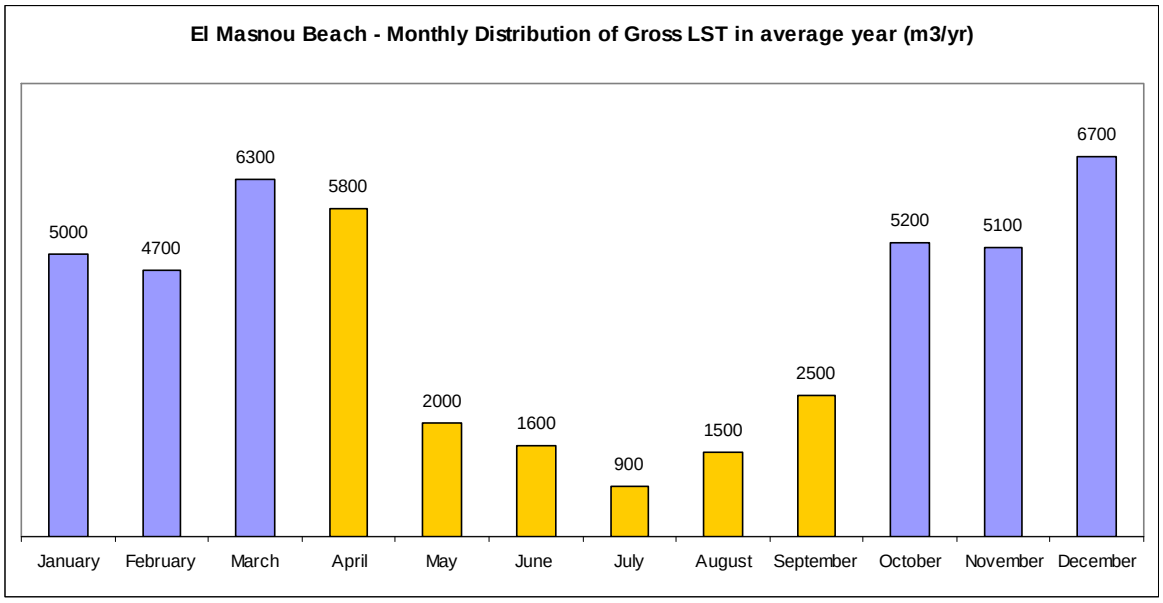

Summer and winter time distribution of Gross LST:

- Oct-Mar: 33 000 (70%)
- Apr-Sep: 24 300 (30%)

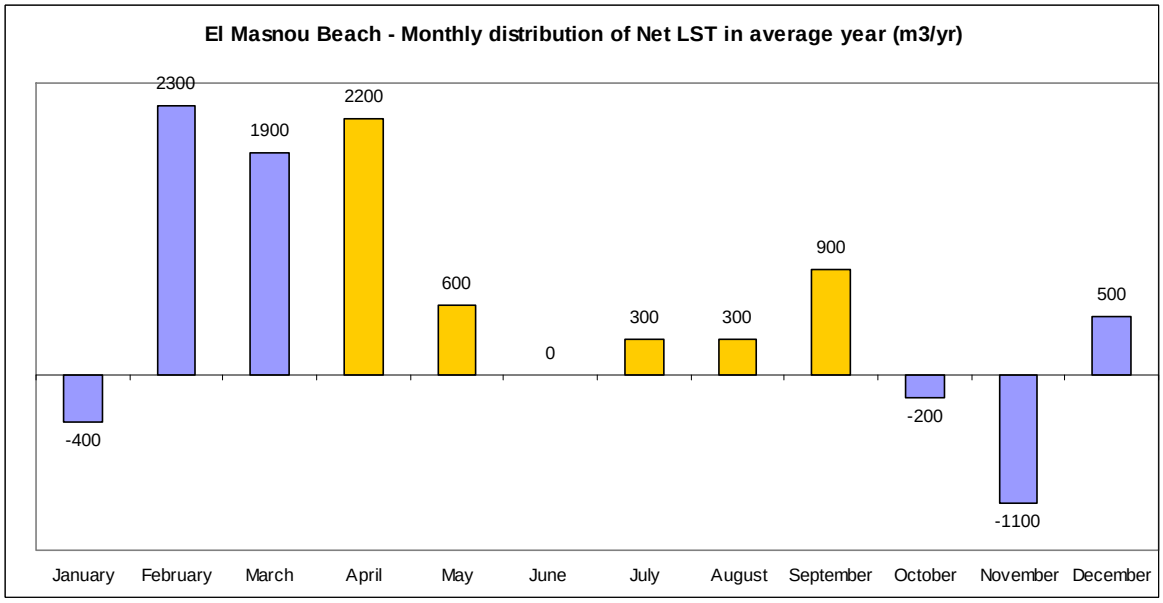

Summer and winter time distribution of Gross LST:

- Oct-Mar: 6 400 (60%)
- Apr-Sep: 4 300 (40%)

LST estimation in average year: total, by wave direction and proportion caused by Hs>2m.

Beach	Direction of Littoral Drift	Total LST (m3/year)	By wave direction			By Hs		Grain size (mm)	Orientation (º)	Slope
			Wave direction	LST (m3/year)	%	LST (Hs>2m)	%			
Masnou	South	27261	ENE	490	1.8	313	63.9	1.12	70	0.19
			ENE	11456	42.0	4674	40.8			
			ESE	11512	42.2	3241	28.2			
			SE	3593	13.2	455	12.7			
			SSE	210	0.8	63	30.0			
	North	19948	SSE	57	0.3	18	31.6			
			S	2812	14.1	574	20.4			
			SSW	17079	85.6	5229	30.6			

Gross LST: 41 200 m^3/yr

Net LST: 7 300 m^3/yr (to South)

Sediment Budget using LST Capacity

Figure 3.16 Evaluation of LST along the beach of El Masnou.

Storm contribution: proportion of transport caused by storm conditions (Hs>2m)

South Direction: 33%

North Direction: 30%

Masnou Drift Rose

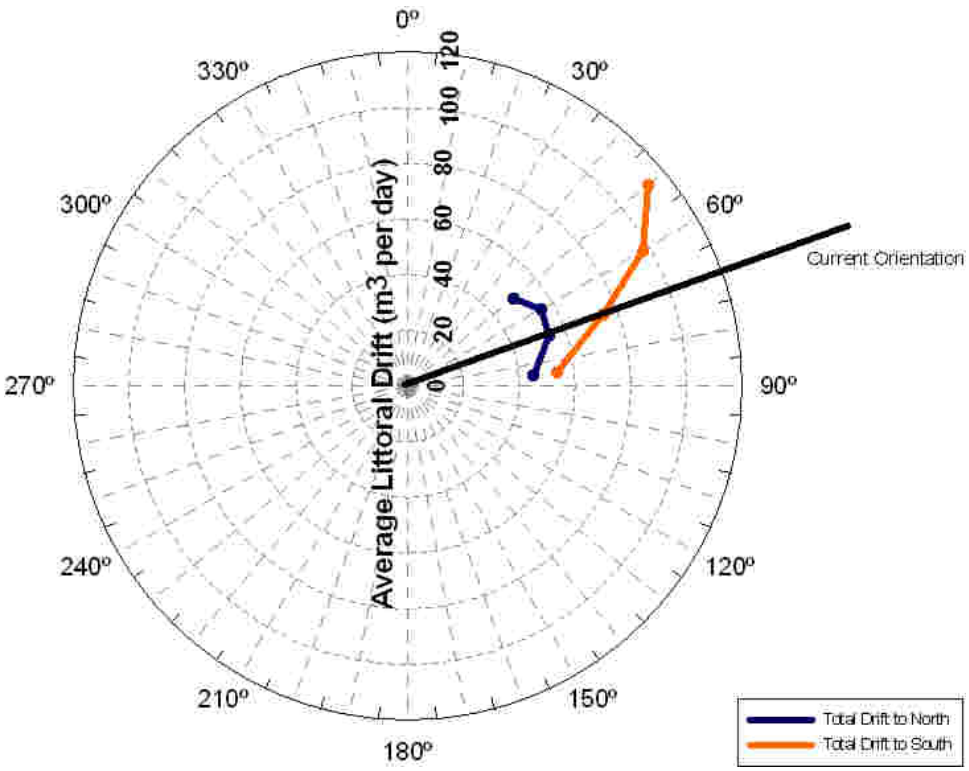

3.2.10 Castelldefels

Situation of Castelldefelsl beach.

Beach definition and main parameters

Figure 3.17 Definition of the beach of Castelldefels.

	Diameter (D_{50})	Orientation (deg)	Slope	Wave effective Dir.
1. Castelldefels East	0.50	65	0.08	65-235
2. Castelldefels West	0.50	90	0.08	90-235
- Castelldefels Drift Rose	0.50	30-85	0.08	65-235

CASTELLDEFELS EAST

Longshore Sediment Transport Time Series

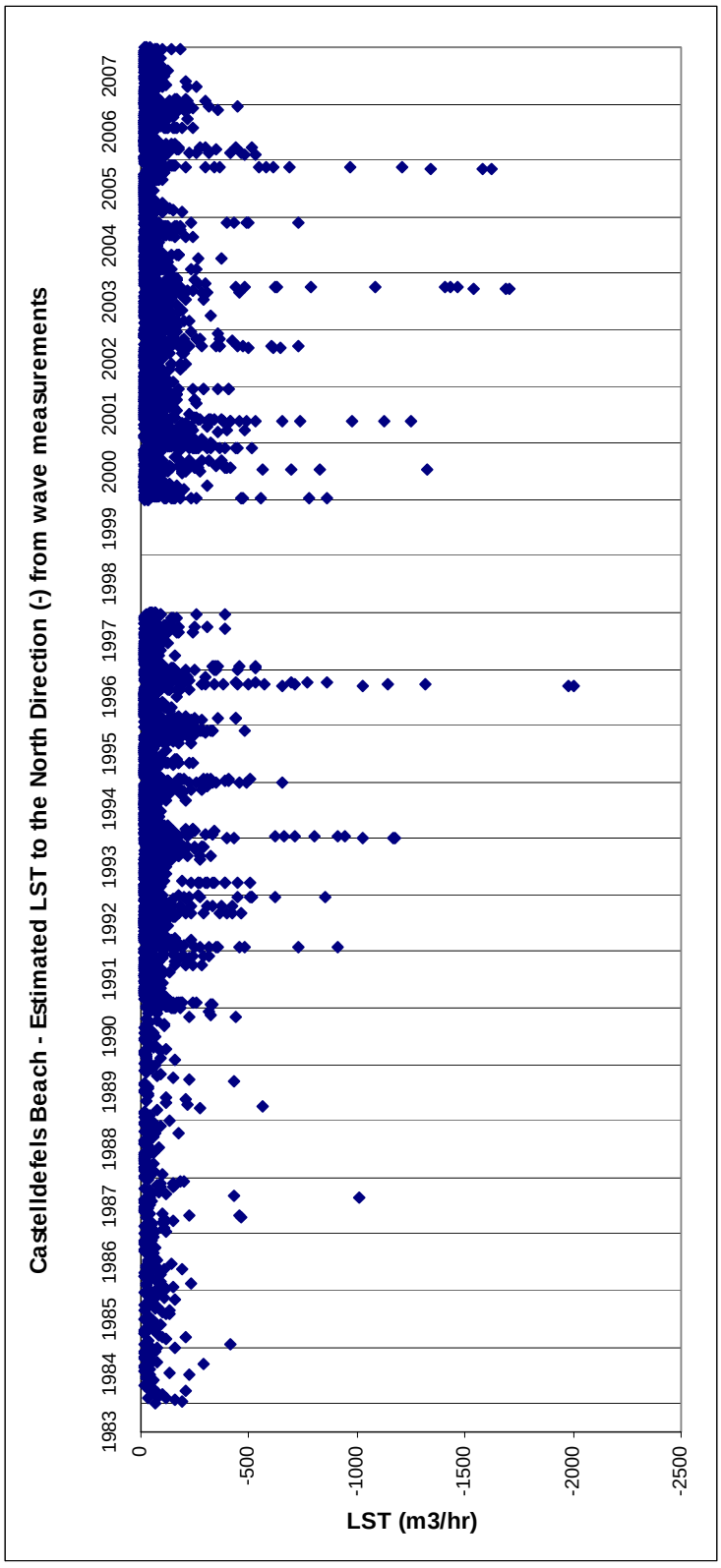

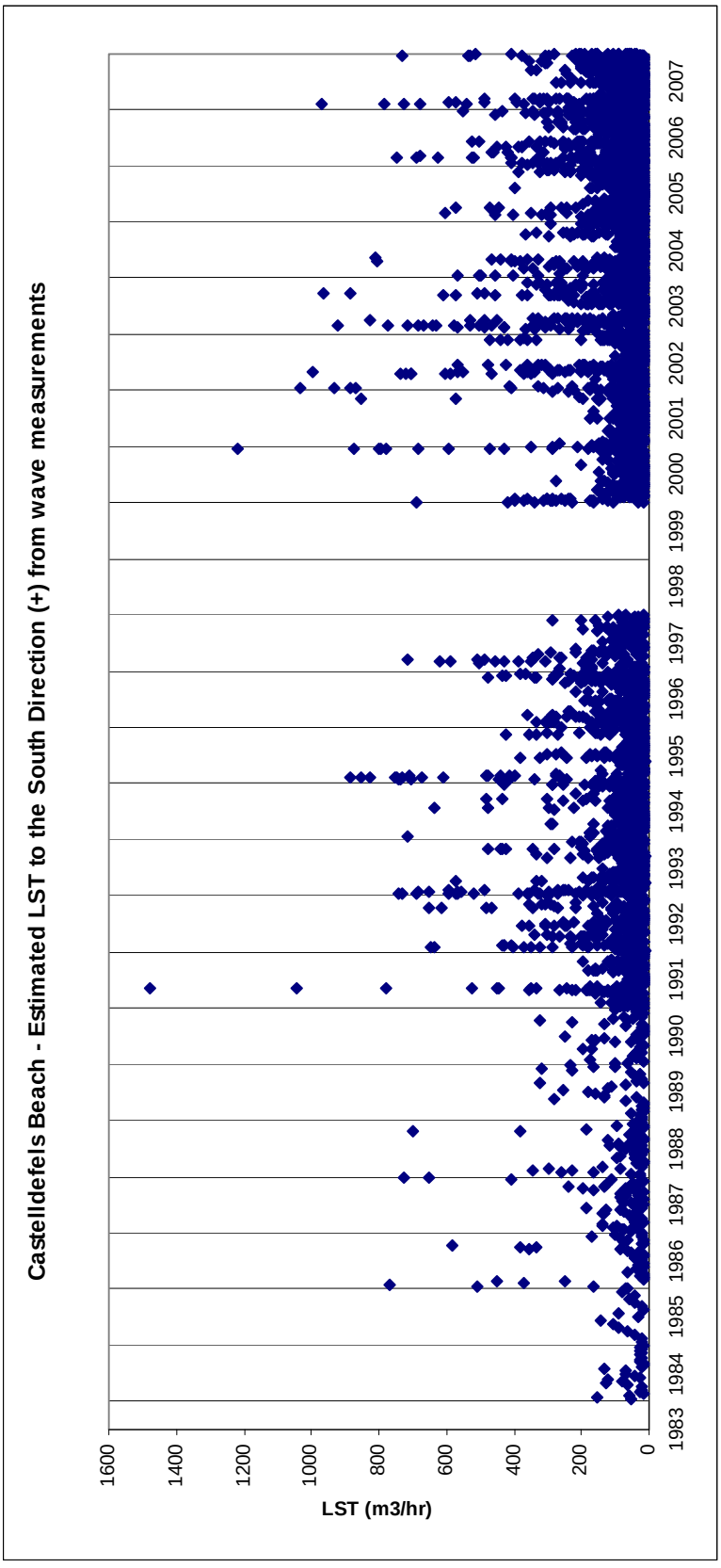
Castelldefels Beach - Estimated LST to the South Direction (+) from wave measurements
LST (m3/hr)
1600
1400
1200
1000
800
600
400
200
0
1983
1984
1985
1986
1987
1988
1989
1990
1991
1992
1993
1994
1995
1996
1997
1998
1999
2000
2001
2002
2003
2004
2005
2006
2007

Monthly Distribution

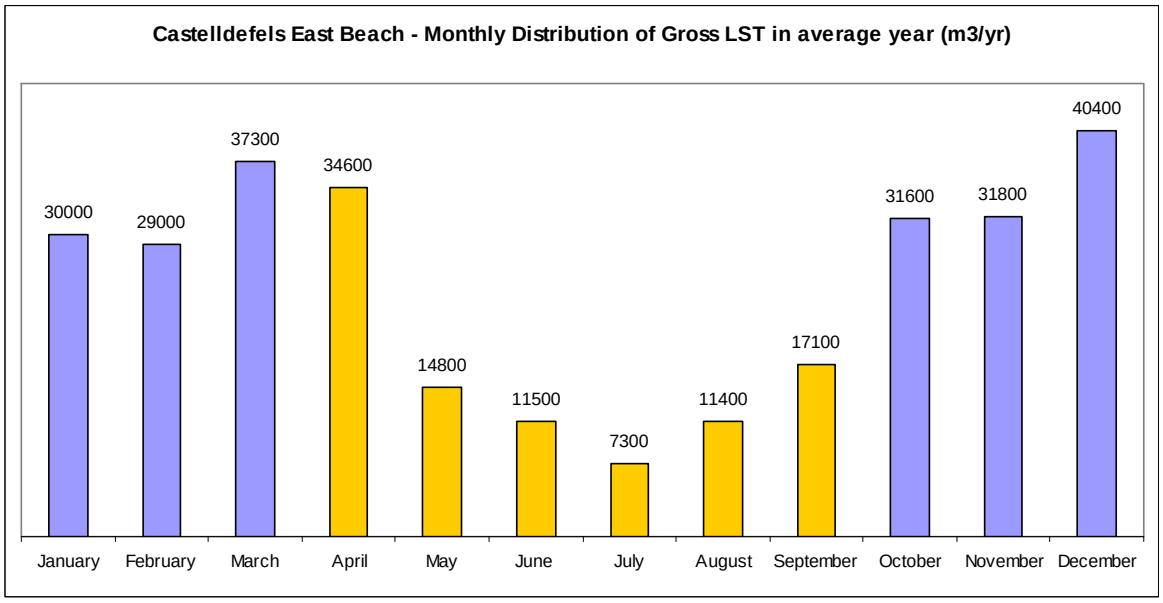

Summer and winter time distribution of Gross LST:

- Oct-Mar: 200 100 (67%)
- Apr-Sep: 96 700 (33%)

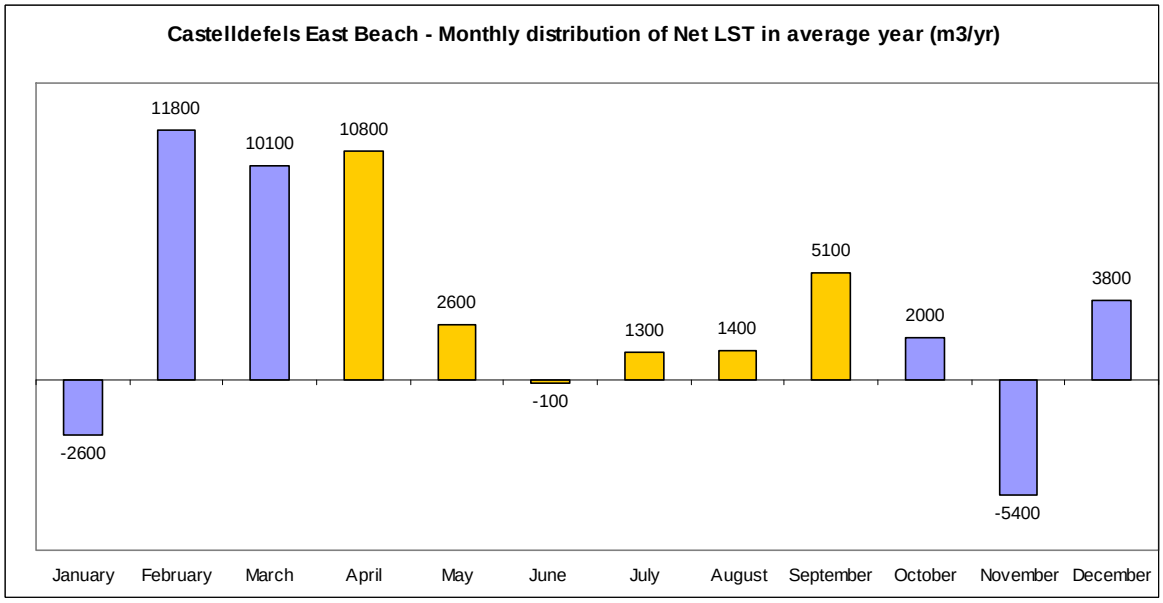

Summer and winter time distribution of Net LST:

- Oct-Mar: 35 700 (63%)
- Apr-Sep: 21 300 (37%)

CASTELLDEFELS WEST

Longshore Sediment Transport Time Series

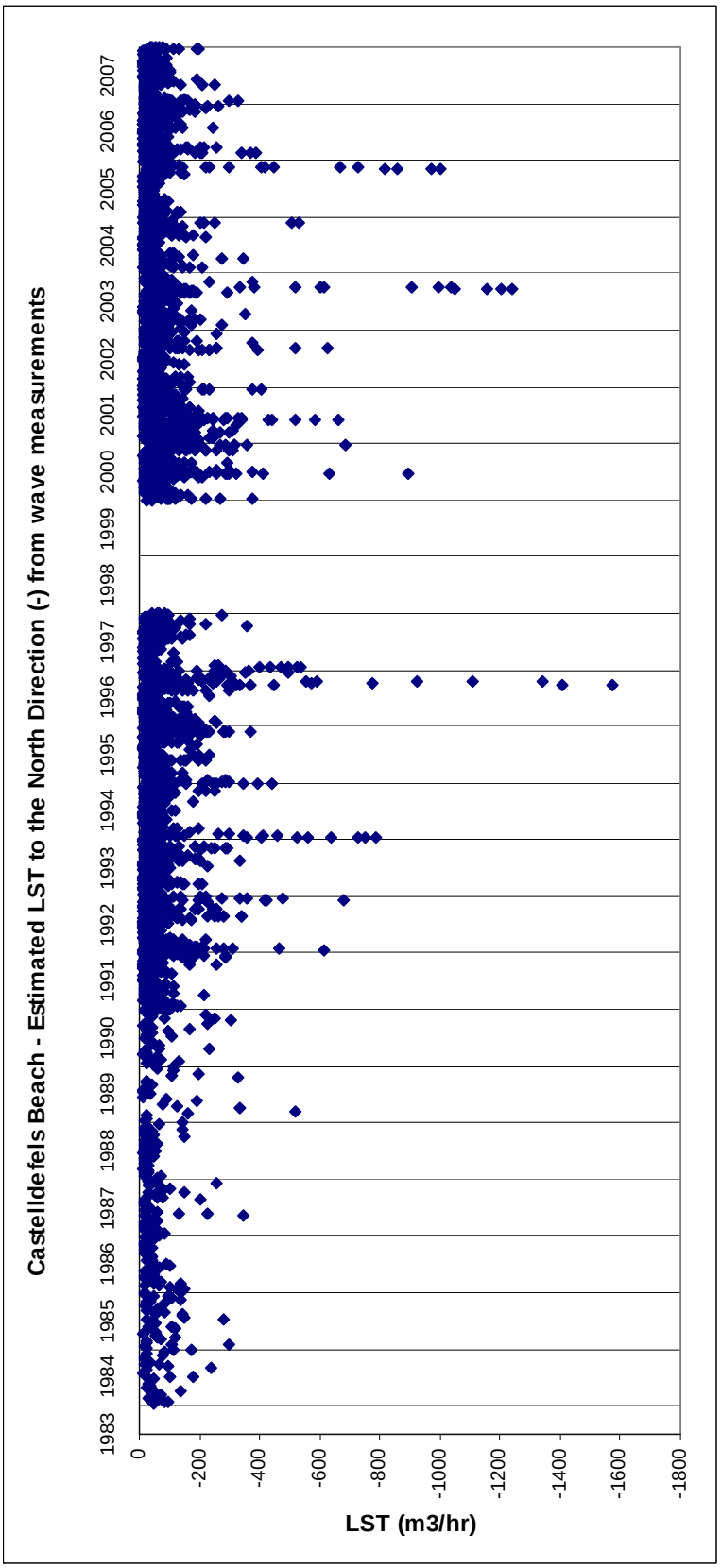

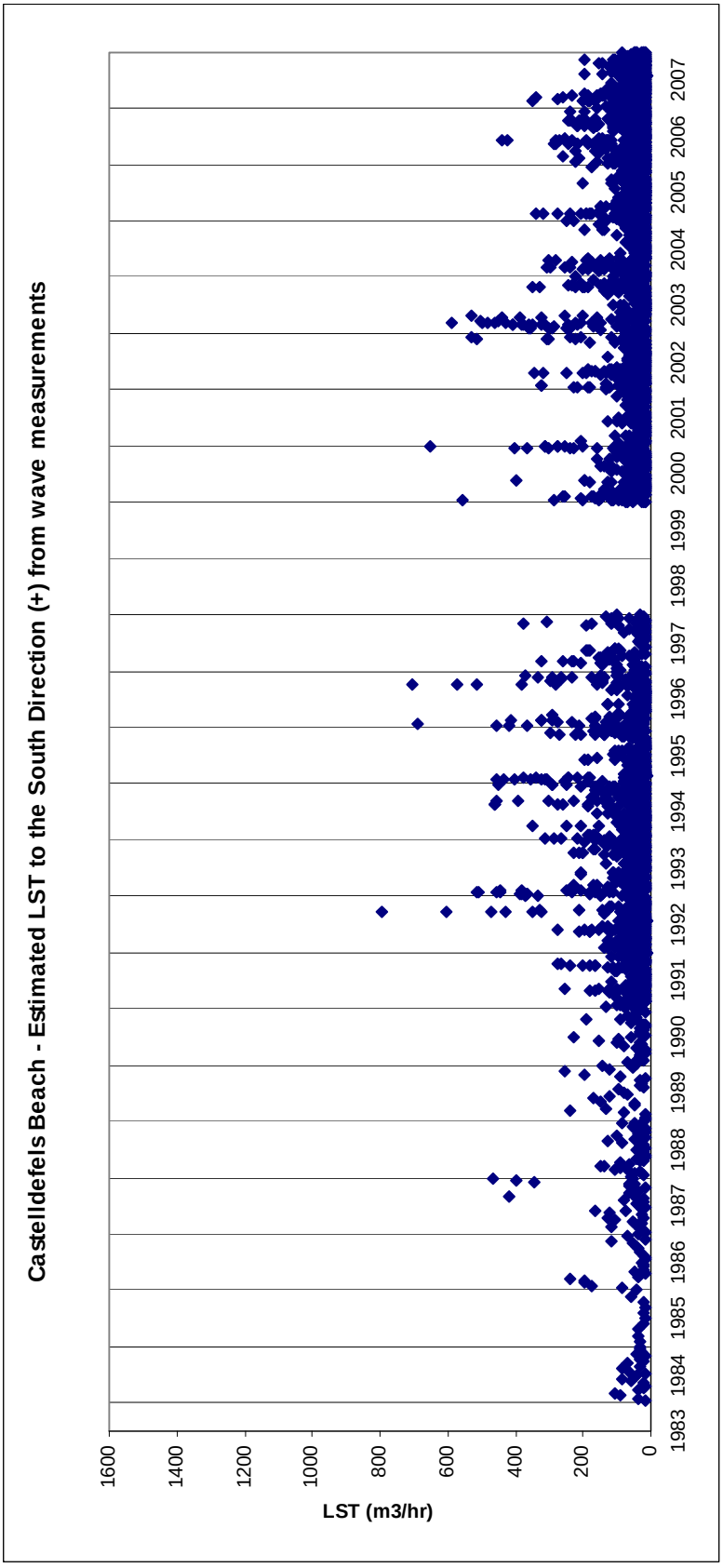
Castelldefels Beach - Estimated LST to the South Direction (+) from wave measurements
LST (m3/hr)
1600
1400
1200
1000
800
600
400
200
0
1983
1984
1985
1986
1987
1988
1989
1990
1991
1992
1993
1994
1995
1996
1997
1998
1999
2000
2001
2002
2003
2004
2005
2006
2007

Monthly Distribution

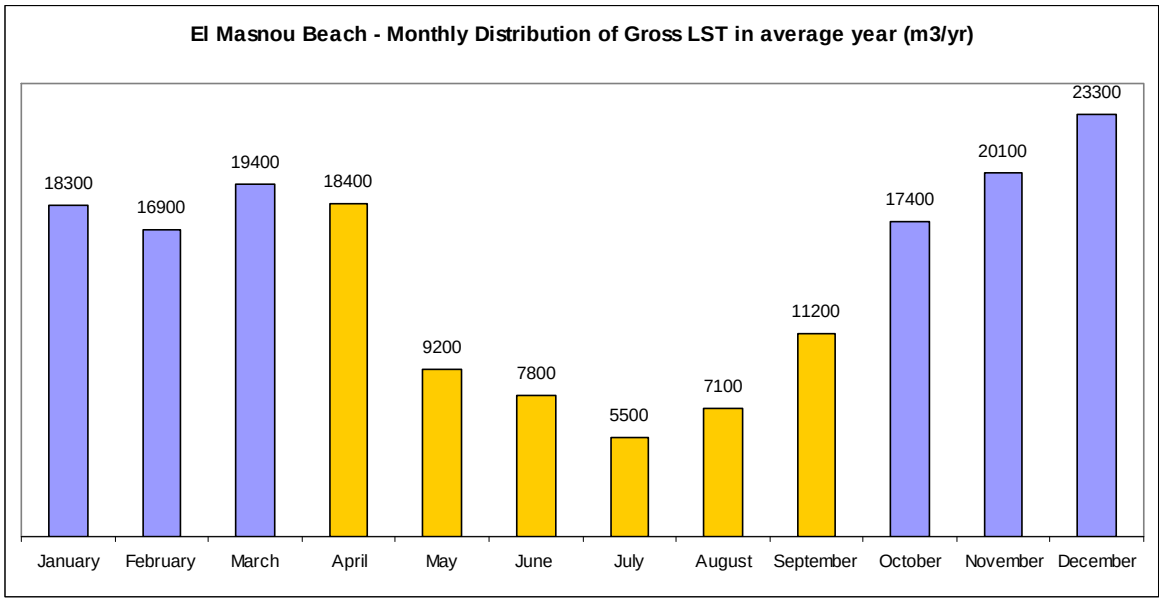

Summer and winter time distribution of Gross LST:

- Oct-Mar: 115 400 (66%)
- Apr-Sep: 59 200 (34%)

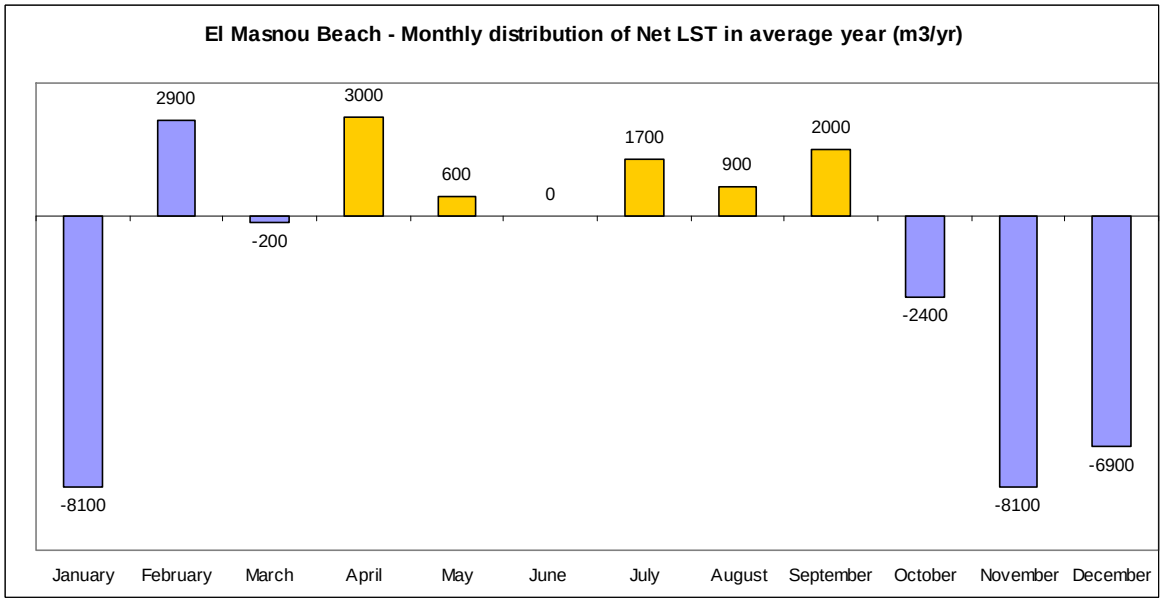

Summer and winter time distribution of Net LST:

- Oct-Mar: 28 600 (78%)
- Apr-Sep: 8 200 (22%)

LST estimation in average year: total, by wave direction and proportion caused by Hs>2m.

Beach	Direction of Littoral Drift	Total LST (m3/year)	Wave direction			Hs		Grain size (mm)	Orientation (º)	Slope
			Wave direction	LST (m3/year)	%	LST (Hs>2m)	%			
Castelldefels East	South	168925	ENE	10851	6.4	4108	37.9	0.5	65	0.08
			E	77566	45.9	27539	35.5			
			ESE	61787	36.6	15823	25.6			
			SE	18177	10.8	1923	10.6			
			SSE	544	0.3	160	29.4			
	North	128028	SSE	1601	1.3	273	17.1			
			S	20601	16.1	3157	15.3			
			SSW	88865	69.4	24945	28.1			
			SW	16961	13.2	1513	8.9			
Castelldefels West	South	80078	E	5925	7.4	2938	49.6	0.5	90	0.08
			ESE	35818	44.7	9104	25.4			
			SE	26271	32.8	2692	10.2			
			SSE	10715	13.4	1334	12.4			
			S	1349	1.7	434	32.2			
	North	94494	S	2669	2.8	614	23.0			
			SSW	62868	66.5	17291	27.5			
			SW	28957	30.6	2255	7.8			

	East Castelldefels	West Castelldefels
Gross LST(m^3/yr)	297 000	174 600
Net LST (m^3/yr)	40 900 (to South)	-14 400 (to North)

Sediment Budget using LST Capacity

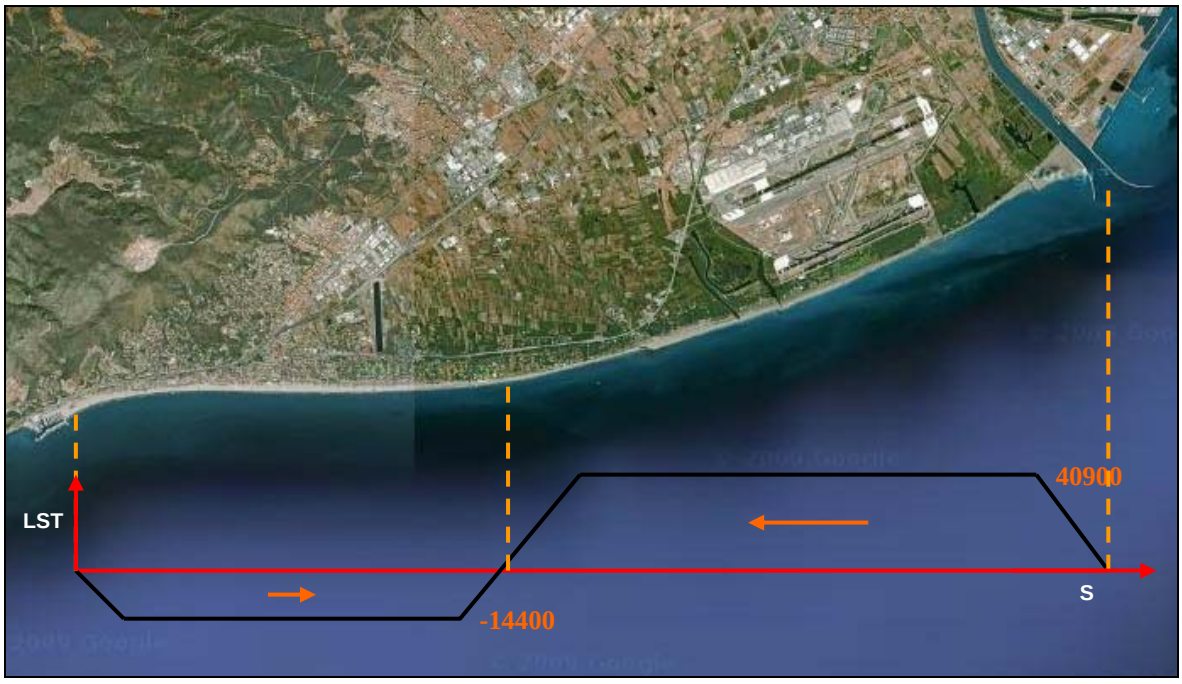

Figure 3.18 Evaluation of LST along the beach of Castelldefels.

Comments on Sediment Budget

Due to its different orientation, littoral drift at East and West stretches of Castelldefels beach is in opposite directions. East side is exposed to waves from East, the typical direction from where storms use to come. The angle of incidence for this waves is oblique and produce a quite important transport to the South. At the end of this first stretch the shoreline changes its orientation until it becomes about 90º along the West side. That means that at this second stretch waves from East come parallel to the coast and hence producing no transport. On the other hand, unlike East stretch this one is exposed to waves from South West direction. Such conditions give as a result a Net transport to the left when looking offshore along the West side. As the orientation changes, the value of Net transport decreases until it takes the opposite direction along the other stretch and increases again, but this time with the opposite sign.

Storm contribution: proportion of transport caused by storm conditions (Hs>2m)

	East Castelldefels	**West Castelldefels .**
South Direction:	29%	21%
North Direction:	23%	21%

3.2.11 Calafell

Situation of El Roc – Creixell beach.

Beach definition and main parameters

Figure 3.17 Definition of the beach of Calafell.

	Diameter (D_{50})	Orientation (deg)	Slope	Wave effective Dir.
1. Calafell	0.17	79	0.06	80-235
Data for Drift Rose:				
- Calafell Drift Rose	0.17	60-100º	0.06	80-235

Longshore Sediment Transport Time Series

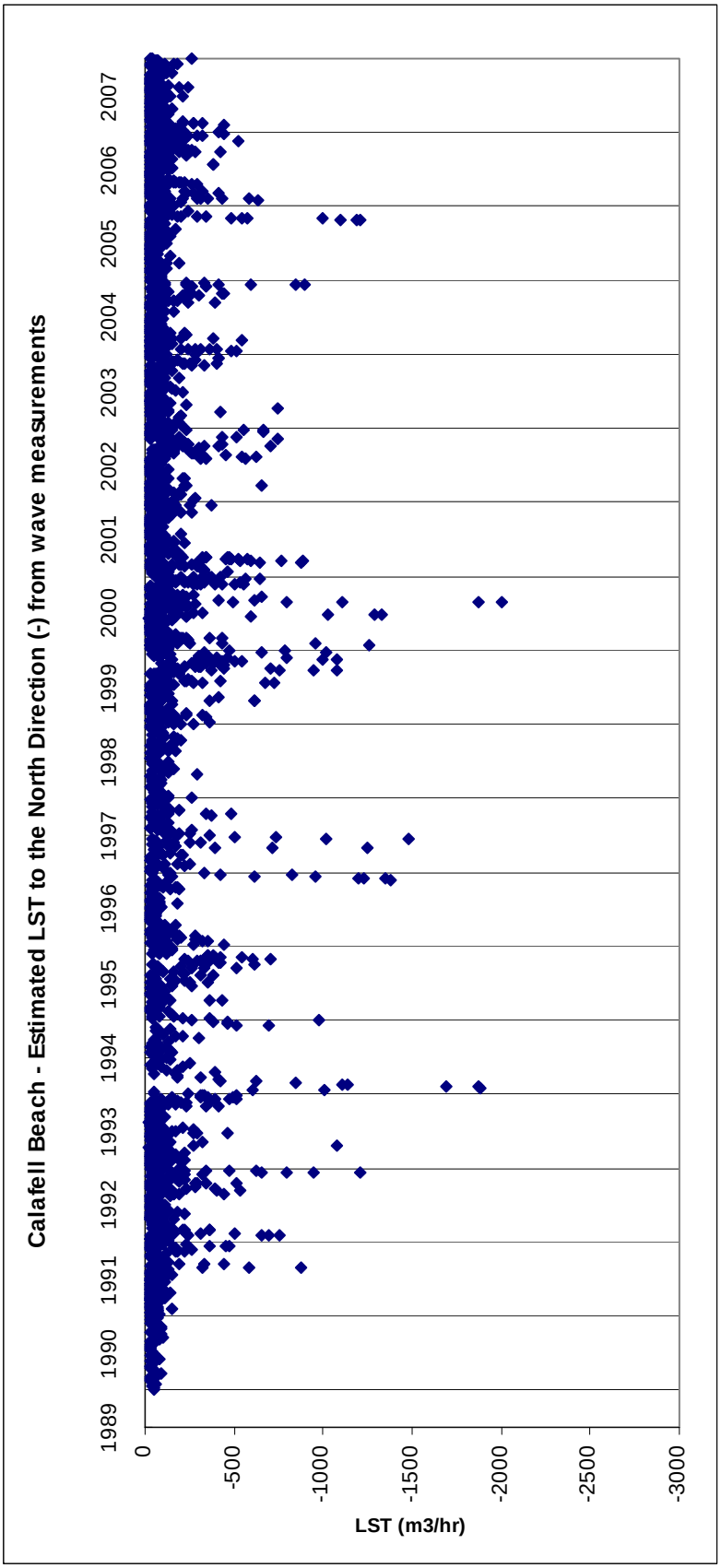

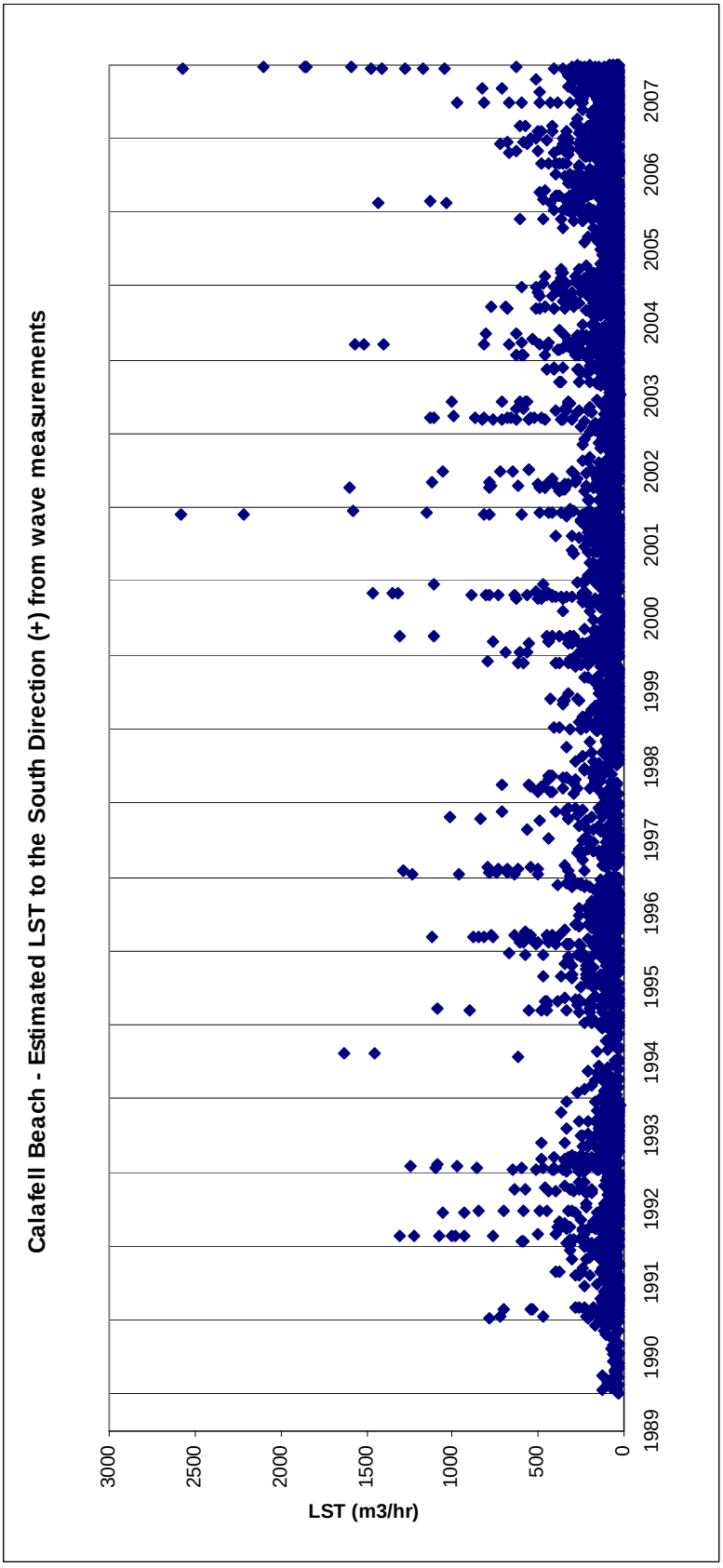
Calafell Beach - Estimated LST to the South Direction (+) from wave measurements
LST (m3/hr)
3000
2500
2000
1500
1000
500
0
1989
1990
1991
1992
1993
1994
1995
1996
1997
1998
1999
2000
2001
2002
2003
2004
2005
2006
2007

Monthly Distribution

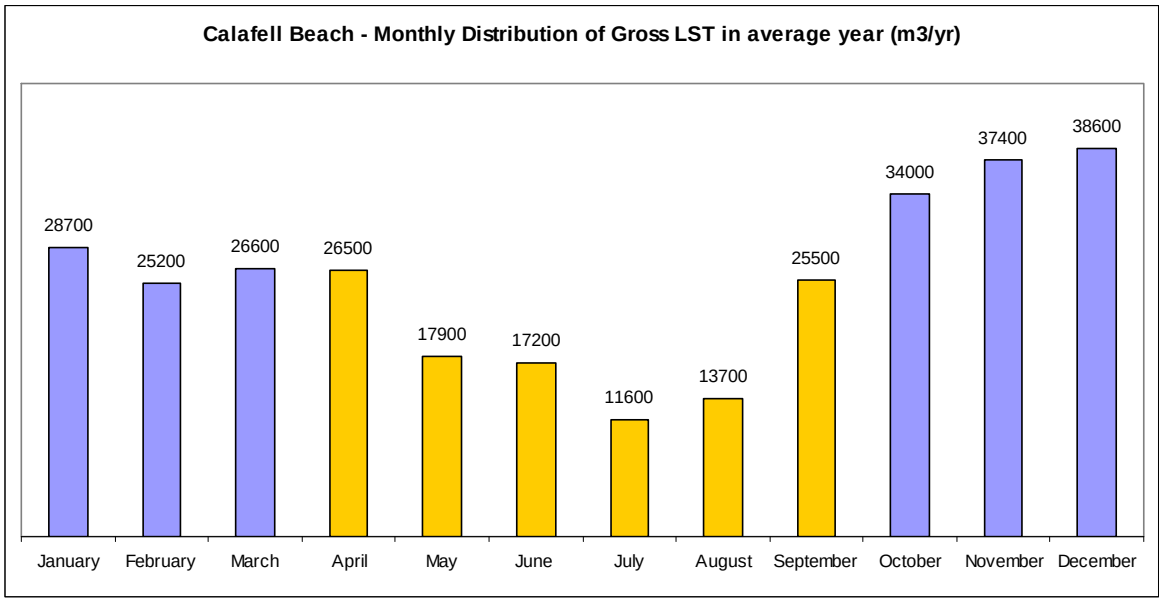

Summer and winter time distribution of Gross LST:

- Oct-Mar: 190 500 (68%)
- Apr-Sep: 112 400 (32%)

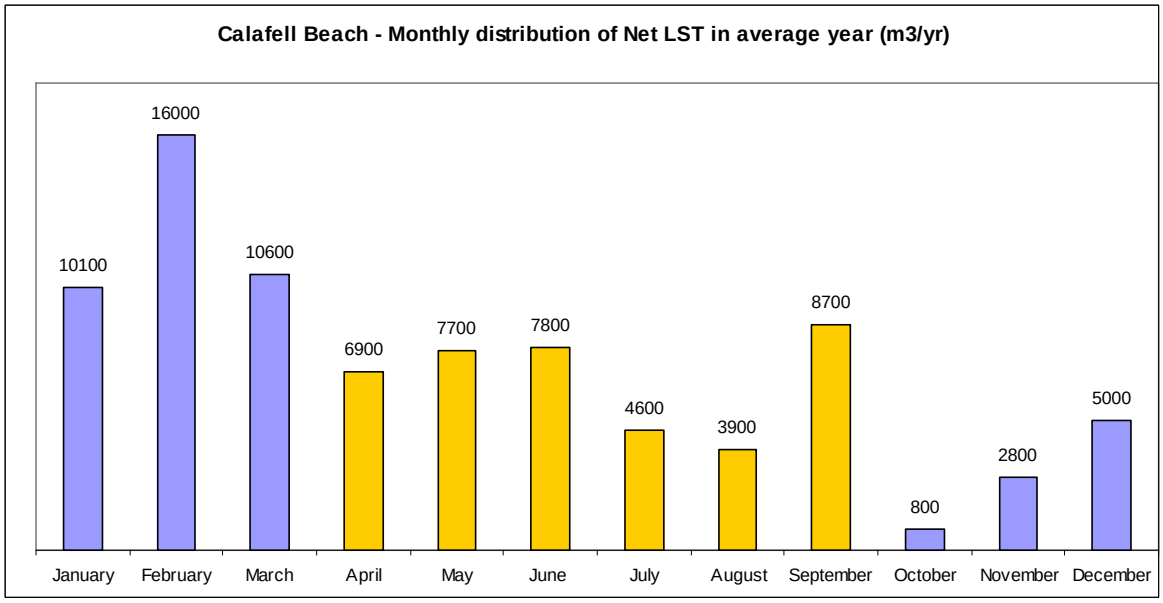

Summer and winter time distribution of Gross LST:

- Oct-Mar: 45 300 (53%)
- Apr-Sep: 39 600 (47%)

LST estimation in average year: total, by wave direction and proportion caused by Hs>2m.

Beach	Direction of Littoral Drift	Total LST (m3/year)	By wave direction			By Hs		Grain size (mm)	Orientation (º)	Slope
			Wave direction	LST (m3/year)	%	LST (Hs>2m)	%			
Calafell	South	193899	E	96428	49.7	38910	40.4	0.17	79	0.06
			ESE	61730	31.8	10023	16.2			
			SE	26073	13.4	2204	8.5			
			SSE	9668	5.0	854	8.8			
	North	108829	S	59090	54.3	12098	20.5			
			SSW	48198	44.3	7777	16.1			
			SW	1541	1.4	0	0.0			

Gross LST: 302 700 m^3/yr

Net LST: 85 100 m^3/yr (to South)

Sediment Budget using LST Capacity

Figure 3.18 Evaluation of LST along the beach of Calafell.

Storm contribution: proportion of transport caused by storm conditions (Hs>2m)

South Direction: 27%

North Direction: 18%

Calafell Drift Rose

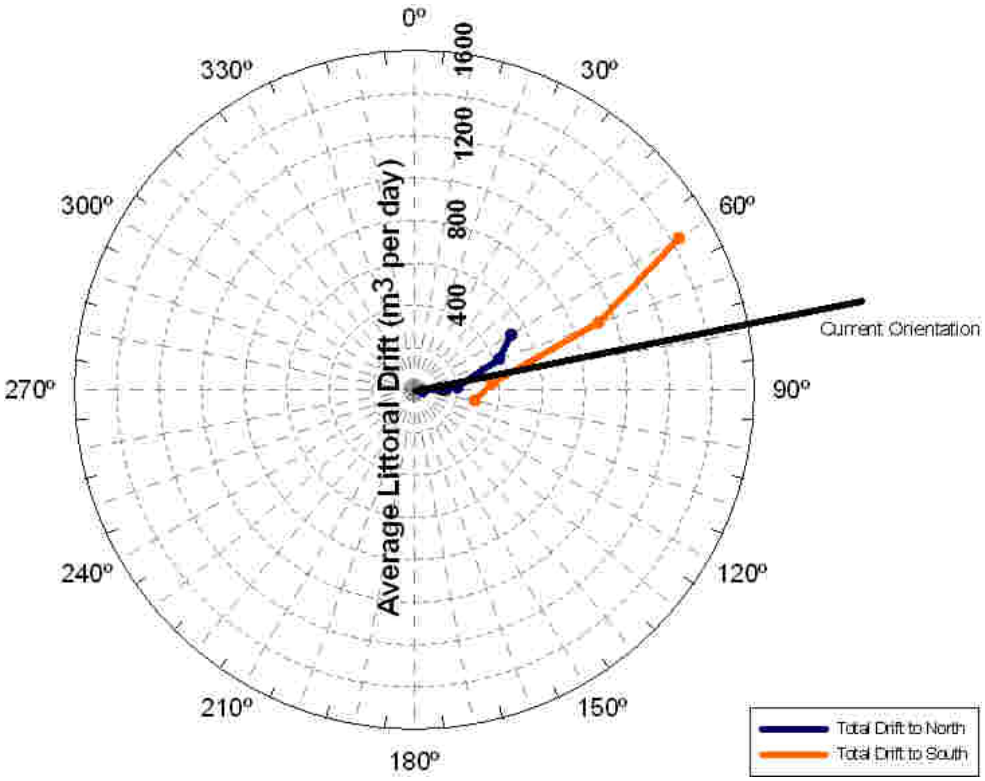

3.2.12 Torredembarra. El Roc - Creixell

Situation of El Roc – Creixell beach.

Beach definition and main parameters

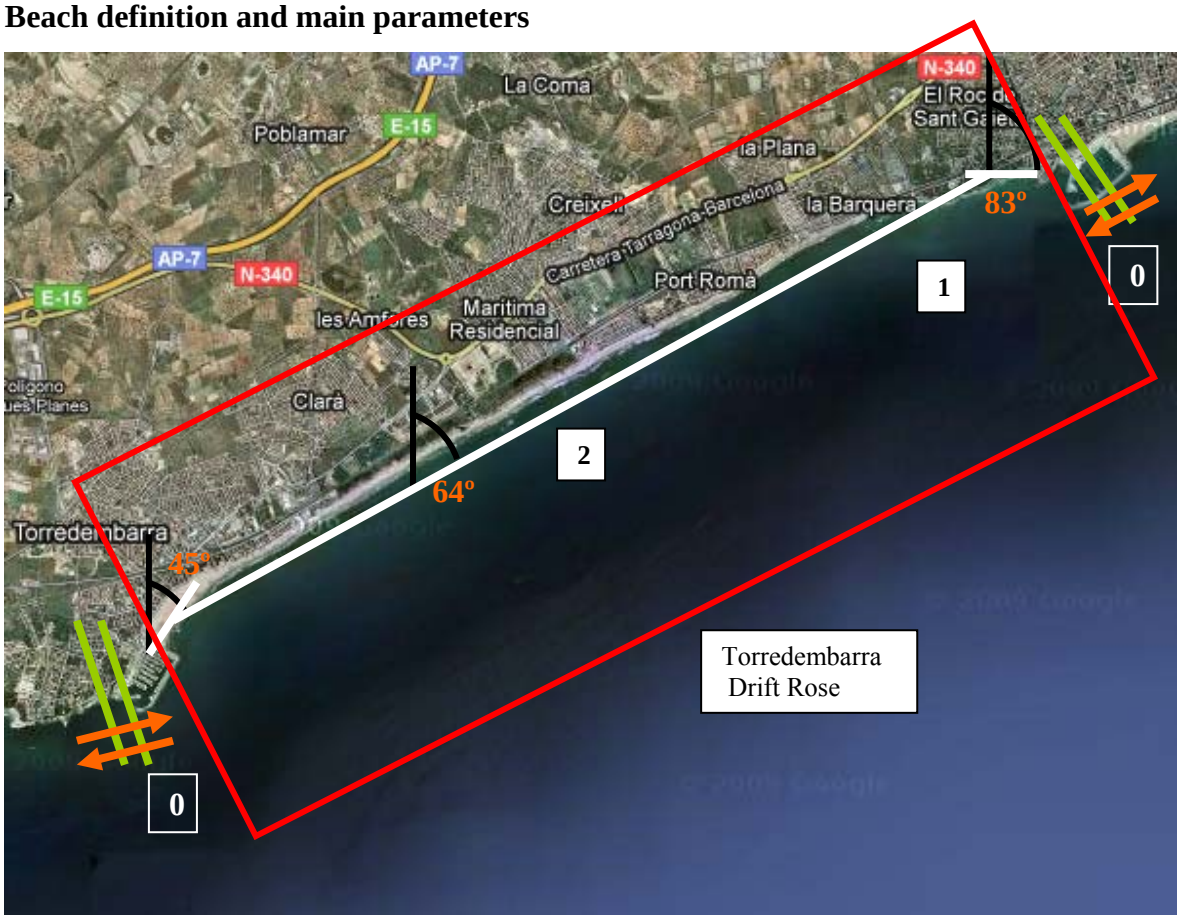

Figure 3.19 Definition of the beach of El Roc – Creixell.

	Diameter (D_{50})	**Orientation (deg)**	**Slope**	**Wave effective Dir.**
1. El Roc	0.34	64	0.02	80-235
2. Creixell	0.15	64	0.02	80-235
Data for Drift Rose:				
- Torredembarra				
Drift Rose	0.25	30-90º	0.02	80-235

EL ROC

Longshore Sediment Transport Time Series

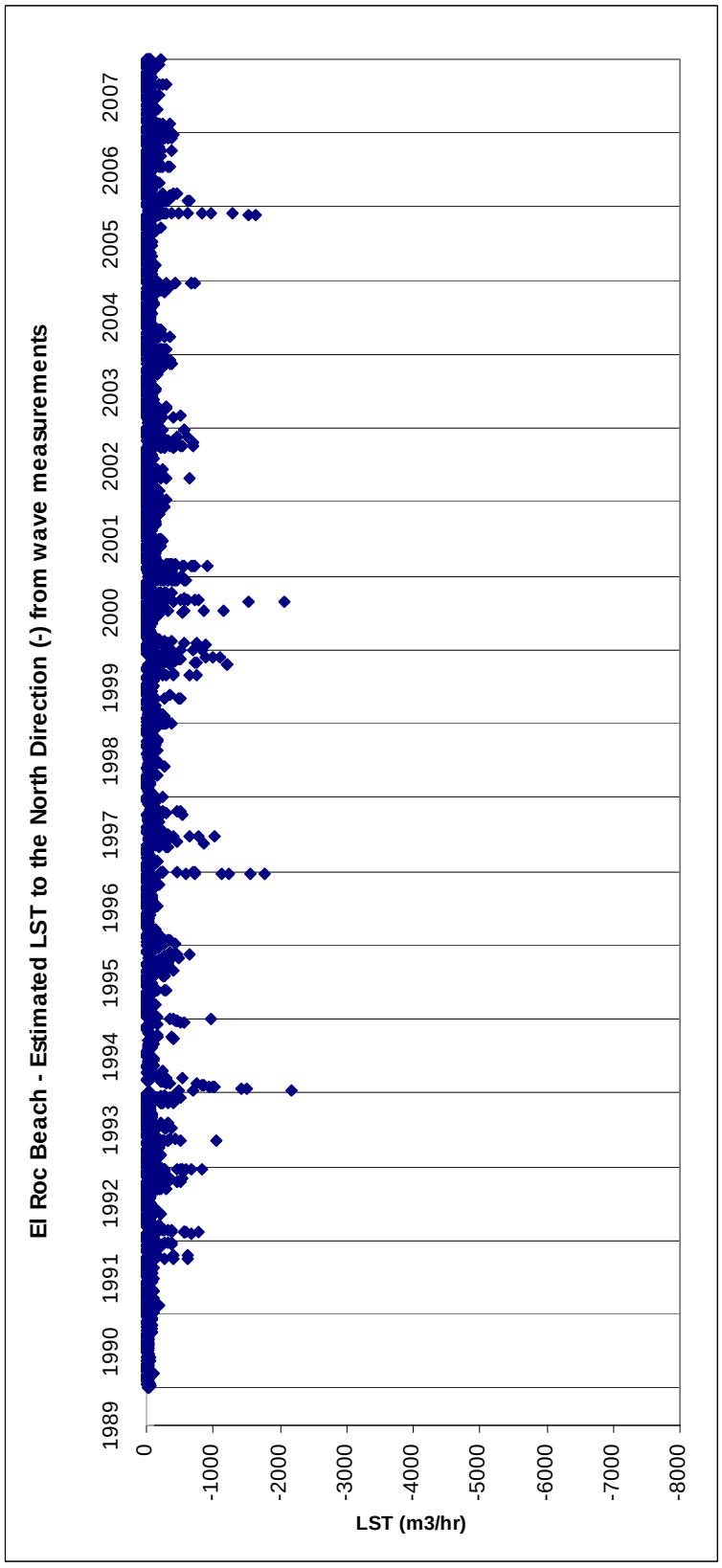

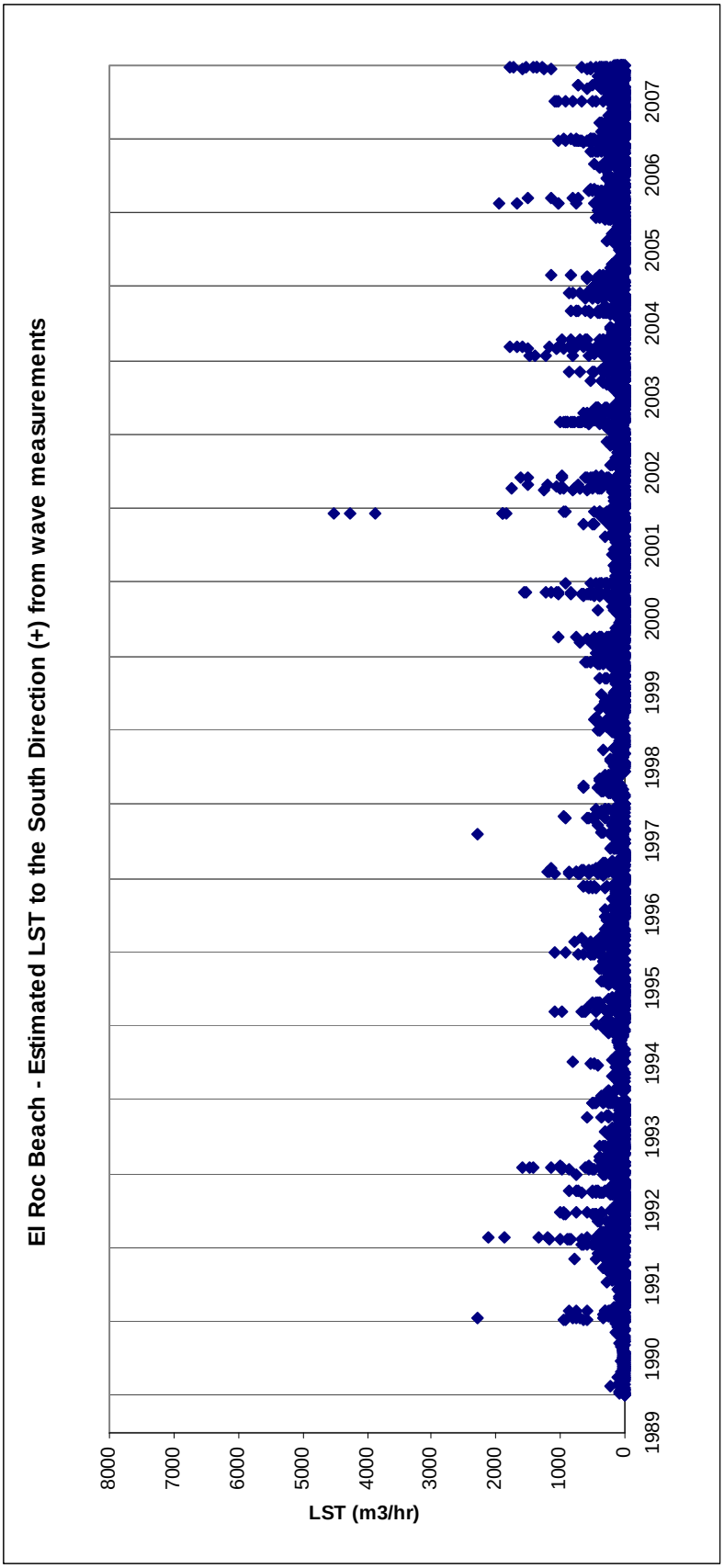
El Roc Beach - Estimated LST to the South Direction (+) from wave measurements
LST (m3/hr)
8000
7000
6000
5000
4000
3000
2000
1000
0
1989
1990
1991
1992
1993
1994
1995
1996
1997
1998
1999
2000
2001
2002
2003
2004
2005
2006
2007

Monthly Distribution

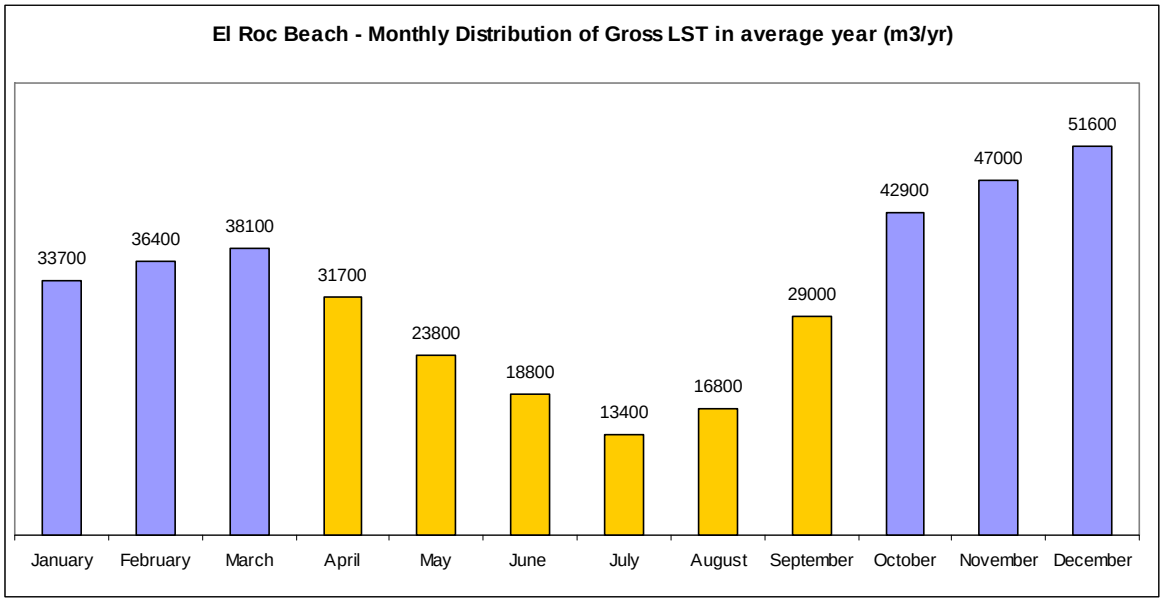

Summer and winter time distribution of Gross LST:

- Oct-Mar: 249 700 (68%)
- Apr-Sep: 133 500 (32%)

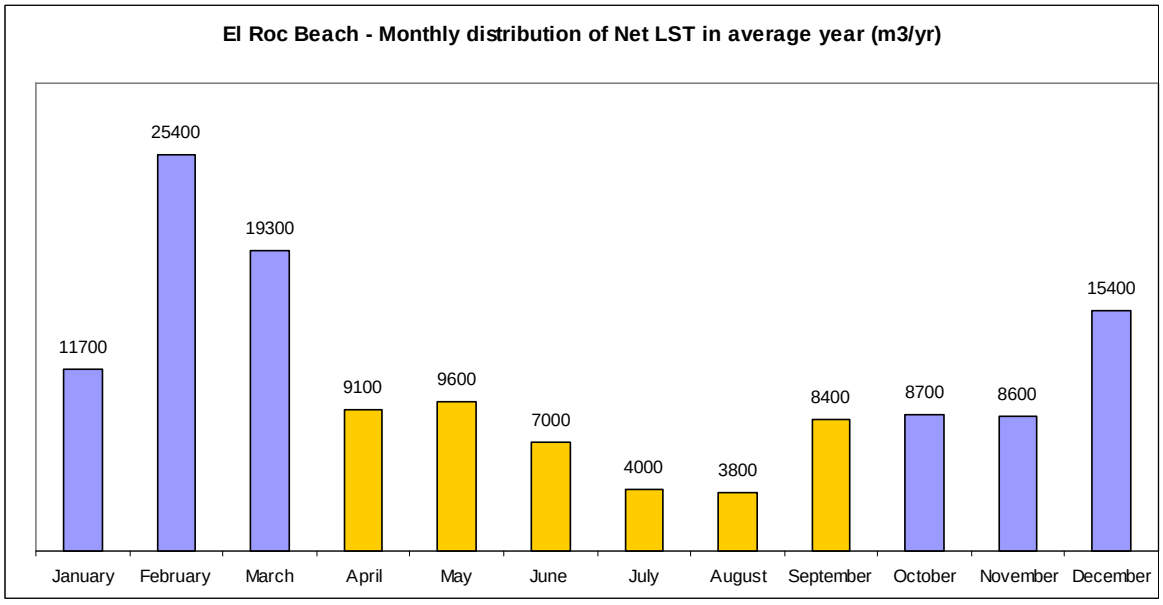

Summer and winter time distribution of Net LST:

- Oct-Mar: 89 100 (68%)
- Apr-Sep: 41 900 (32%)

CREIXELL

Longshore Sediment Transport Time Series

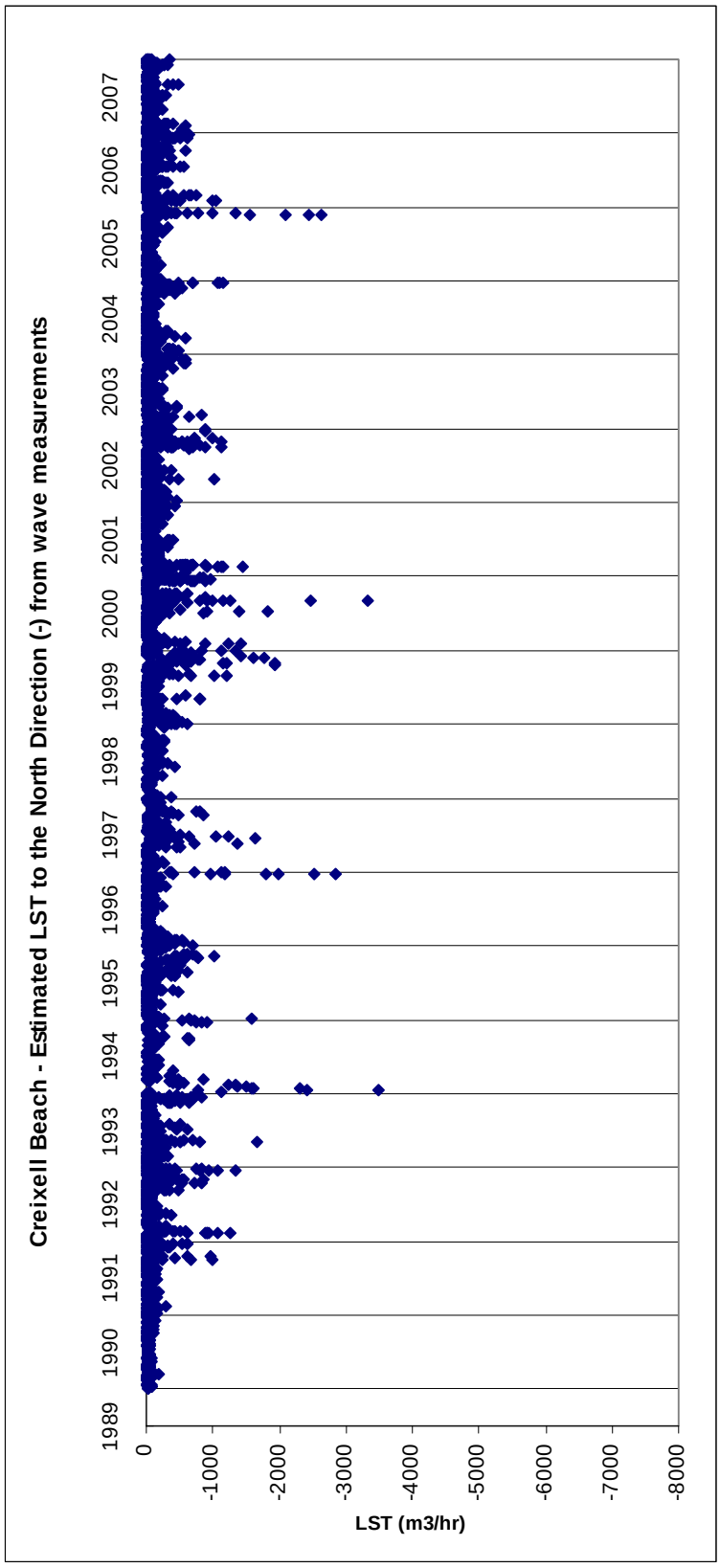

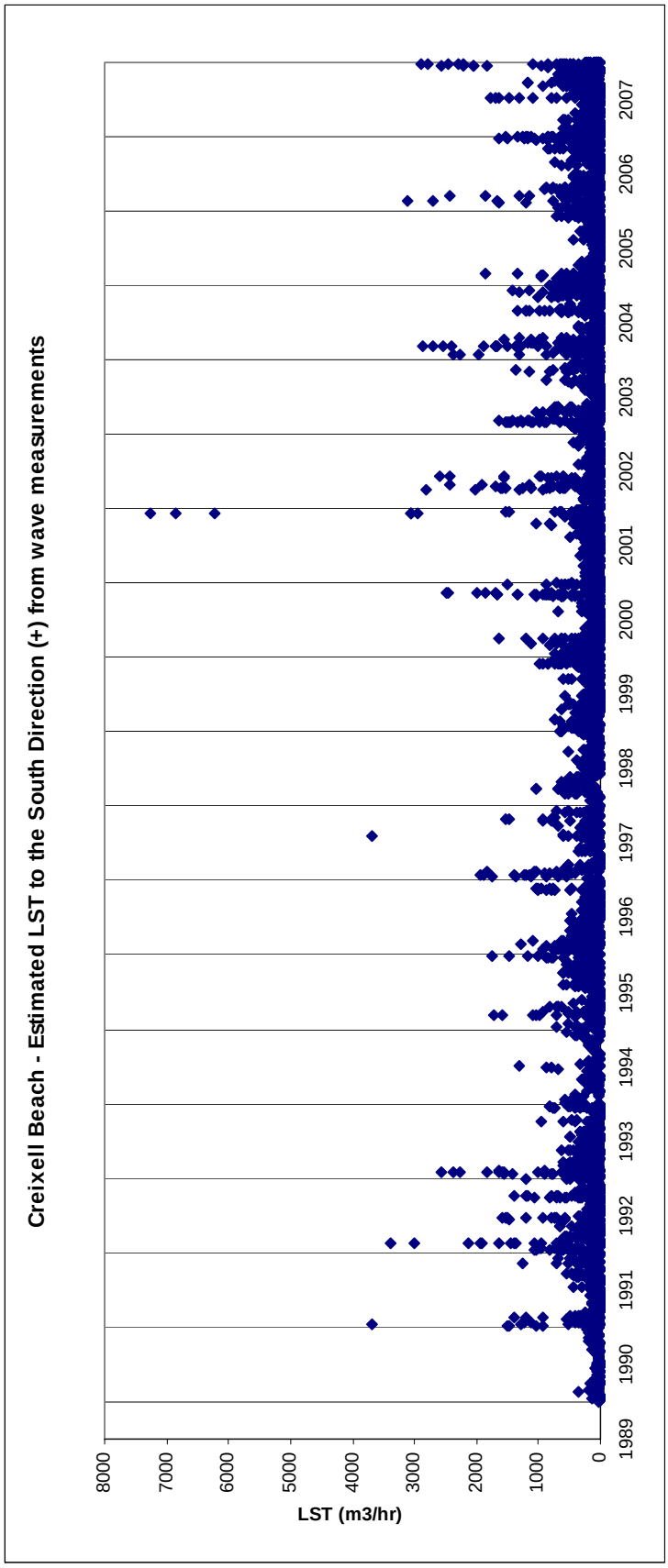
Creixell Beach - Estimated LST to the South Direction (+) from wave measurements
LST (m3/hr)
8000
7000
6000
5000
4000
3000
2000
1000
0
1989
1990
1991
1992
1993
1994
1995
1996
1997
1998
1999
2000
2001
2002
2003
2004
2005
2006
2007

Monthly Distribution

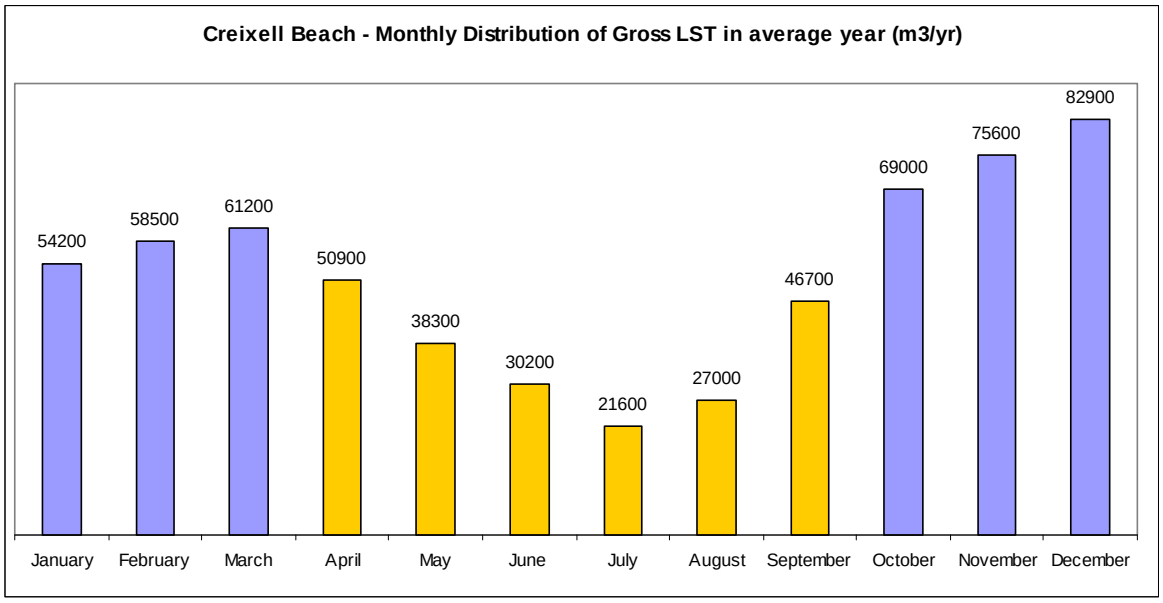

Summer and winter time distribution of Gross LST:

- Oct-Mar: 401 400 (65%)
- Apr-Sep: 214 700 (35%)

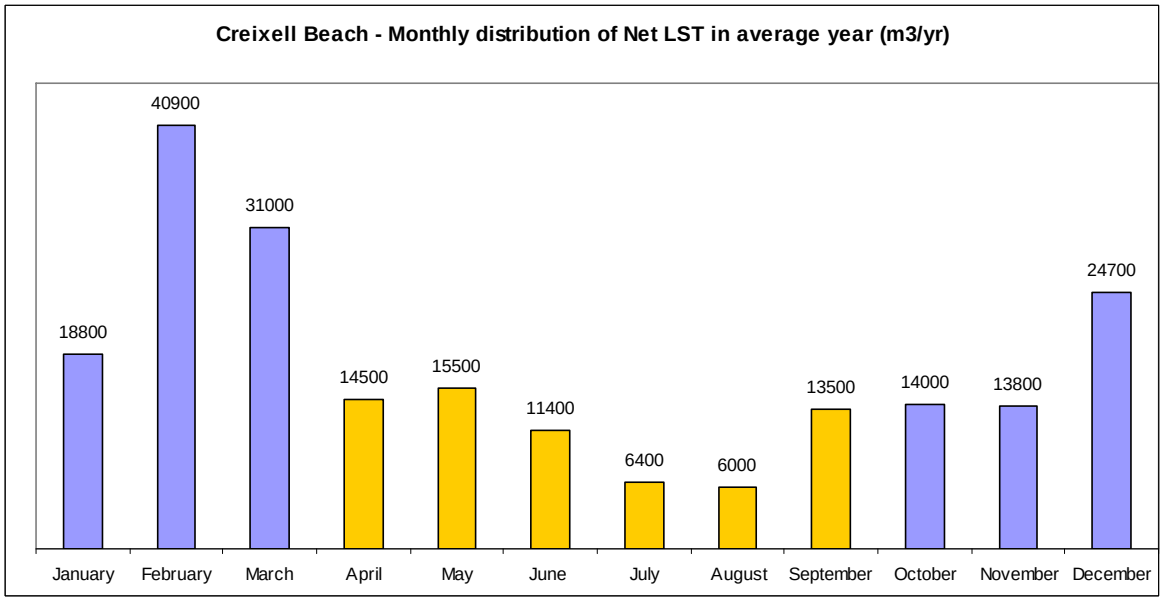

Summer and winter time distribution of Gross LST:

- Oct-Mar: 143 200 (68%)
- Apr-Sep: 67 300 (32%)

LST in average year: total, wave direction and proportion caused by Hs>2m.

Beach	Direction of Littoral Drift	Total LST (m3/year)	Wave direction			Hs		Grain size (mm)	Orientation (º)	Slope
			Wave direction	LST (m3/year)	%	LST (Hs>2m)	%			
El Roc	South	264535	E	190936	72.2	75933	39.8	0.34	64	0.02
			ESE	60388	22.8	10026	16.6			
			SE	12508	4.7	893	7.1			
			SSE	703	0.3	53	7.5			
	North	126048	SSE	3787	3.0	420	11.1			
			S	83405	66.2	14213	17.0			
			SSW	37992	30.1	5795	15.3			
			SW	864	0.7	0	0.0			
Creixell	South	416306	E	307840	73.9	122101	39.7	0.15	64	0.01
			ESE	85819	20.6	13449	15.7			
			SE	21137	5.1	1290	6.1			
			SSE	1510	0.4	84	5.6			
	North	204687	SSE	6810	3.3	675	9.9			
			S	135010	66.0	22854	16.9			
			SSW	61393	30.0	9318	15.2			
			SW	1474	0.7	0	0.0			

	El Roc	**Creixell**
Gross LST(m^3/yr)	390 600	620 993
Net LST (m^3/yr)	138 500 (to North)	211 600 (to West)

Sediment Budget using LST Capacity

Figure 3.20 Evaluation of LST along the beach of Calafell – Torrebembarra.

Storm contribution: proportion of transport caused by storm conditions (Hs>2m)

	El Roc	Creixell
South Direction:	33%	33%
North Direction:	16%	16%

Torredembarra Drift Rose

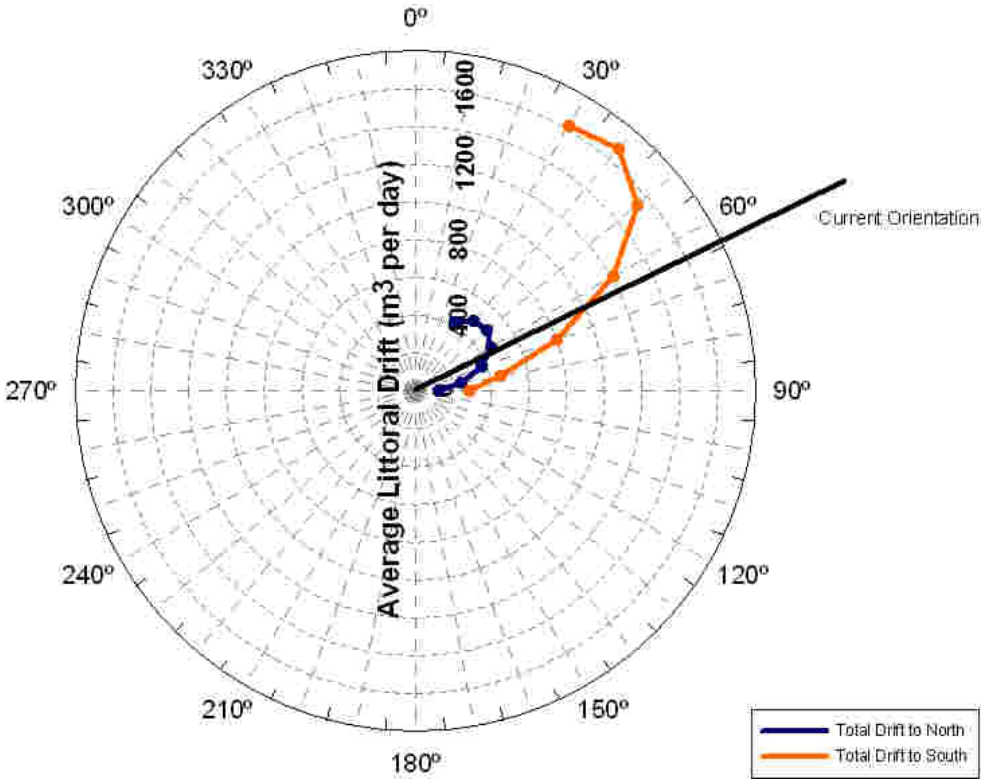

3.2.13 Tarragona. El Miracle

Situation of Tarragona – El Miracle.

Beach definition and main parameters

Figure 3.21 Definition of the beach of El Miracle.

	Diameter (D_{50})	Orientation (deg)	Slope	Wave effective Dir.
1. El Miracle	0.19	44	0.02	80-218
Data for Drift Rose:				
- El Miracle Drift Rose	0.19	20-80º	0.02	80-218

Longshore Sediment Transport Time Series

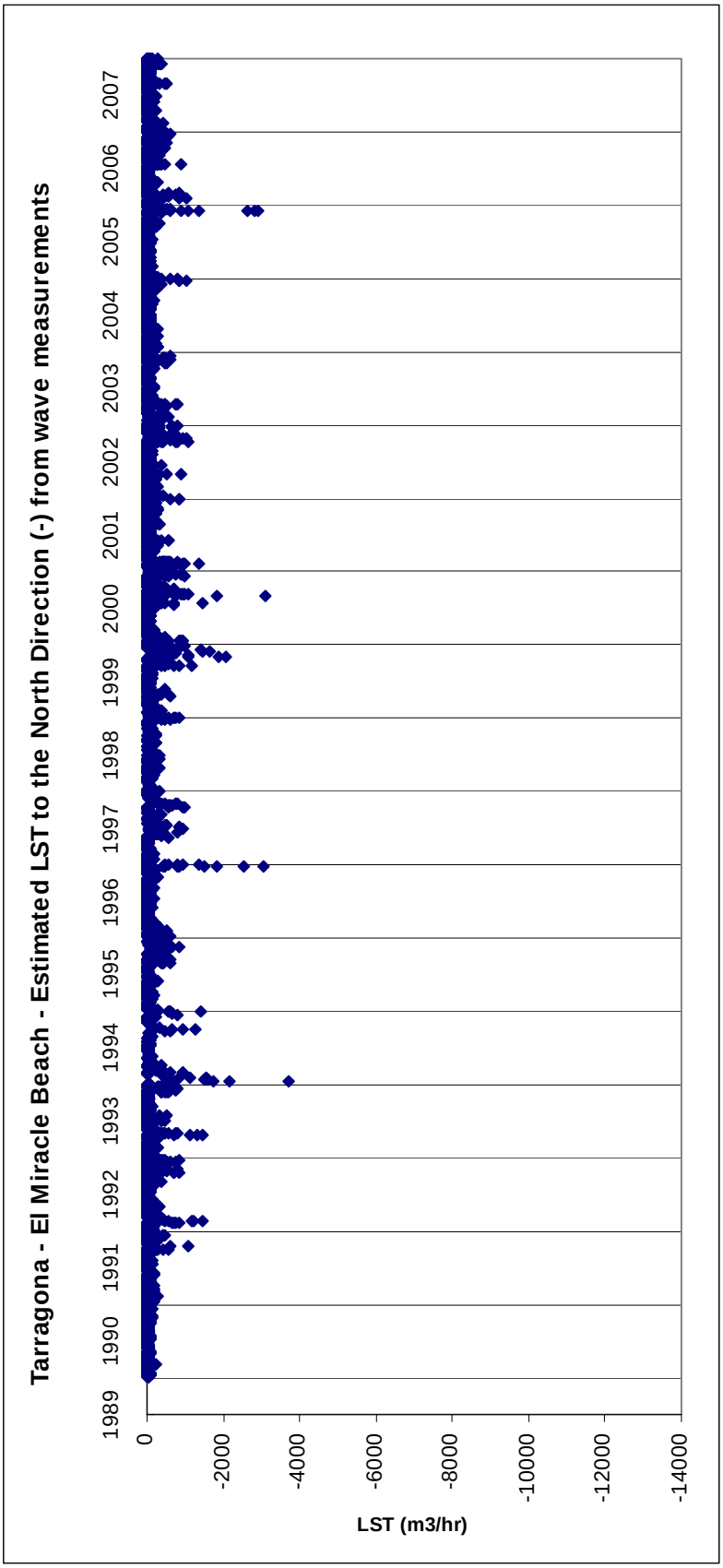

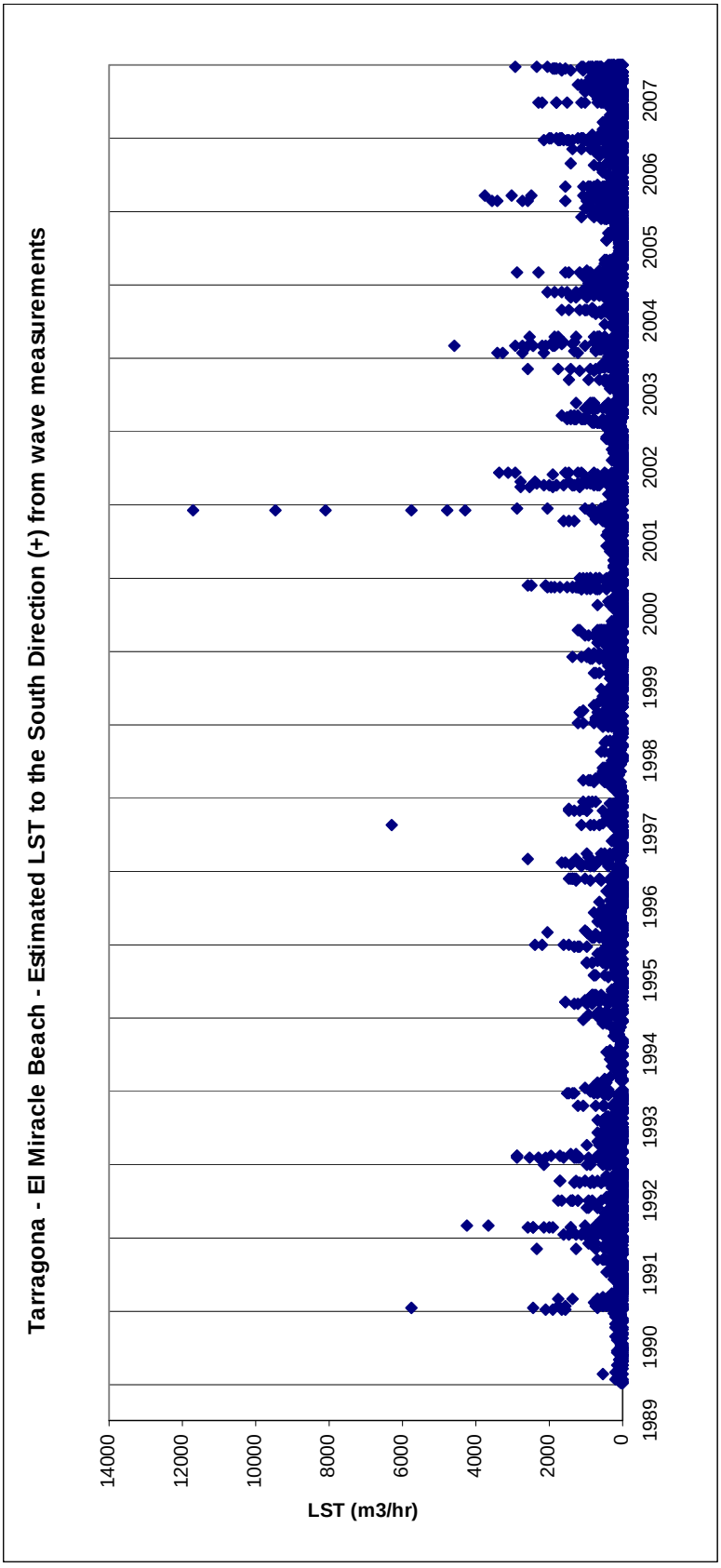
Tarragona - El Miracle Beach - Estimated LST to the South Direction (+) from wave measurements
LST (m3/hr)
14000
12000
10000
8000
6000
4000
2000
0
1989
1990
1991
1992
1993
1994
1995
1996
1997
1998
1999
2000
2001
2002
2003
2004
2005
2006
2007

Monthly Distribution

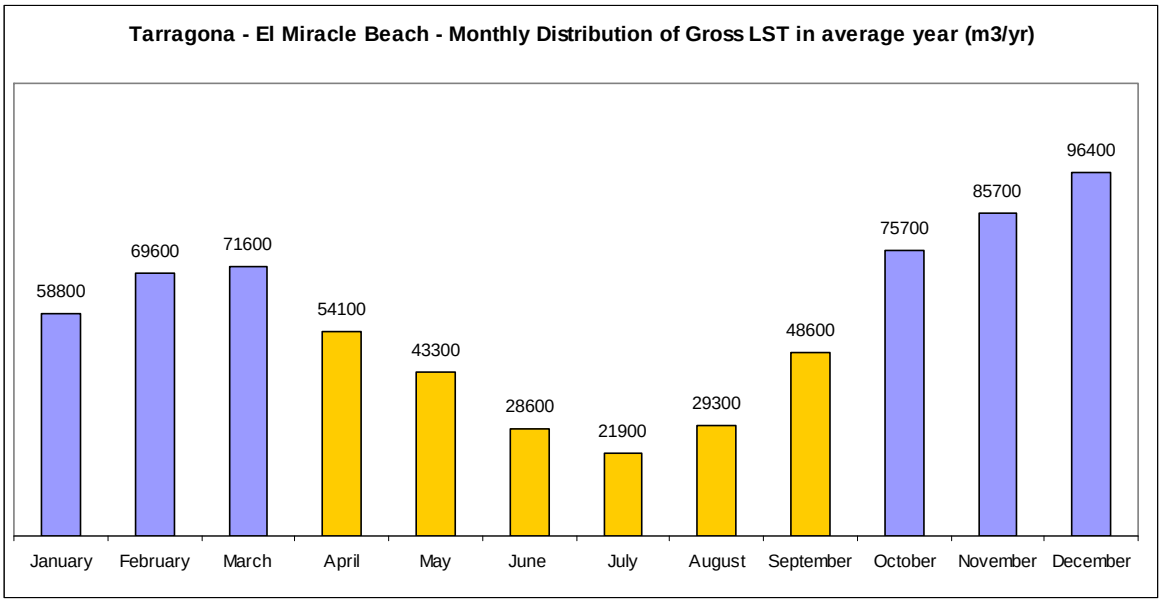

Summer and winter time distribution of Gross LST:

- Oct-Mar: 457 800 (67%)
- Apr-Sep: 64 000 (33%)

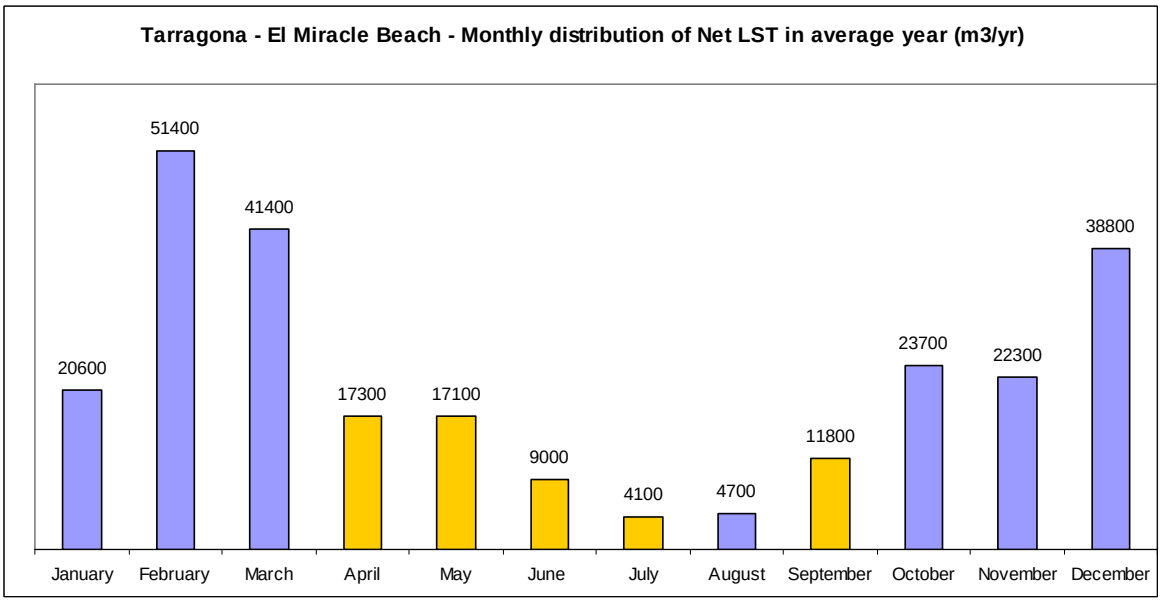

Summer and winter time distribution of Net LST:

- Oct-Mar: 198 200 (76%)
- Apr-Sep: 64 000 (24%)

LST estimation in average year: total, by wave direction and proportion caused by Hs>2m.

Beach	Direction of Littoral Drift	Total LST (m3/year)	Wave direction			Hs		Grain size (mm)	Orientation (º)	Slope
			Wave direction	LST (m3/year)	%	LST (Hs>2m)	%			
El Miracle	South	472678	E	410119	86.8	167816	40.9	0.19	44	0.02
			ESE	60428	12.8	10212	16.9			
			SE	2131	0.5	49	2.3			
	North	210635	SE	4076	1.9	640	15.7			
			SSE	26753	12.7	2020	7.6			
			S	140268	66.6	23165	16.5			
			SSW	39365	18.7	6067	15.4			
			SW	173	0.1	0	0.0			

Gross LST: 683 300 m^3/yr

Net LST: 262 000 m^3/yr (to South)

Sediment Budget using LST Capacity

Figure 3.22 Evaluation of LST along the beach of El Miracle (Tarragona).

Storm contribution: proportion of transport caused by storm conditions (Hs>2m)

South Direction: 60%

North Direction: 34%

El Miracle Drift Rose

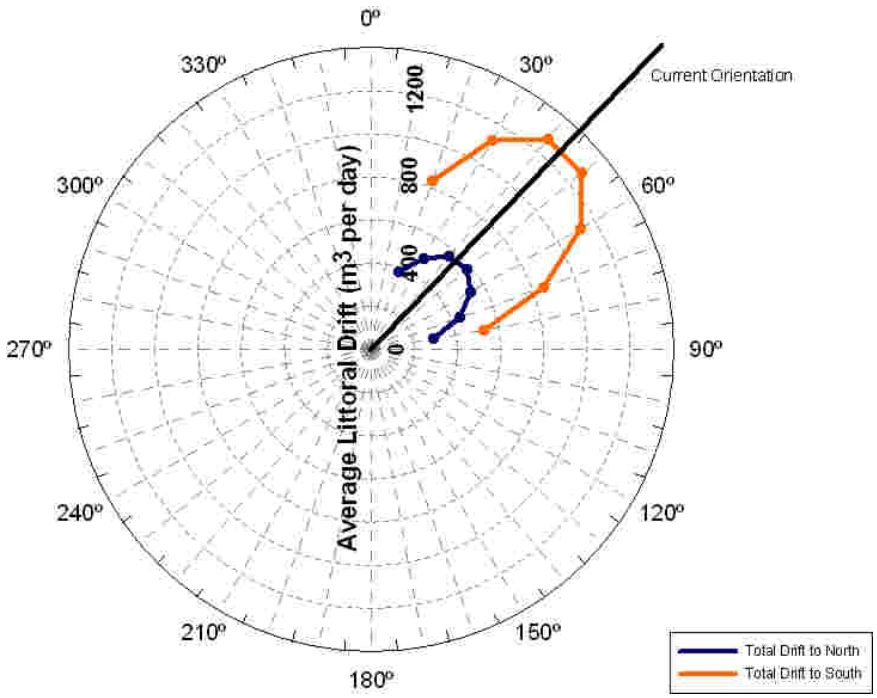

3.2.9 Tarragona. La Pineda

Situation of Tarragona – La Pineda.

Beach definition and main parameters

Figure 3.23 Definition of the beach of La Pineda (Tarragona).

	Diameter (D_{50})	Orientation (deg)	Slope	Wave effective Dir.
1. La Pineda	0.21	33	0.03	60-200
Data for Drift Rose:				
- La Pineda Drift Rose	0.21	330-60º	0.03	60-200

Longshore Sediment Transport Time Series

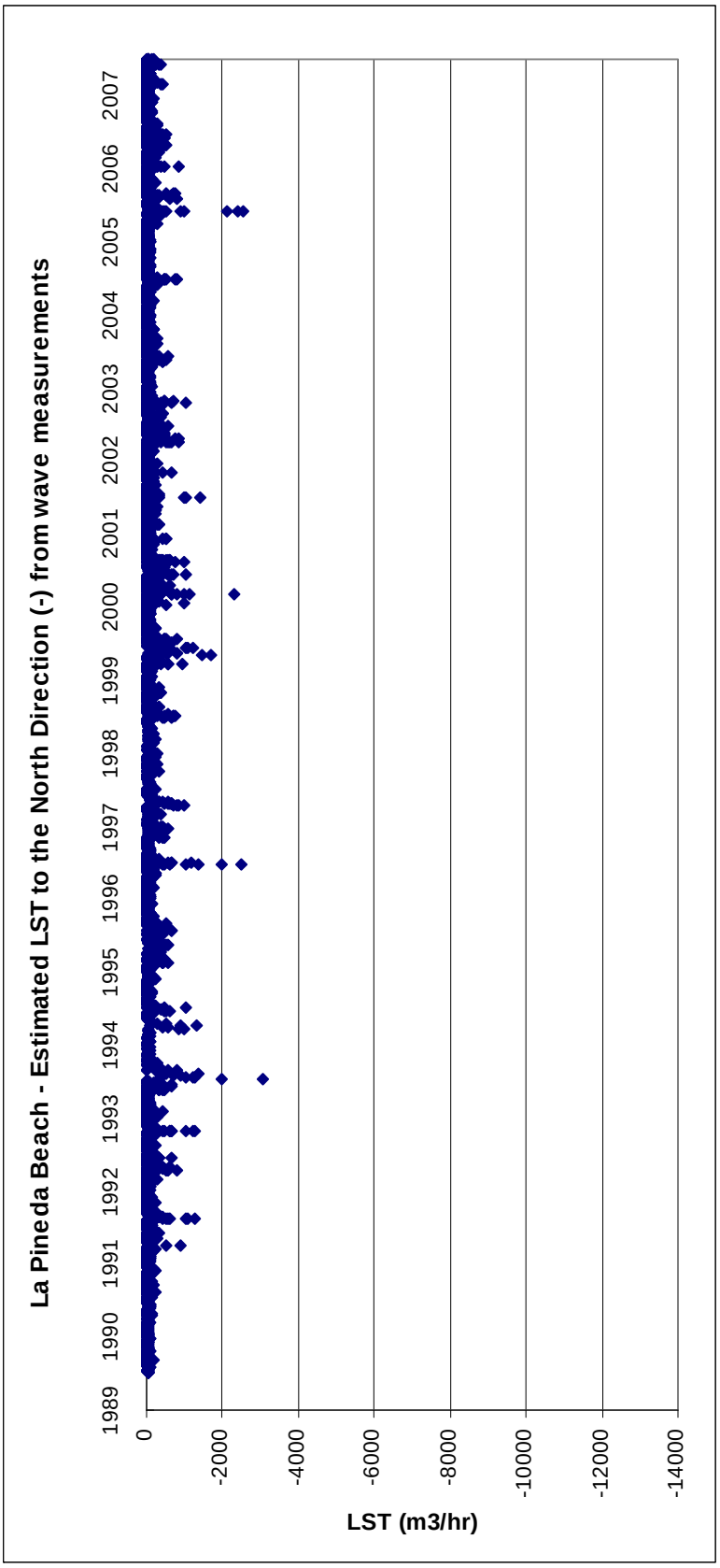

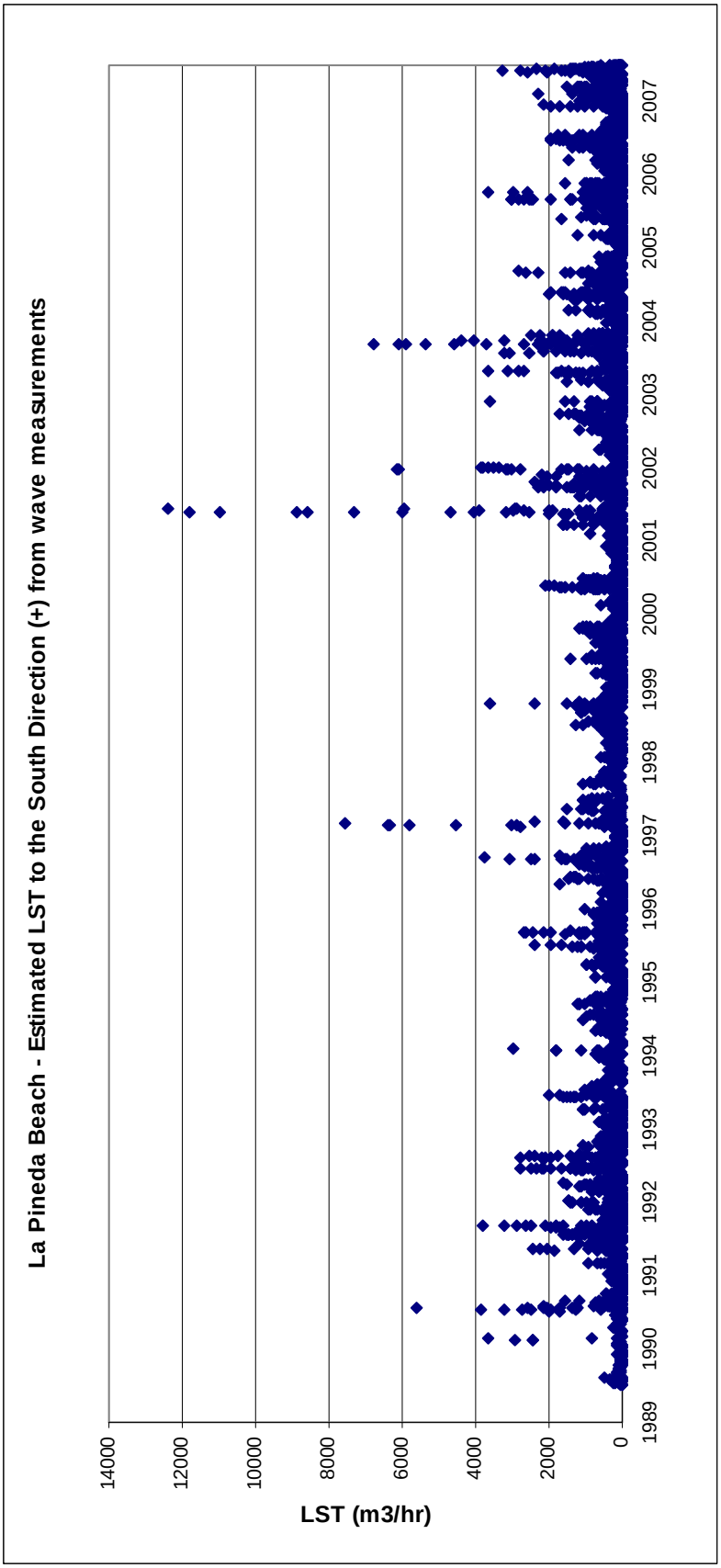
La Pineda Beach - Estimated LST to the South Direction (+) from wave measurements
LST (m3/hr)
14000
12000
10000
8000
6000
4000
2000
0
1989
1990
1991
1992
1993
1994
1995
1996
1997
1998
1999
2000
2001
2002
2003
2004
2005
2006
2007

Monthly Distribution

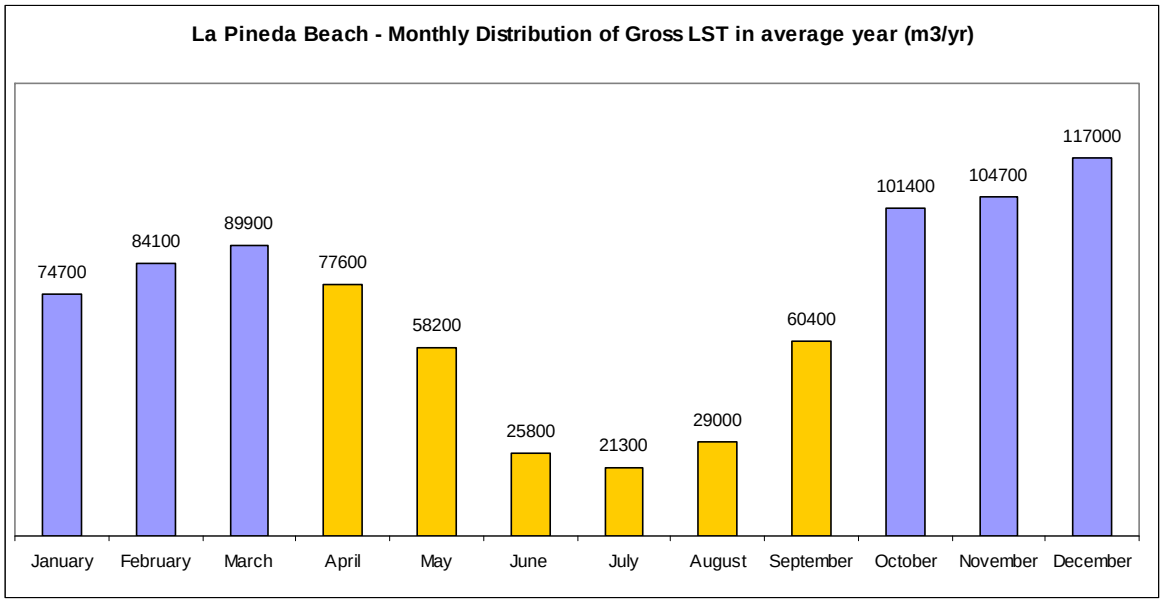

Summer and winter time distribution of Gross LST:

- Oct-Mar: 571 800 (68%)
- Apr-Sep: 272 300 (32%)

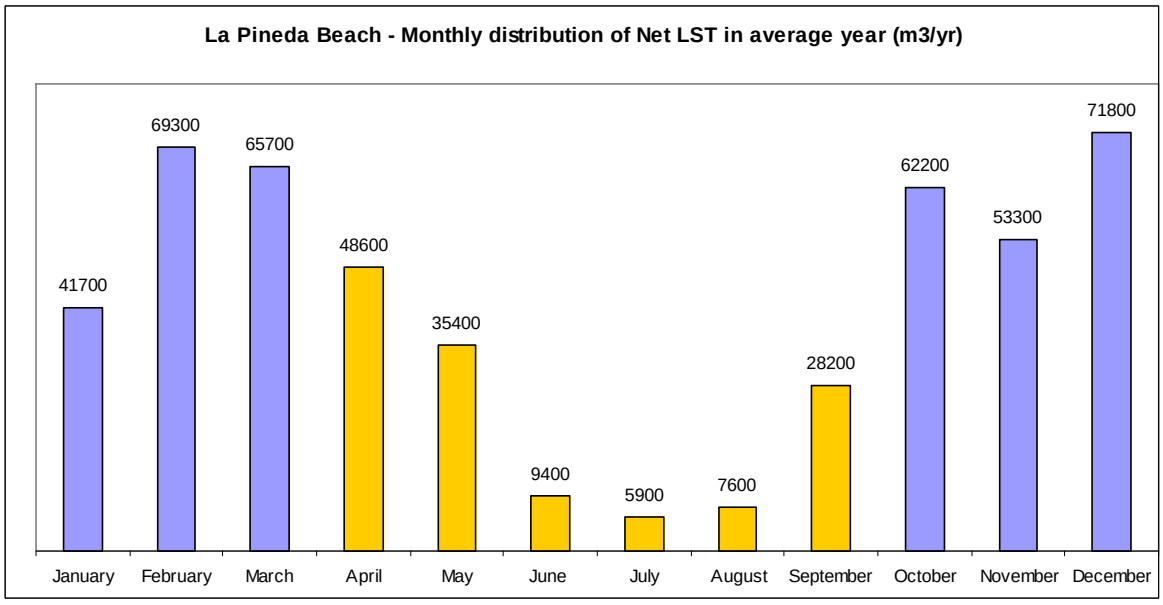

Summer and winter time distribution of Gross LST:

- Oct-Mar: 364 000 (73%)
- Apr-Sep: 135 100 (27%)

LST estimation in average year: total, by wave direction and proportion caused by Hs>2m.

Beach	Direction of Littoral Drift	Total LST (m3/year)	Wave direction			Hs		Grain size (mm)	Orientation (º)	Slope
			Wave direction	LST (m3/year)	%	LST (Hs>2m)	%			
La Pineda	South	447683	E	414224	92.5	142183	34.3	0.21	33	0.03
			ESE	33459	7.5	6371	19.0			
	North	172605	SE	11842	6.9	1353	11.4			
			SSE	31336	18.2	2304	7.4			
			S	111934	64.8	18428	16.5			
			SSW	17493	10.1	2569	14.7			

Gross LST: 620 300 m^3/yr

Net LST: 275 100 m^3/yr (to South)

Sediment Budget using LST Capacity

Figure 3.24 Evaluation of LST along the beach of La Pineda.

Storm contribution: proportion of transport caused by storm conditions (Hs>2m)

South Direction: 46%

North Direction: 14%

La Pineda Drift Rose

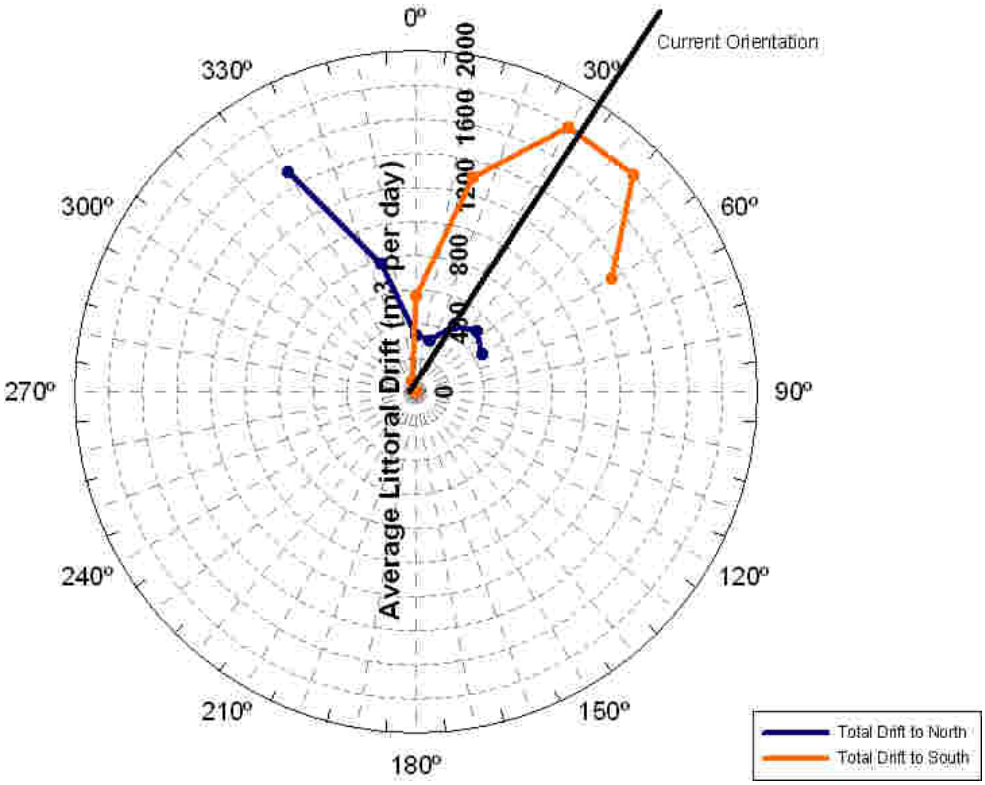

3.2.14 Cambrils – Salou

Situation of Cambrils-Salou

Beach definition and main parameters

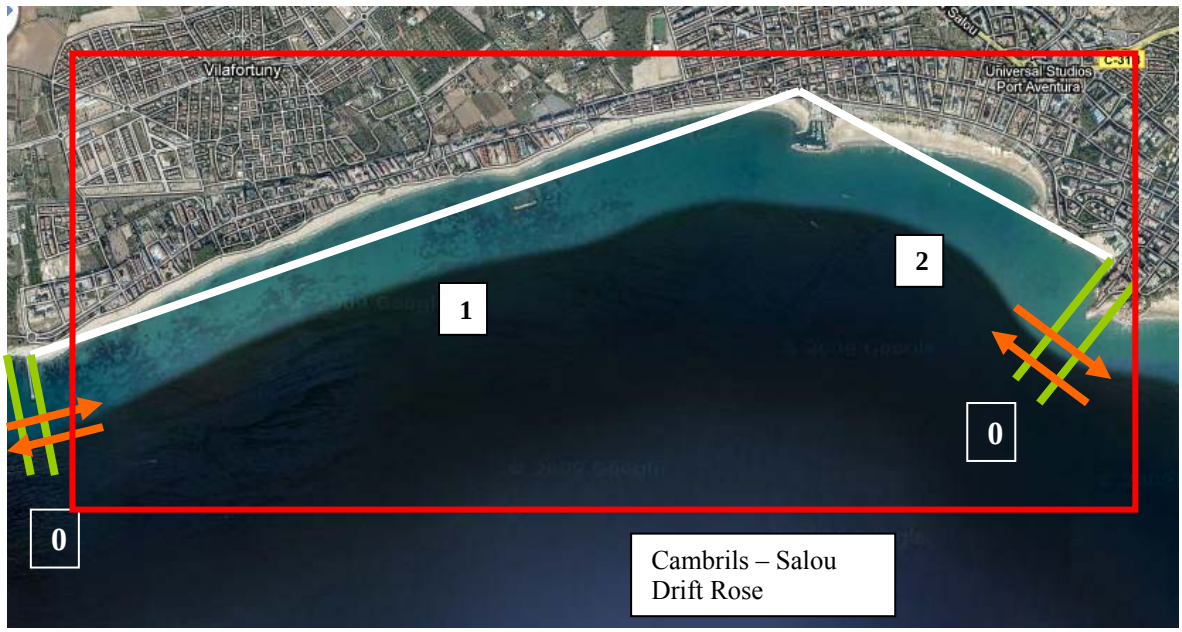

Figure 3.25 Definition of the beach of Cambrils - Salou .

	Diameter (D_{50})	Orientation (deg)	Slope	Wave effective Dir.
1. Cambrils	0.15	70	0.03	103-235
2. Salou	0.15	116	0.03	125-225
- Cambrils-Salou Drift Rose	0.15	50-150º	0.03	103-225

CAMBRILS

Longshore Sediment Transport Time Series

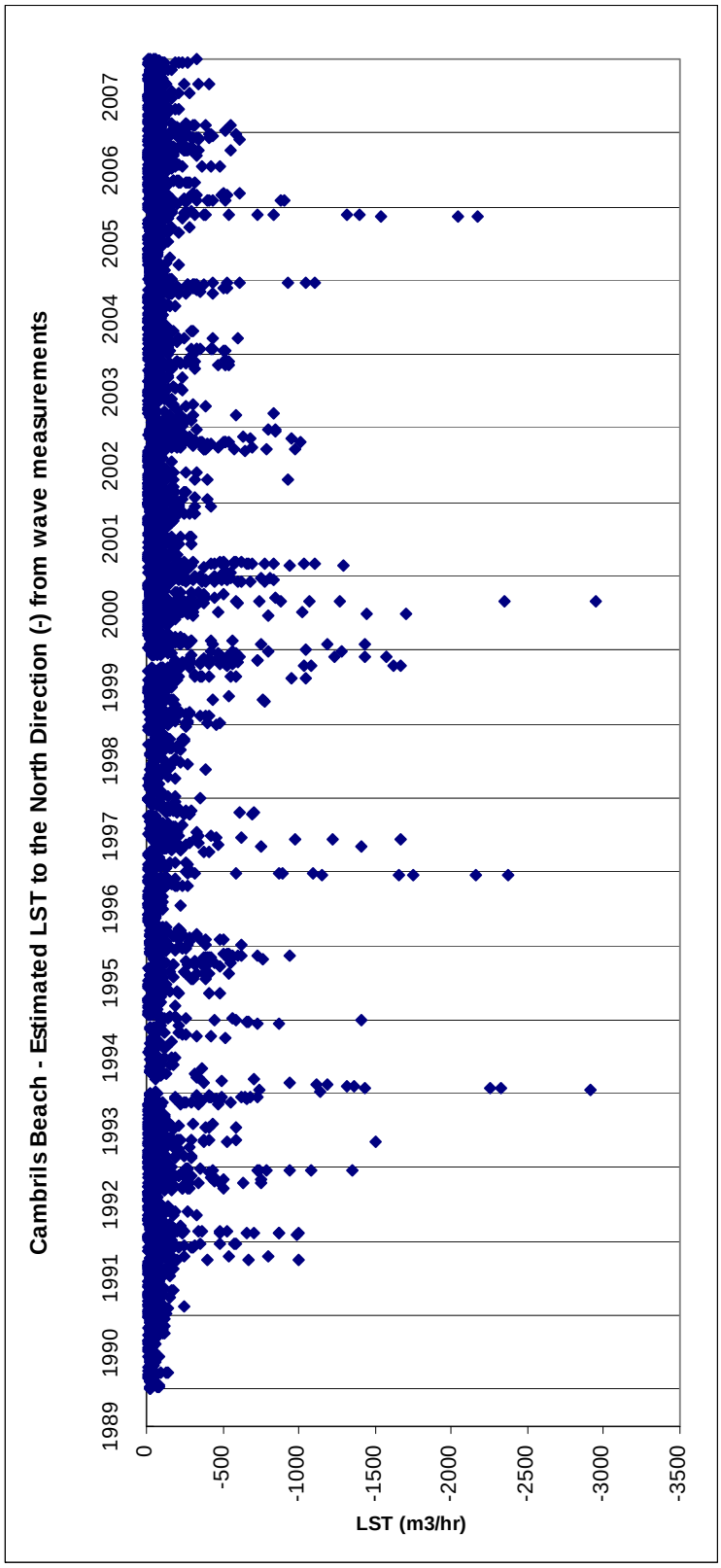

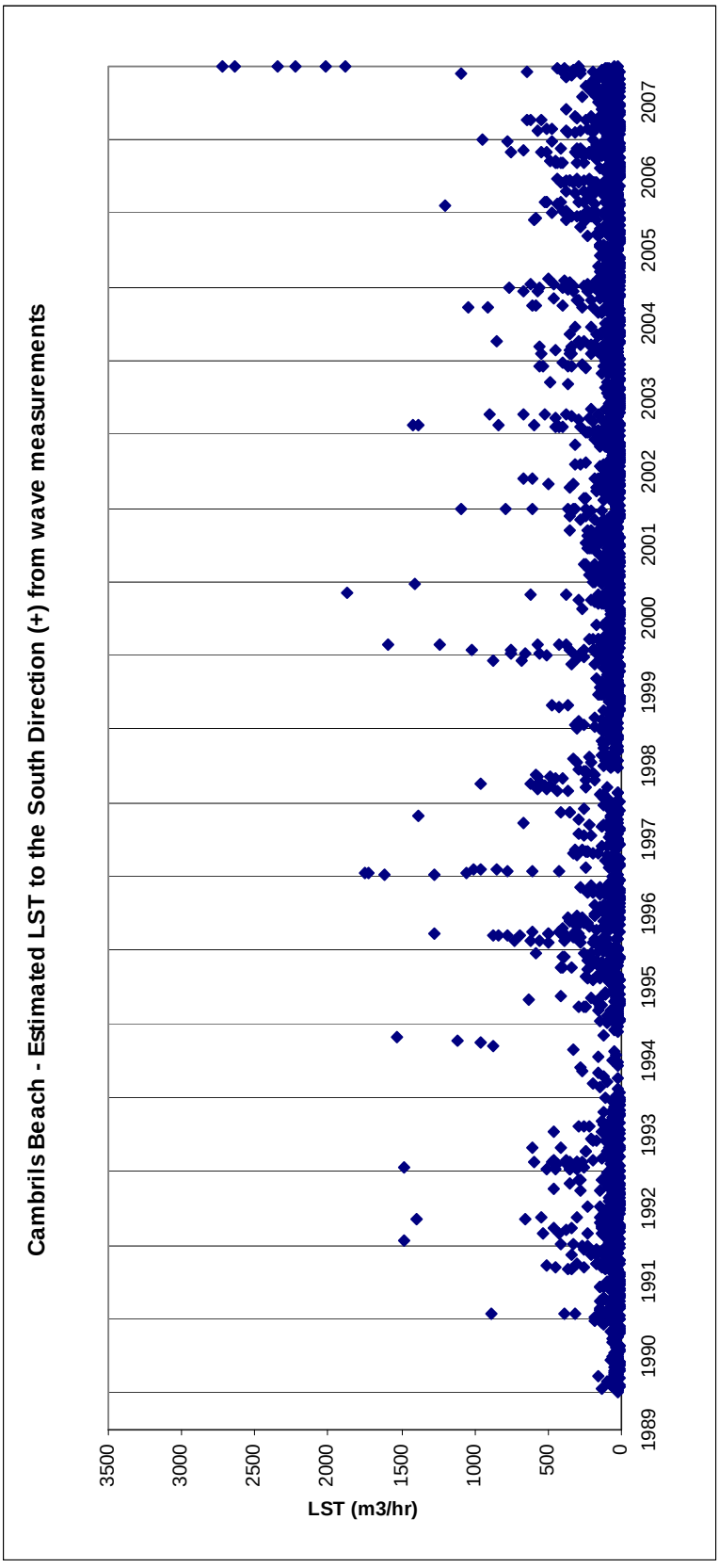
Cambrils Beach - Estimated LST to the South Direction (+) from wave measurements
LST (m3/hr)
3500
3000
2500
2000
1500
1000
500
0
1989
1990
1991
1992
1993
1994
1995
1996
1997
1998
1999
2000
2001
2002
2003
2004
2005
2006
2007

Monthly Distribution

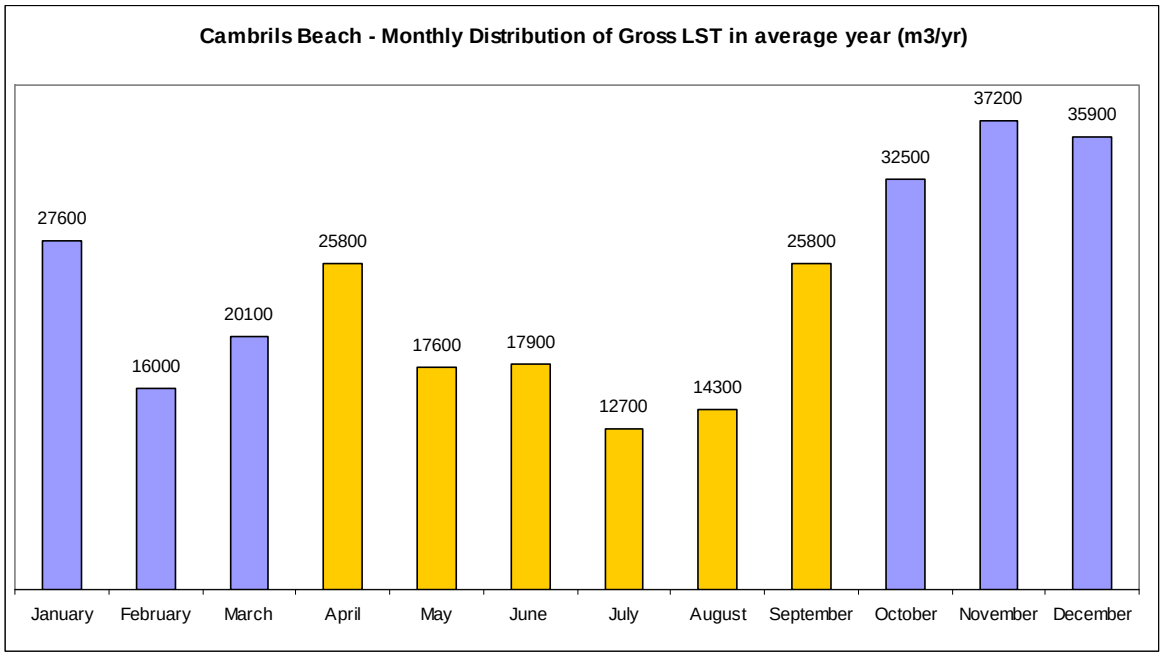

Summer and winter time distribution of Gross LST:

- Oct-Mar: 169 300 (60%)
- Apr-Sep: 114 100 (40%)

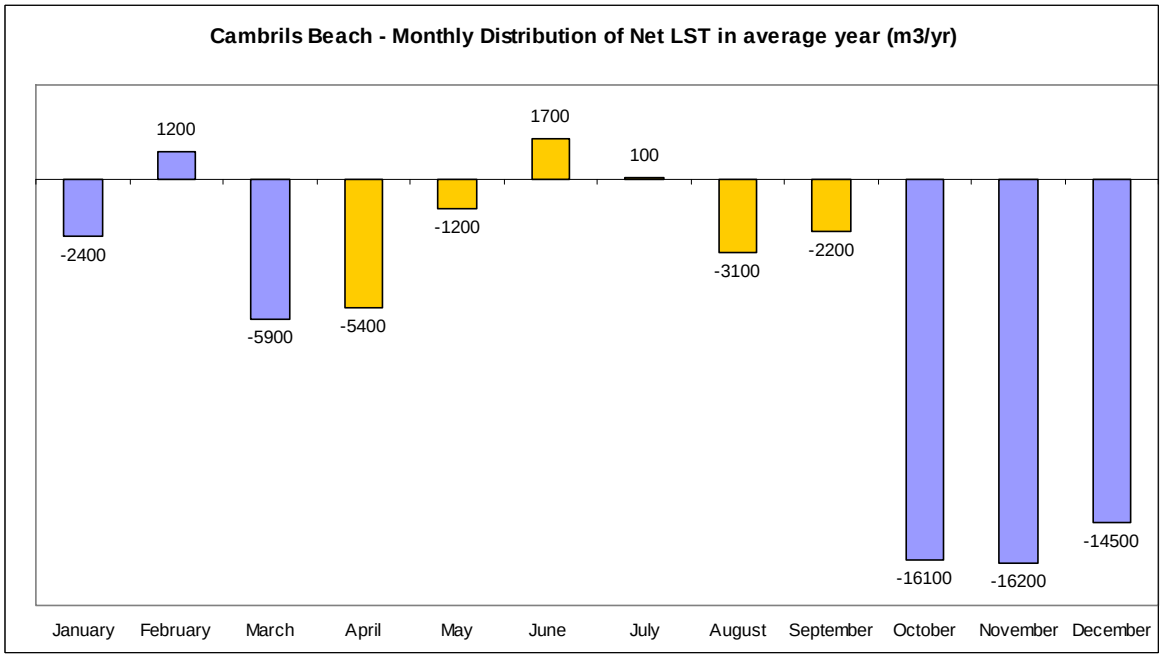

Summer and winter time distribution of Net LST:

- Oct-Mar: 56 300 (80%)
- Apr-Sep: 13 700 (20%)

SALOU

Longshore Sediment Transport Time Series

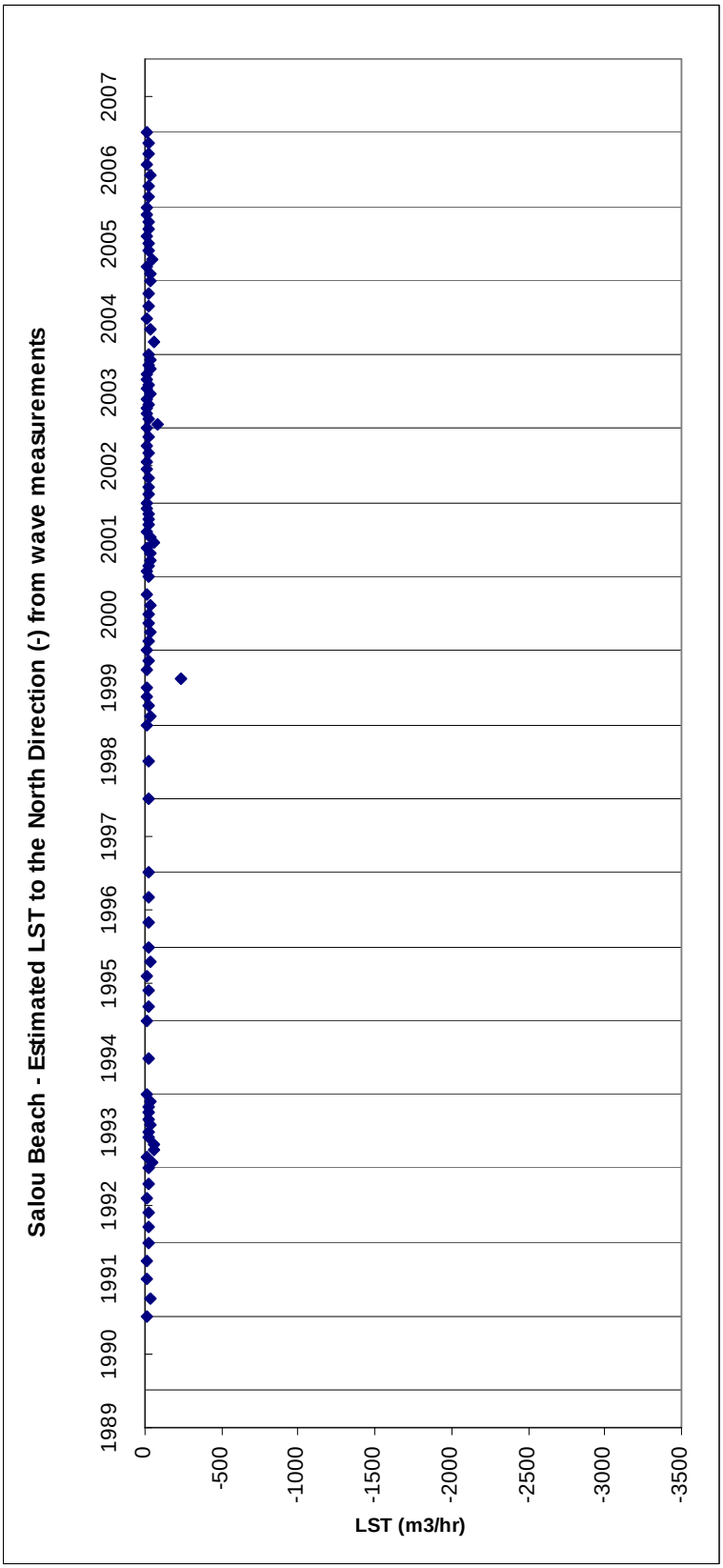

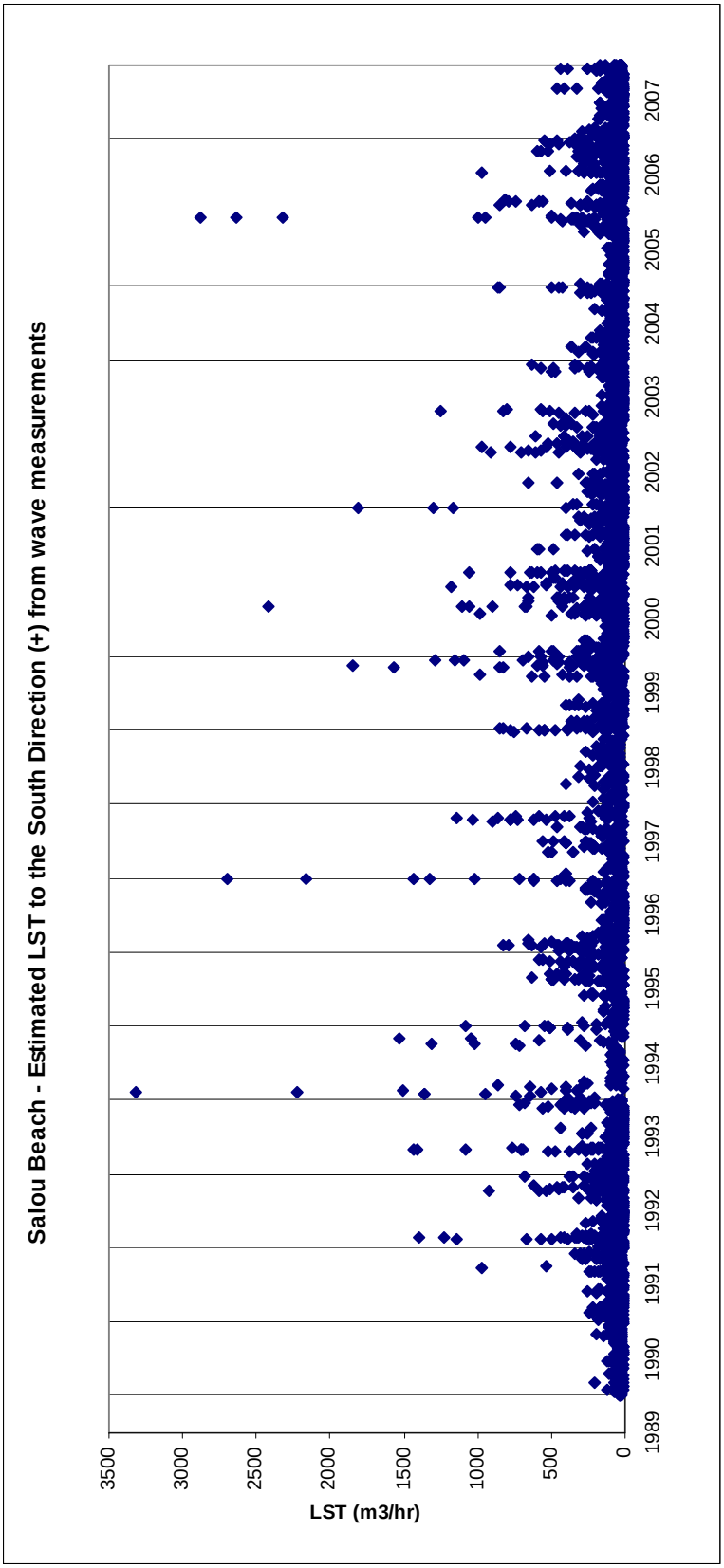
Salou Beach - Estimated LST to the South Direction (+) from wave measurements
LST (m3/hr)
3500
3000
2500
2000
1500
1000
500
0
1989
1990
1991
1992
1993
1994
1995
1996
1997
1998
1999
2000
2001
2002
2003
2004
2005
2006
2007

Monthly Distribution

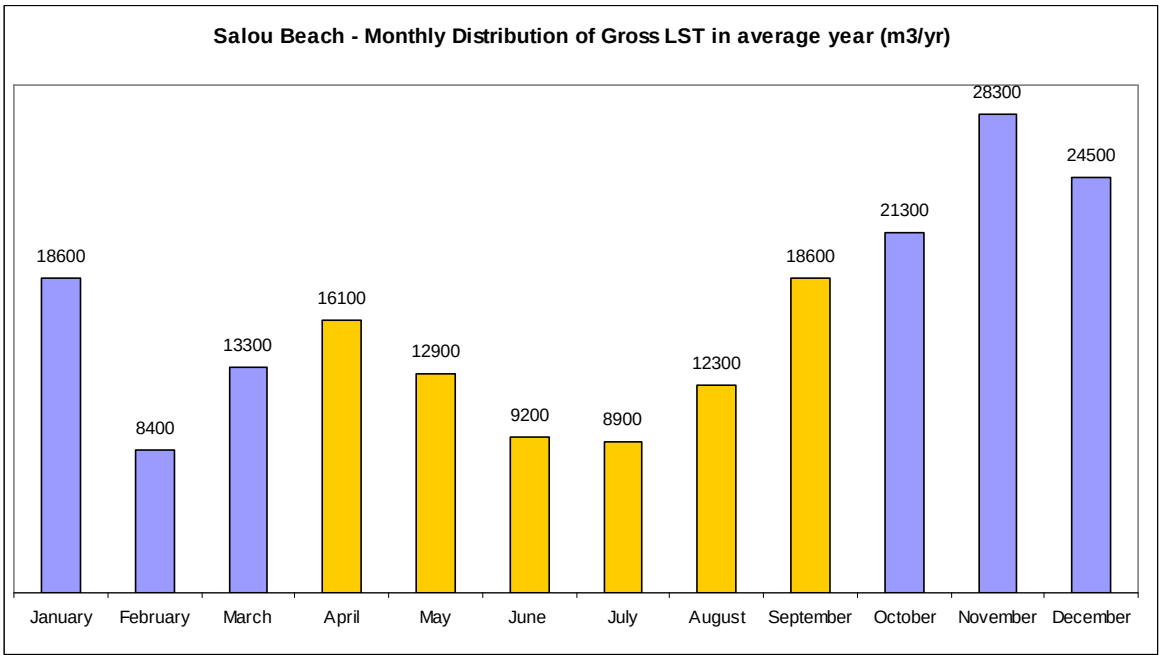

Summer and winter time distribution of Gross LST:

- Oct-Mar: 114 400 (59%)
- Apr-Sep: 78 000 (41%)

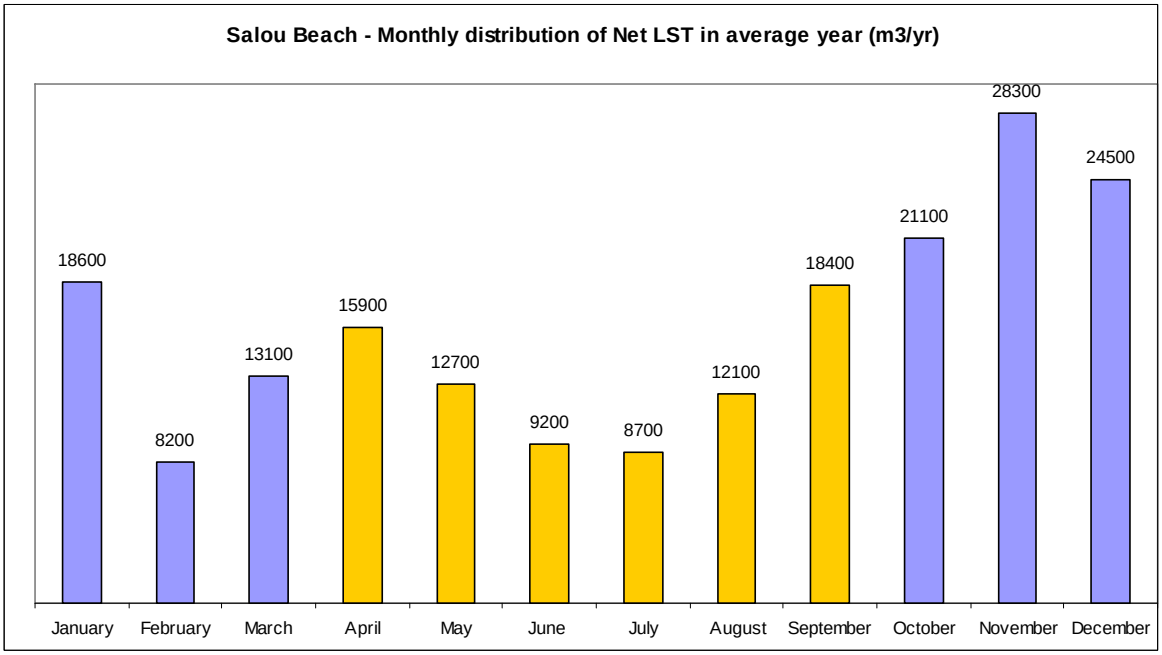

Summer and winter time distribution of Net LST:

- Oct-Mar: 113 800 (60%)
- Apr-Sep: 77 000 (40%)

LST estimation in average year: total, by wave direction and proportion caused by Hs>2m.

Beach	Direction of Littoral Drift	Total LST (m3/year)	Wave direction			Hs		Grain size (mm)	Orientation (º)	Slope
			Wave direction	LST (m3/year)	%	LST (Hs>2m)	%			
Cambrils	South	109823	ESE	80861	73.6	12715	15.7	0.15	70	0.03
			SE	24801	22.6	1768	7.1			
			SSE	4161	3.8	303	7.3			
	North	173767	SSE	1721	1.0	294	17.1			
			S	110599	63.6	19484	17.6			
			SSW	59839	34.4	9191	15.4			
			SW	1608	0.9	0	0.0			
Salou	West	191466	SE	16954	8.9	1804	10.6	0.15	116	0.03
			SSE	37226	19.4	2718	7.3			
			S	120856	63.1	19781	16.4			
			SSW	16430	8.6	2727	16.6			
	East	787	SSW	264	33.5	66	25.0			
			SW	523	66.5	0	0.0			

	Cambrils	**Salou**
Gross LST(m^3/yr)	283 600	190 679
Net LST (m^3/yr)	-63 900 (to East)	192 253 (to West)

Sediment Budget using LST Capacity

Figure 3.25 Evaluation of LST along the beach of Cambrils – Salou.

Storm contribution: proportion of transport caused by storm conditions (Hs>2m)

	Cambrils	Salou
South Direction:	14%	14%
North Direction:	17%	8%

Cambrils – Salou Drift Rose

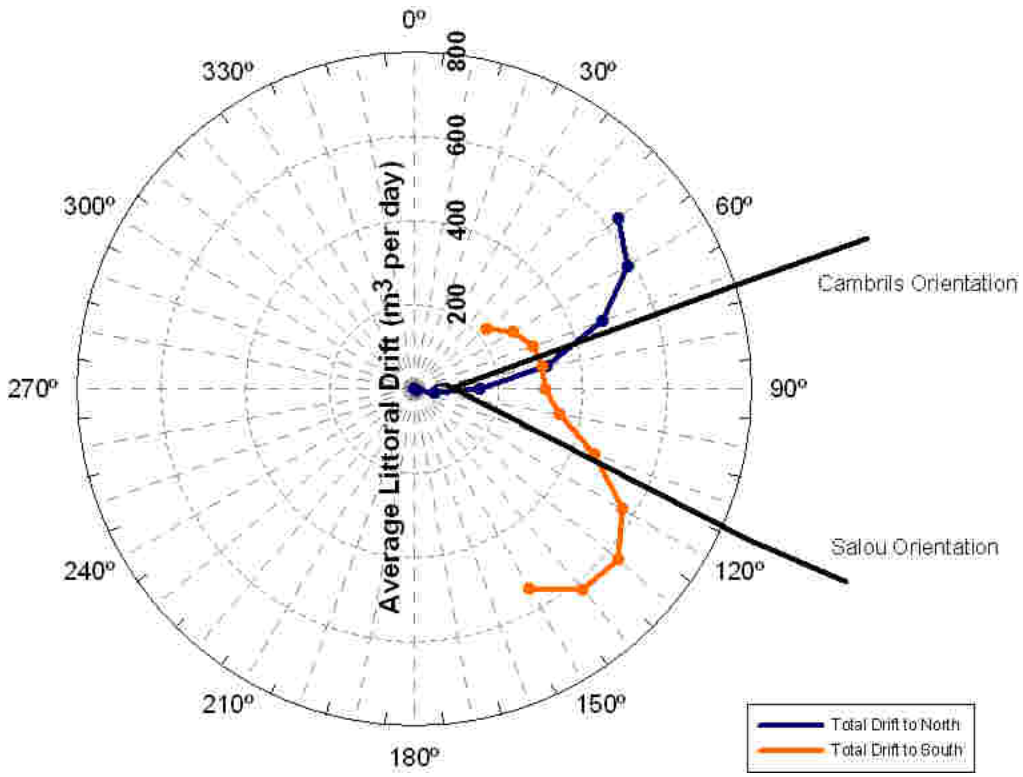

3.2.15 L'Hospitalet de l'Infant – Arenal

Situation of L'Hospitalet de l'Infant - Arenal

Beach definition and main parameters

Figure 3.26 Definition of the beach of L'Hospitalet de l'Infant – Arenal.

	D_{50}(mm)	Orientation (deg)	Slope	Wave effective Dir.
1. L'H. de l'Infant	0.19	44	0.02	70-190
- L'H. de l'I. Drift Rose	0.19	20-140º	0.02	70-190

Longshore Sediment Transport Time Series.

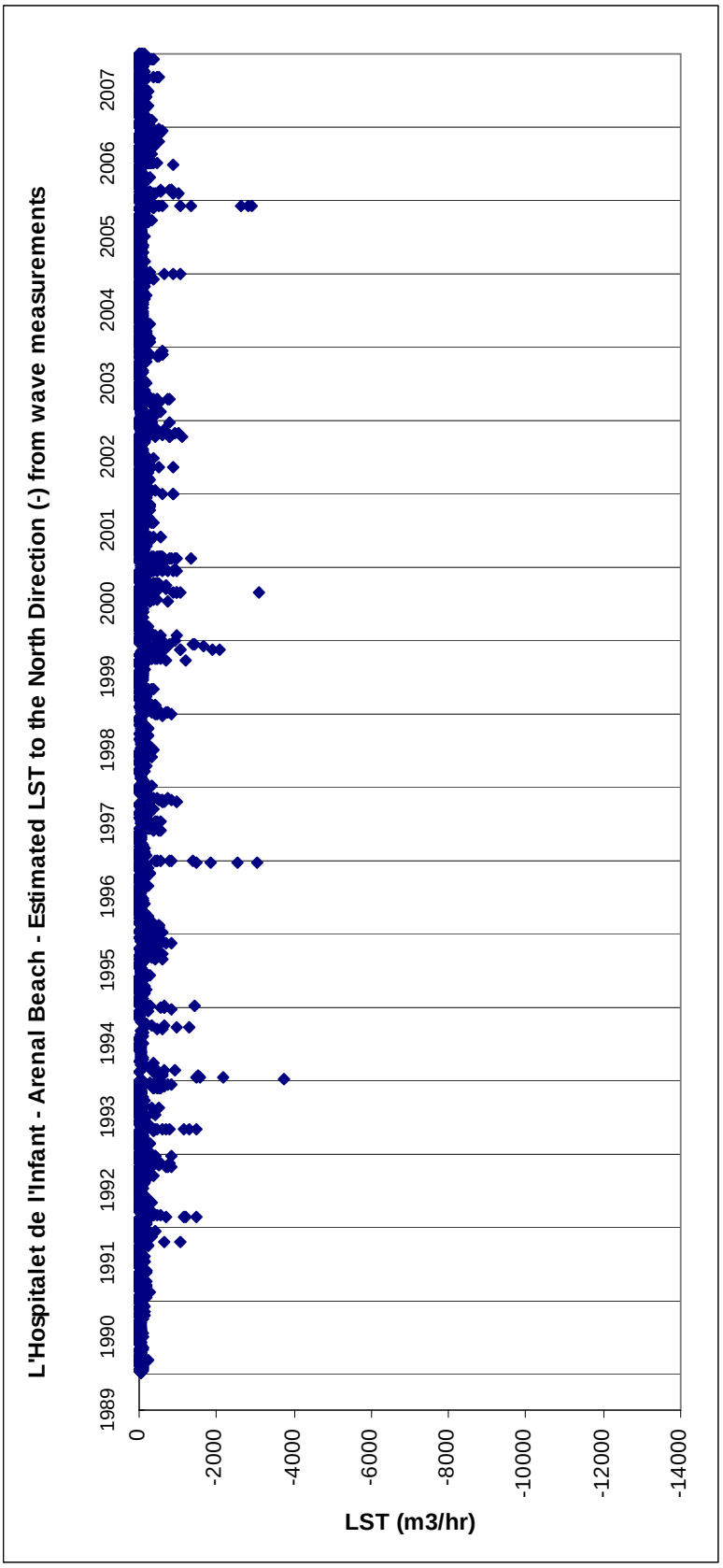

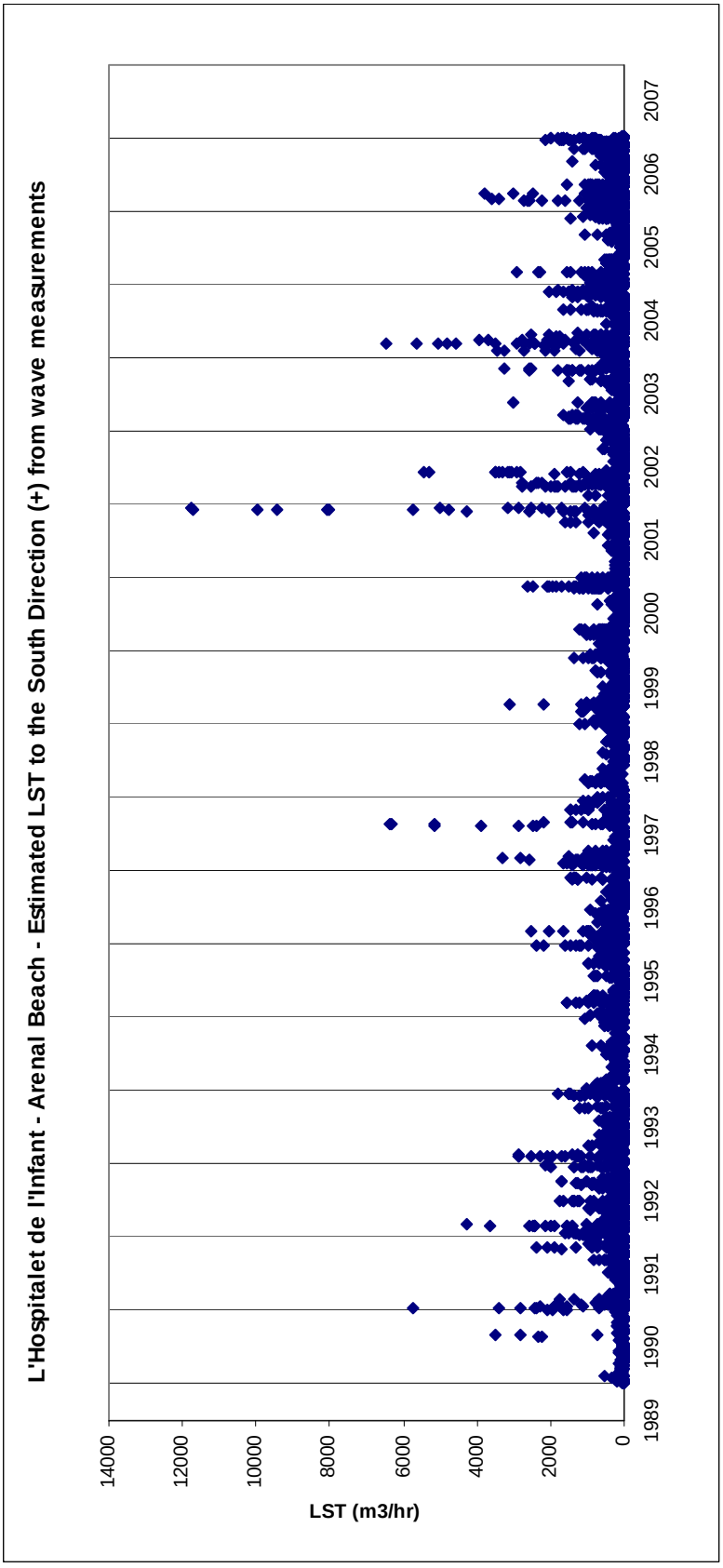
L'Hospitalet de l'Infant - Arenal Beach - Estimated LST to the South Direction (+) from wave measurements
LST (m3/hr)
14000
12000
10000
8000
6000
4000
2000
0
1989
1990
1991
1992
1993
1994
1995
1996
1997
1998
1999
2000
2001
2002
2003
2004
2005
2006
2007

Monthly distribution

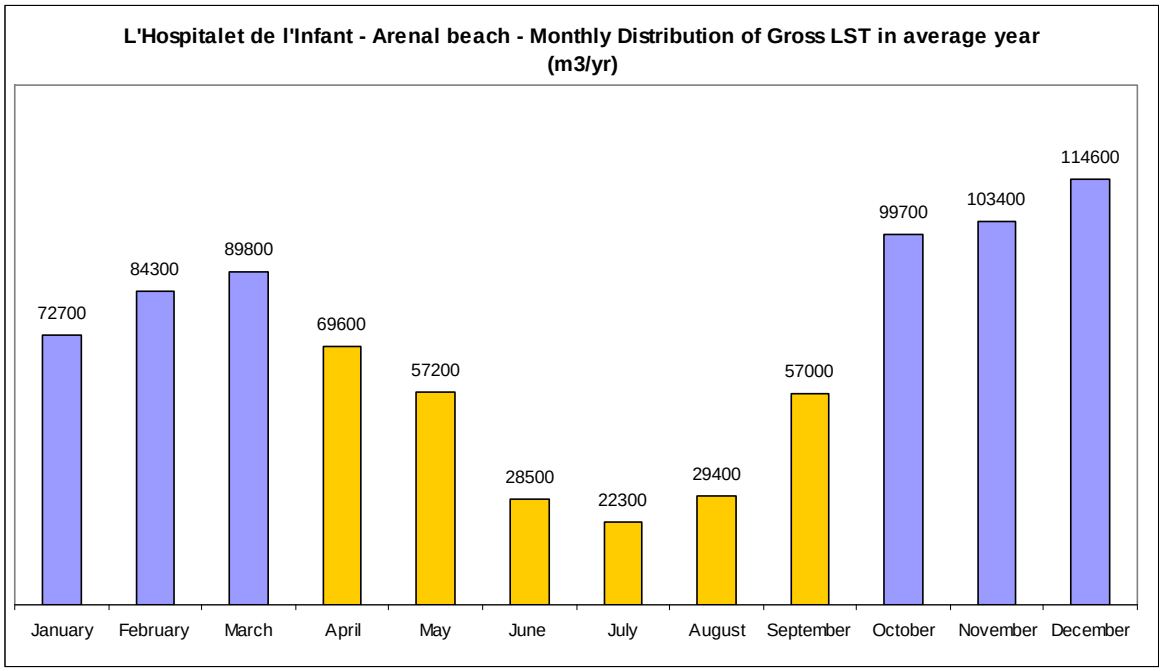

Summer and winter time distribution of Gross LST:

- Oct-Mar: 564 500 (68%)
- Apr-Sep: 264 000 (32%)

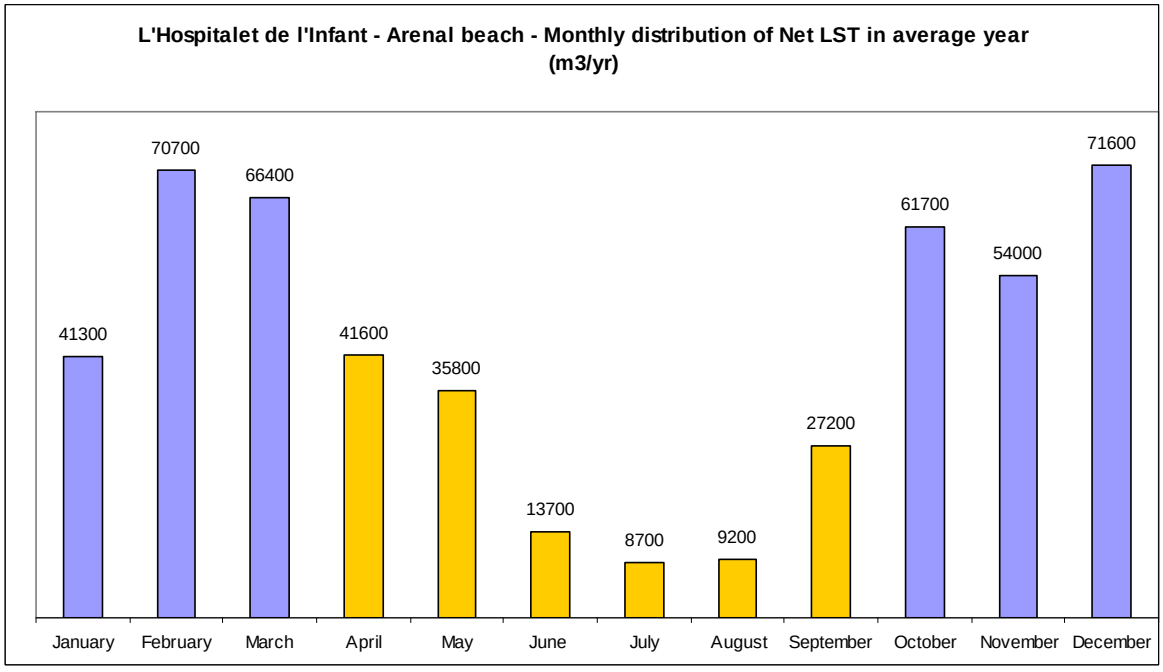

Summer and winter time distribution of Net LST:

- Oct-Mar: 365 700 (73%)
- Apr-Sep: 136 200 (27%)

LST estimation in average year: total, by wave direction and proportion caused by Hs>2m.

Beach	Direction of Littoral Drift	Total LST (m3/year)	Wave direction			Hs		Grain size (mm)	Orientation (º)	Slope
			Wave direction	LST (m3/year)	%	LST (Hs>2m)	%			
L'Hospitalet de l'Infant	South	665100	ENE	155819	23.4	89926	57.7	0.19	44	0.02
			E	446762	67.2	187142	41.9			
			ESE	60428	9.1	10212	16.9			
			SE	2131	0.3	49	2.3			
	North	163300	SE	4076	2.5	640	15.7			
			SSE	26753	16.4	2020	7.6			
			S	132457	81.1	21782	16.4			

Gross LST: 828 400 m^3/yr

Net LST: 501 800 m^3/yr (to South)

Sediment Budget using LST Capacity

Figure 3.27 Evaluation of LST along the beach of L'Hospitalet de l'Infant – Arenal.

Storm contribution: proportion of transport caused by storm conditions (Hs>2m)

South Direction: 43%

North Direction: 15%

L'Hospitalet de l'Infant Drift Rose

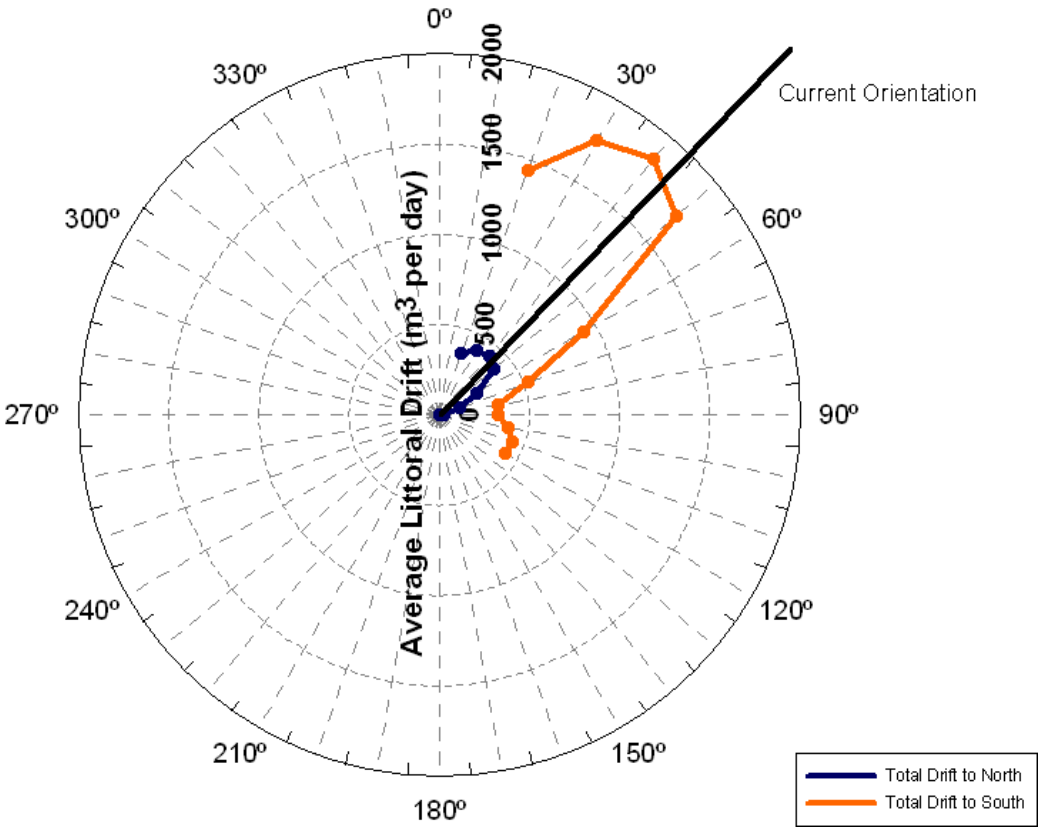

L'Hospitalet de l'Infant is not an equilibrium beach. Littoral drift to the South is huge and it can be noticed just looking at the picture (Fig 3.27). A great amount of sand is displaced to the Southern part of the beach while at the Northern part we can see the decrease of the beach width. Equilibrium beaches use to show a constant width of sand along them. Contribution from the Northern part of the port situated at the upper end must be almost zero as there is no even a little deposit of sand attached to the south side of the port as consequence of wave diffraction.

3.2.16 Ebre Delta

Situation of Ebre Delta.

Beach definition and main parameters

Figure 3.28 Definition of the zone of South Ebre Delta. Borders of the stretches studied are open and sediment is capable to cross from inside to outside of the unit or vice versa.

	Diameter (D_{50})	Orientation (deg)	Slope	Wave Dir (deg)
1. Calaix Gran	0.20	27	0.02	27-207
2. Urbanització l'Eucaliptus	0.20	62	0.02	62-213
3. Barra del Trabucador	0.20	33	0.02	62-213
4. Salines	0.20	75	0.02	75-215
5. Cap Tortosa	0.20	288	0.02	27-108
6. Platja Riumar	0.20	325	0.02	27-145
- South Ebre Drift Rose	0.19	27-215º	0.02	27-215

CALAIX GRAN

Longshore Sediment Transport Time Series.

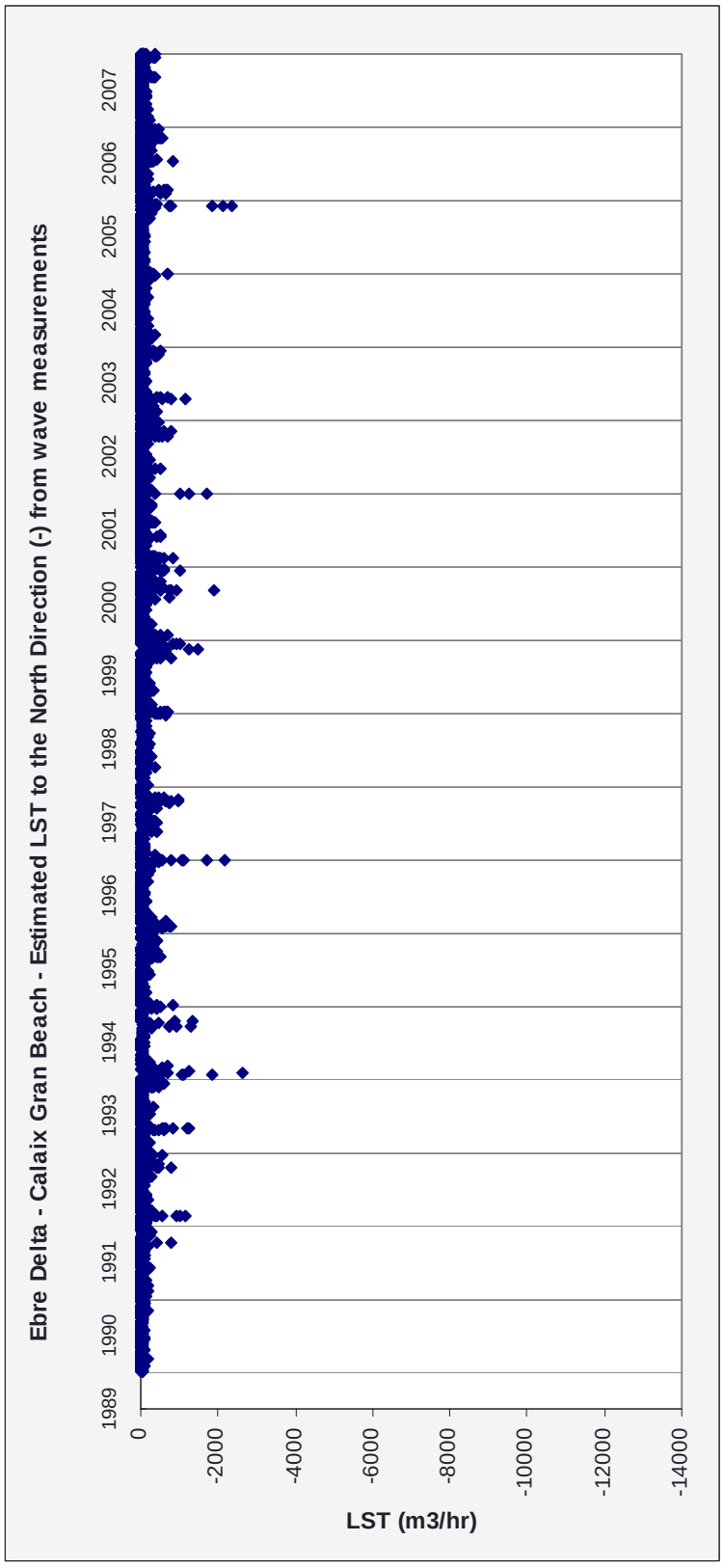

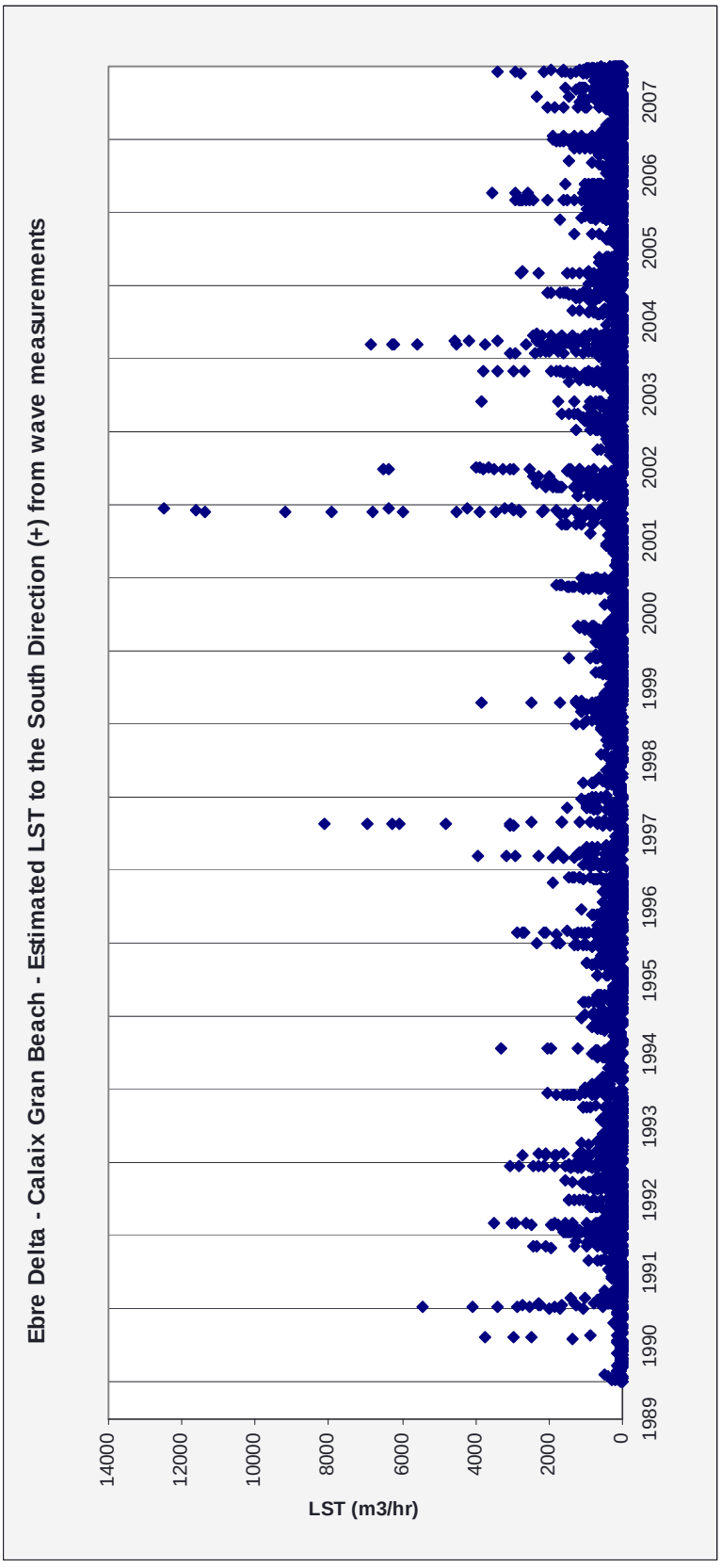
Ebre Delta - Calaix Gran Beach - Estimated LST to the South Direction (+) from wave measurements
LST (m3/hr)
14000
12000
10000
8000
6000
4000
2000
0
1989
1990
1991
1992
1993
1994
1995
1996
1997
1998
1999
2000
2001
2002
2003
2004
2005
2006
2007

Monthly distribution

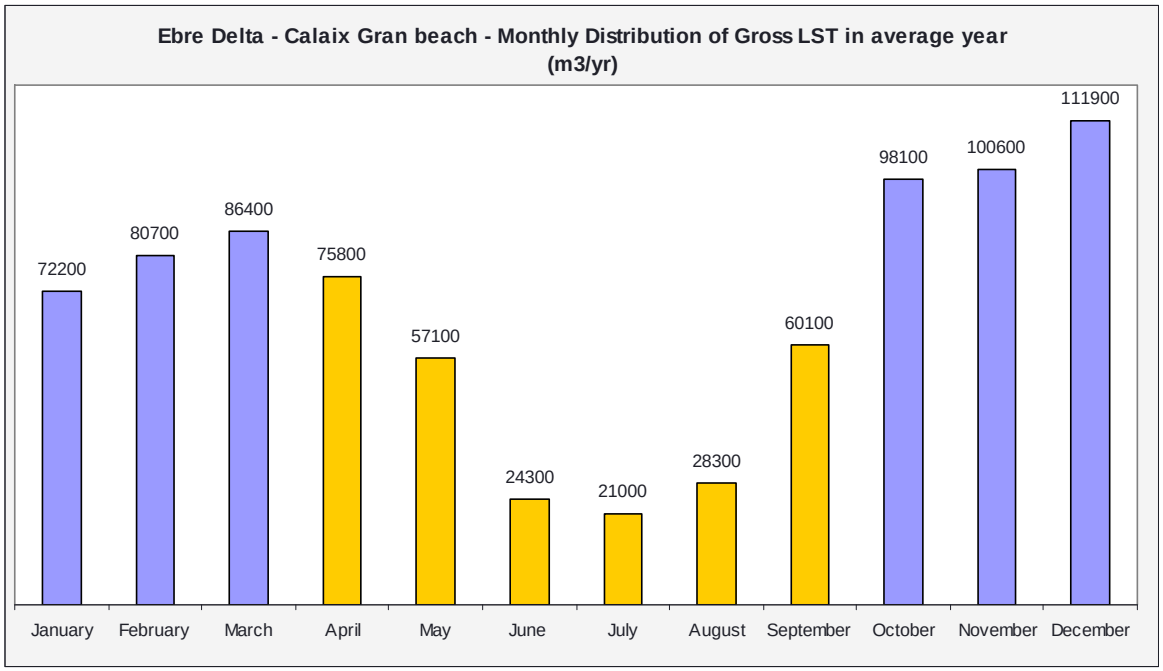

Summer and winter time distribution of Gross LST:

- Oct-Mar: 549 900 (67%)
- Apr-Sep: 266 600 (33%)

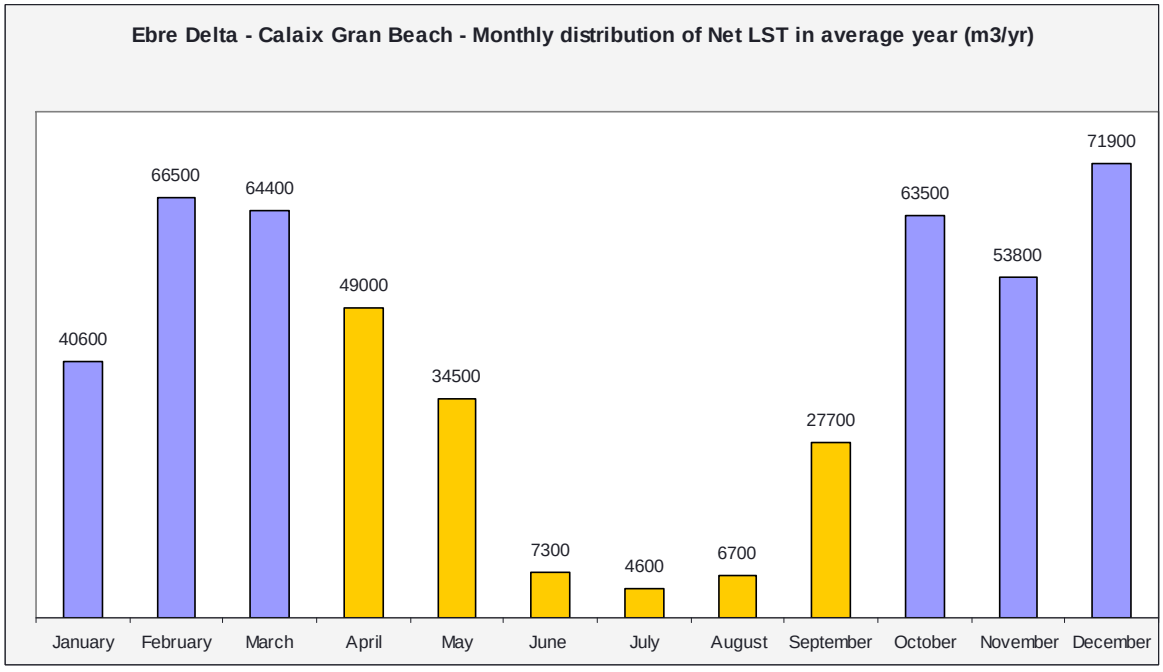

Summer and winter time distribution of Net LST:

- Oct-Mar: 360 700 (74%)
- Apr-Sep: 129 900 (26%)

EUCALIPTUS

Longshore Sediment Transport Time Series.

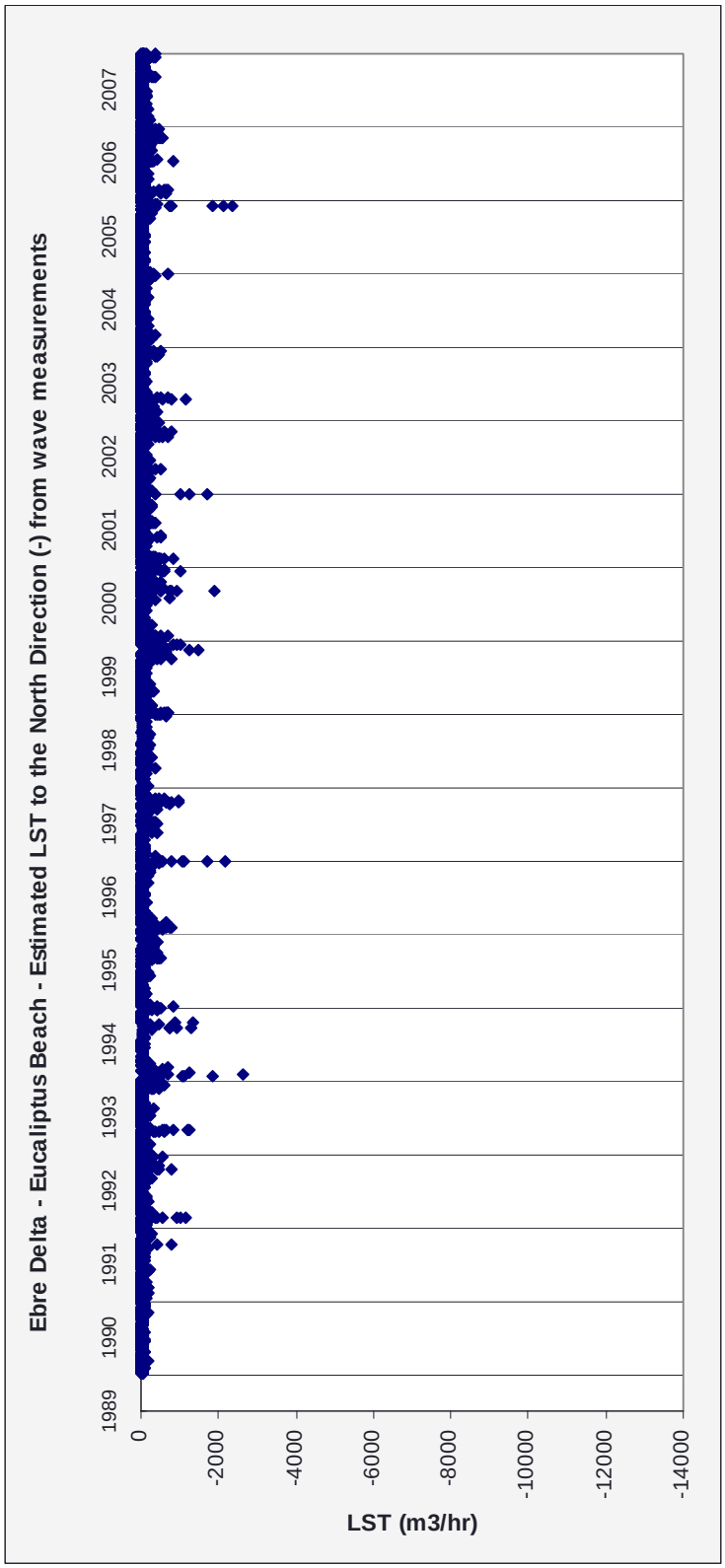

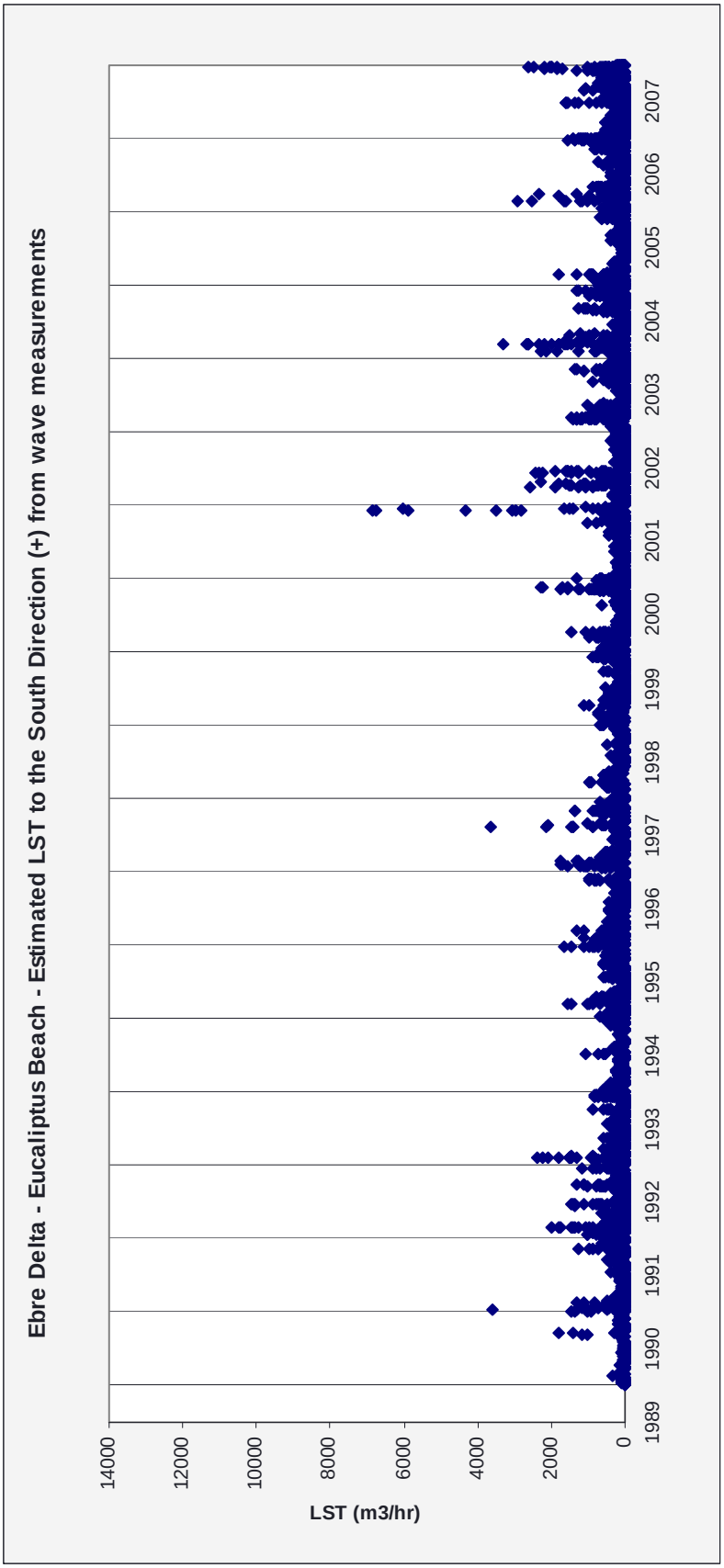
Ebre Delta - Eucaliptus Beach - Estimated LST to the South Direction (+) from wave measurements
LST (m3/hr)
14000
12000
10000
8000
6000
4000
2000
0
1989
1990
1991
1992
1993
1994
1995
1996
1997
1998
1999
2000
2001
2002
2003
2004
2005
2006
2007

Monthly distribution

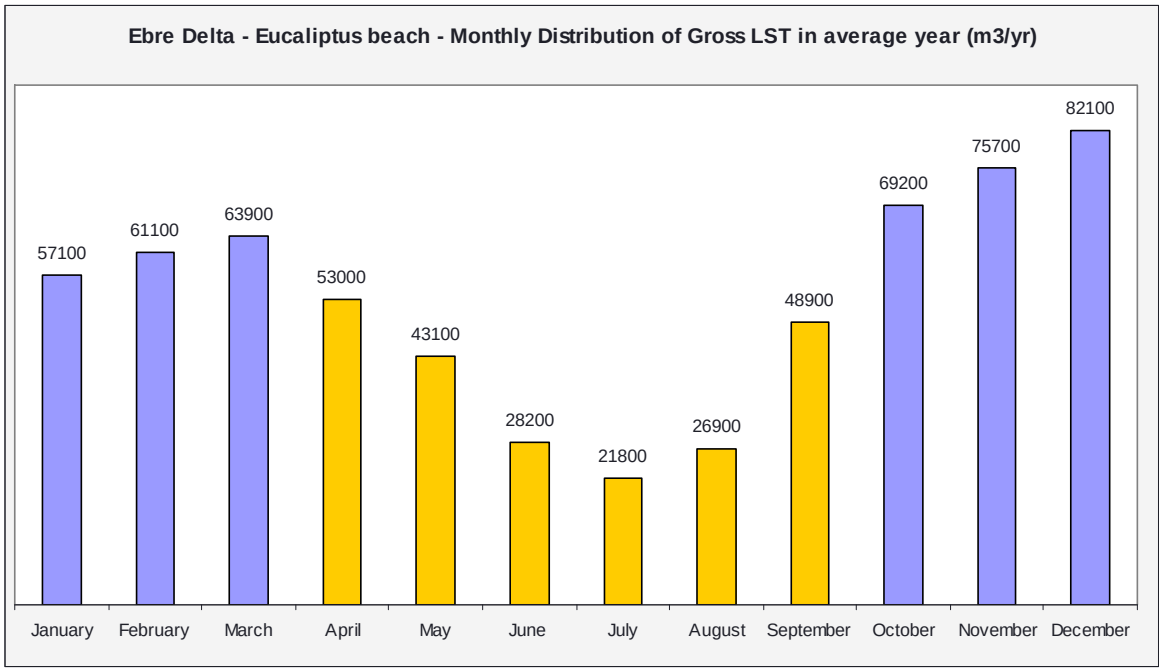

Summer and winter time distribution of Gross LST:

- Oct-Mar: 409 100 (65%)
- Apr-Sep: 221 900 (35%)

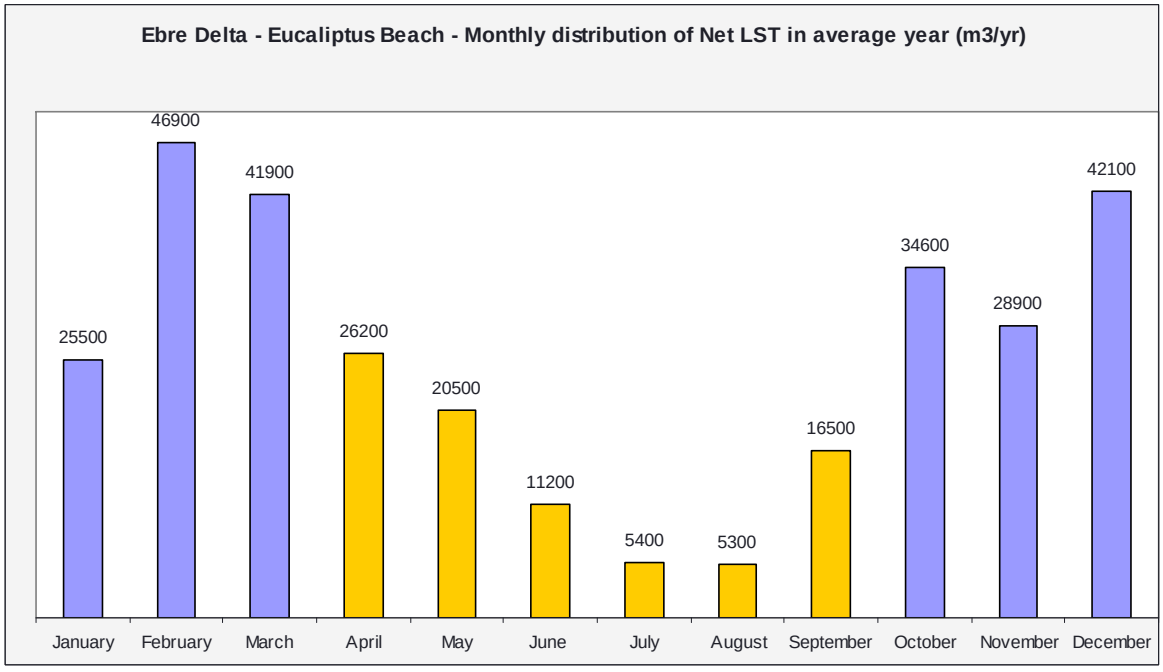

Summer and winter time distribution of Net LST:

- Oct-Mar: 219 900 (72%)
- Apr-Sep: 85 100 (28%)

BARRA DEL TRABUCADOR

Longshore Sediment Transport Time Series.

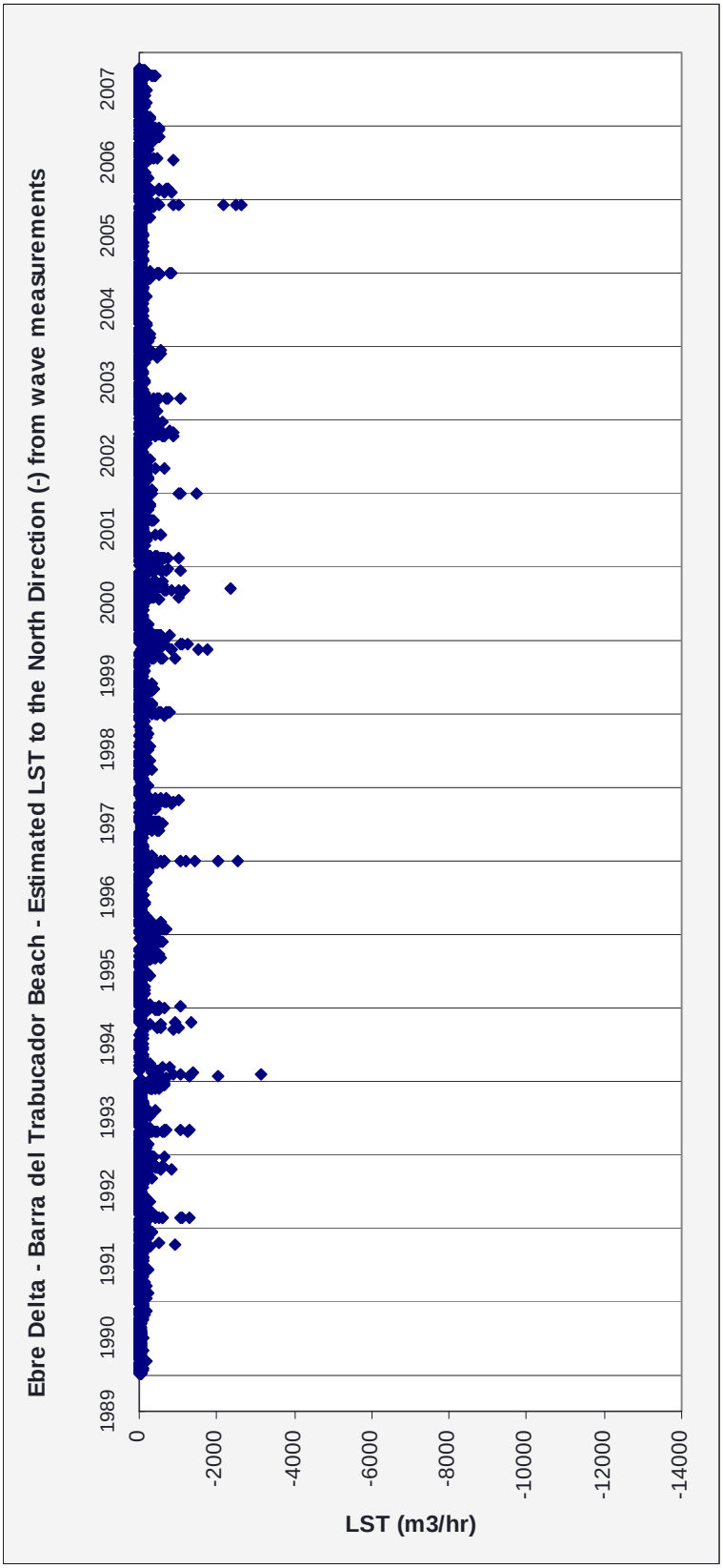

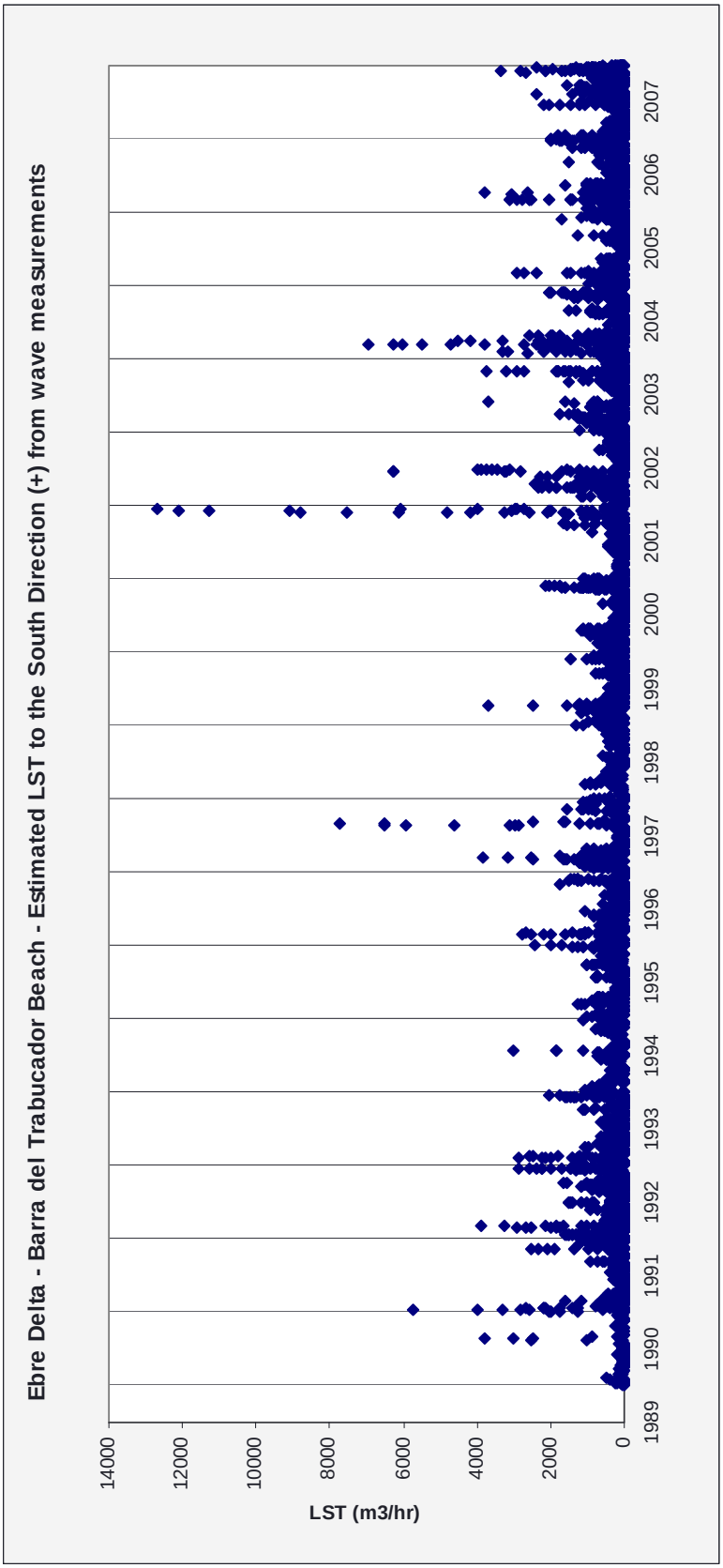
Ebre Delta - Barra del Trabucador Beach - Estimated LST to the South Direction (+) from wave measurements
LST (m3/hr)
14000
12000
10000
8000
6000
4000
2000
0
1989
1990
1991
1992
1993
1994
1995
1996
1997
1998
1999
2000
2001
2002
2003
2004
2005
2006
2007

Monthly distribution

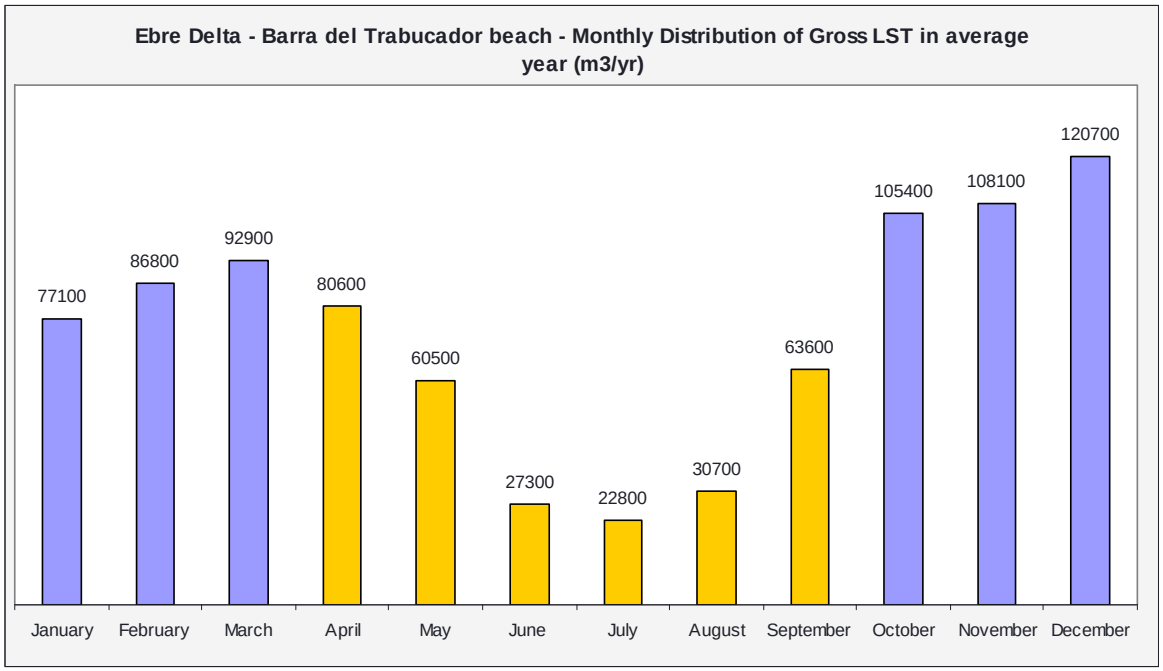

Summer and winter time distribution of Gross LST:

- Oct-Mar: 591 000 (67%)
- Apr-Sep: 285 500 (33%)

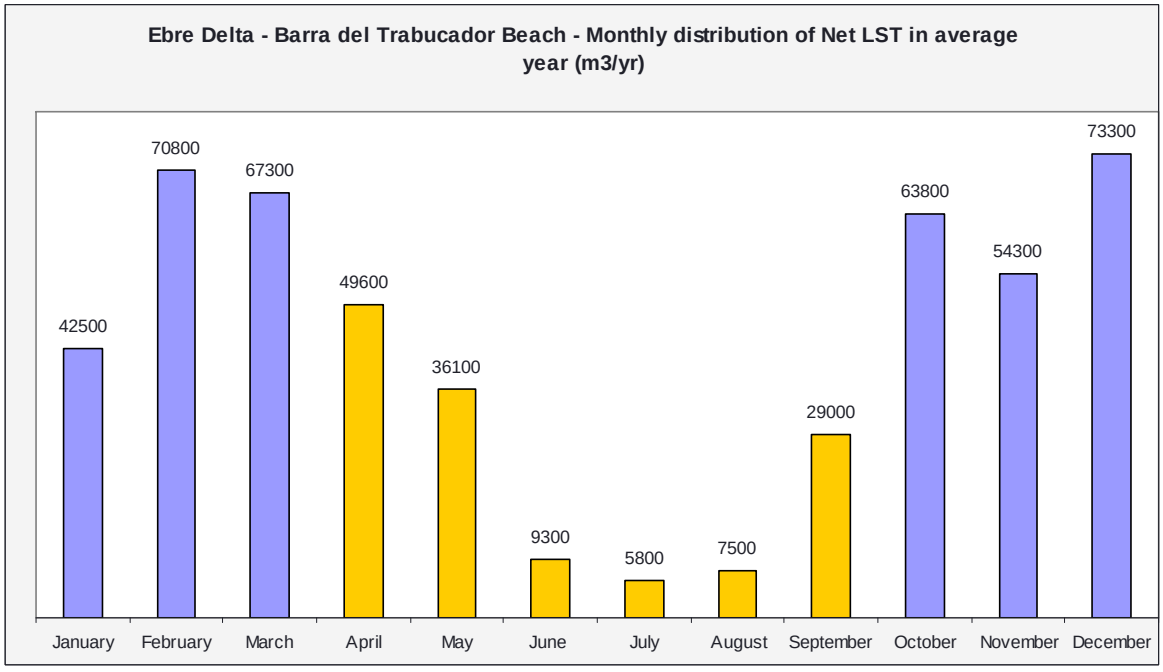

Summer and winter time distribution of Net LST:

- Oct-Mar: 372 000 (73%)
- Apr-Sep: 137 300 (27%)

SALINES

Longshore Sediment Transport Time Series.

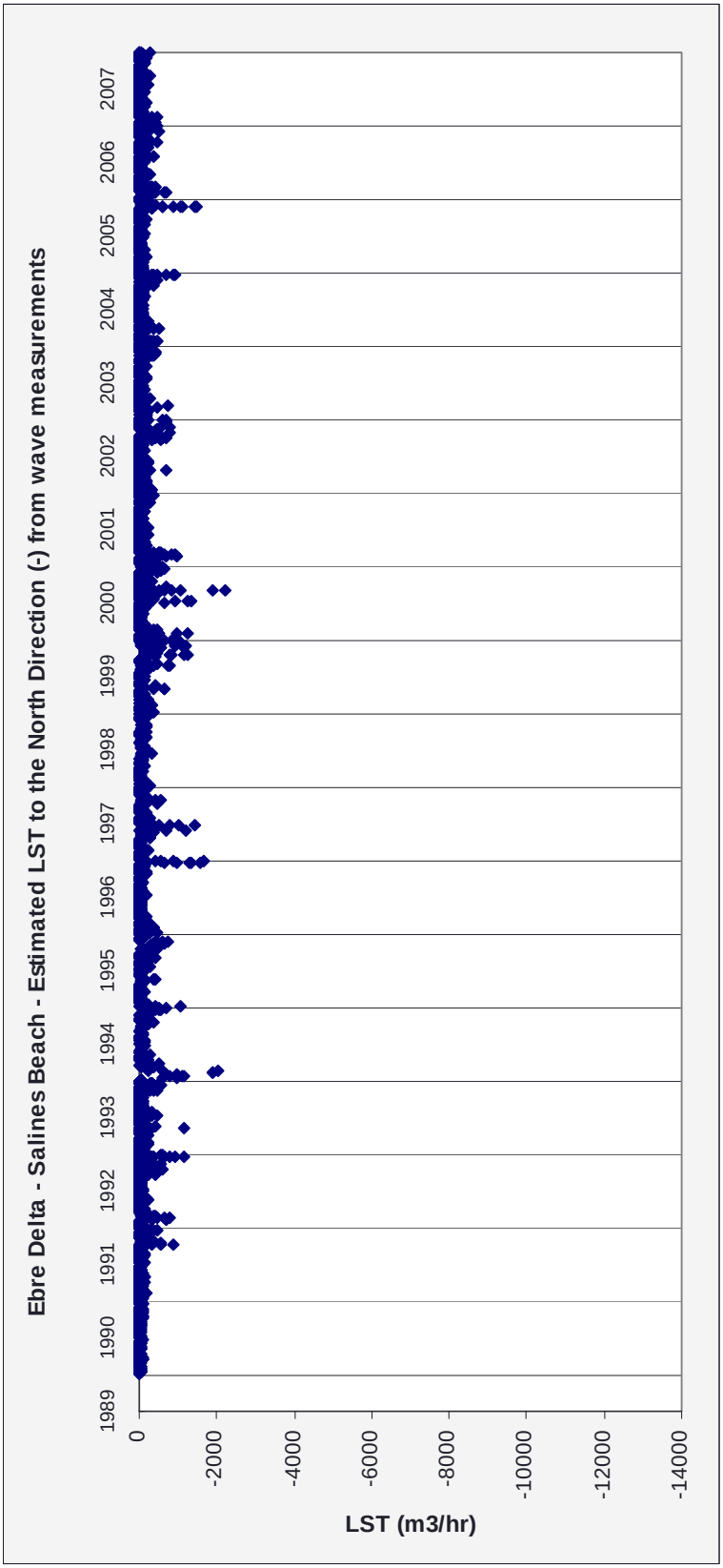

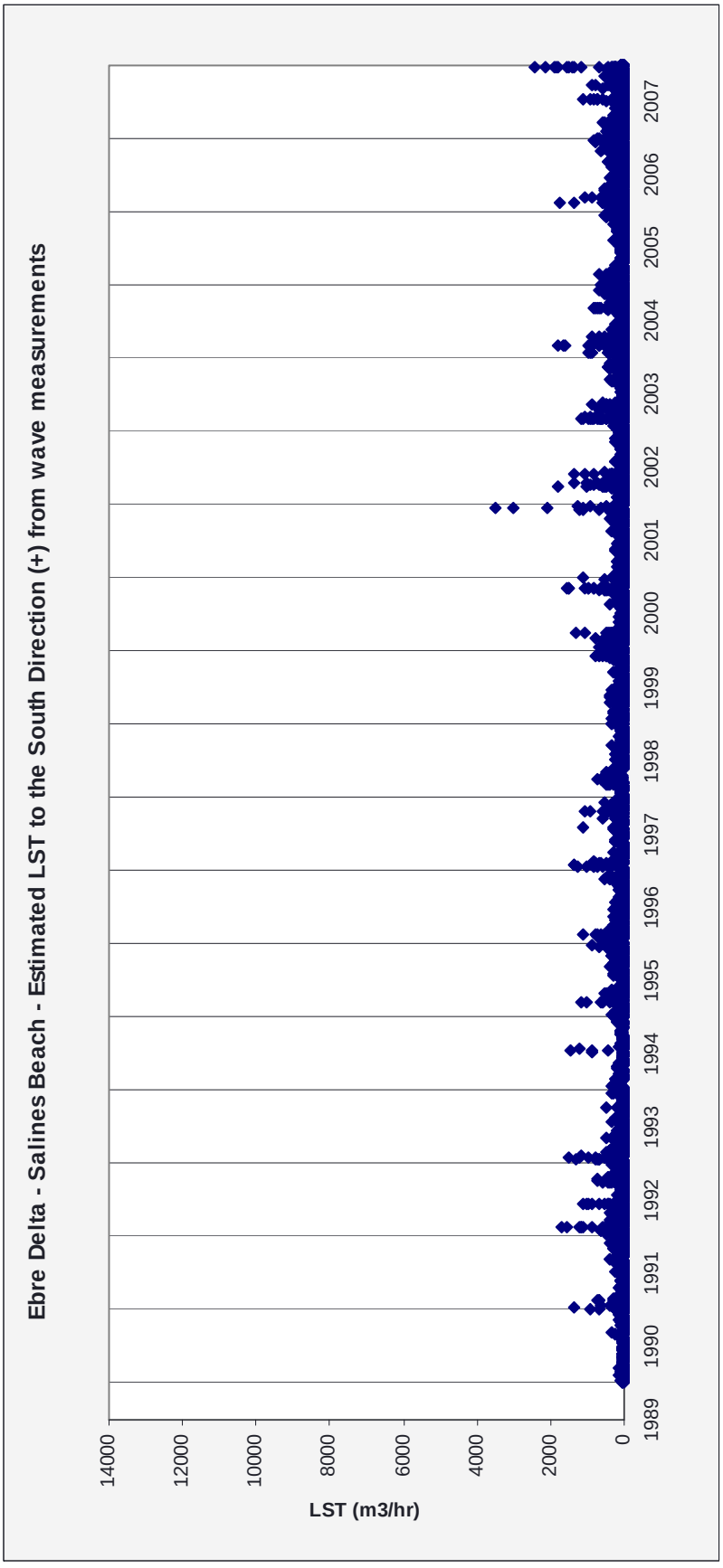
Ebre Delta - Salines Beach - Estimated LST to the South Direction (+) from wave measurements
LST (m3/hr)
14000
12000
10000
8000
6000
4000
2000
0
1989
1990
1991
1992
1993
1994
1995
1996
1997
1998
1999
2000
2001
2002
2003
2004
2005
2006
2007

Monthly distribution

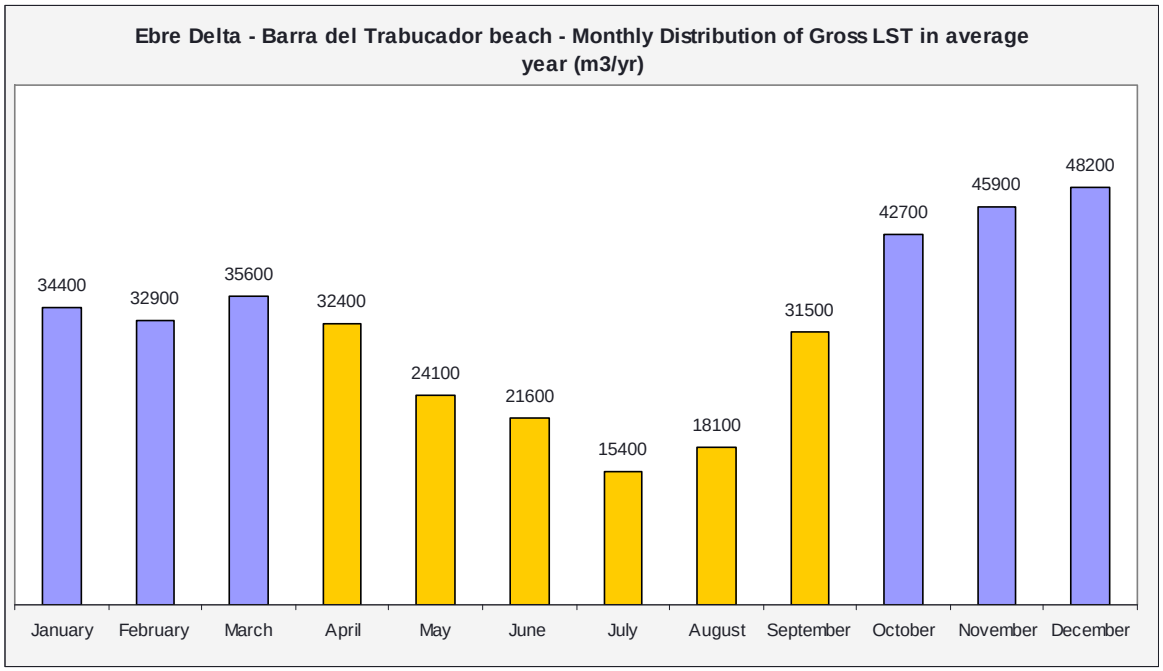

Summer and winter time distribution of Gross LST:

- Oct-Mar: 239 700 (63%)
- Apr-Sep: 143 100 (37%)

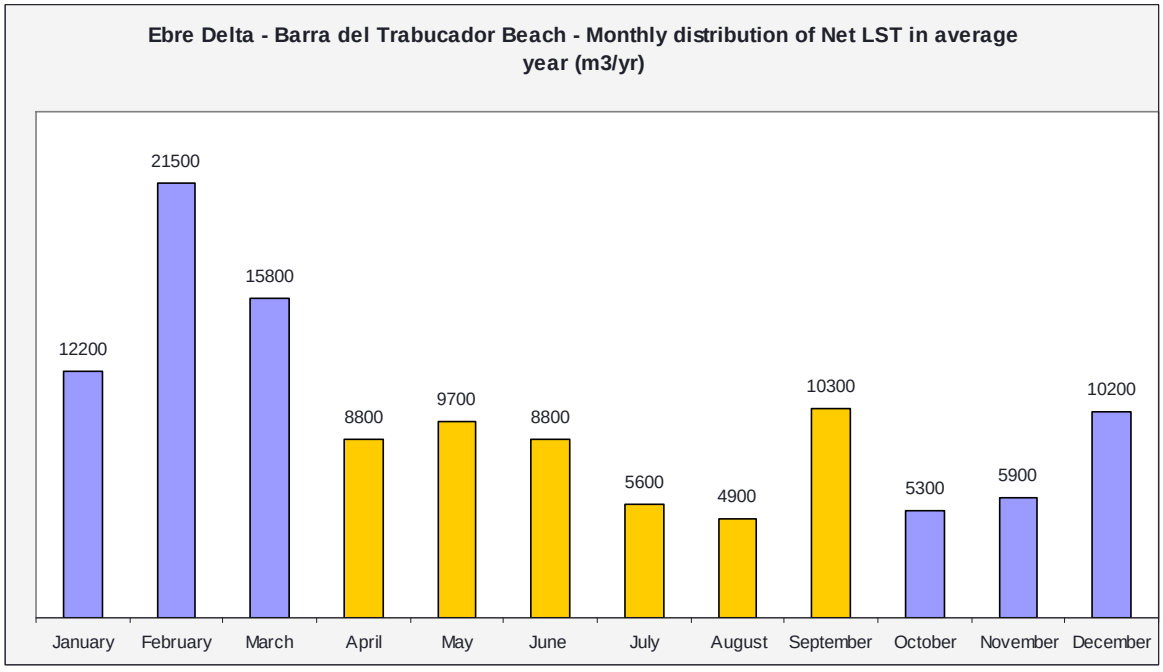

Summer and winter time distribution of Net LST:

- Oct-Mar: 70 900 (60%)
- Apr-Sep: 48 100 (40%)

CAP TORTOSA

Longshore Sediment Transport Time Series.

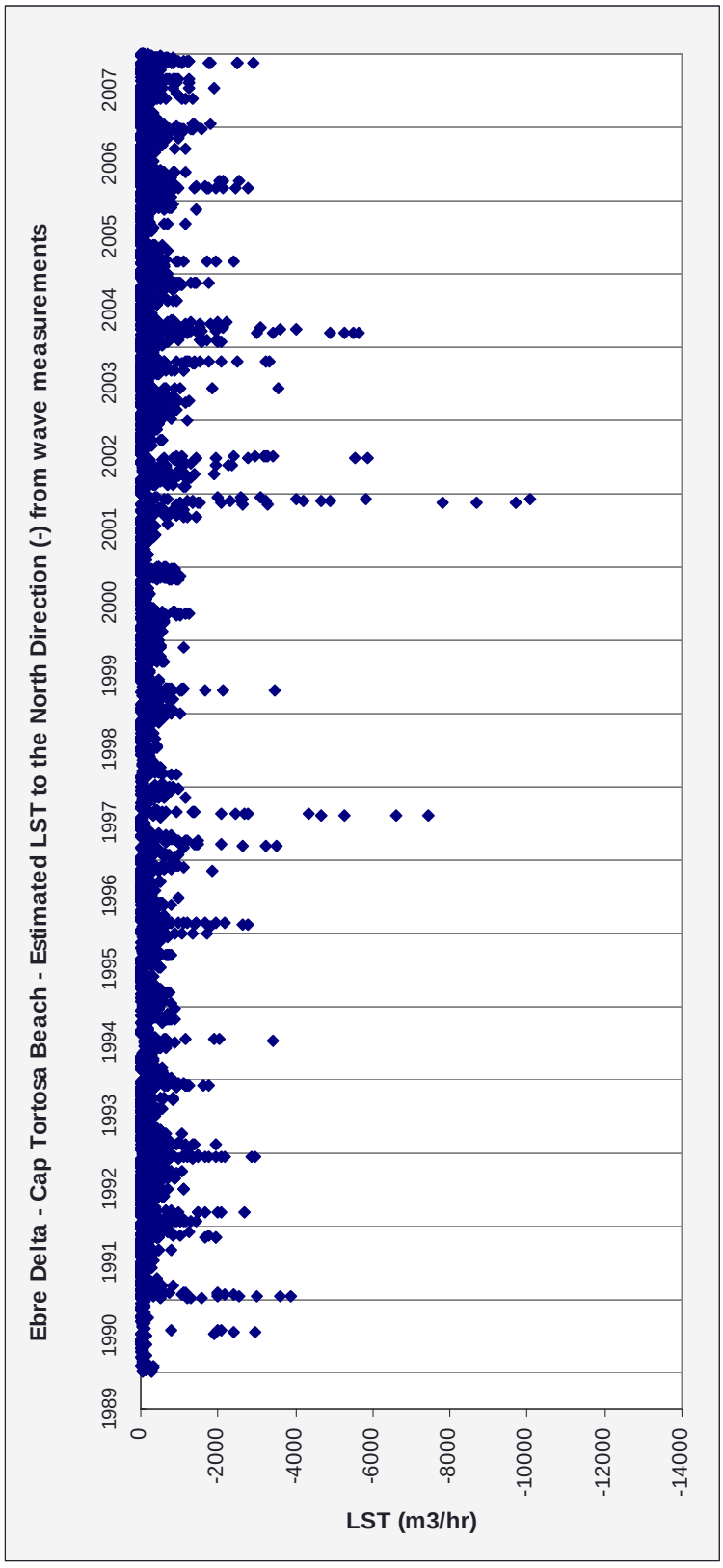

Monthly distribution

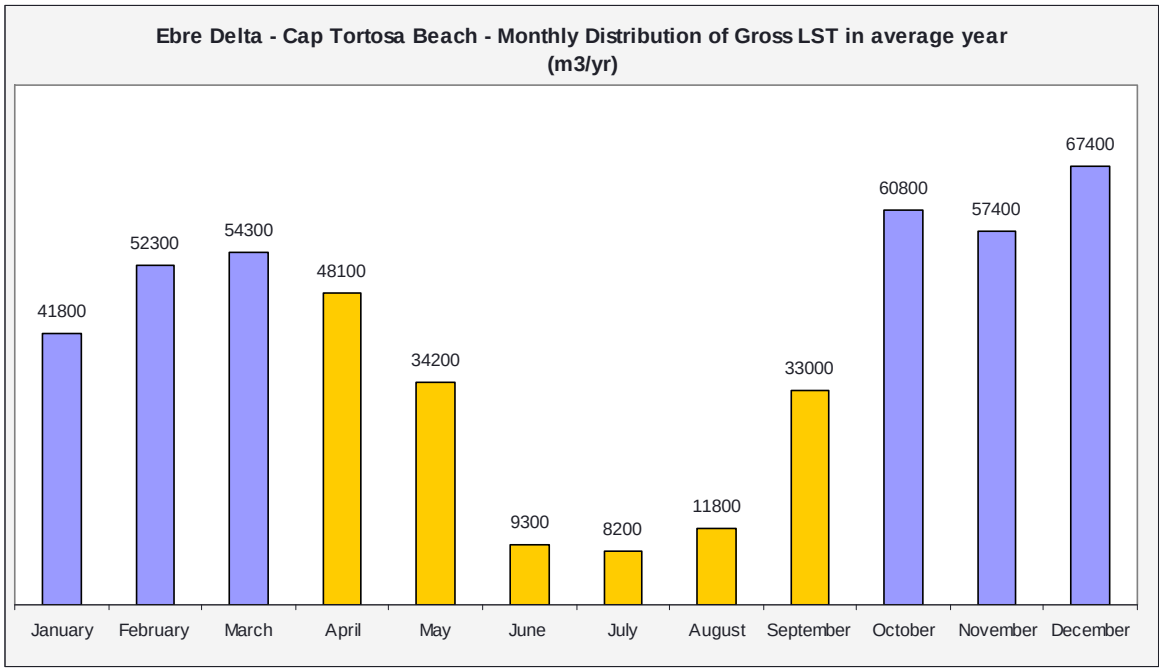

Summer and winter time distribution of Gross LST:

- Oct-Mar: 334 000 (70%)
- Apr-Sep: 144 600 (30%)

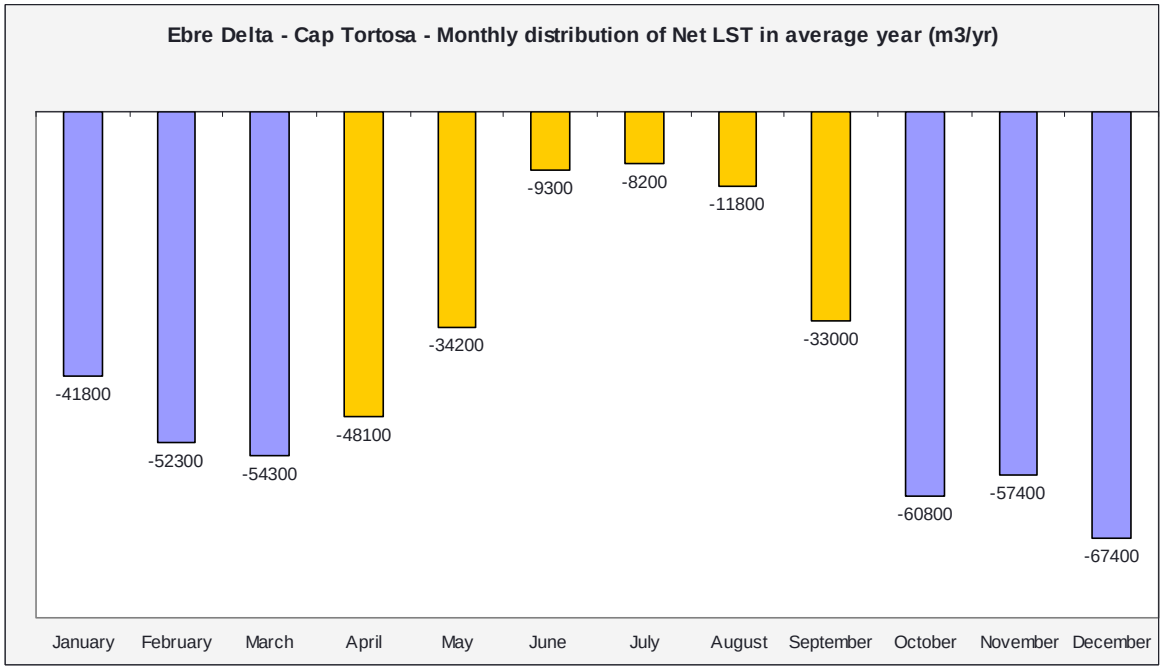

Summer and winter time distribution of Net LST:

- Oct-Mar: 334 000 (70%)
- Apr-Sep: 144 600 (30%)

PLATJA RIUMAR

Longshore Sediment Transport Time Series.

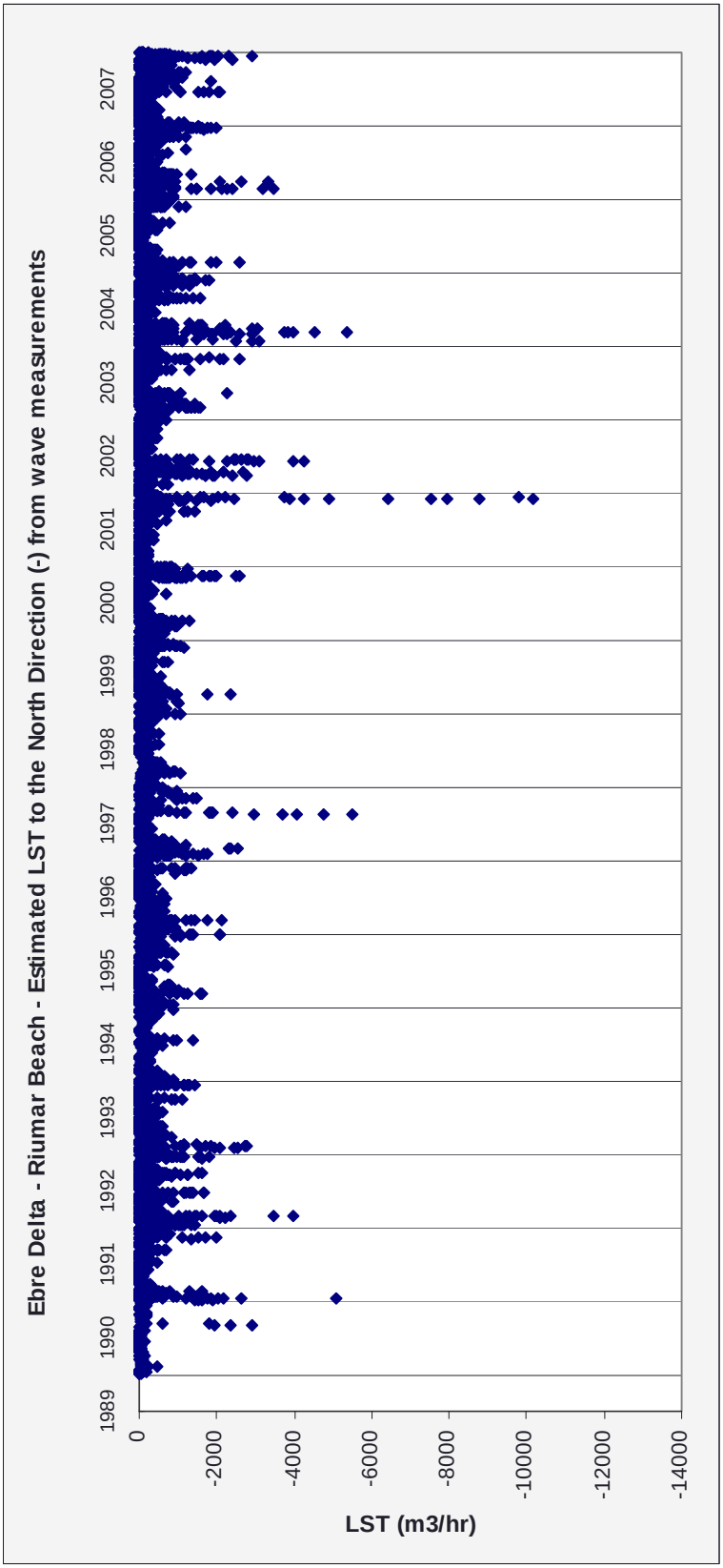

Monthly distribution

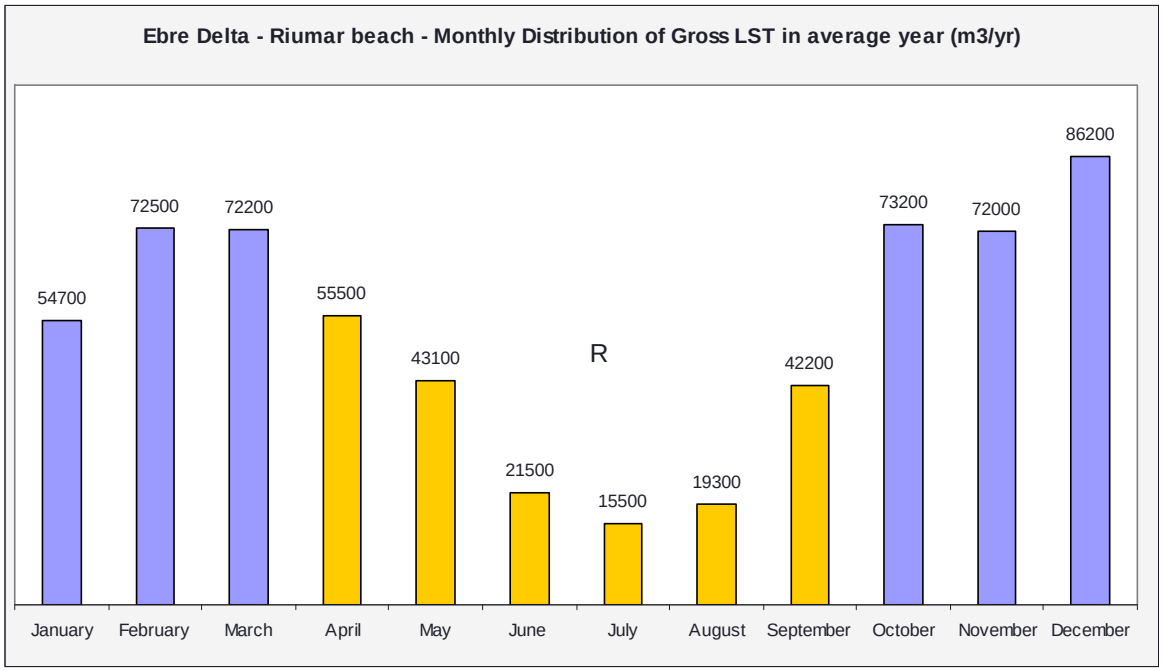

Summer and winter time distribution of Gross LST:

- Oct-Mar: 430 800 (69%)
- Apr-Sep: 197 100 (31%)

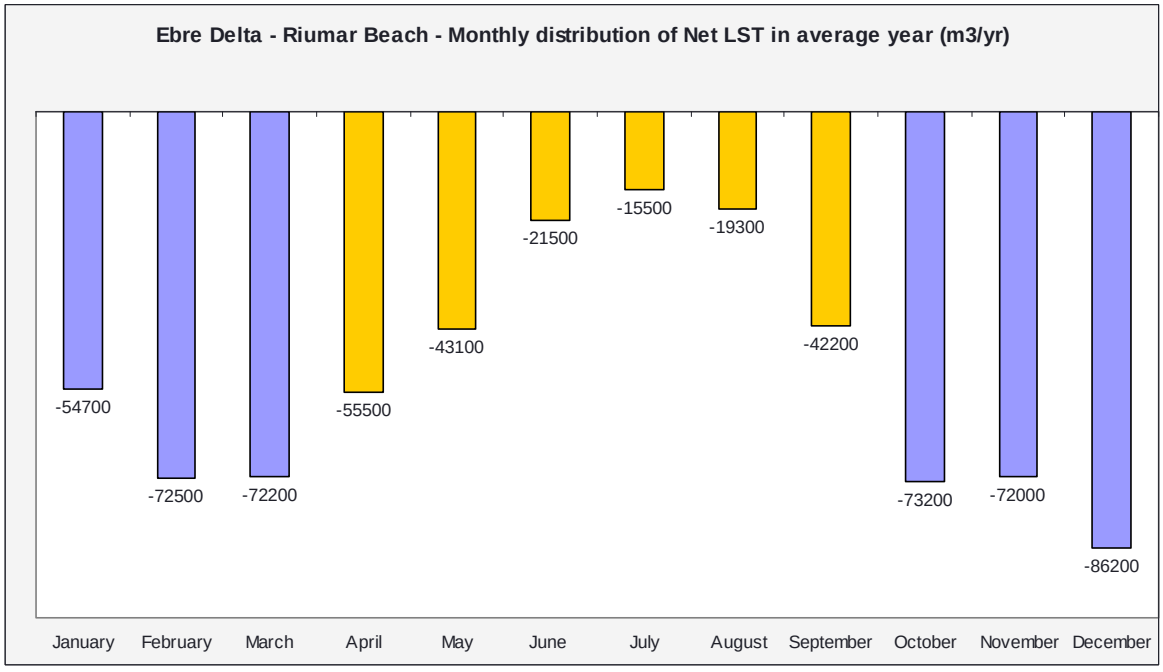

Summer and winter time distribution of Net LST:

- Oct-Mar: 430 800 (69%)
- Apr-Sep: 197 100 (31%)

LST estimation in average year: total, by wave direction and proportion caused by Hs>2m.

Beach	Direction of Littoral Drift	Total LST (m3/year)	Wave direction			Hs		Grain size (mm)	Orientation (º)	Slope
			Wave direction	LST (m3/year)	%	LST (Hs>2m)	%			
Calaix Gran	South	653419	NE	1540	0.2	376	24.4	0.2	27	0.02
			ENE	240237	36.8	132831	55.3			
			E	390614	59.8	167571	42.9			
			ESE	21028	3.2	4307	20.5			
	North	163017	ESE	784	0.5	651	83.0			
			SE	18781	11.5	1768	9.4			
			SSE	34465	21.1	2418	7.0			
			S	97045	59.5	15660	16.1			
			SSW	11942	7.3	1951	16.3			
L'Eucaliptus	South	484027	ENE	66797	13.8	38659	57.9	0.2	62	0.02
			E	309777	64.0	126093	40.7			
			ESE	91213	18.8	12945	14.2			
			SE	15856	3.3	985	6.2			
			SSE	384	0.1	21	5.5			
	North	184031	SSE	7001	3.8	714	10.2			
			S	123477	67.1	20949	17.0			
			SSW	53553	29.1	8173	15.3			
Barra del Trabucador	South	689186	ENE	228359	33.1	127393	55.8	0.2	33	0.02
			E	425615	61.8	180892	42.5			
			ESE	35212	5.1	6532	18.6			
	North	183497	SE	12988	7.1	1388	10.7			
			SSE	33039	18.0	2362	7.1			
			S	116094	63.3	18894	16.3			
			SSW	21376	11.6	3397	15.9			
Salines	South	250571	E	149391	59.6	58455	39.1	0.2	75	0.02
			ESE	67083	26.8	10282	15.3			
			SE	25762	10.3	1502	5.8			
			SSE	8335	3.3	484	5.8			
	North	130777	SSE	176	0.1	35	19.9			
			S	79301	60.6	14071	17.7			
			SSW	50655	38.7	7717	15.2			
			SW	645	0.5	0	0.0			

Beach	Direction of Littoral Drift	Total LST (m3/year)	Grain size (mm)	Orientation (º)	Slope
Cap Tortosa	East	0	0.2	288	0.02
	West	478600			
Platja Riumar	East	0	0.2	325	0.02
	West	627900			

	Calaix Gran	**Eucaliptus**	**Barra del Trabucador**
Gross LST (m^3/yr)	816 400	668 000	872 700
Net LST (m^3/yr)	490 400 (to South)	300 000 (to South)	505 700 (to South)

	Salines	**Cap Tortosa**	**Platja Riumar .**
Gross LST (m^3/yr)	381 400	478 600	627 900
Net LST (m^3/yr)	119 800 (to South)	478 600 (to West)	627 900 (to West)

Storm contribution: proportion of transport caused by storm conditions (Hs>2m)

	Calaix Gran	**Eucaliptus**	**Barra del Trabucador**	**Salines**
South Direction	47%	38%	46%	29%
North Direction	14%	16%	14%	17%

	Cap Tortosa	**Platja Riumar .**
East Direction	-	-
West Direction	49%	42%

Less than a half of sediment transport at Ebre Delta is caused by storms. Non storm periods produce the major part of littoral drift, since the bottom is composed by very small grain sand, easily moved by not very strong waves. Note that the magnitude of the drift is huge and reaches more than 600 000 m^3/year of net transport in some zones.

Sediment Budget using LST capacity

Figure 3.29 Evaluation of LST along the Ebre Delta.

Ebre Delta Drift Rose

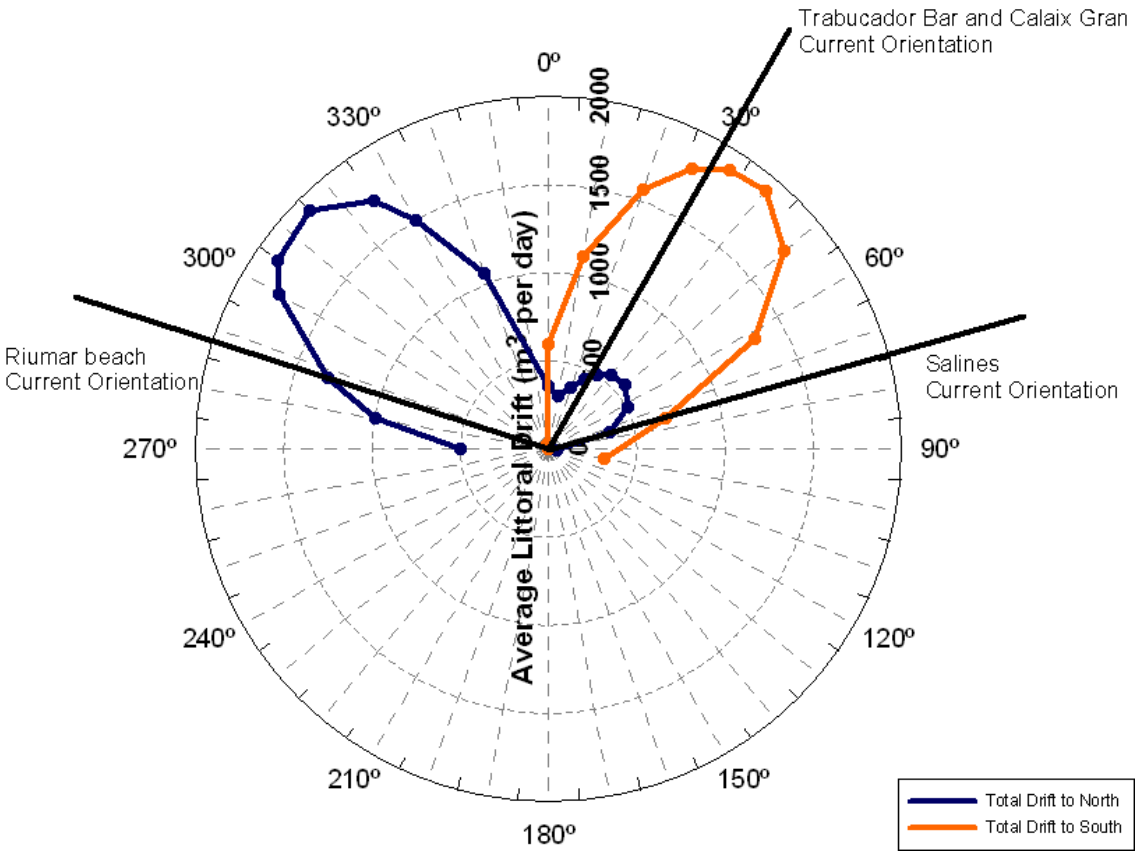

The Ebre Delta is a very special zone of the Catalan coast. Formed by a very small size grain, the littoral drift there is much higher than at any other stretch of this coast. Created from the sediment coming through Ebre River, it has been decreasing since the dam construction and river regulation reduced highly the amount of sediment brought by the stream. Currently the wave climate is producing the littoral drift seen on the sediment budget image. Many studies focused on this aspect of the Catalan coast sediment transport have been carried out in order to estimate the magnitude of the Delta Ebre retreat. That is quite complicated due to the huge annual drift of about 500 000 m^3 at some zones.

3.3 GENERAL CONCLUSIONS

3.3.1 LST by Net/Gross and by direction of transport (South/North)

Beach	Net LST*	Gross LST	Direction		Buoy Zone
			To South	To North	
x 1000 m3/yr					
La Rovina	-4	105	50	54	1
Sant Pere Pescador	-87	264	88.9	175.4	1
Sant martí d'Empúries	-38	252	106.9	145.2	1
L'Estartit	86	597	342	256	2
Pals	26	432	229	203	2
Palamós	-2	3	0	2	2
St. Antoni de C.	32	117	75	43	2
Platja d'Aro	13	121	66.9	54	2
Sant Pol	-98	203	52.3	150.3	2
Lloret North	5	22	14	9	3
Lloret South	3	18	11	8	3
Santa Cristina	45	120	82	38	3
S'Abanell North	18	35	26	8	3
S'Abanell South	9	16	13	4	3
La Tordera	110	187	148	39	3
La Tordera-Arenys	53	283	168	115	3
Arenys - Port Balis	61	287	174	113	3
Mataró	61	287	174	113	3
Mataró 2	7	234	121	113	3
El Masnou	7	47	27	20	4
East Castelldefels	41	297	169	128	4
West Castelldefels	-14	175	80	95	4
Calafell	85	303	194	109	6
El Roc	139	391	265	126	6
Creixell	212	621	416	205	6
El Miracle	262	683	473	211	6
La Pineda	275	620	448	173	6
Cambrils	-64	284	110	174	6
Salou	191	192	192	1	6
L'Hospitalet de l'Infant	502	828	665	163	6
Ebre Delta:					
Calaix Gran	490	816	653	163	6
L'Eucaliptus	300	668	484	184	6
Barra del Trabucador	506	873	689	184	6
Salines	120	381	251	131	6
Cap Tortosa	-479 (to West)	479	0 (to East)	479 (to West)	6
Platja Riumar	-628 (to West)	628	0 (to East)	628 (to West)	6

Table 3.1 LST estimations at points along the Catalan coast.

In almost all beaches along the coast of Catalonia littoral drift is from North East to South West. Although most of the waves come from South direction rather than from East, those coming from this direction have greater Hs in some periods of the year.

3.3.3 Monthly Distribution

In all coastal zones analyzed sediment transport is produced largely in autumn and winter, which is the time in which most of the storms take place and the average wave height is in general higher. Graphics of Monthly Distribution of sediment transport throughout an average year show in different color the period from October to March and the period from April to September. The following table is a resume of the proportion of transport produced in winter time (October to March) and summer time (April to September). To know the monthly distribution of Hs see "Appendix 2: *Monthly Distribution of Hs*".

	Gross Sediment Transport	**Net Sediment Transport**
	Oct-Mar/Apr-Sep	Oct-Mar/Apr-Sep
La Rovina	64/36	70/30
Sant Pere Pescador	75/25	71/29
Sant Martí d'Empúries	76/24	71/29
L'Estartit	74/26	83/17
Pals	72/28	55/45
Palamós	84/16	79/21
Sant Antoni de Calonge	74/26	68/32
Platja d'Aro	69/31	74/26
Sant Pol	70/30	74/26
Lloret North	69/31	61/39
Lloret South	69/31	73/28
Santa Cristina	69/31	83/17
S'Abanell North	74/36	82/18
S'Abanell South	80/20	88/13
Tordera	80/20	87/13
Tordera – Arenys	74/26	80/20
Arenys – Port Balis	74/26	80/20
Mataró	74/26	80/20
El Masnou	70/30	60/40
Calafell	63/37	53/47
El Roc	68/32	68/32
Creixell	65/35	68/32
El Miracle	67/33	76/24
La Pineda	68/32	73/27

Cambrils	60/40	80/20
Salou	59/41	60/40
L'Hospitalet de l'Infant – Arenal	68/32	73/27
Average	**70/30**	**72/28**

It is clear that, with very little deviation, 70% of annual sediment transport takes place during autumn – winter time. This proportion is close to this value for any beach along the Catalan Coast.

Influence of Grain Size

Regarding Gross Sediment Transport the proportion of transport produced in October – April is quite higher at beaches placed in the North Catalan Coast. These beaches are composed in general by greater grain size sand than the ones placed towards the South Coast. The cause of this fact is quite simple: the grater grain size the greater wave height needed to start sediment movement (smaller threshold) and hence it'll be smaller the quantity of sediment moved during the summer time non storm period. In coast zones composed by small grain size sand there will exist sediment transport most of the time even during periods in which the beach is not reached by great wave heights.

3.3.4 Proportion of LST caused by storms

An important goal of this research was to evaluate how important is the quantity of sediment transport produced by storm conditions. It was suspected that this proportion was high but we weren't able to say if storm conditions periods explain almost all the transport or not. In other words, to decide if to consider only storm periods is enough to obtain a sufficiently approximated value to the real LST. The conclusion, as we'll see on this chapter, is that we cannot do so.

In the following table we can see the proportion of sediment transport caused by storm conditions (Hs > 2m).

	South Direction (%)	North Direction (%)
La Rovina	51	31
Sant Pere Pescador	74	50
Sant Martí d'Empúries	71	52
L'Estartit	45	51
Pals	29	62
Palamós	40	31
Sant Antoni de Calonge	68	32
Platja d'Aro	68	49
Sant Pol	65	33
Lloret North	53	23
Lloret South	51	23
Santa Cristina	55	23
S'Abanell North	58	31
S'Abanell South	58	31
Tordera	58	31
Tordera – Arenys	50	19
Arenys – Port Balis	50	19
Mataró	50	19
El Masnou	33	30
East Castelldefels	29	23
West Castelldefels	21	21
Calafell	27	18
El Roc	33	16
Creixell	33	16
El Miracle	60	34
La Pineda	46	44
Cambrils	14	17
Salou	14	8
L'Hospitalet de l'Infant – Arenal	43	15

Storms have a clear greater influence on transport to the South direction. That makes sense, as important storms tend to come from the East direction and waves from this direction produce in almost al beaches in the Catalan Coast transport to the South. Transport to the North is in general lower and caused by normal non storm wave conditions. Great storms from the South are not very common in this area (see *Appendix 1. Wave Height Roses*).

On the other hand, transport caused by storms is higher in the North zone of Catalonia and tends to decrease as we go to the South, from values over 70% in the Gulf of Roses to almost all values lower than 50% in the southern coast of Tarragona and until the Ebre Delta. Northern beaches are composed in general by greater sediment sizes than southern and have in consequence greater slopes. These two factors make that a greater wave is

needed to start the movement of sediment, so during certain periods of not very high waves transport will occur at southern beaches but not at northern. That's right that if a beach is composed by a smaller size sediment storms will move a larger quantity of sediment than whether the same storms reach a beach with a bigger sediment. Taking this into account it seems that there shouldn't be any influence of grain size and beach slope on the proportion moved by storms. In practice, at the Catalan coast it exist such influence (due to the fact already exposed) and looking at the results of this study that's clear that in beaches with a higher threshold for sediment movement it will be higher the proportion of sediment caused by storm conditions. But never such conditions will determinate the total transport and we'll have to take always in consideration both storm and non storm wave periods.

In general, we can say that in exposed beaches the proportion of transport to the South direction produced by storm conditions will be between 40% and 70% at the northern coast (from Barcelona to Roses) and between 20% and 50% at the southern coast (from Barcelona to the Ebre Delta). For transport to the North direction this proportion will be between 30% and 50% from Barcelona to Roses and between 10% and 30% from Barcelona to the Ebre Delta.

3.3.5 Annual deviation over the mean

Here it has been plotted the variation of the total LST in each year over the average value of LST of all the years since measurements are available. The objective is to see if there is any kind of evolution in the quantity of sediment transport occurred in the course of the years. For all beaches it has been used an index of deviation over the mean that has been plotted on the following graphics. This index is what is represented with the variable "Deviation" on the graphics and is calculated as:

$$\text{Deviation}_{\text{YEAR i}} = \frac{LST_{YEARi} - LST_{AVERAGE}}{LST_{AVERAGE}}$$

Using this coefficient the plot is centered in the zero. The value of the coefficient for a certain year will be null if the LST of this year coincides with the mean, positive if is higher and negative if lower. Despite of data series might not be long enough to define a long term sediment transport behavior, we need to see if something like a trend can be observed. Probably in the future years more accurate long term studies could be done when the length of data series is increased.

Analyzing the graphics, is possible to identify certain cycles on some of them. On the following graphics, we can appreciate two types of cycles with different shape but with the same period of repetition. That period is about 6-7 years. Most southern beaches from Calafell to L'Hospitalet de l'Infant do not seem to follow any type of cycle or evolution. At the end are represented the graphics for all beaches with each identification number.

Issues for variability

Another aspect of the analysis of the graphics consist in investigate which beaches tend to suffer a high variability of the values of sediment transport. Furthermore, it would be interesting to identify which characteristics or elements make the annual values of a beach more or less steady.

Following are listed the beaches and classified regarding to their annual variability of sediment transport values. The variability is considered to be very low, low and high.

It may be observed that, in general, exposed beaches tend to have less variability than closed and protected beaches. An explanation for this fact could be that exposed beaches are always receiving waves so at the end of a year it has received more or less the same number of great height waves than in another year. Protected waves only receive the waves coming from the direction towards they are open. It can be possible that in a certain year the waves do not come from this direction any day but the do in another year. Between these two years the magnitude of sediment transport will be quite different.

Shape 1. Constant with peaks (6-7 year cycles).

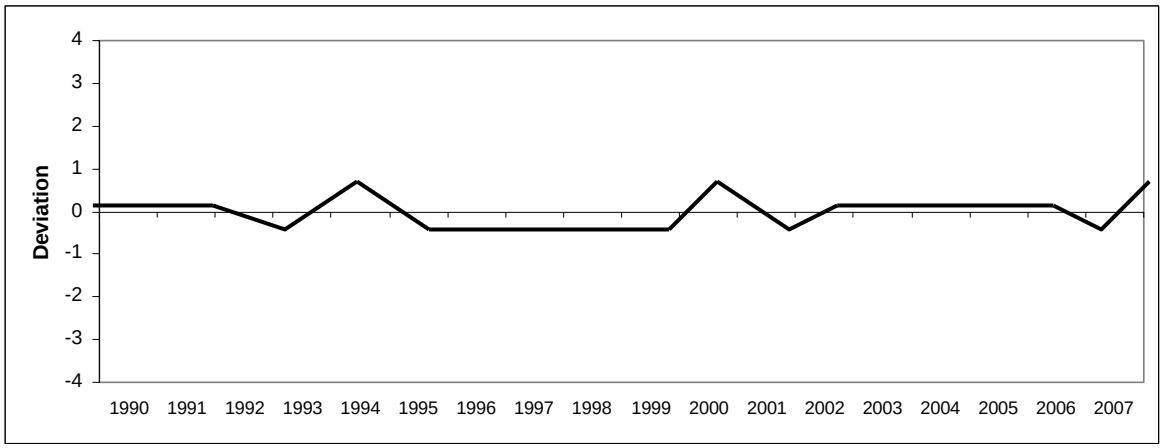

With this shape:

4. L'Estartit Unit - L'Estartit

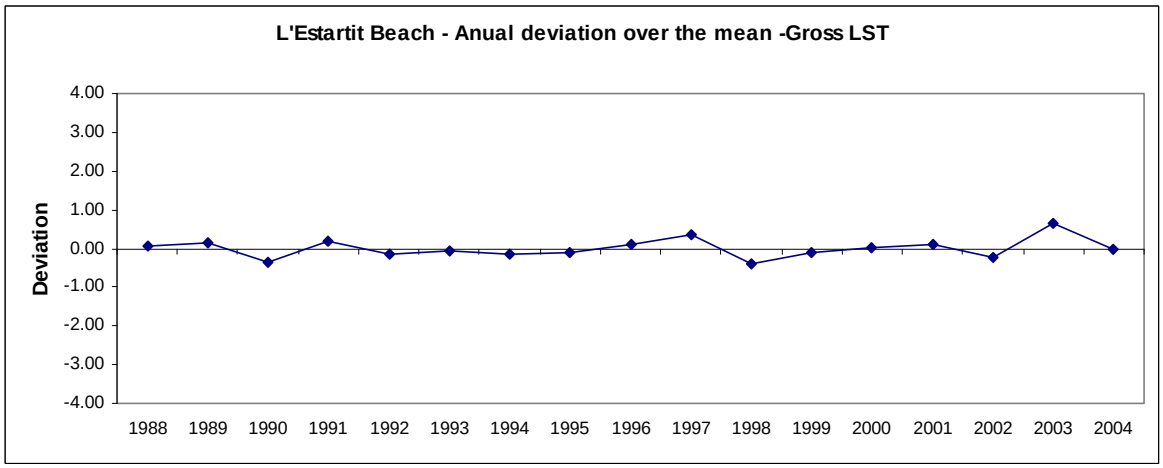

5. L'Estartit Unit – Pals

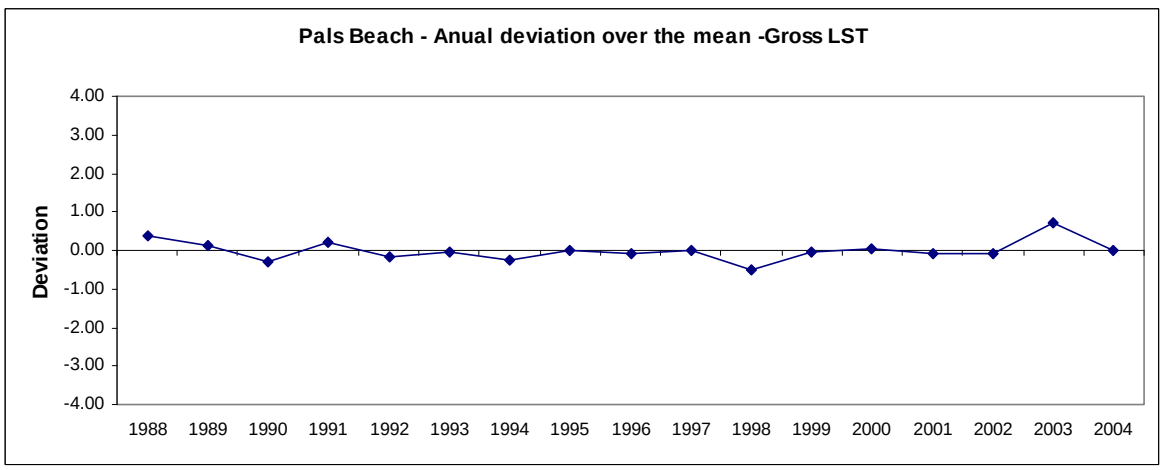

7. Palamós Unit - Sant Antoni de Calonge

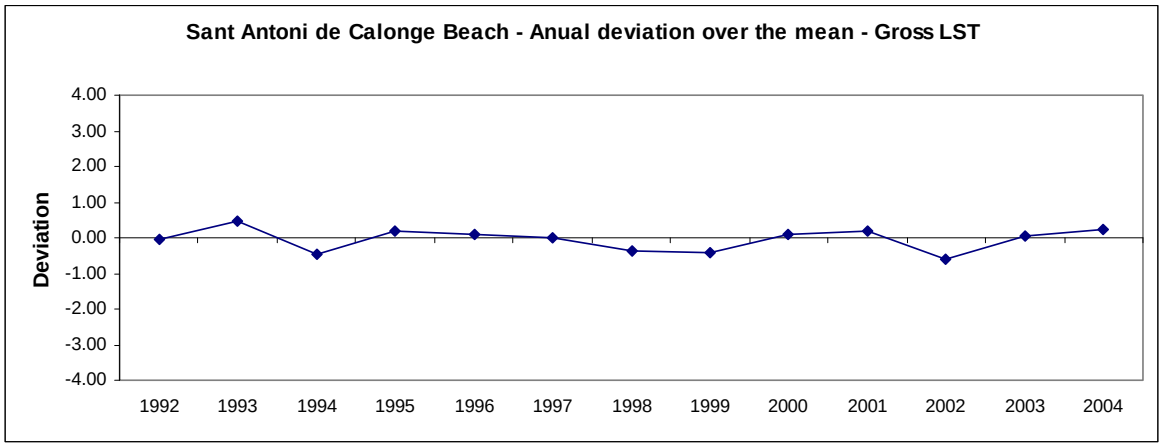

8. Platja d'Aro Unit – Platja d'Aro

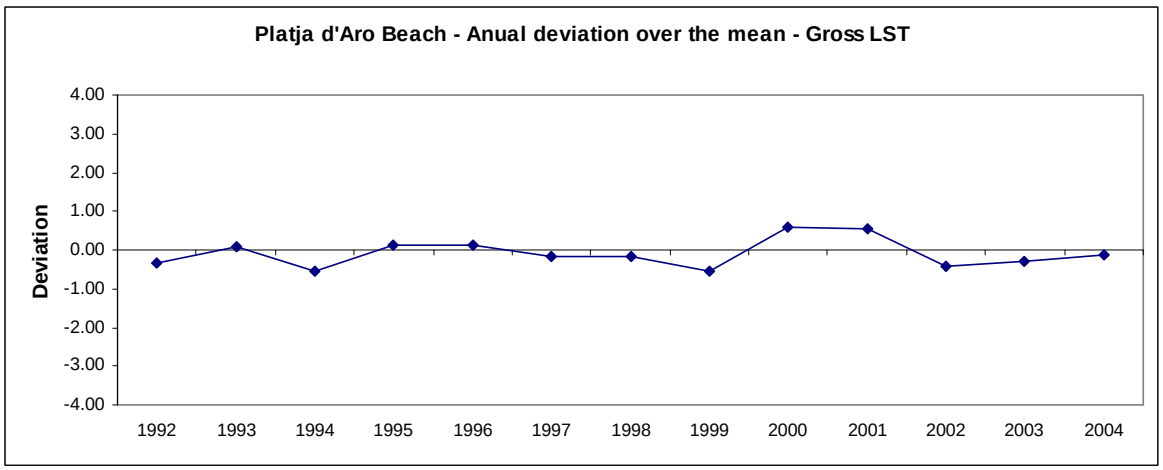

Shape 2. Alternative arcs (6 year cycles).

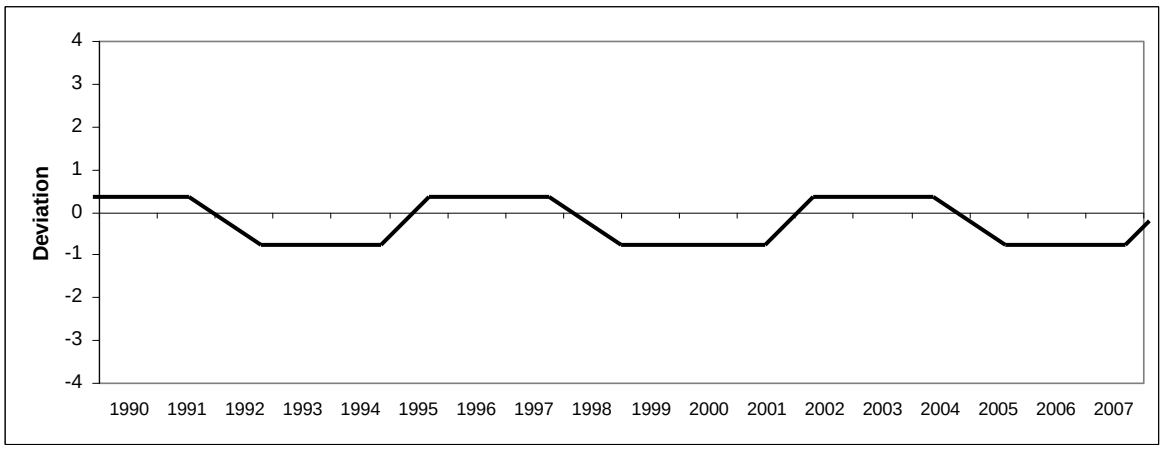

With this shape:

9, 10, 11 Lloret North and Lloret South Unit – Lloret North

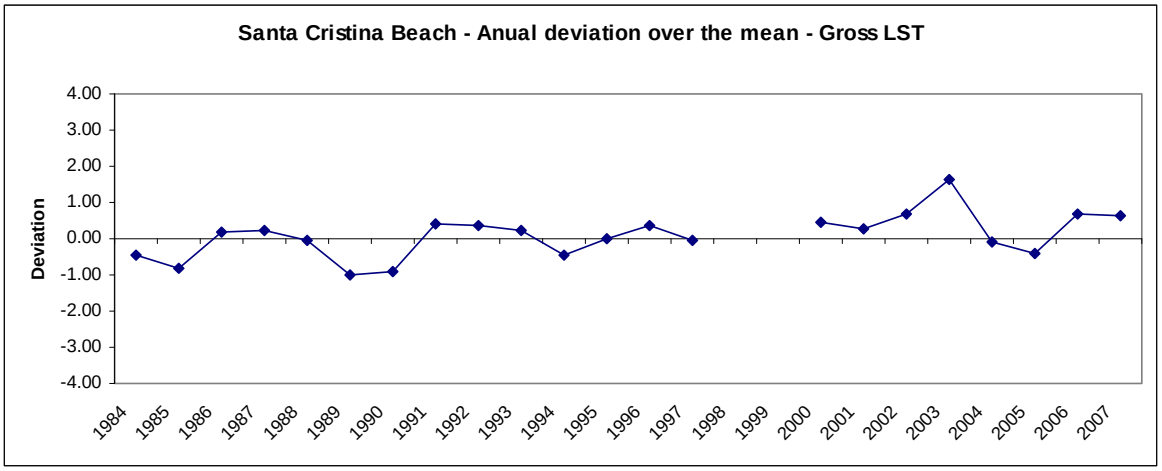

12, 13, 14 Blanes Unit

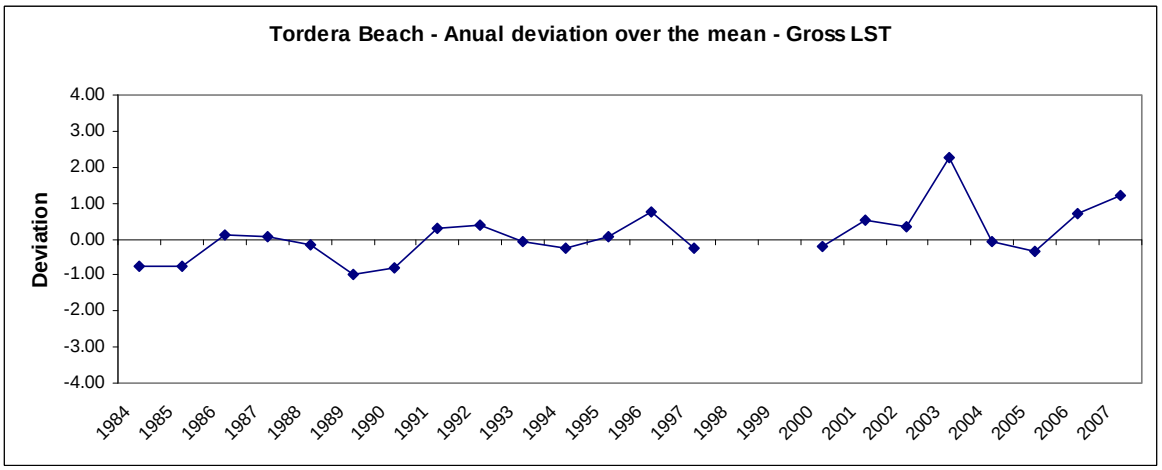

In the two last cases (Lloret and Blanes) only one from graphic from the unit is shown, as they're all similar. At the end of the chapter it can be seen all graphics.

15. Mataró Unit – Mataró

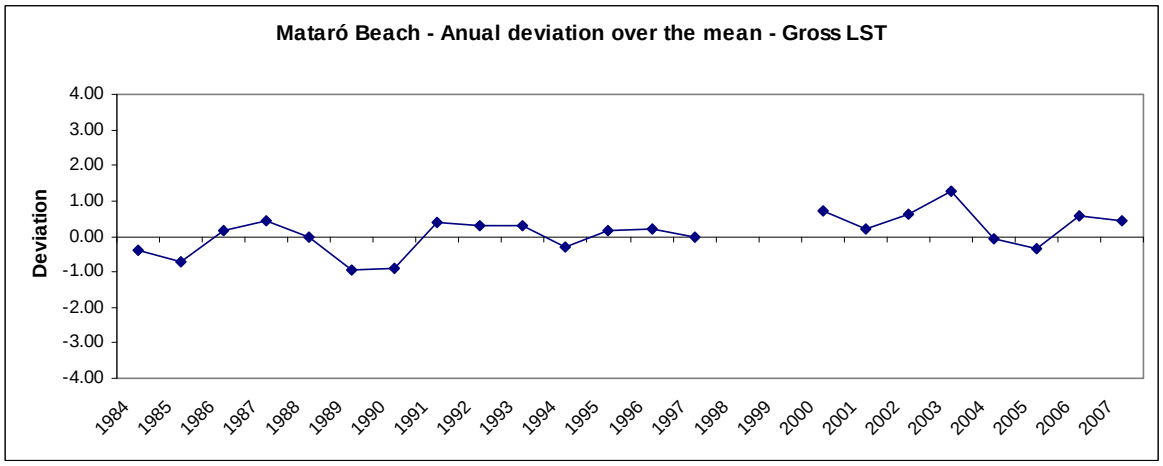

16. Masnou Unit - Masnou

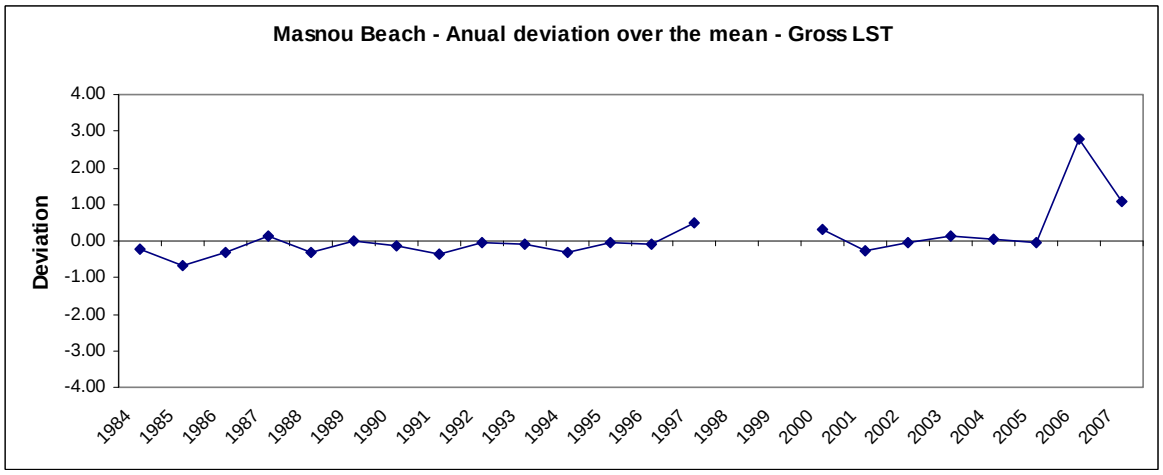

Conclusion

Cycles of 6-7 years can be observed in the behavior of the sediment transport in the course of the years. Although it is not clear in all the beaches it does in a great number of them. This subject could be investigated further in specific studies. In the case of beaches performing Shape 1 we have a peak with an extremely height or low value of transport in every cycle. After this peak we have always an opposite value the following year. That means that after an extreme high value there's a moderately low value and after an extremely low value there's a quite high value.

Annual Deviation Graphics of all beaches

1. Roses Unit - **La Rovina**

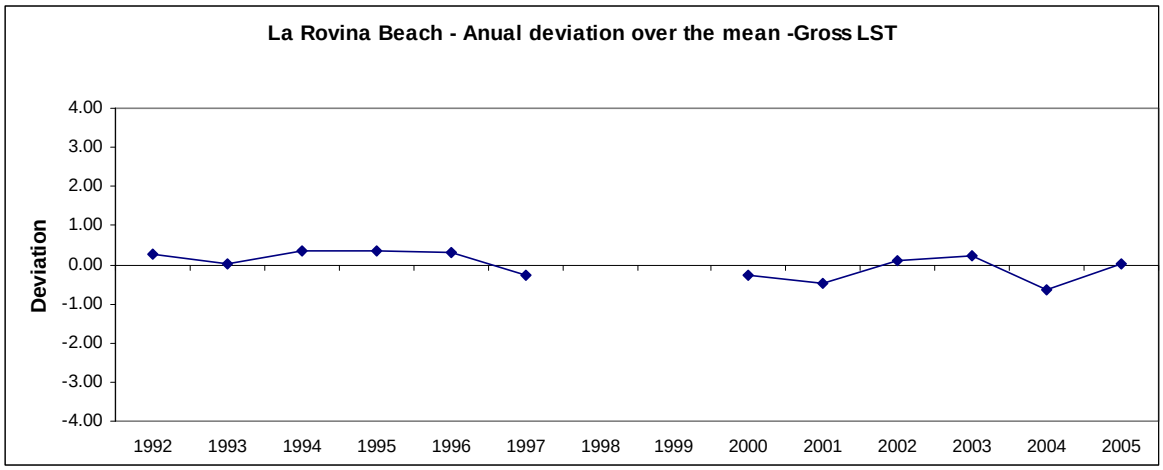

2. Roses Unit - **Sant Pere Pescador**

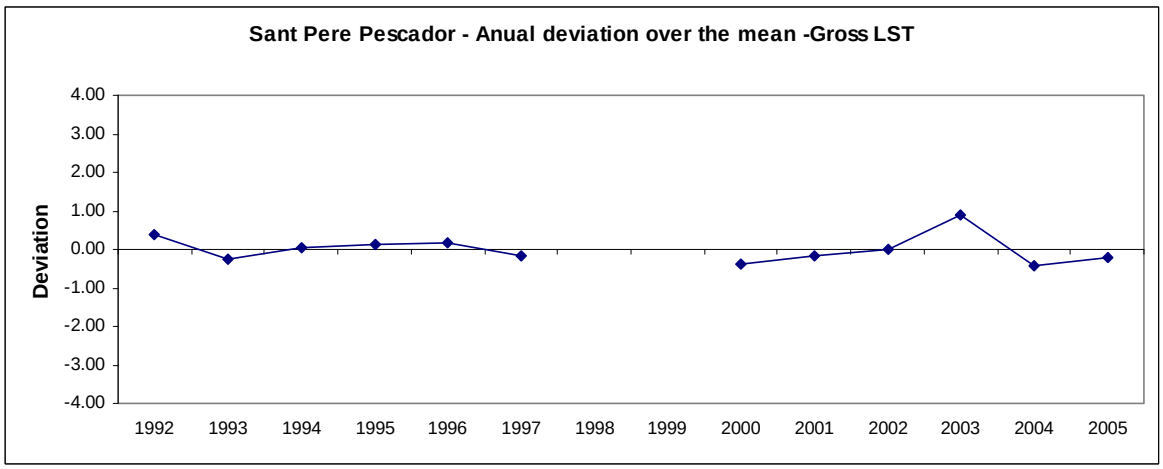

3. Roses Unit - **Sant Martí d'Empúries**

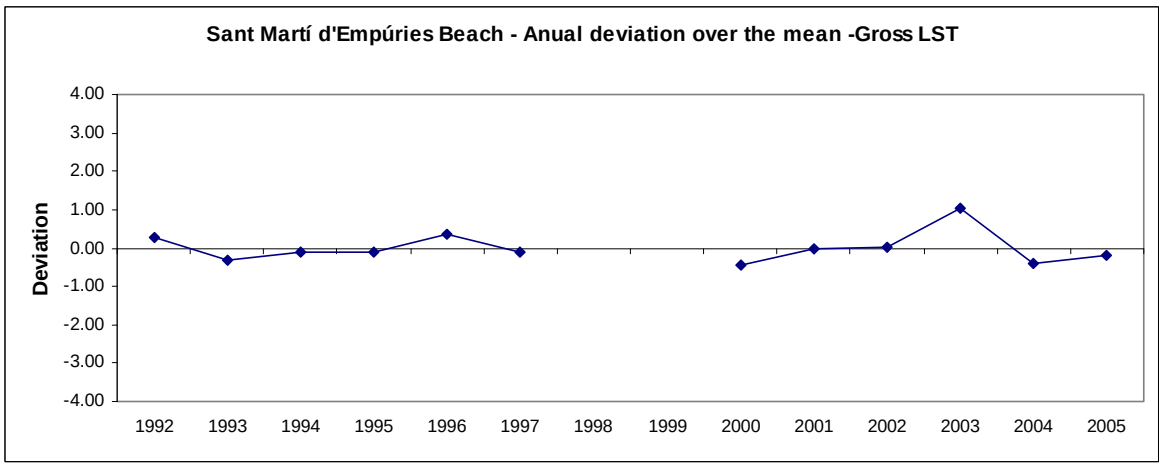

4. L'Estartit Unit - **L'Estartit**

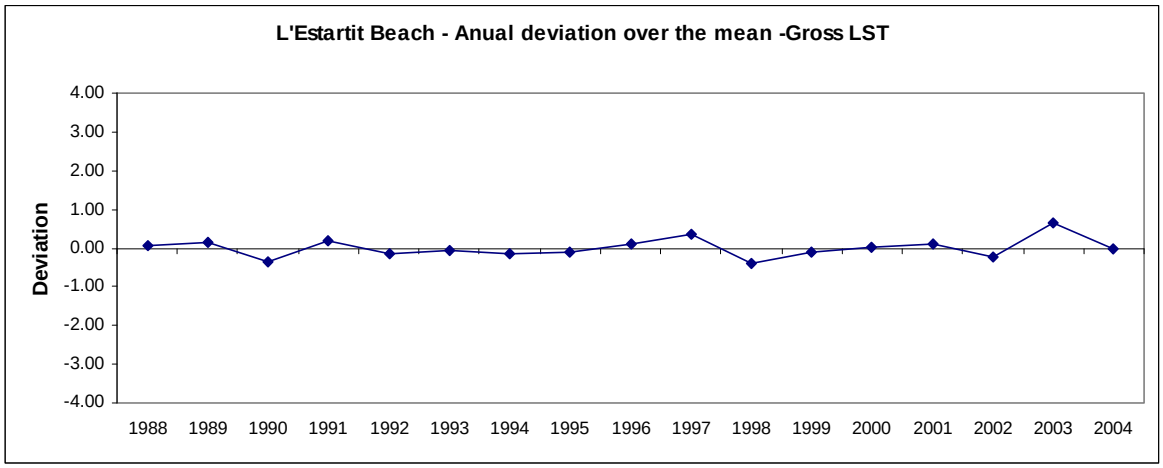

5. L'Estartit Unit - **Pals**

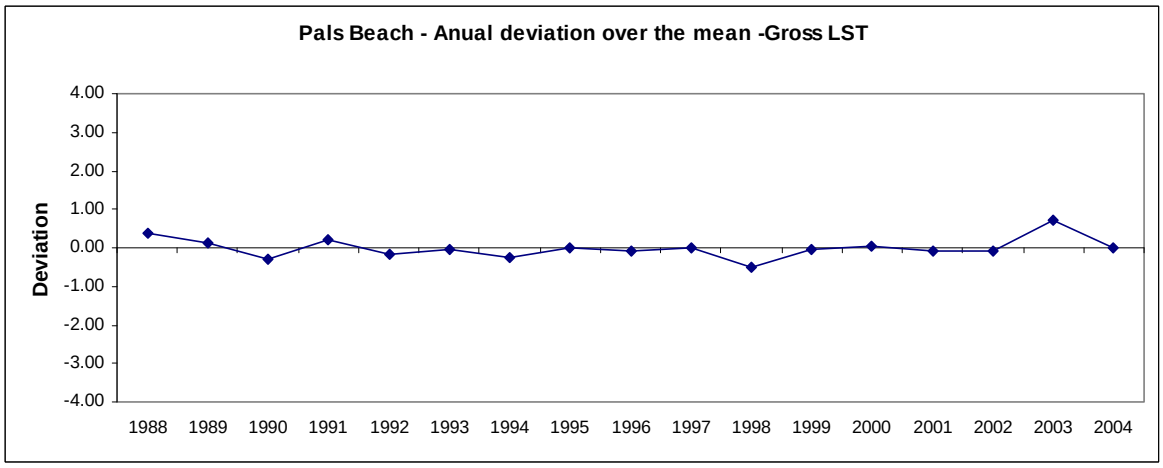

6. Palamós Unit - **Palamós**

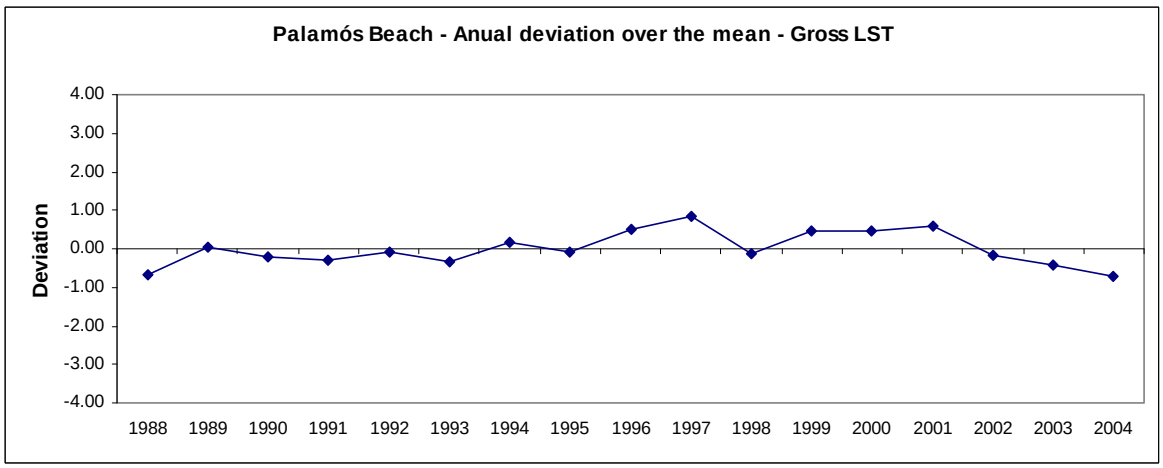

7. Palamós Unit - **Sant Antoni de Calonge**

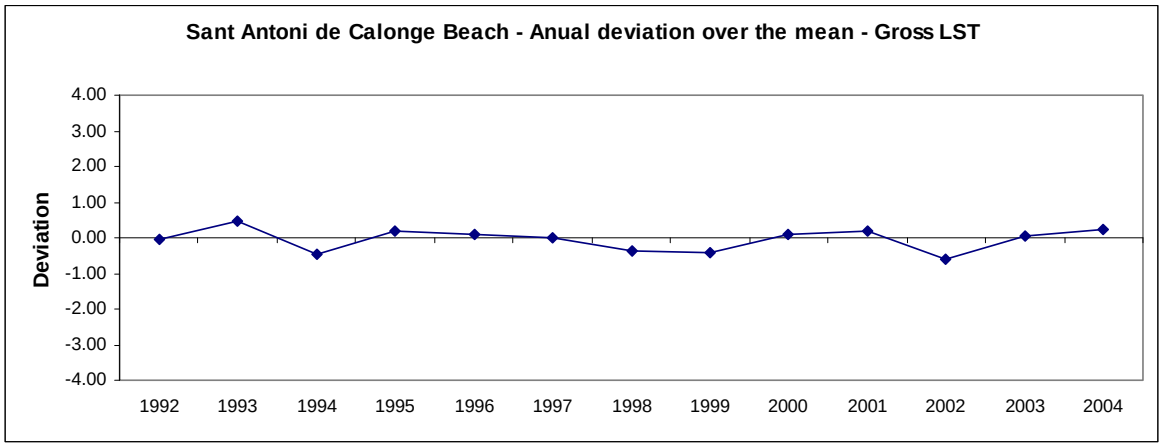

8. Platja d'Aro Unit – **Platja d'Aro**

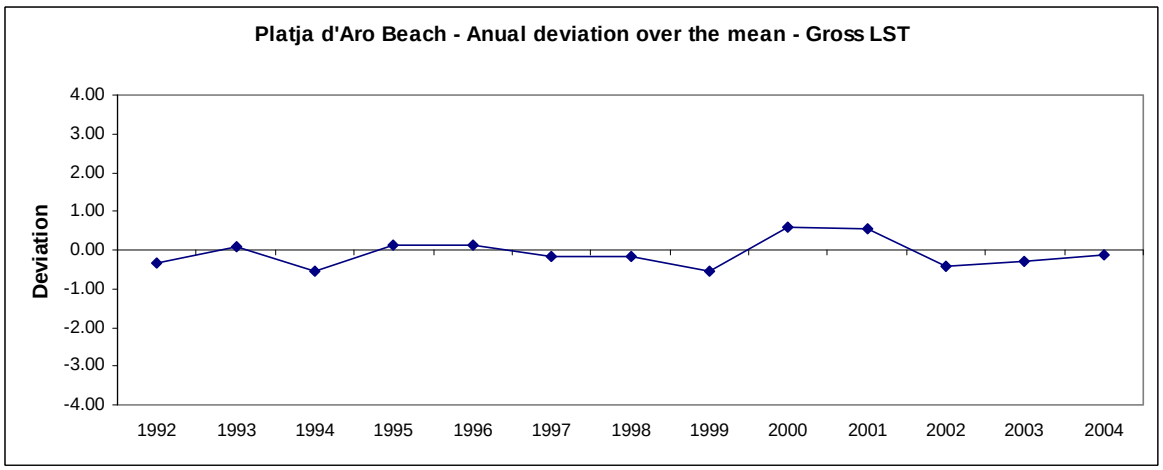

9. Lloret North Unit – **Lloret North**

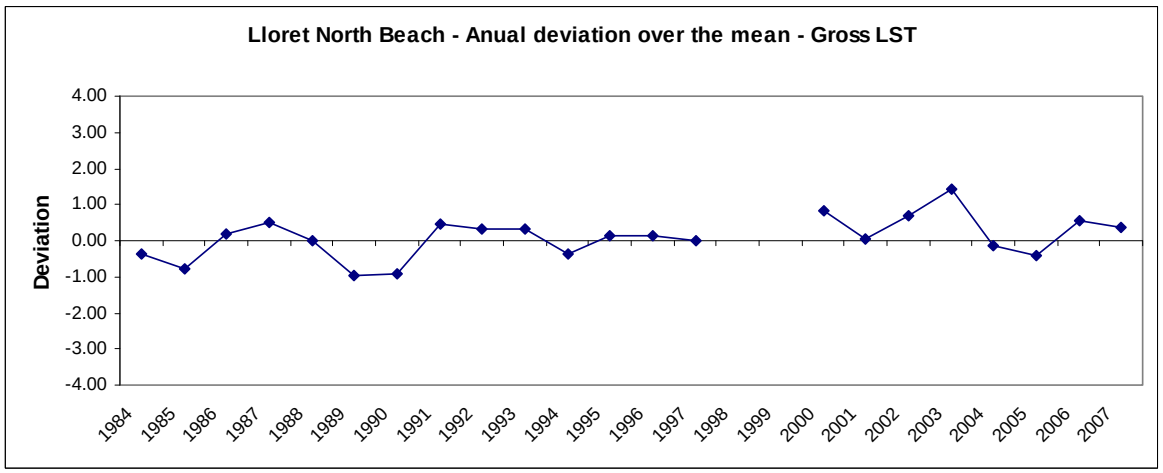

10. Lloret South Unit – **Lloret South**

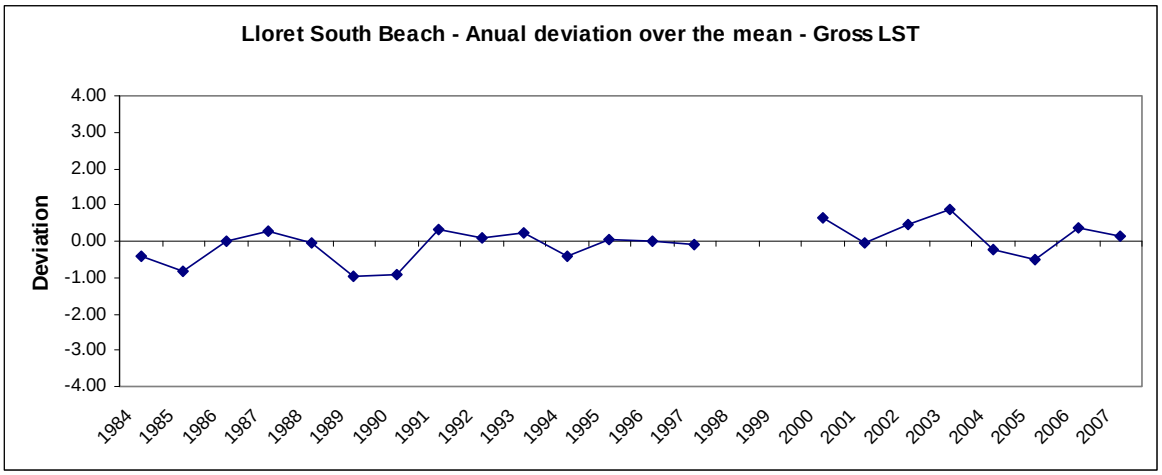

11. Lloret South Unit – **Santa Cristina**

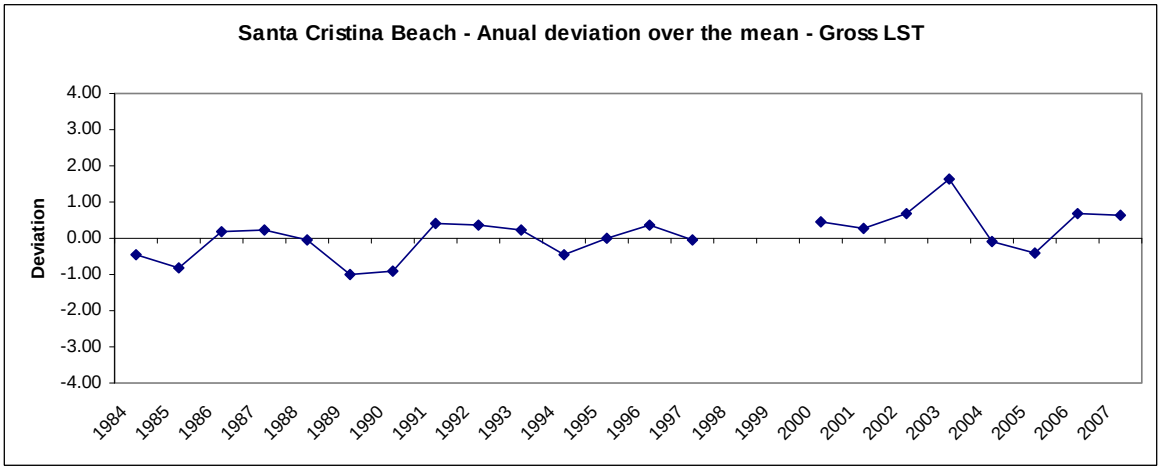

12. Blanes Unit – **S'Abanell North**

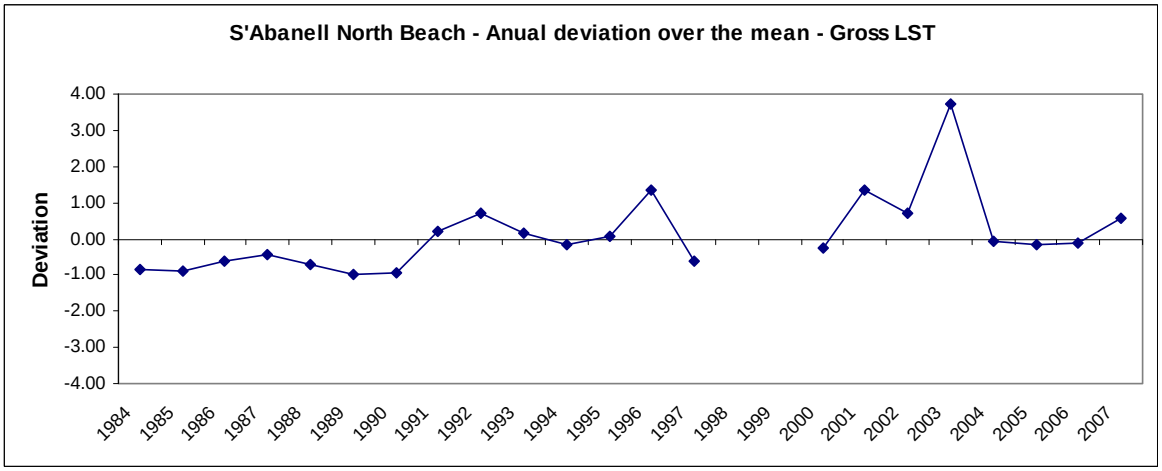

13. Blanes Unit – **S'Abanell South**

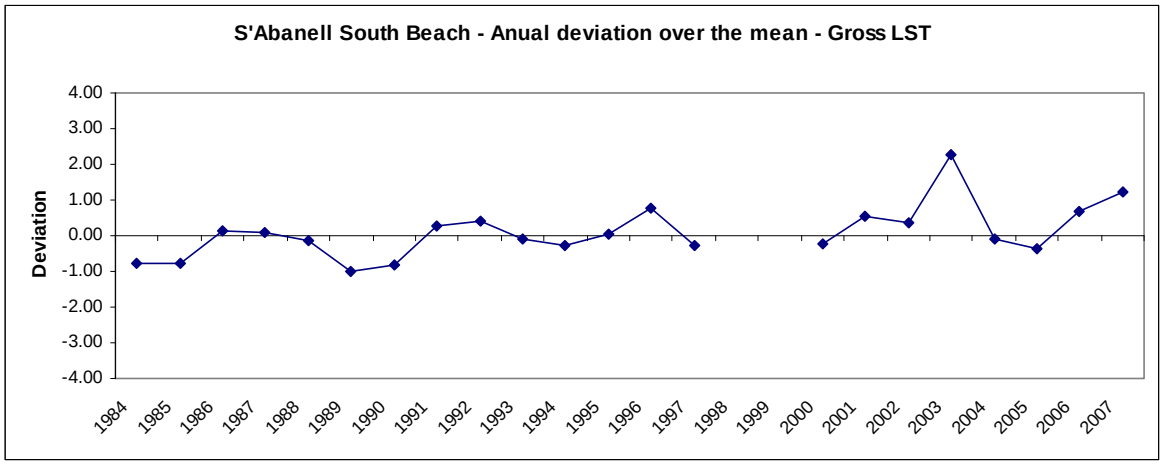

14. Blanes Unit – **La Tordera**

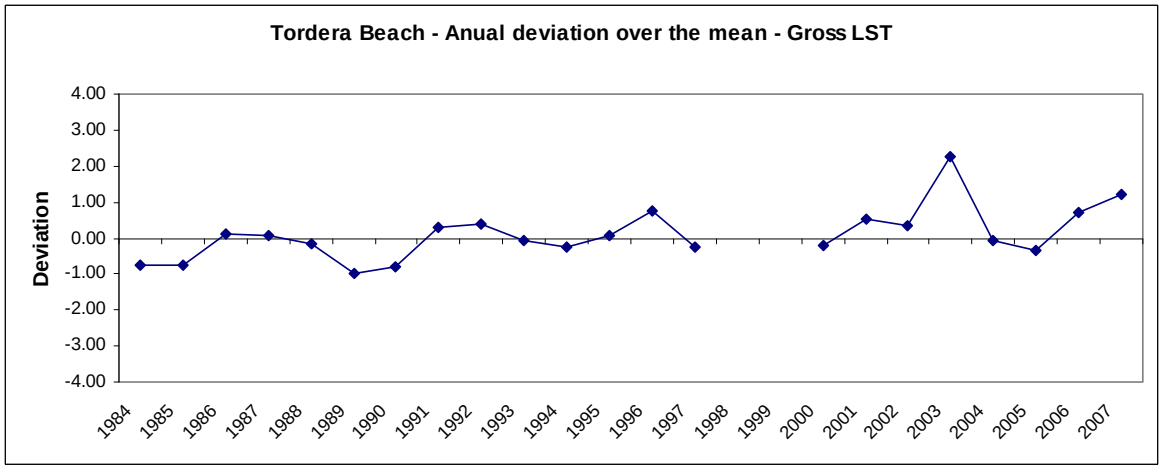

15. Mataró Unit - **Mataró**

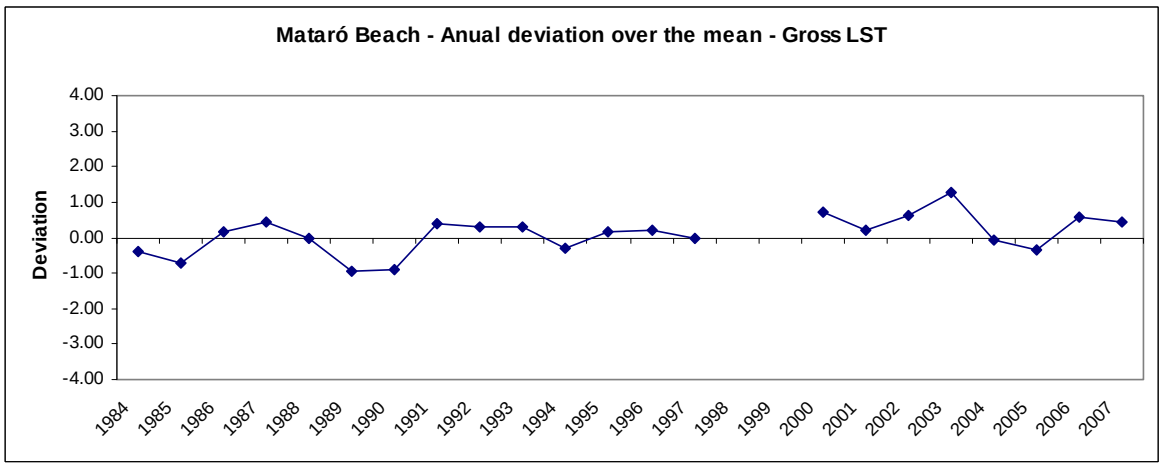

16. Masnou Unit - **Masnou**

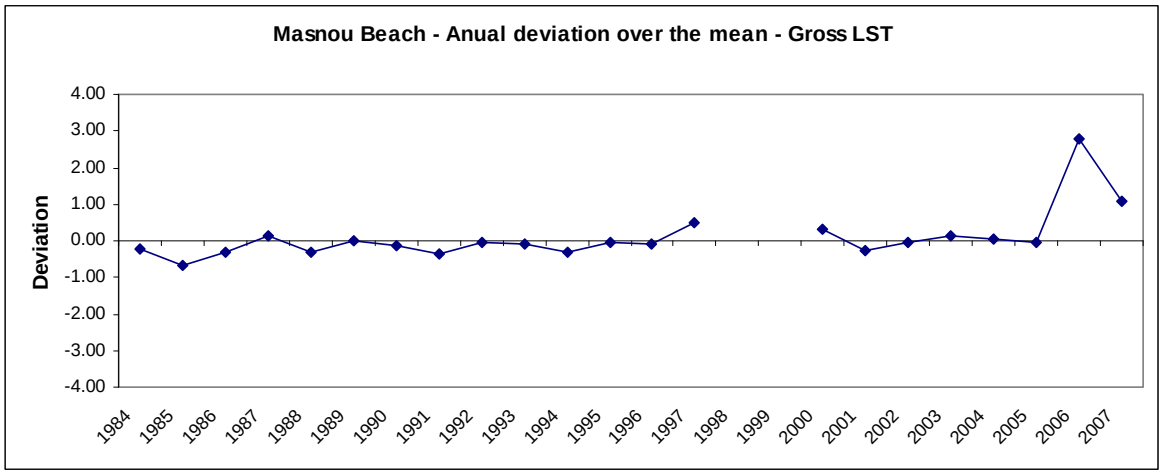

17. Calafell Unit - **Calafell**

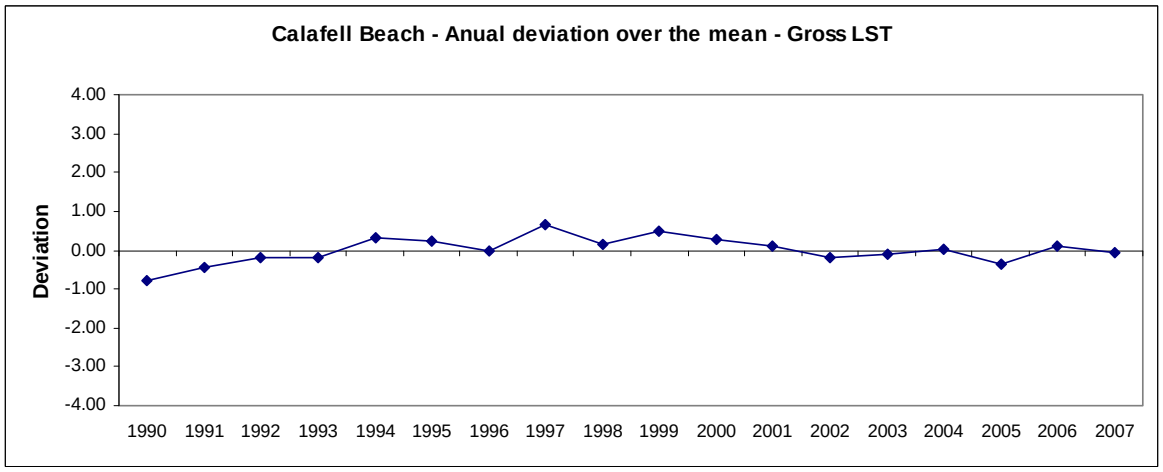

18. Torredembarra Unit - **Creixell**

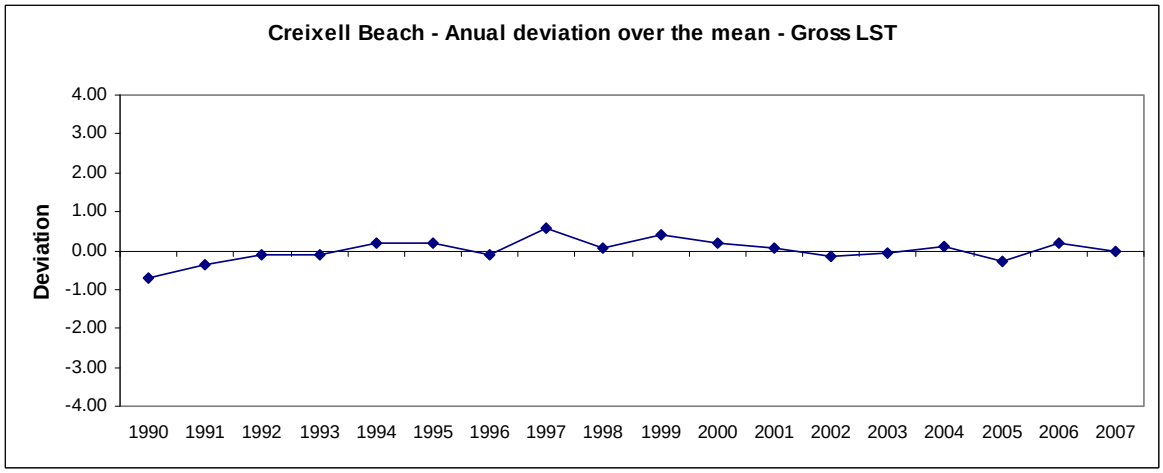

19. Torredembarra Unit – **El Roc**

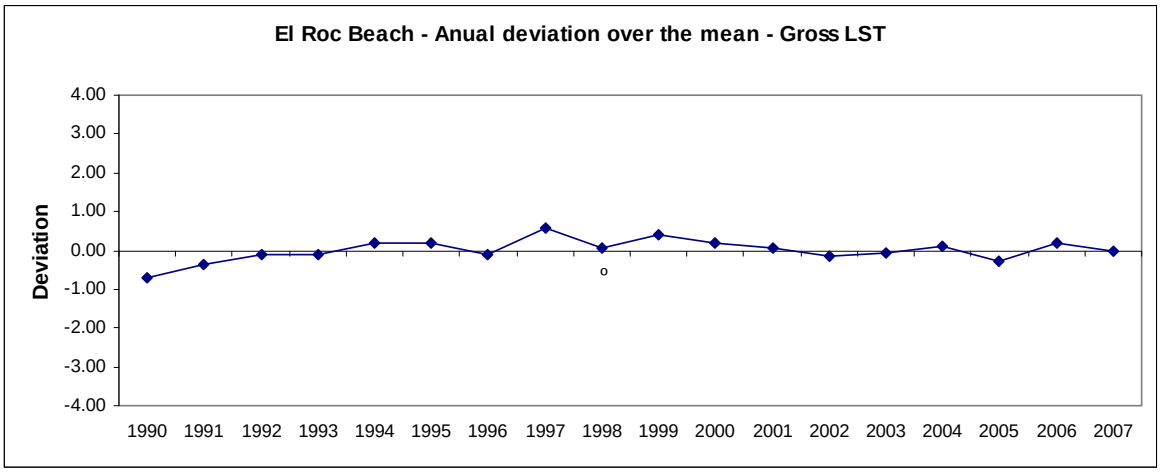

20. El Miracle Unit – **El Miracle**

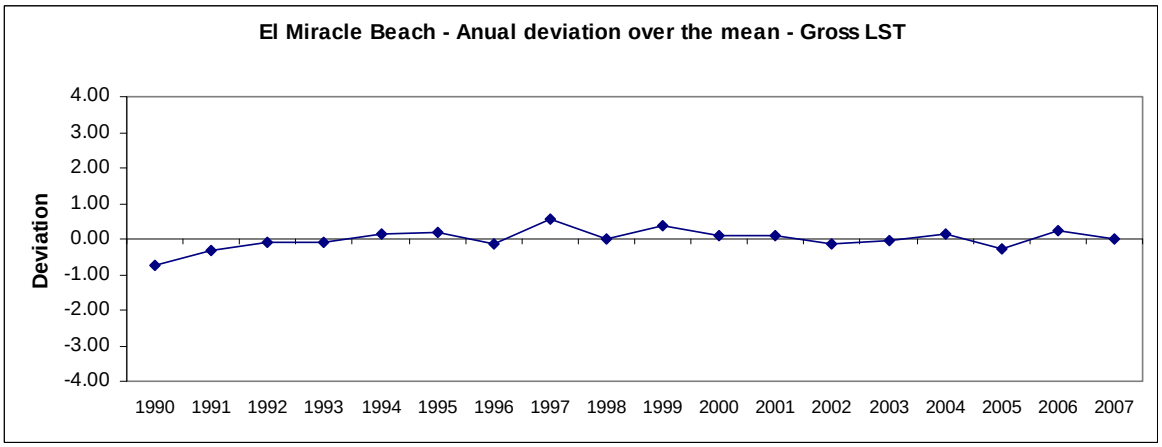

21. La Pineda Unit – **La Pineda**

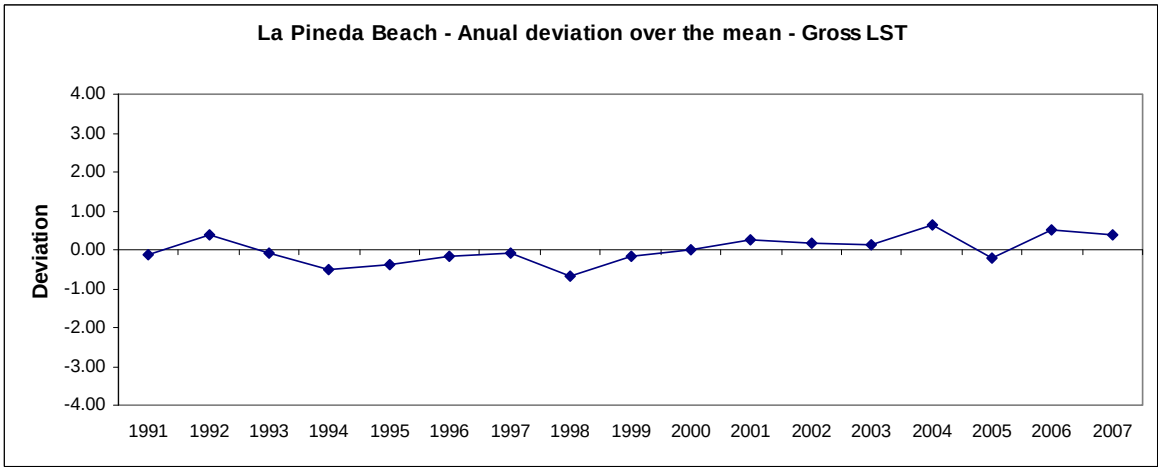

22. Cambrils Unit – **Cambrils**

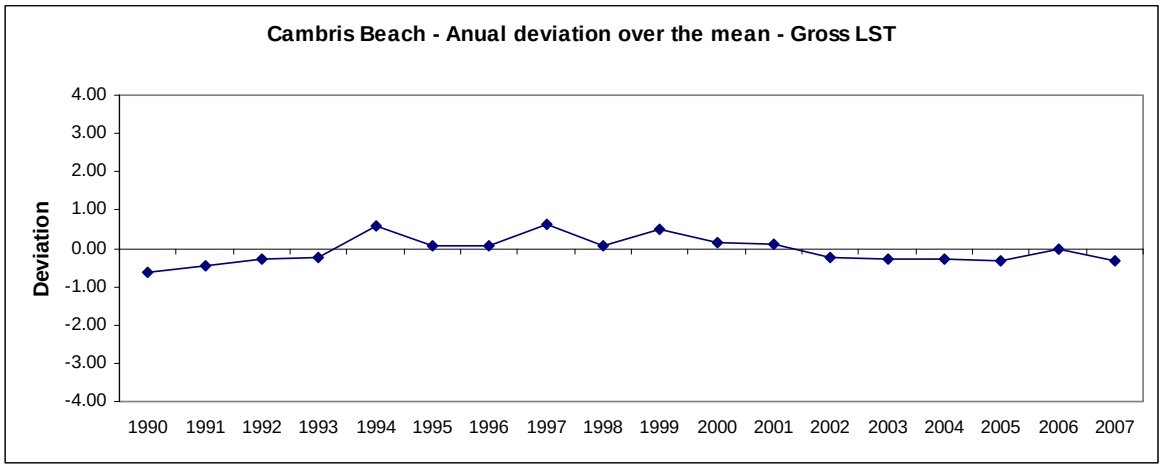

23. Cambrils Unit – **Salou**

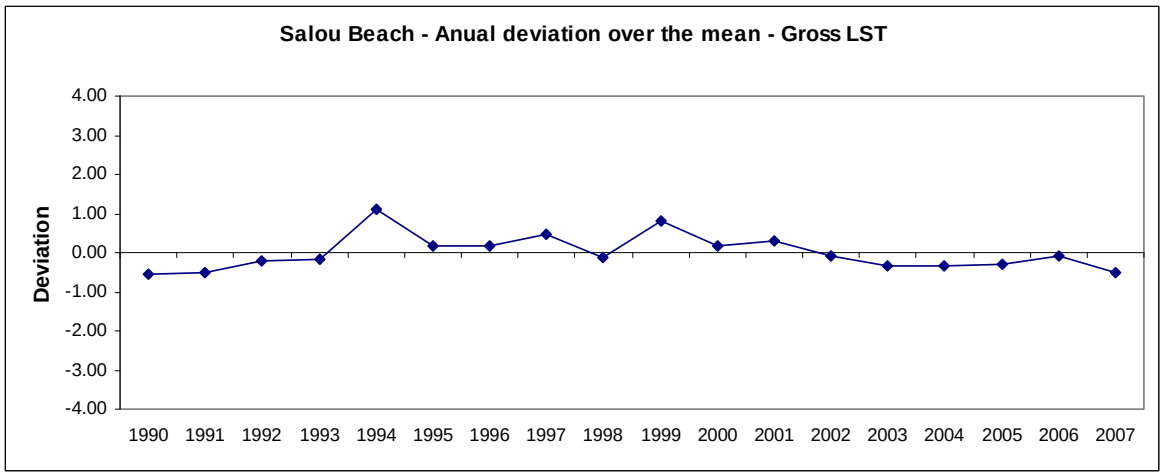

24. L'Hospitalet de l'Infant Unit – **L'Hospitalet de l'Infant**

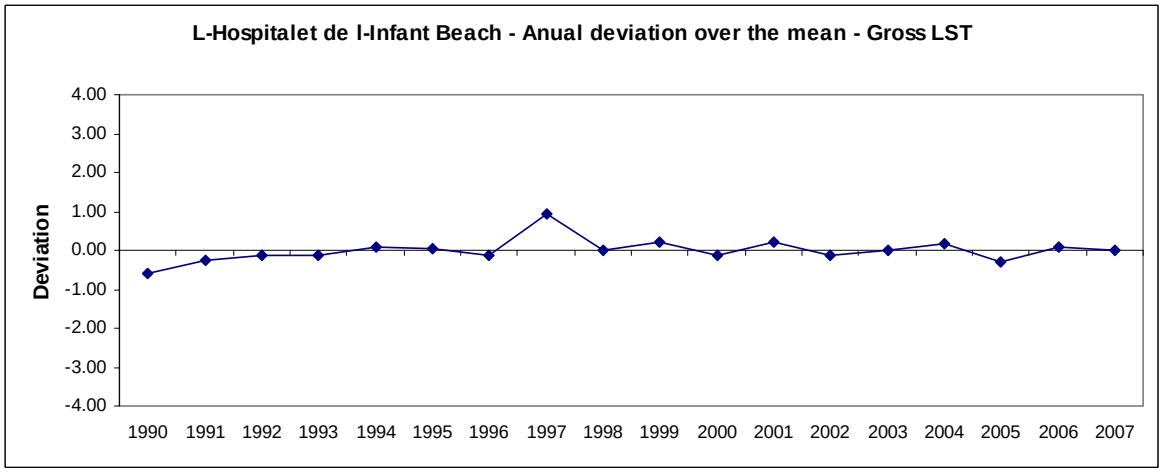

Appendix 1

Wave Height Roses

Buoy Zone 1

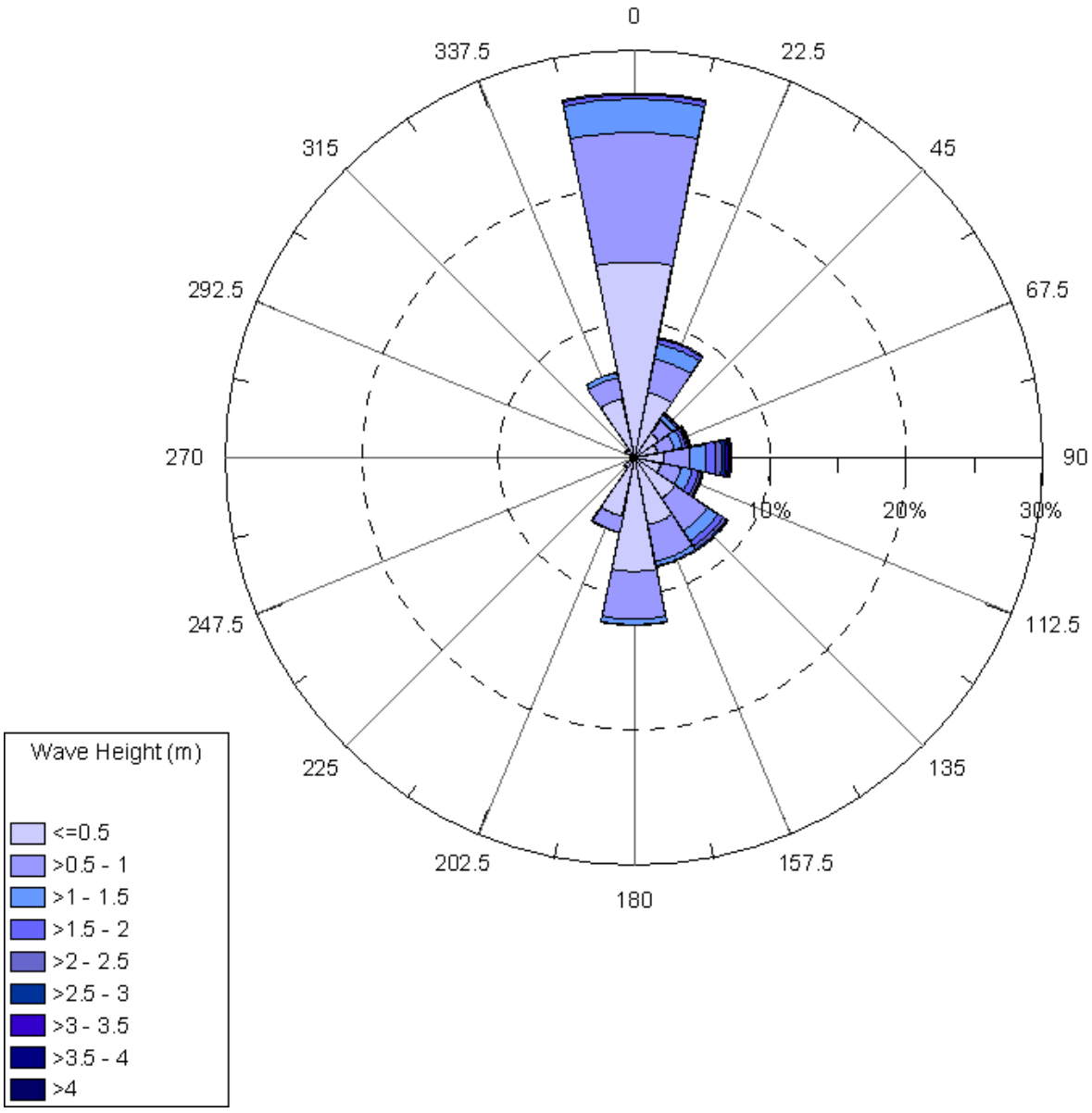

Appendix 1 *Wave Height Roses*

Buoy Zone 2

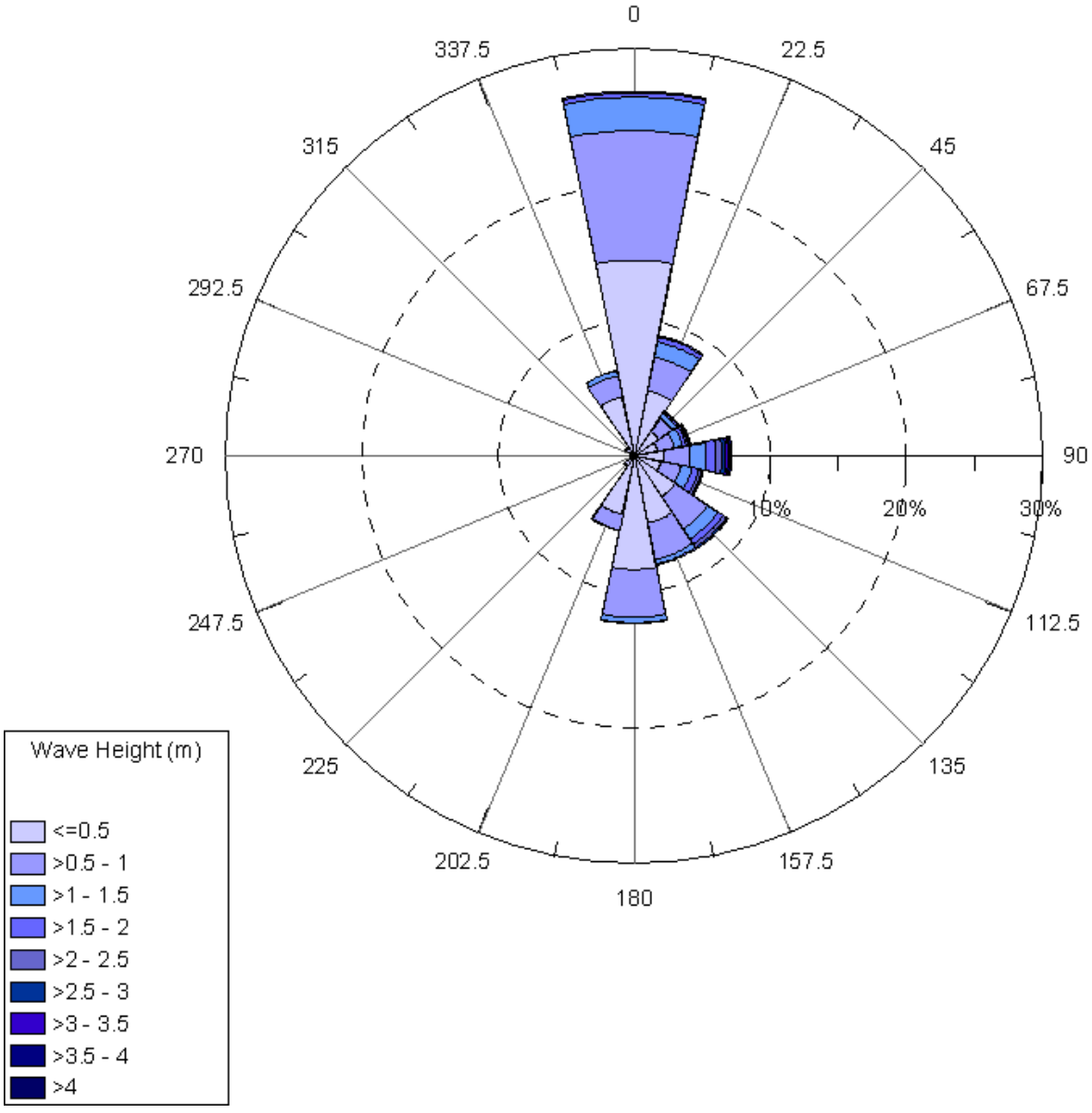

Appendix 1 *Wave Height Roses*

Buoy Zone 3

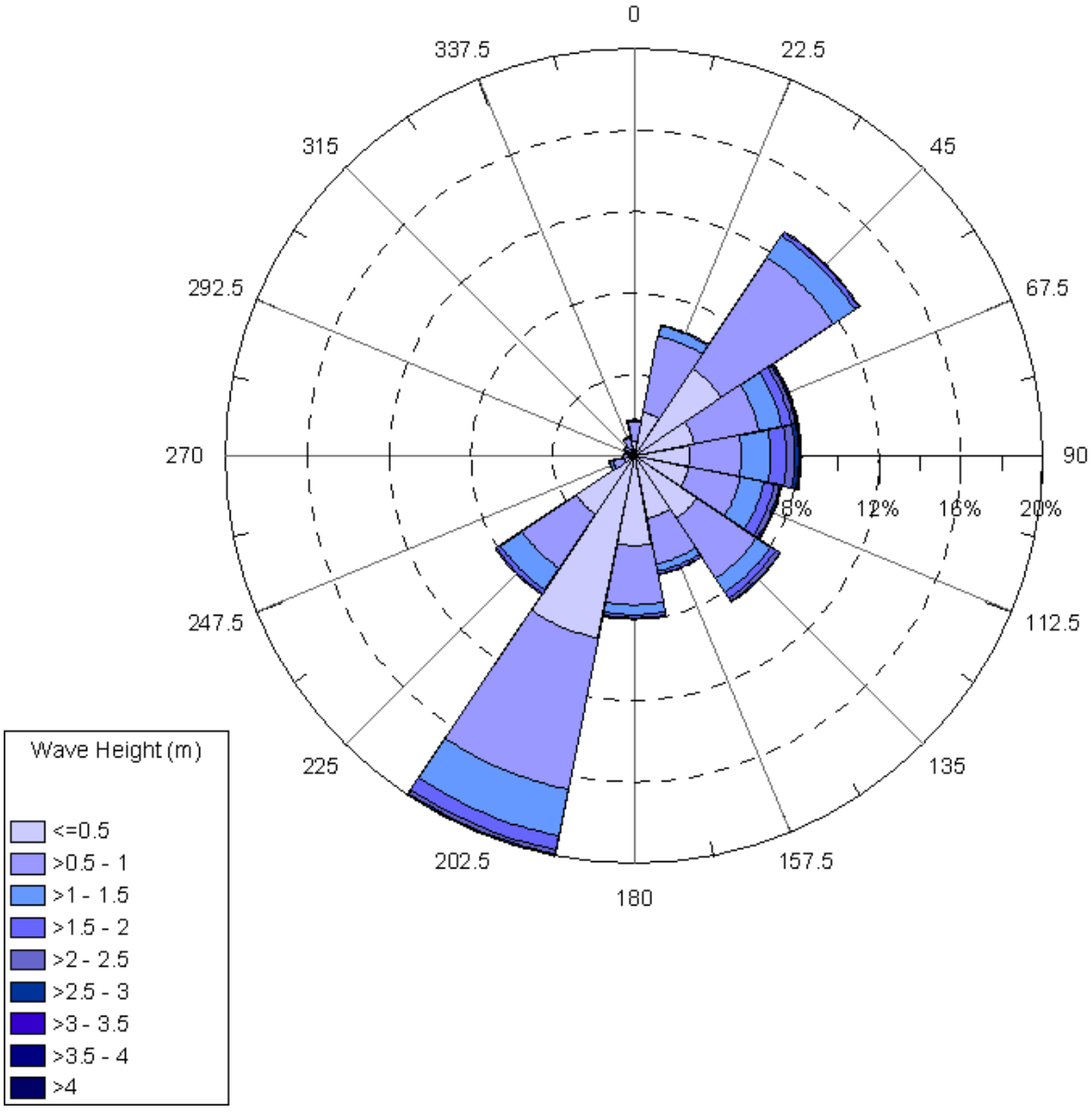

Buoy Zone 4

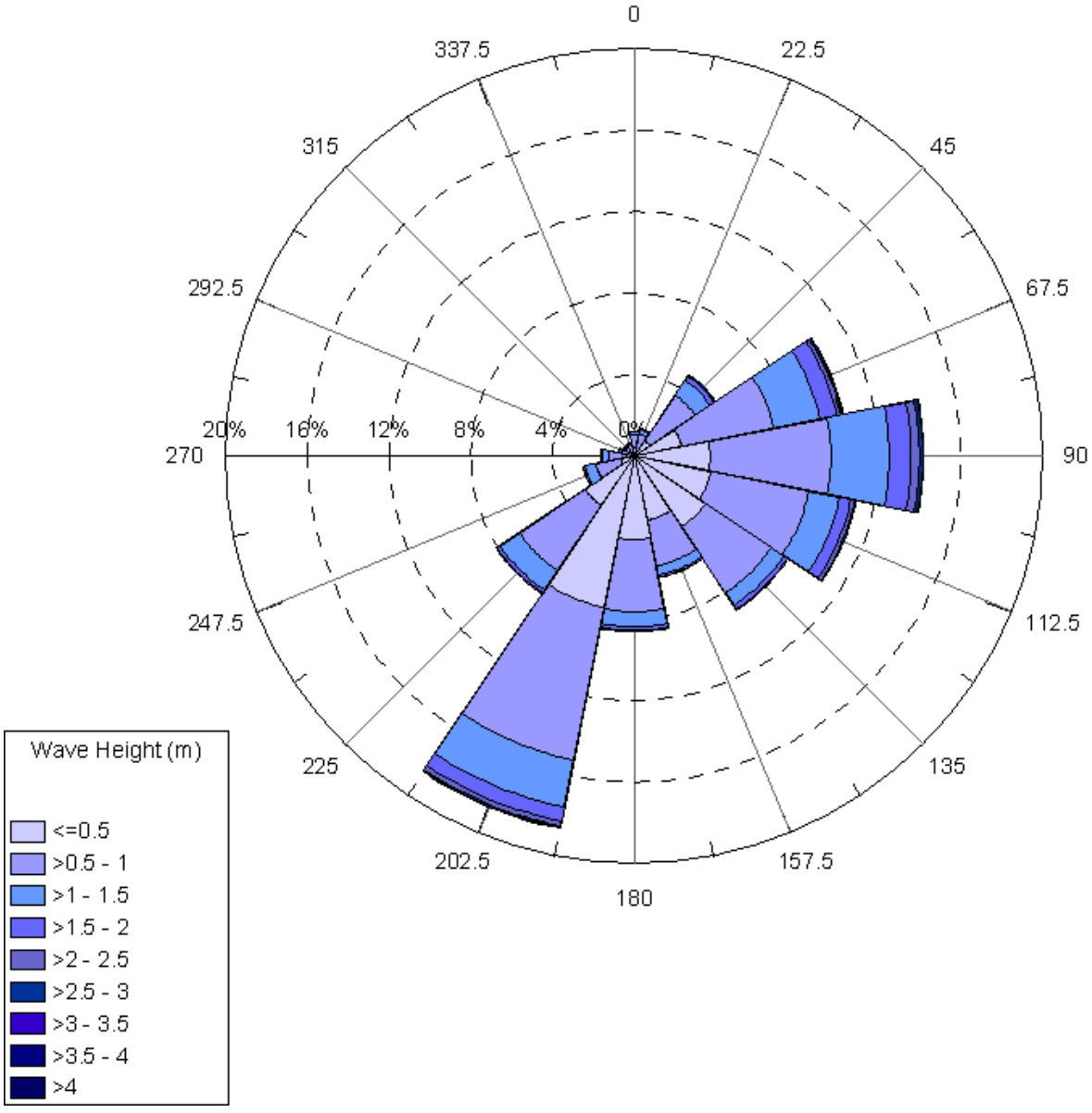
0
22.5
45
67.5
90
112.5
135
157.5
180
202.5
225
247.5
270
292.5
315
337.5
20%
16%
12%
8%
4%
0%
Wave Height (m)
<=0.5
>0.5 - 1
>1 - 1.5
>1.5 - 2
>2 - 2.5
>2.5 - 3
>3 - 3.5
>3.5 - 4
>4

Appendix 1 Wave Height Roses

Buoy Zone 6

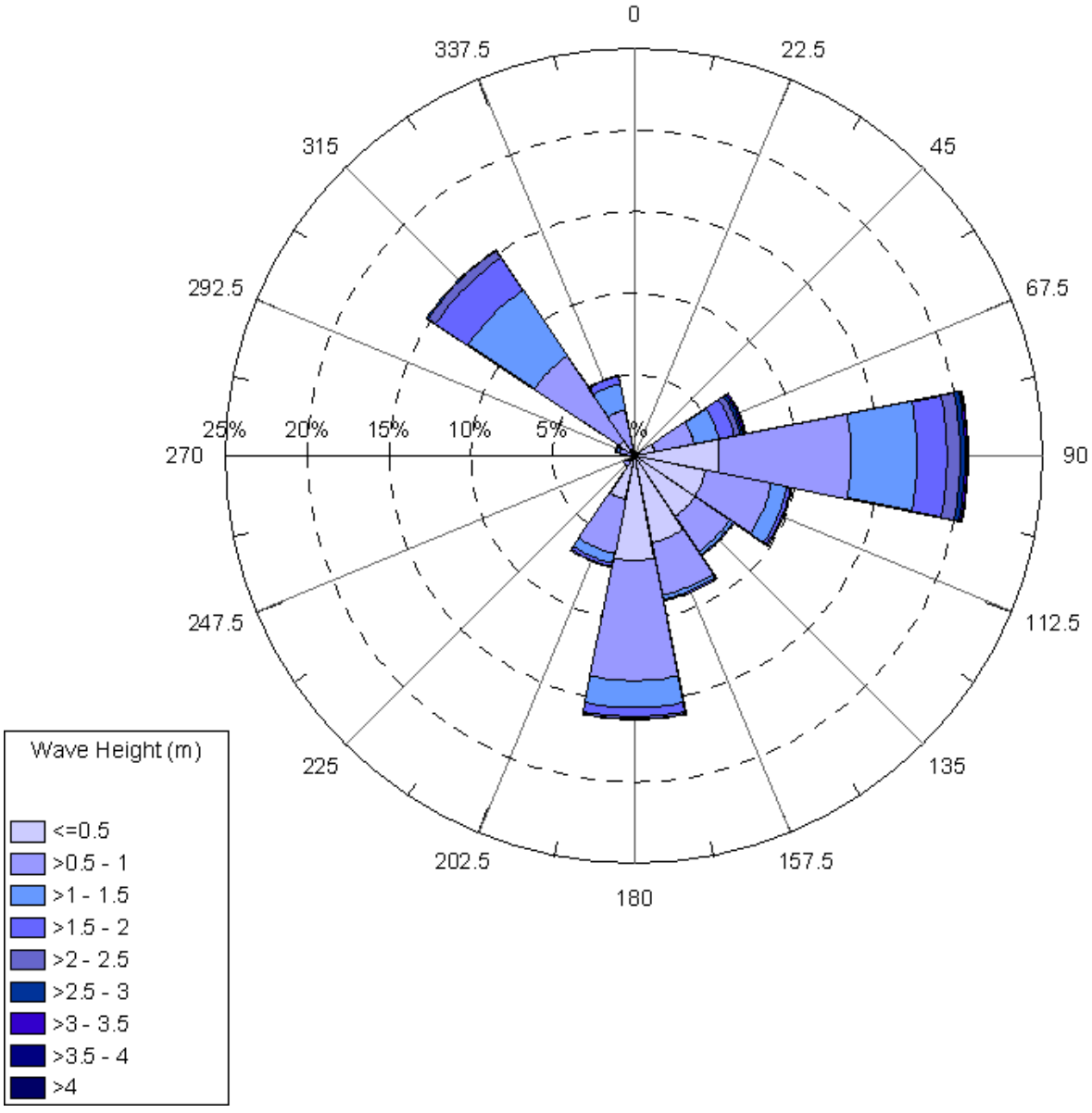

Appendix 2

Monthly Distribution of Hs

Buoy Zone 1

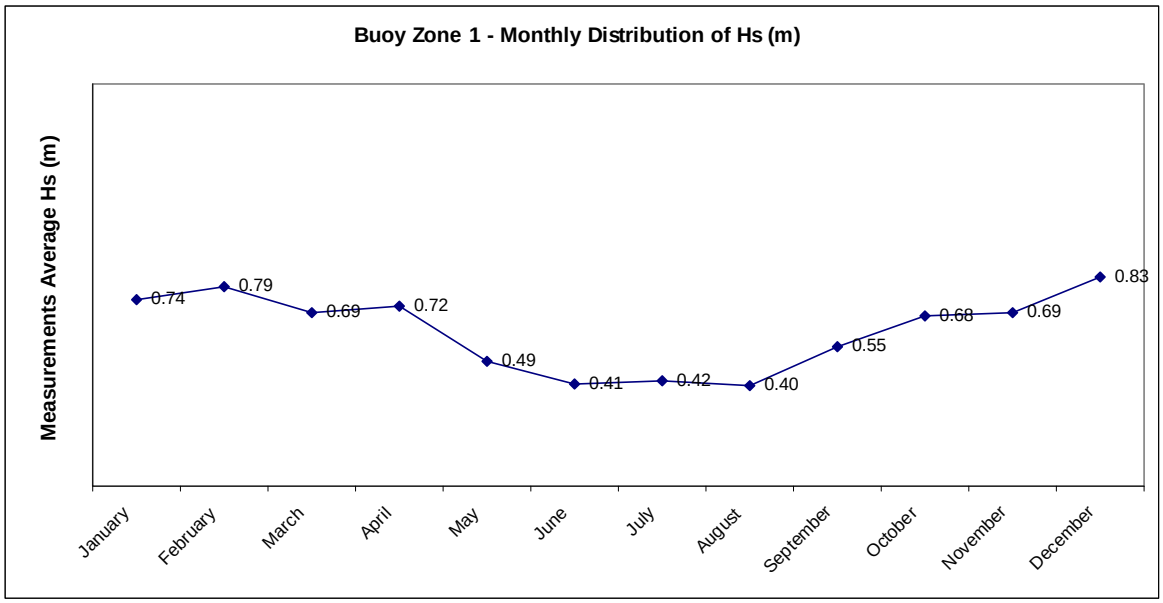

Buoy Zone 2

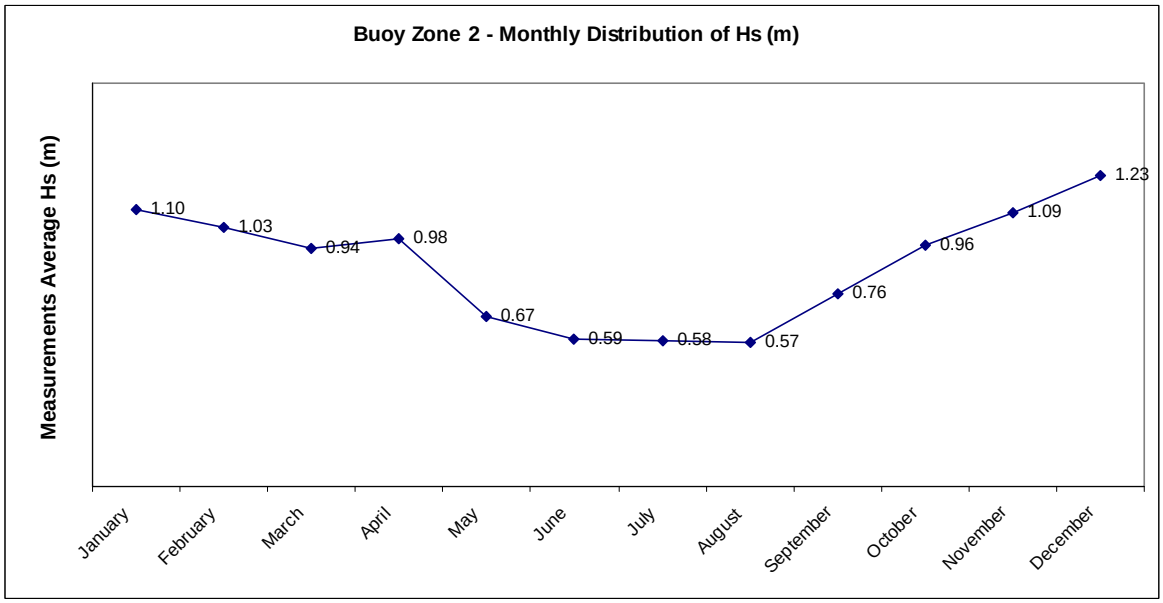

Buoy Zone 3

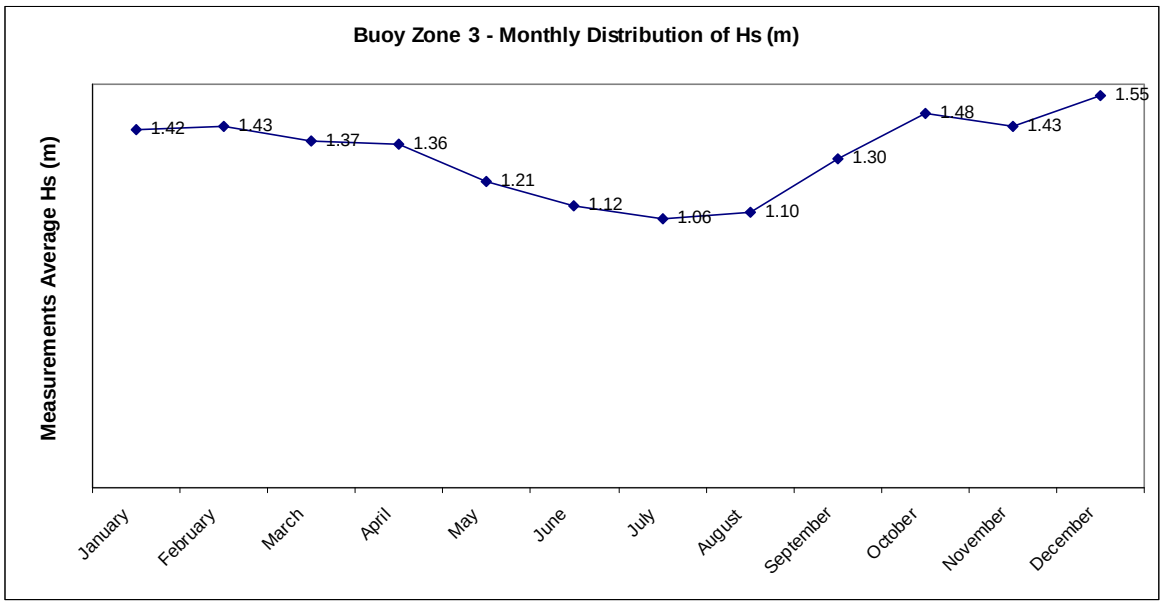

Buoy Zone 4

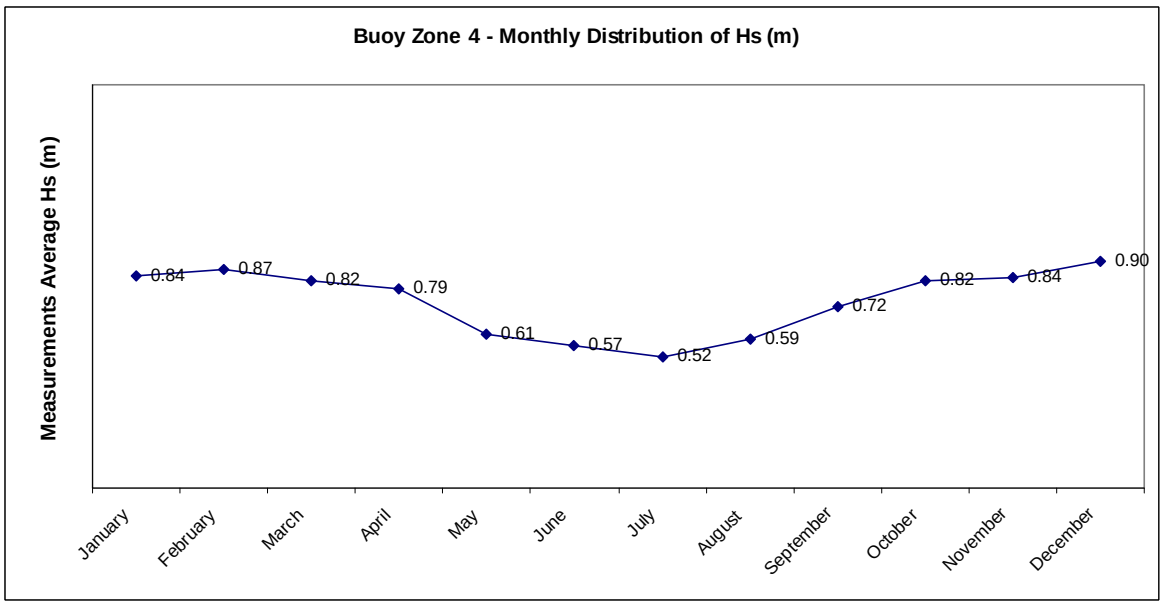

Buoy Zone 6

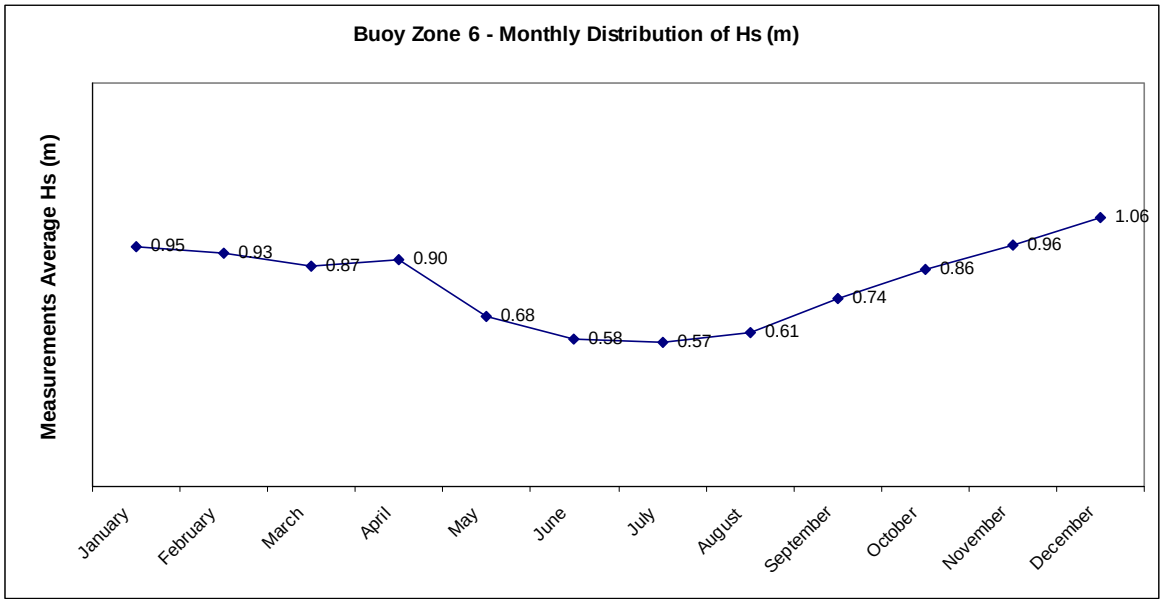
Buoy Zone 6 - Monthly Distribution of Hs (m)
Measurements Average Hs (m)
0.95
0.93
0.87
0.90
0.68
0.58
0.57
0.61
0.74
0.86
0.96
1.06
January
February
March
April
May
June
July
August
September
October
November
December

Chapter 4

References

Bayram, A., Larson, M., Hanson, H. *A new formula for the longshore sediment transport rate*. Coastal Engineering 54 (2007) 700–710.

Bayram, A., Larson, M., Miller, H.C., Kraus, N.C. *Cross-shore distribution of longshore sediment transport: comparison between predictive formulas and field measurements*. Coastal Engineering 44 (2001) 79– 99.

Camenen, B., Larroude´, P., *Comparison of sediment transport formulae for the coastal environment*.

Coastal Engineering Manual. Coastal and Hydraulics Laboratory. US Army Corps of Engineers. Part III-Chapter 2, Part V-Chapter 4.

Gimenez i Esgleas, D. *Observacio i estudi geologic del fons mari a la costa del Maresme*. L'Atzavara.

Gual, I. *Estat actual del fons mari a la platja de Torredembarra*. September 2002.

Heathershaw, A.D., Carr, A.P., Blackley, M.W. *Final Report: Coastal erosion and nearshore sedimentation processes*. Institute of ocanographic sciences, Surrey (UK).

Munilla, T., Corrales, M.J., San Vicente, C. Suprabenthic assemblages from Catalan beaches: zoological groups. Universitat Autònoma de Barcelona. Laboratori de Zoologia.

Oficina Catalana del Canvi Climatic. *Estudis de base per a una estratègia de prevenció i d'adaptació al canvi climàtic N1: Delta de l'Ebre. Prognosi dels efectes del canvi climàtic sobre el delta. Impactes sobre la costa.*

Universitat Politecnica de Catalunya. *Granulometria de la costa gerundense*. Atached document 5: Resultados del analisis granulometrico.

Kamphuis, J.W. *Alongshore transport of sand*. Presented at: ICCE '02 Cardiff, Wales, July 2002.

References

Sanchez-Arcilla, A., Jimenez, Jose. A. *Evolucion en planta/perfil de una playa. Metodos predictivos*. Laboratori d'Enginyeria Marítima, E.T.S. Ingenieros de Caminos, Canales y Puertos de Barcelona, Universitat Politécnica de Catalunya.

Sanchez-Arcilla, A., Jimenez, Jose. *El problema erosivo en el Delta del Ebro*. Revista de Obras Publicas, Septiembre 1997/Nº3368.

Sanchez-Arcilla, A. Regressio costanera al Delta de l'Ebre.CIIRC, LIM-UPC. 2007.

Schoonees, J.S. *Annual variation in the net longshore sediment transport rate*. Coastal Engineering 40_2000.141–160.

Van Rijn, L.C. *Longshore sand transport*.

Van Rijn, L.C., Boer, S. *Effect of grain diameter on sand transport in active coastal zone*.

Van Rijn, L.C., Boer, S. *The effects of grain size and bottom slope on sand transport in the coastal zone*.

Walton, T.L., Dean, R.G. *Longshore sediment transport via littoral drift rose*. Ocean Engeenering 37 (2010) 228-235.